

SELECTIVITY AND DETECTION
IN CAPILLARY ELECTROPHORESIS

by

Maha Yehia Khaled

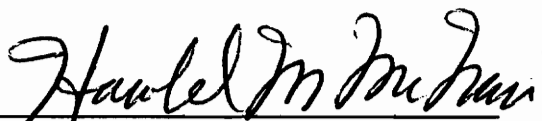
Dissertation Submitted to the Faculty of the
Virginia Polytechnic Institute and State University
in partial fulfillment of the requirements for the degree of

DOCTOR OF PHILOSOPHY

IN

CHEMISTRY

APPROVED



Harold M. McNair, Chairman



Mark R. Anderson



Neal Castagnoli, Jr.



Raymond E. Dessy



John G. Mason



Joseph S. Merola

August, 1994

Blacksburg, Virginia

C.2

LD
5655
V856
1994
K535
C.2

SELECTIVITY AND DETECTION IN CAPILLARY ELECTROPHORESIS

by

Maha Yehia Khaled
Committee Chairman: Harold M. McNair
Chemistry

(ABSTRACT)

This work is a contribution to the minimization of some of the selectivity and detection limitations in capillary electrophoresis. A more practical design of an electrochemical detector is introduced with simultaneous on-line UV detection (1), for the selective detection of a number of pungent and neurological compounds, the piperines and the capsacinoids. Commercially available microelectrodes together with large 25 μm id fused silica capillary columns are used for the first time in the presence of an auxiliary electrode. Minimum detectable quantities and efficiencies are sample dependent and were found to be comparable to the earlier more laborious electrochemical cell designs.

To exploit the benefits of common additives that enhance the selectivity of electrolyte systems, various additives including α , β and γ Cyclodextrins, organic modifiers, as well as a series of cationic surfactants are explored for the separation of a number of industrially important isomeric aromatic carboxylic acids (2). The separation was found to depend largely on the analyte's geometry, degree of ionization as well as on the buffer pH and composition.

The resultant separations were compared for best efficiency, resolution and ruggedness.

In addition, to add to the arsenal of CE selectors, a number of new micellar systems are investigated. Oligomeric sodium 10-undecylenate, a recently introduced oligomeric surfactant (3) is structurally investigated through the separation of vitamins and the resultant selectivity and resolution is compared to the more commonly used surfactant sodium dodecyl sulfate (4). Additionally, a number of phospholipids and lysophospholipids, common constituents of cell membranes, are investigated not only as possible MECC surfactants but also as highly hydrophobic analytes needing themselves separation (5).

Finally, as a contribution to methods development, the effect of variations in system parameter conditions is examined in a successful separation of a number of enzymes.

ACKNOWLEDGMENTS

Professor Dr. Harold McNair taught me that; *"To give a man a fish you have provided him with a meal but if you teach him how to fish, you have given him a thousand meals"* (Chinese Proverb). I would like to thank Dr. McNair not only for giving me one of the greatest fishing rods ever, but also for pointing and sending me out to where the 'fishing' is best and on occasions, allowing me to accompany him on his own various 'fishing trips' (the short courses), to watch him perform one of his best 'fishing tricks', the gift of teaching. One, in my opinion, usually makes a few good decisions in one's life; coming to Virginia Tech and joining the McNair group has been one of my best. Professor McNair has been a great mentor and I shall for ever be in debt to him for furnishing many an opportunity for me to learn.

I would also like to thank my scientific committee members Prof. Mark Anderson, Prof. Neal Castagnoli, Prof. Raymond Dessy, Prof. John Mason and Prof. Joe Merola for their patience and guidance through out the course of my study and stay, here at Tech.

The long hours in the lab would not have been possible were it not for my colleagues and friends. I would like to thank Dr. George Reiner, Dr. Nicholas Snow, Dr. Greg Slack , Dr. Lisa Goebel, Laura Perry, Dr. Vince Remcho, Dr. Robert Klute , Dr. Christopher Palmer, Angelica Marochi, Dr. Lee Polite, Dr. Richard Pauls, Dr. Yuri Kazakavich and Dr. Markus Lyman, for their friendship and for the many fruitful scientific discussions. Scott Smith, Yuwen Wang, Josette Heng, Xiaowei Sun, Bai Hong, Marshall Penny, Stefanie Armstrong and

lately Donna Blankenship, Lori McDaniel and Elena Cabusas also deserve my thanks for reasons too plentiful to enumerate.

I must also thank some of the people whom have been a constant source of support and encouragement and have helped me settle in and understand America; Dr. Jehane Ragaii, Dr. Mona El Sheikh, Dr. George Janini, Mrs Marijke McNair, Mrs Kay Castagnoli and Dr. Pam Perrone.

Last but not least, I am grateful to my parents and my brothers for their support, constant caring, belief in me and for setting the high standards that I am constantly struggling to achieve. Were it not for their encouragement, I would have never ventured to seek my scientific and cultural freedom.

***Fired at first sight with what muse imparts,
In fearless youth we tempt the heights of arts,
While from the bounded level of our mind
Short views we take, nor see the length behind;
But more advanced behold with strange surprise
New distant scenes of endless science rise!
So pleased at first the towering Alps we try,
Mount o'er the vales, and seem to tread the sky,
The eternal snows appear already past,
And the first clouds and mountains seem the last;
But those attained we tremble to survey
The growing labors of the lengthened way,
The increasing prospect tires our wandering eyes,
Hills peep o'er hills, and Alps on Alps arise!***

Alexander Pope

To my family.

*Yehia, Afaf,
Waleed, Amro
Halima,*

and my friend,

Mona

TABLE OF CONTENTS

	Page
CHAPTER I INTRODUCTION	1
1.1 ELECTROPHORESIS	1
1.2 HISTORICAL	3
1.3 BASIC HARDWARE COMPONENTS	6
CHAPTER II. SEPARATION THEORY	9
2.1 THE ELECTRICAL DOUBLE LAYER	9
2.2 ELECTROOSMOSIS	12
2.2.1. PLUG PROFILE	15
2.2.2. MEASURING ELECTROOSMOSIS	15
2.3 SEPARATION IN CAPILLARY ELECTROPHORESIS	17
2.4 BASIC PRINCIPLES	19
2.4.1. MIGRATION TIMES	19
2.4.2. EFFICIENCY	20
2.4.3. RESOLUTION	22
CHAPTER III FACTORS INFLUENCING PERFORMANCE	
3.1 FUNDAMENTAL DISPERSIVE EFFECTS	23
3.1.1. JOULE HEATING AND TEMPERATURE GRADIENTS	24
3.1.2. INJECTION PLUG LENGTH.	28
3.1.3. ELECTRODISPERSION.	28
3.1.4. SOLUTE WALL EFFECTS.	31
3.1.5. COMPARATIVE EVALUATION OF THE DIFFERENT DISPERSIVE EFFECTS.	32
3.2 OPERATIONAL PARAMETERS	34
3.2.1. CAPILLARY DIMENSIONS	34
3.2.2. APPLIED POTENTIAL	35

3.3.	THE ELECTROLYTE SYSTEM	38
3.3.1.	THE BUFFER IONIC STRENGTH	39
3.3.2.	THE PH	40
3.3.3.	BUFFER ADDITIVES	42
	a)Complex Formation	42
	Ion pairing agents	
	Metal additives	
	Cyclodextrins	
	Surfactants	
	b)Organic Modifiers	57

CHAPTER IV. INSTRUMENTATION

4.1.	SAMPLE INTRODUCTION	58
4.2.1.	HYDRODYNAMIC INJECTION	58
4.2.2.	ELECTROKINETIC INJECTION	61
4.2.	POWER SUPPLY	62
4.3.	DETECTION	64
4.3.1.	U.V. DETECTION	66
4.3.2.	FLUORESCENCE	
4.3.3.	ELECTROCHEMICAL	71
4.3.4.	MASS SPECTROMETRY	80
4.2.5.	INDIRECT DETECTION	81

CHAPTER V. EXPERIMENTAL

5.1.	MEKC OF PUNGENT COMPOUNDS USING SIMULTANEOUS ON-LINE ULTRAVIOLET AND MODIFIED ELECTROCHEMICAL DETECTION.	82
5.1.1.	APPARATUS AND INSTRUMENTATION	82
5.1.2.	CHEMICALS.	82
5.2.	CAPILLARY ZONE ELECTROPHORETIC SEPARATION OF ISOMERIC BENZOIC CARBOXYLIC ACIDS; THE EFFECT OF ADDITIVES.	88

5.2.1.	APPARATUS	88
5.2.2.	MATERIALS	89
5.2.3.	PROCEDURE	89
5.3.	EVALUATION OF AN OLIGOMERIZED SODIUM UNDECYLENATE AS A SURFACTANT FOR THE SEPARATION OF VITAMINS.	91
5.3.1.	APPARATUS	91
5.3.2.	EXPERIMENTAL CONDITIONS.	92
5.3.3.	SYNTHESIS OF OLIGOMER.	94
5.4.	THE SEPARATION OF PHOSPHOLIPIDS AND THEIR USE AS SURFACTANTS IN MICELLAR ELECTROKINETIC CHROMATOGRAPHY.	97
5.4.1	APPARATUS	97
5.4.2.	CHEMICALS	98
5.5.	THE ANALYTICAL SEPARATION OF <i>TRICHODERMA REESEI</i> CELLULASES BY CAPILLARY ZONE ELECTROPHORESIS; MANIPULATION OF THE OPERATING CONDITIONS.	100
5.5.1.	APPARATUS	100
5.5.2	MATERIALS	101

CHAPTER VI. RESULTS AND DISCUSSIONS

6.1.	MEKC OF PUNGENT COMPOUNDS USING SIMULTANEOUS ON-LINE ULTRAVIOLET AND MODIFIED ELECTROCHEMICAL DETECTION.	102
6.2.	CAPILLARY ZONE ELECTROPHORETIC SEPARATION OF ISOMERIC BENZOIC CARBOXYLIC ACIDS; THE EFFECT OF ADDITIVES.	125
6.3.	EVALUATION OF AN OLIGOMERIZED SODIUM UNDECYLENATE AS A SURFACTANT FOR THE SEPARATION OF VITAMINS.	154
6.4.	THE SEPARATION OF PHOSPHOLIPIDS AND THEIR USE AS SURFACTANTS IN MICELLAR ELECTROKINETIC CHROMATOGRAPHY.	178

6.5. THE ANALYTICAL SEPARATION OF <i>TRICHODERMA REESEI</i> CELLULASES BY CAPILLARY ZONE ELECTROPHORESIS; MANIPULATION OF THE OPERATING CONDITIONS.	199
CHAPTER VII. CONCLUSIONS	211
REFERENCES	216
VITA	225

LIST OF FIGURES

		Page
Fig. 1.1	Modes of separation science	3
Fig. 1.2	Basic capillary electrophoresis Instrumentation	7
Fig. 2.1	Stern model of the double Layer	13
Fig. 2.2	Flow profiles: HPLC vs CE	16
Fig. 2.3	Separation in Capillary Zone Electrophoresis	18
Fig. 3.1	Schematic of temperature gradient from capillary center to the surrounding	26
Fig. 3.2	Effect of Electrophoretic Dispersion	30
Fig. 3.3	On-Column detection	36
Fig. 3.4	Effect of pH on surface silanols and electroosmotic flow	43
Fig. 3.5	Cyclodextrins	45
Fig. 3.6	Separation in Micellar Electrokinetic Capillary Chromatography	49
Fig. 3.7	Addition of cationic surfactants	53
Fig. 4.1	Modes of sample introduction Capillary Electrophoresis	59
Fig. 4.2	Schematic diagram of two different UV/VIS detection devices in CE	67
Fig. 4.3	Method for sensitivity enhancement	69
Fig. 4.4	Conductivity detection	73
Fig. 4.5	Post-column CE electrochemical detection	76
Fig. 4.6	End-column CE electrochemical detection	77
Fig. 4.7	Schematic of a liquid junction and coaxial interface between CE and MS	80
Fig. 5.1	Experimental set-up for simultaneous on-line Ultra-Violet and electrochemical detection.	83
Fig. 5.2	Modified amperometric electrochemical detection cell	85
Fig. 6.1	Molecular structure of pungent compounds	103

Fig. 6.2	Separation of capsaicin and dihydrocapsaicin	107
Fig. 6.3	Effect of Injection Time	108
Fig. 6.4	Effect of separation potential	110
Fig. 6.5	Effect of organic modifier	111
Fig. 6.6	Separation of the capsaicins and homovanillic acid	112
Fig. 6.7	Ultra-violet detection pungent compounds	113
Fig. 6.8	Ultra-Violet spectra	115
Fig. 6.9	Cyclic voltammetry of the pungent compounds.	116
Fig. 6.10	Simultaneous on-line detection.	117
Fig. 6.11	End-column electrochemical detection linear range for hydroquinone	120
Fig. 6.12	Calibration curve for homovanillic acid, capsaicin and dihydrocapsaicin	121
Fig. 6.13	End-column ED of hydroquinone.	123
Fig. 6.14	End-column ED of Dopamine and 3,4-hydroxybenzylamine.	124
Fig. 6.15	Molecular structures of the aromatic carboxylic acids	127
Fig. 6.16	Separation of acids under positive polarity.	130
Fig. 6.17	Electrophoretic dispersion with lower applied potentials.	131
Fig. 6.18	Effect of pH on retention time, resolution and peak shape.	133
Fig. 6.19	Effect of pH.	138
Fig. 6.20	% Relative standard deviation in a) Time. b) Area.	136
Fig. 6.21	Addition of β cyclodextrin for the separation of the aromatic carboxylic acids.	137
Fig. 6.22	3-D plot for the separation of the acids.	138
Fig. 6.23	Separation mechanism for the aromatic carboxylic acids using cyclodextrins	140
Fig. 6.24	Effect of β cyclodextrin concentration on elution order of the acids.	141

Fig. 6.25	Effect of addition of γ cyclodextrin on the separation of the aromatic carboxylic acids.	142
Fig. 6.26	Separation of acids using cyclodextrins.	143
Fig. 6.27	Effect of cyclodextrin type on retention of the aromatic acids.	144
Fig. 6.28	a) Effect of voltage on resolution of TA from OA. b) Effect of voltage on Retention time.	146
Fig. 6.29	% Relative standard deviation	147
Fig. 6.30	Calibration curve for acids.	148
Fig. 6.31	Addition of cationic surfactants; Reversal of polarity.	151
Fig. 6.32	Industrial samples.	153
Fig. 6.33	Electrokinetic separation of catechols using a monodisperse sulfonated polymer.	155
Fig. 6.34	Separation of PAHs using sodium undecylenate Oligomer (35%ACN).	157
Fig. 6.35:	Carbon-13 NMR spectra of the Oligomerized Sodium 10-Undecylenate.	159
Fig. 6.36	Proton NMR of sodium undecylenate oligomer	161
Fig. 6.37	Molecular structure of water soluble vitamins.	162
Fig. 6.38	Absorbance spectra of Vitamins.	163
Fig. 6.39	Effect of Oligomer (UDO) concentration on the elution order of water soluble vitamins.	164
Fig. 6.40	Effect of pH on the elution of the water soluble vitamins.	166
Fig. 6.41	Separation of water soluble vitamins using the Oligomer.	169
Fig. 6.42	% RSD of the peak area	170
Fig. 6.43	% RSD of the elution time.	171
Fig. 6.44	Effect of micelle type on the elution order of the water soluble vitamins	173
Fig. 6.45	Efficiency comparison between SDS and UDO.	175
Fig. 6.46	Effect of addition of acetonitrile with oligomer on the elution of water soluble vitamins.	176

Fig.6.47	Effect of addition of Acetonitrile on the water soluble vitamin's separation.	178
Fig. 6.48	Structures of common phospholipid classes	181
Fig. 6.49	Phospholipids verses Lysophospholipids as possible surfactants	184
Fig. 6.50	Separation of alkyl parabens.	188
Fig. 6.51	Separation of alkyl parabens with 2.2 mM of the anionic surfactant lysophosphatidylglycerol;	190
Fig. 6.52	Enhancement of alkyl paraben separation with mixed micellar systems.	193
Fig. 6.53	Chromatograms of commercially available phospholipids.	194
Fig. 6.54	The separation of two classes of phospholipids	195
Fig. 6.55	Separation of commercially available lysophospholipids.	197
Fig. 6.56	Separation of phosphatidylcholines based on different chain length.	198
Fig. 6.57	Separation of Enzymes.	203
Fig. 6.58	Effect of pH on Enzyme Separation.	206
Fig. 6.59	Effect of Ionic Strength on enzyme separation.	210

LIST OF TABLES

		Page
Table 1.1	Commercial CE instrumentation	8
Table 3.1	Cyclodextrin physical parameters	46
Table 3.2	CE surfactants.	50
Table 3.3	Typical values for several plate height contributions	55
Table 4.1	Available methods of detection in CE.	67
Table 6.1	Resultant efficiencies and minimum detectable quantities using the modified end column detection cell	119
Table 6.2	% RSD for peak areas.	122
Table 6.3	pKa and molecular weight values of the aromatic carboxylic acid isomers	129
Table 6.4	Electrophoretic and electroosmotic parameters of the different micellar systems	186
Table 6.5	Elution Window Ranges	189
Table 6.6	Characteristics of purified <i>Trichoderma Reesei</i> Cellulases.	200
Table 6.7	% Relative Standard Deviations of enzyme areas and retention times.	204

CHAPTER I

INTRODUCTION

1.1. ELECTROPHORESIS

Electrophoresis is the separation of molecules based on their movement under the influence of an applied potential. Molecules migrate differentially in a buffered electrolyte that provides the required pH and conductivity necessary for the separation (6). Capillary Electrophoresis (CE) is a form of electrophoresis where the separation takes place within a fused silica capillary with on-line (and in most cases on-column) detection. The transformation from the conventional slab-gel format to columns was first investigated by Hjertén (7), miniaturized by Mikkers, Everaerts and Verheggen (8), and finally made practical in a capillary format by Jorgenson (9).

Capillary Electrophoresis is a rapidly developing analytical technique, with an exponential rise in the number of publications that has resulted in its rapid transfer from the research laboratory into routine industrial labs. The theoretical background was developed for electrophoresis by Kohlrausch over 100 years ago, and the instrumentation is largely adapted from chromatography. From High Performance Liquid Chromatography (HPLC), CE has borrowed and modified the detectors, and from Gas Chromatography (GC) it has taken the capillary columns and benefits from state of the art column coating and deactivation technology. This merger of techniques has, as a consequence, brought together scientists from diverse disciplines. The

problems originated in the bioanalytical and macromolecular labs; the separation required the knowledge of chromatographers, polymer and organic chemists; and finally the detection has involved the spectroscopists.

Mobility differences can be exploited in a variety of ways to obtain a separation, resulting in number of possible modes of operation (Fig. 1.1). Using the same basic instrumentation these modes differ only in the constituents of the buffer and the mechanisms of separation offering complementary and orthogonal information. In addition to the conventional Slab Gel Electrophoresis, the basic methods encompassed by Capillary Electrophoresis include Capillary Zone Electrophoresis (CZE), Micellar Electrokinetic Capillary Chromatography (MEKC), Isotachopheresis (ITP), Isoelectric focusing (IEF), and Gel Capillary Electrophoresis (GCE).

Utilizing these variations, CE is capable of separating ionic, ionizable and neutral compounds (both large and small). The major thrust behind the technique comes from its simple instrumentation, ease in method development, superior peak efficiencies (over 1 million theoretical plates), high resolution, low mass sensitivities (zeptomoles), relatively short analysis times, low solvent and analyte consumption (single cells have been analyzed) and low waste disposal. Preliminary predictions were that CE would replace HPLC and Slab Gel Electrophoresis. However, this is not realistic. CE remains limited in some respects, lagging behind in concentration sensitivities, selectivity, analysis of highly hydrophobic compounds and availability of commercial detectors. Capillary Electrophoresis, consequently, is emerging as a complementary technique working orthogonally with the other more established chromatographic methods.

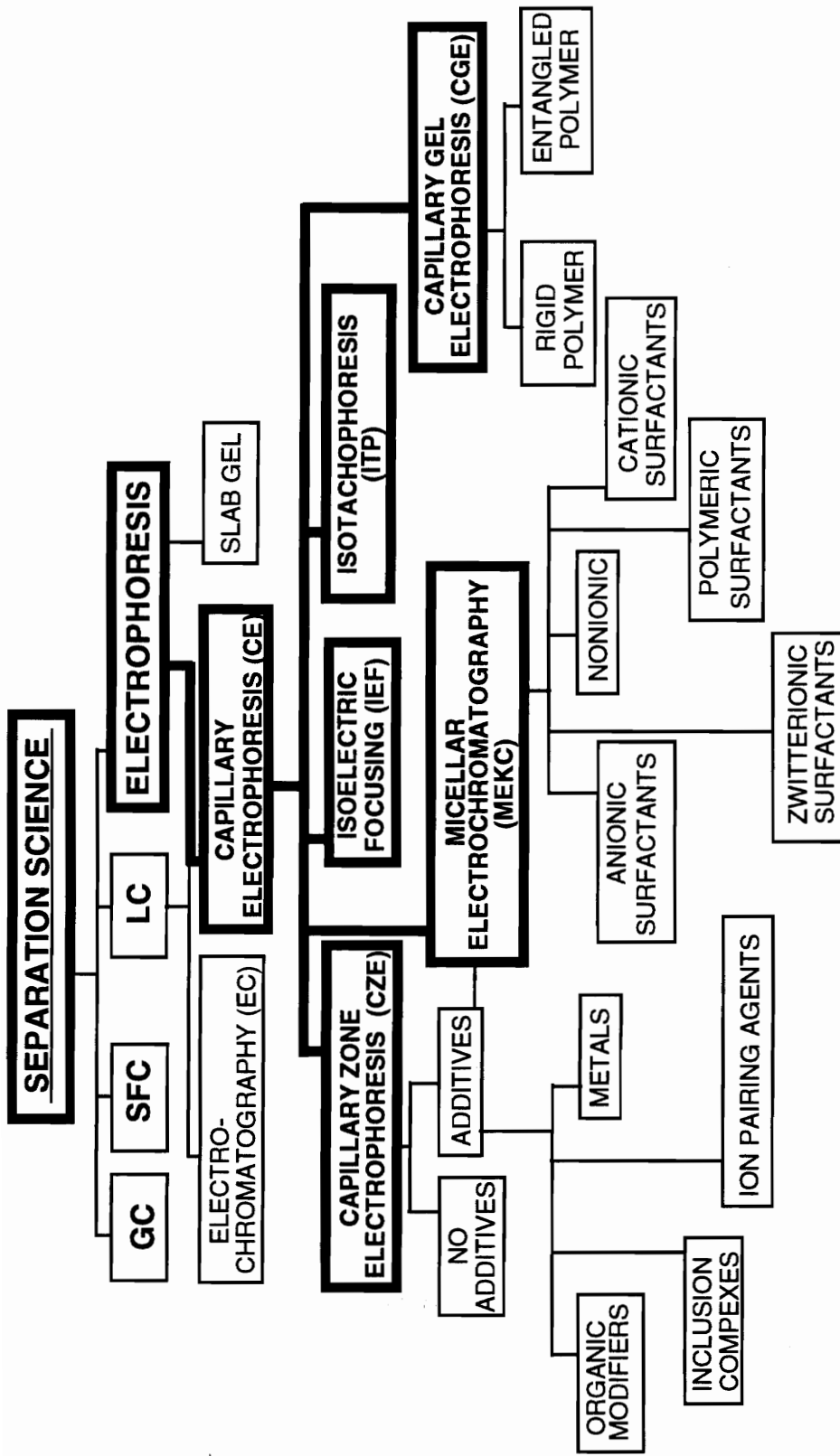


Figure 1.1

1.2. HISTORICAL

While the principles of ionic migrations in an electrolyte solution go back to 1897, to Kohlrausch ⁽¹⁰⁾, the term Electrophoresis was not used until 1909 when Michaelis described the migration of colloids in an electric field ⁽¹¹⁾. The use of electrophoresis to separate proteins was first reported in 1937 by the Swedish biochemist Arne Tiselius ⁽¹²⁾. In his "moving boundary electrophoresis" technique a protein solution is placed in a U-shaped tube and a protein-free buffer solution is carefully layered over both ends of the protein solution. Two electrodes immersed into either ends of the tube at a potential difference caused migration of the charged proteins. The proteins differentially migrated forming separate moving boundaries. Due to the cumbersome apparatus necessary to prevent convective mixing, the large sample added and the subsequent poor resolution of the less mobile components, the method, although one of the most powerful in the early years of protein chemistry, is not widely used today.

The moving boundary method led to Zone Electrophoresis, a technique in which the sample is constrained to move in a solid support such as filter paper, cellulose or a gel. This largely eliminated the convective mixing of the sample which was added only as a narrow band, permitting the various sample components to migrate as more discrete bands (better resolution). The gel, when used as the separation media, provides the physical support, mechanical stability and helps reduce diffusion and convection for the fluidic buffer system. Gels, such as polyacrylamide, may even participate in the separation

mechanism through molecular sieving. This technique requires several labor intensive and time consuming steps which include the gel preparation, sample application, staining and eventually quantification of the zones by densitometry. Subsequently, development efforts headed towards elimination of the stabilizing gels and performing the electrophoresis in free solution.

Free Solution Zone Electrophoresis, first described by Hjertén⁽⁷⁾ in 1967, was carried out without the use of gel support in a tube of 1-3 mm internal diameter quartz tubes. The quartz tubes were coated with methylcellulose to eliminate electroosmosis and rotated constantly around their longitudinal axis to counteract gravity caused convection. The detection was achieved by scanning the length of the tube with a U.V. detector. With Free Zone Capillary Electrophoresis Hjertén was able to separate proteins, nucleic acids and viruses.

The use of narrow-bore capillary tubes of sub millimeter diameter (0.4 mm) was further exploited by Everaerts and coworkers in the mid 1970s ⁽¹³⁾. Heat dissipation is enhanced when the ratio of the cross-section of the separation compartment to its surface area is high. This anticonvection effect with miniaturization allowed the use of larger currents, resulting in faster separations, better resolution and contributed to the development of capillary isotachopheresis (ITP) in narrow-bore Teflon tubes. The use of teflon instead of glass tubes has the advantage of minimizing the distortions of the isotachopheretic separations caused by electroosmosis. Unfortunately the scientific interest in this technique was low at that time and introduced ITP instrumentation was not a significant commercial success.

By 1974, Pretorius (14), dealing with chromatography, had recognized the potential of electroosmosis as a propulsive principle in elution chromatography, and derived equations for (at the time) unattainable miniature instrumentation. In the meantime, Virtanen reported zone electrophoresis in glass tubes of 200-500 μm bores (15), and detected the separated compounds by potentiometry. Several years later, and always the first credited for Capillary Electrophoresis, Mikkers, Everaerts and Verheggen, performed zone electrophoresis in narrow-bore Teflon tubes with an internal diameter of 200 μm (8). The separation of 16 small anions ranging from chloride to benzylaspartate, was achieved within 10 minutes employing conductometric detection. Although plate heights of less than 10 μm were attained, this detection mode was relatively insensitive and required sample overloading, resulting in poor resolution.

Despite these developments, however, two major problems still prevailed: namely the low sensitivity of the detection systems for narrow bore tubes and the problem of electroosmosis. It was not until Jorgenson and co-workers who helped to achieve the rapid development of this method in the last decade (16-18). Instead of suppressing electroosmosis by using electrically inert capillaries, advantage was taken of the unique plug flow profile of electroosmotic flow. This flow, which is generated in fused silica capillaries of very narrow internal diameters, allows movement of all the analytes through the capillary in one direction allowing their on-column detection and with much less dispersion than observed in HPLC. In their first publication, separation of danysl and fluorescamine derivatized amines with plate heights of only a few micrometers, was demonstrated using on-column fluorescence detection (16-17).

Adaptation of Gel Electrophoresis ⁽¹⁹⁾ and Isoelectric focusing ⁽²⁰⁾ to CE were followed by Terabe's efforts in 1984 ⁽²¹⁾ to confront one of the technique's major draw backs; namely that of the separation of neutral molecules. This was accomplished through the introduction of micelles to the system electrolyte. Surfactants added in concentrations above their critical micellar concentration (cmc), form labile micelles within which neutral compounds may partition. Based on their hydrophobicities and thus retention within the micellar hydrophobic interior, analytes will elute with different retention times.

The late eighties saw great advances in detection and instrumentation. Laser fluorescence in 1985, introduced by Gassman et al, improved detection limits. In 1987 Olivaries et al interfaced ⁽²²⁾ CZE to mass spectrometry and various forms of electrochemical detection were employed ⁽²³⁾. In 1988, the first commercial CE instrument was introduced while Khur and Yeung employed, for the first time, indirect fluorescence detection. Moreover, field manipulation were conducted in 1990 to externally control electroosmosis.

While the pace in instrumental development slowed down in the early 90's, concentration on improvement in injection techniques, capillary surface deactivation as well as methods development employing new electrophoretic buffer systems seems to dominate today.

1.3. BASIC HARDWARE COMPONENTS

There are six basic components to a Capillary Electrophoresis instrument: 1) column; 2) buffer reservoirs; 3) injection system; 4) power supply; 5) detector; and 6) data collection system. An example of a home made system

is depicted in (fig. 1.2). The capillary filled with buffer extends between the buffer reservoirs after being threaded through a detector. A power supply generates the necessary electric field through platinum electrodes dipped into each of the buffer reservoirs. Sample introduction is performed by a temporary placement of one end of the capillary into the sample reservoir. Data is collected through an integrator or computer where the detector response in the form of peaks is collected versus migration time. This output form is known as an Electropherogram. When partitioning between two phases is involved in the separation due to additives in the buffer the out-put becomes a Chromatogram.

It was not until 1988 that the first commercial CE system was introduced by Microphoretics. To date there are over 12 companies producing commercial systems with 1993 world wide sales estimated at \$ 40 million. The availability of commercial systems has greatly facilitated growth of the technique. In addition to the basic components found in home made systems, most commercial systems offer thermostating of the capillary chamber and the buffer / sample compartments. Furthermore, sample introduction automation as well as voltage, wavelength and mobile phase programming by microprocessors are possible. Table 1.1 lists some of these companies and their system capabilities.

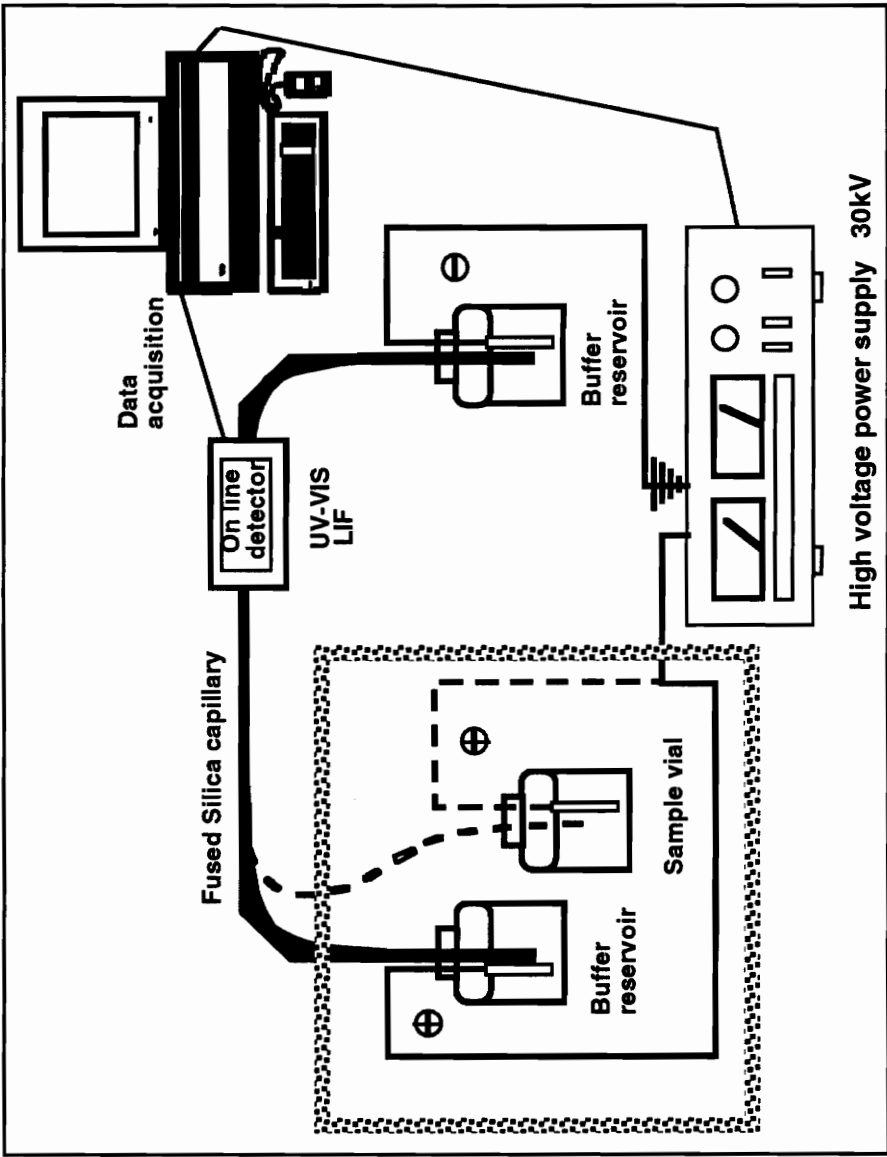


Figure 1.2 : Basic Capillary Electrophoresis Instrumentation

Table 1.1: Commercial Capillary Electrophoresis instrumentation. (24)

INSTRUMENT	MODEL	CAPILLARY FORMAT	DETECTOR METHOD	CAPILLARY HEATING	POLARITY REVERSAL
HEWLETT PACKARD	HP 3DCE	CARTRIDGE	Diode Array UV-VIS 190-600nm	FAC* (peltier)	Software
BECKMAN	PACE 5010 / 5510	CARTRIDGE	Filter/Diode Array 190-600nm LIF/MS Interface	Liquid (peltier)	Manual
APPLIED BIOSYSTEMS	270A-HT	FREE	UV 190-700nm	FAC	Software
THERMO-SEPARATIONS	SPECTRA - PHORESIS 2000	CARTRIDGE	Low Inertial Scanning 190-800 nm	FAC (peltier)	Software
BIORAD	BIOFOCUS 3000	CARTRIDGE	Fast scanning 190-800 nm	Liquid	Software
DIONEX	CES-1	FREE	UV 190-800 nm fluorescence	FAC	Manual
ISCO	3850	FREE	UV 190-365 nm	FAC	Manual
WATERS	QUANTA 4000E	FREE	UV filter	FAC (peltier)	Manual
ATI/JUNICAM	CRYSTAL/PRINCE	FREE	UV Filter / Scanning / Diode Array / Fluorescence / Radio - metric / MS interface	FAC (peltier)	Software

FAC*=Forced Air Convection

CHAPTER II

SEPARATION THEORY

2.1. THE ELECTRIC DOUBLE LAYER

Mobility of ions in solution under the influence of an electric field is governed by their charge to mass ratio. The size of the molecule is based on its molecular weight, the hydrodynamic volume and the degree of solvation. Separation in capillary electrophoresis relies on mobility differences and the ability to control them.

In a homogeneous electric field, a charged compound present in an electrolyte solution at infinite dilution, is accelerated by an electric force F_e :

$$F_e = z_i e_0 E \tag{2.1}$$

where z_i is charge of component i , e_0 the electron charge and E is the electric field strength. The force accelerates the sample in its respective direction in the potential gradient.

In a viscous hydrodynamic medium, as the ion accelerates, it is retarded by a drag force F_d :

$$F_d = k\eta v_i^0 \tag{2.2}$$

where, according to Stoke's law, k is a constant that can be substituted by $6\pi r$ for a spherical particle, η is the media viscosity and v_i^0 is the ionic velocity.

When the acceleration caused by the electric force F_e is counterbalanced by the drag force F_d , the charged species moves with a constant migration velocity given by:

$$v_i^0 = \frac{z_i e_0}{6\pi\eta r_i} E \quad (2.3)$$

The ionic velocity is proportional to the electric field strength, with the proportionality factor known as the Absolute Electrophoretic Mobility, μ_i^0 :

$$\mu_i^0 = \frac{v_i^0}{E} = \frac{z_i e_0}{6\pi\eta r_i} \quad (2.4)$$

For a given ion, μ_i^0 is a characteristic constant, dependent only on the viscosity (and temperature) of the media, and theoretically independent of voltage and column length.

Although this equation is useful to describe changes in mobility as a function of hydrodynamic radius and charge, it is limited in a number of respects. Stokes radius applies only to rigid spherical ions. Friction calculations for the more complex irregular shapes are not easily evaluated. Forces originating from the electrostatic interactions with other ions in the electrolyte solution are not taken into account. Additionally, the net charge of a weak electrolyte is smaller than it's theoretical charge $z_i e_0$ because of

incomplete dissociation (25). Therefore, it is more accurate to describe the mobility according to Hückel (26) as a function of the zeta potential ζ and the permittivity ϵ (dielectric constant) of the buffer;

$$\mu_{ep} = \frac{\zeta \cdot \epsilon}{6 \pi \eta} \quad (2.5)$$

The ζ potential, however, is in itself not an easily accessible quantity and consequently, of little use for mobility prediction. However its physical meaning allows qualitative evaluation of the influence of several parameters on ion mobility. It is a quantity that originated from the double layer theory (27-29), which describes the interface between the ion and the surrounding ionic atmosphere. Several theories are available, differing in their description of this interface structure (30). The Helmholtz model introduced in 1879, envisions the counter ions in the surrounding electrolyte to be tightly associated with the central ion. There is a linear decay in potential from the center just as in a capacitor. Goüy in 1910 and Chapman in 1913 however assumed that the counter ions were freely associated with the central ion with freedom of ion exchange and an exponential decay in potential. The Stern model on the other hand combines the two above theories, assuming that there is one layer tightly associated (the rigid layer) overlaid by a second layer of loose association (the diffuse layer). In the presence of an electric field , a shear force is exerted between the two layers as the central ion is attracted towards its oppositely charged electrode. The ζ -potential is the value of the ion potential at the shear plane.

As is apparent from equation (2.4) the larger the charge, and the smaller the hydrodynamic and solvation radius the faster the ion's mobility. Neutral molecules, intuitively should have no mobility. However, this was found not to be the case in capillary electrophoresis conducted in fused silica tubes. Neutral molecules as well as oppositely charged ions, generally, all travel in the same direction due to the presence of a unique phenomenon known as electroosmosis.

2.2. ELECTROOSMOSIS

Fused silica, the most frequently used material in capillary electrophoresis, behaves like a weak acid and changes its surface characteristics depending on the pH of the aqueous buffer inside the capillary. In an acidic medium ($\text{pH} < 2.5$), silica is protonated to form positive silanols SiOH_2^+ ; at $\text{pHs} \approx 2.5$, the silanols are neutral, SiOH ; and at $\text{pH} > 2.5$, the surface is negative SiO^- . As is the case with an ion in solution, counter ions tend to adsorb electrostatically to the silica surface to counteract the surface charge. The potential difference Ψ between the silica surface and the bulk electrolyte in the center of the capillary results in a double layer formation with a rigid layer of the adsorbed counter ions, superimposed by a diffuse layer extending into the bulk solution (fig. 2.1). The potential in the rigid layer ϕ , decreases linearly, and that of the diffuse layer ζ exponentially, towards the

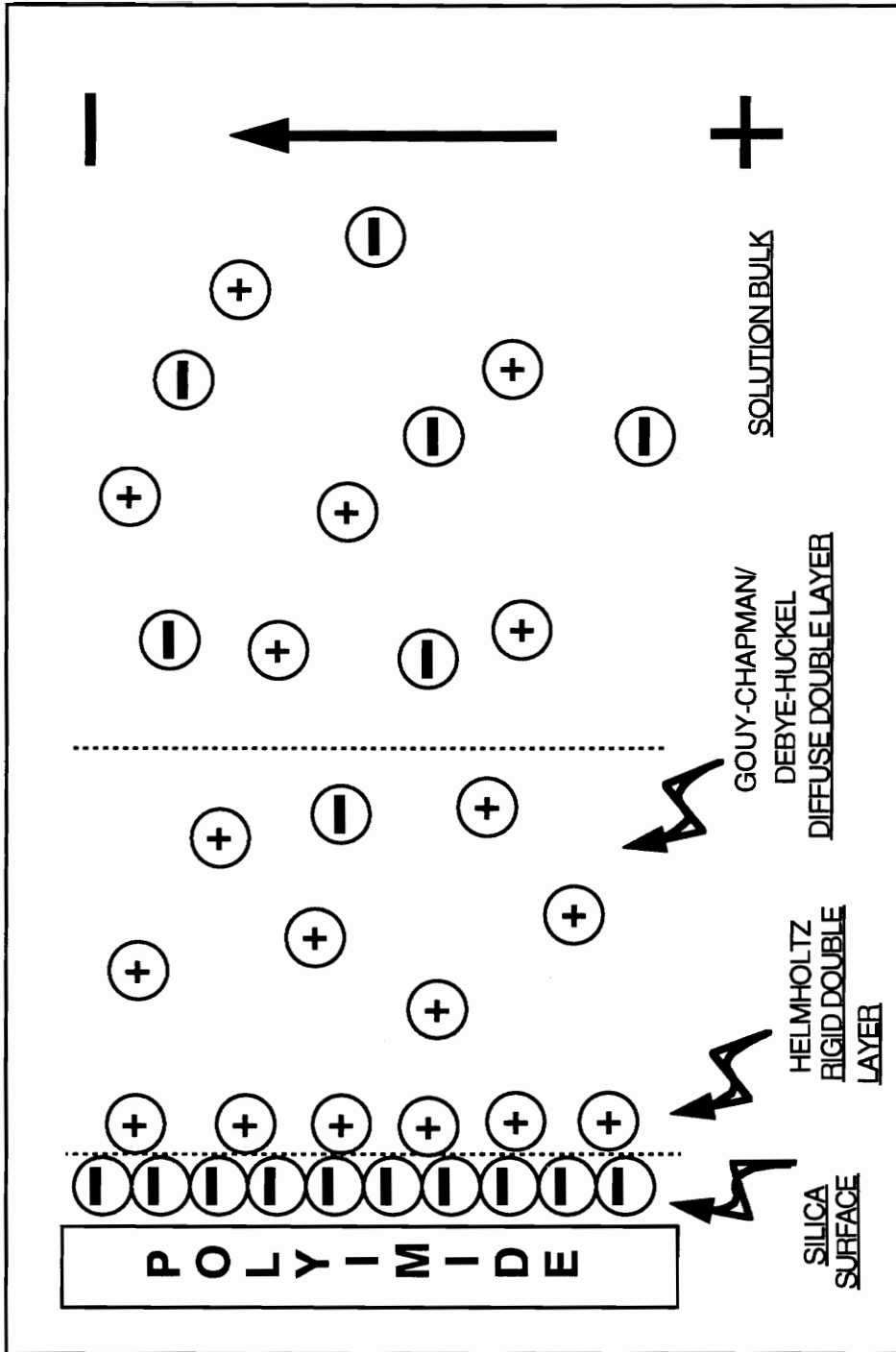


Figure 2.1: Stern Model of the Double Layer

center of the capillary. The thickness of the diffuse layer ranges from 0.5-100 nm depending on ionic strength, type of buffer, pH and surface characteristics of the capillary column. On application of a potential difference along the capillary axis of the capillary, the diffuse layer is swept towards the oppositely charged electrode. This flow drags along with it, the contents of the capillary. This relative motion of a liquid against a fixed charged surface is known as electroosmosis. Also known as electroendoosmosis, this is a basic phenomenon that occurs in all electrophoretic separations in the presence of an applied potential.

Rice and Whitehead ⁽³¹⁾ described electroosmotic flow in capillaries with circular cross section, addressing the effects of tube diameter on flow profile:

$$v_{eo}(r) = \frac{\epsilon \zeta E}{4 \pi \eta} * \left[\frac{1 - I_0[\kappa_d a]}{I_0[\kappa_d r]} \right] \quad (2.6)$$

κ_d is the reciprocal of the thickness of the double layer, while a is the distance from the center of the capillary, r is the radius of the capillary and I_0 is a zero order Bessel function of the first kind. The $6 \pi \eta$ factor of equation (2.3) is exchanged by $4 \pi \eta$ in the above equation reflecting the transition from curved to flat geometry. The ionic surface, in this case that of the fused silica capillary, is large relative to the thickness of its double layer. For the typically small double layer thickness in capillary electrophoresis, Pretorius in 1974 deduced the following equation to describe electroosmotic velocity ⁽¹⁴⁾;

$$v_{eo} = \frac{\zeta \cdot \epsilon}{4\pi\eta} E \quad (2.7)$$

Where,

$$u_{eo} = \frac{\zeta \cdot \epsilon}{4\pi\eta} \quad (2.8)$$

2.2.1. PLUG PROFILE

Electroosmosis has a plug like profile relative to the parabolic, pressure driven, flow profile found in both HPLC and GC (fig 2.2). Equation (2.7) reveals that there is no radial dependence of the velocity or flow, implying that no matter where an ion is in solution from the surface to the center, it should experience the same electroosmotic flow. This theoretically results in a flat flow profile of all constituents in the electrolyte. It is this flat plug profile that results in the superior efficiencies for which this technique is famous. Nevertheless, capillaries with large diameters ($\geq 200 - 300 \mu\text{m}$) start to exhibit parabolic flow, while capillaries with too small a diameter disrupt the existence of the double layer, a condition known as the double layer overlap. The capillary internal diameter has to be at least 10 times the size of the double layer (31).

2.2.2. MEASURING ELECTROOSMOSIS

Electroosmosis can be measure in a number of ways (32): a) Addition of a UV-active marker to one electrode vessel and monitoring the absorbance at the other electrode ; b) Direct observation of volume or level increase in the destination vessel ; c) weighing the mass of buffer transferred ; d) monitoring

A) Pressure-driven system (GC, LC)



B) Electrically-driven system (CZE)

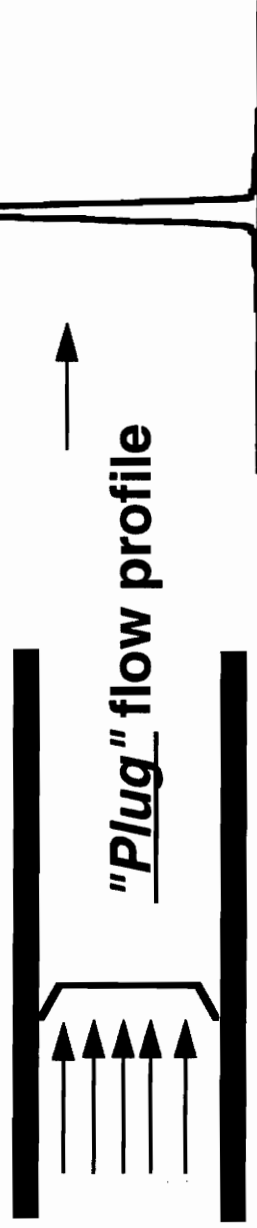


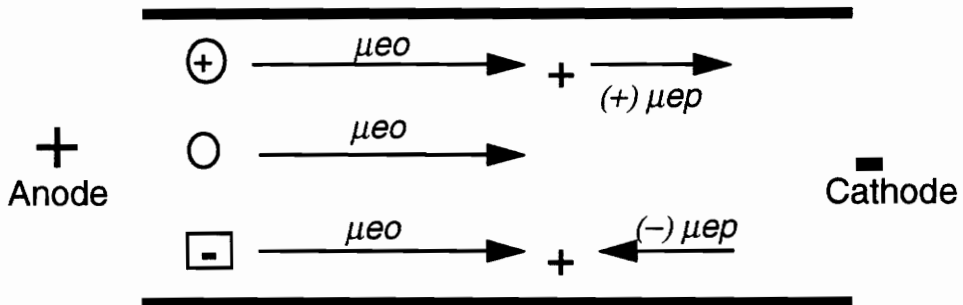
Figure 2.2: Flow profiles: HPLC vs CE

electric current while a buffer with different conductivity is drawn into the capillary by electroosmotic flow ; and e) monitoring the migration time of a neutral marker. The last method is the one in most common use and examples of neutral markers include mesityl oxide, methanol, acetone, and DMSO.

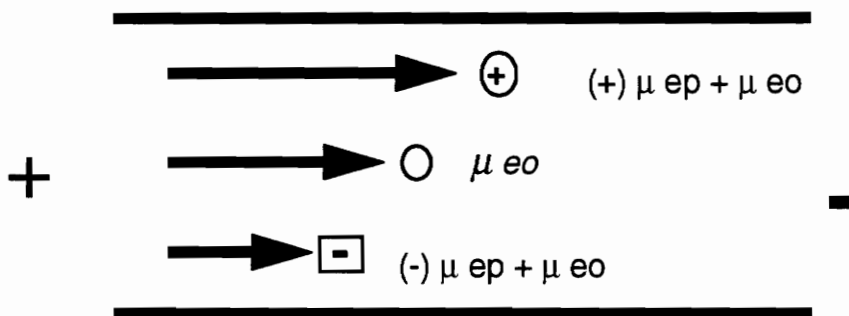
2.3. SEPARATION IN CAPILLARY ZONE ELECTROPHORESIS

In the absence of electroosmotic flow and in the presence of an electric field, anions would migrate towards the anode, neutral molecules would not migrate and cations would head towards the cathode. However, when the surface of the capillary generates electroosmotic flow, (usually stronger than the inherent electrophoretic mobility of the anions) all analytes migrate to the anode. Cations move the fastest, neutral molecules migrate with the electroosmotic flow and anions move the slowest. Thus CZE can separate both cations and anions in a single run, with all neutral molecules lumped together in a single peak (fig. 2.3). To provide separation of the neutrals, additives such as micelles would have to be included in the buffer to affect some sort of partitioning. This branch of CE is better known as Micellar Electokinetic Capillary Chromatography (MEKC) (21).

A) Schematic representation of migration rates of anions, neutral and cations



B) Vector sum of electroosmotic velocity and electrophoretic mobility



C) Typical electropherogram

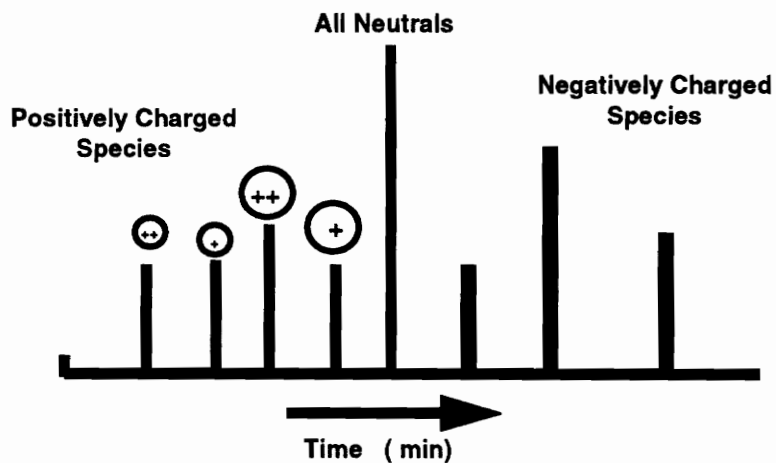


Figure 2.3 : Separation in Capillary Zone Electrophoresis

2.4. BASIC PRINCIPLES

2.4.1. MIGRATION TIMES

The time t_{R_i} required for a solute to migrate to the point of detection is called its "migration time", and can be calculated from the relationships between its mobility, the applied voltage and column length.

$$t_{R_i} = \frac{L_d}{v_i} = \frac{L_d}{\mu_i E} = \frac{L_d L_v}{\mu_i V} \quad (2.9)$$

where L_v is the total column length; L_d is the column length to the detector window; V is the applied voltage; v_i is the solute velocity; and μ_i is the apparent solute mobility in the presence of electroosmotic flow. Short columns and high voltage reduce analysis times.

Through the independent measurement of electroosmotic flow μ_{eo} , using a neutral marker and its elution at t_0 ;

$$\mu_{eo} = \frac{L_v \cdot L_D}{t_0 \cdot V} \quad (2.10)$$

the solute's effective mobility can be calculated;

$$\mu_{ep_i} = \mu_i - \mu_{eo} \quad (2.11)$$

2.4.2. EFFICIENCY

The high efficiencies in capillary electrophoresis relative to HPLC is a consequence of both the flat radial profile across the capillary (as opposed to the radial velocity gradient and resultant parabolic flow) and the absence of stationary phase which leads to resistance to mass transfer and eddy diffusion.

Jorgenson and Lucas (33,34) using basic principles and the assumption that molecular diffusion is the only source of band broadening, derived the equations for efficiency of electrophoretic systems.

Diffusion of ions in solution leads to broadening can be expressed by Einstein's equation:

$$\sigma_L^2 = 2D_m t = \frac{2D_m L_d L_v}{\mu V} \quad (2.12)$$

where D_m is the diffusion coefficient of the solute in solution. The height equivalent of the theoretical plates is given by:

$$HETP = \frac{\sigma_L^2}{L_d} = \frac{2D_m L_d L_v}{L_d \mu V} = \frac{2D_m L_v}{\mu V} \quad (2.13)$$

and,

$$N = \frac{L_d}{HETP} = \frac{\mu V L_d}{2D_m L_v} \quad (2.14)$$

when $L_d \approx L_v$ (34,35)

$$N = \frac{\mu V}{2D_m} \quad (2.15)$$

From the above equation (2.15) it follows that high voltages give the greatest number of theoretical plates, by limiting the residence time in the column, and thereby limiting the effect of diffusion. This is valid up to the limit where heat dissipation becomes inadequate and deviations from Ohm's law results. Efficiency will also be highest when the molecules have fast mobilities or very low diffusion coefficients. In this respect capillary electrophoresis is capable of high efficiencies for both large and small molecules. Worth noting also, N in CE, is theoretically independent of column length (when $L_d \approx L_v$) and migration time. However, efficiencies were found, in practice (36), to decrease dramatically in capillaries shorter than 100 cm. This loss has been attributed to the lower heat dissipation of the shorter columns.

Knox (37) discussed the ultimate possible performance of capillary electrophoresis and was able to show that up to a million theoretical plates per meter are in principle achievable. However, due to the non-diffusional band broadening, such as joule heating, capillary adsorption, sample introduction effects, and detection effects, lower efficiencies will generally be observed.

2.4.3. RESOLUTION

Giddings ⁽⁸⁾ derived the equation for resolution from the same basic equations used for HPLC to calculate the resolution between two solutes:

$$R_s = \frac{(\mu_1 - \mu_2)}{\bar{\mu}} * \frac{\sqrt{N}}{4} \quad (2.16)$$

where μ_1 and μ_2 are the electrophoretic mobilities of two different but closely eluting ions and $\bar{\mu}$ is the mean of the mobilities of the two ions. Substituting N of equation (2.15) results in:

$$R = 0.177 \cdot (\mu_1 - \mu_2) \cdot \sqrt{\frac{V}{D_m \cdot (\bar{\mu} + \mu_{eo})}} \quad (2.17)$$

This equation suggests that increasing the voltage improves the resolution, but only as the square root. To double the resolution, the voltage has to be quadrupled. Since the voltage is usually in the 10-30 kV range, Joule heating limitations are quickly approached ⁽³⁹⁾.

For more effective resolution results, adjustment in mobility differences would induce the same effect as selectivity (α) would in HPLC. The control of selectivity is first achieved by first selecting the proper CE mode followed by proper selection of buffer, concentration, pH and additives.

Furthermore, if μ_{e0} can be adjusted to be equal and opposite to $\bar{\mu}$, infinite resolution is theoretically possible. The same, unfortunately, would also be true for migration time.

CHAPTER III

FACTORS INFLUENCING PERFORMANCE

3.1. FUNDAMENTAL DISPERSIVE EFFECTS

Column efficiency as described by equation (2.12) was derived with the assumption that the only contribution to band broadening is molecular diffusion. In actuality, the deviation from theory can best be explained by the total variance of the system, which is given by the sum of the contributing variances:

$$\sigma_T^2 = \sigma_{DIF}^2 + \sigma_{INJ}^2 + \sigma_{TEMP}^2 + \sigma_{ADS}^2 + \sigma_{DET}^2 + \sigma_{ELEC.DISP}^2 + \dots \quad (3.1)$$

were the subscripts refer to molecular diffusion, injection, temperature gradients, adsorption, detection and electrodispersion respectively. Should any of these factors approach diffusion term, theoretical limits cannot be obtained and equation (2.14) becomes invalid.

3.1.1. JOULE HEATING AND TEMPERATURE GRADIENTS

The heat generated by the passage of an electrical current, known as the Joule effect, has traditionally limited electrophoretic techniques. Ion mobilities and thus current are a function of the media's viscosity. As the system's temperature increases the viscosity decreases, further increasing

current flow and heat generated. Should this heat not be dissipated, nonuniform temperature gradients and local viscosity variances result in subsequent zone broadening. If the temperature rises to the boiling point, bubble formation inhibits further passage of current. While the theoretical equations of efficiency and resolution advocate the use of high voltages, Joule heating ultimately limits this parameter.

One of the reasons behind the success of capillary electrophoresis, relative to conventional slab gel electrophoresis, lies in the former's capability to employ higher voltages. Capillary columns have a large surface area to volume ratio, which allows relatively more efficient heat dissipation. Nevertheless, there is still an increase in the column temperature and temperature gradients. The variance contribution from Joule heating has been extensively studied by Hjerten (7), Foret et al (40), Grushka et al (42) and Knox (37). The temperature profile in the liquid inside the capillary, is parabolic with high temperatures at the center and dropping logarithmically to the capillary wall and the surrounding medium (fig 3.1). Heat dissipates through the silica wall mainly by conduction and is transferred through the surrounding air by convection and radiation. The central parabolic temperature profile results in a parabolic variation of the migration velocity and consequently produces a significant reduction in column efficiency. Such adverse effects are amplified with larger capillary diameters, highly conductive buffers and high buffer concentrations.

Temperature differences depend on the inner radius, the wall thickness, the polyimide coating thickness and the heat transfer coefficient to the surrounding. This can be expressed through the following equation (37,34):

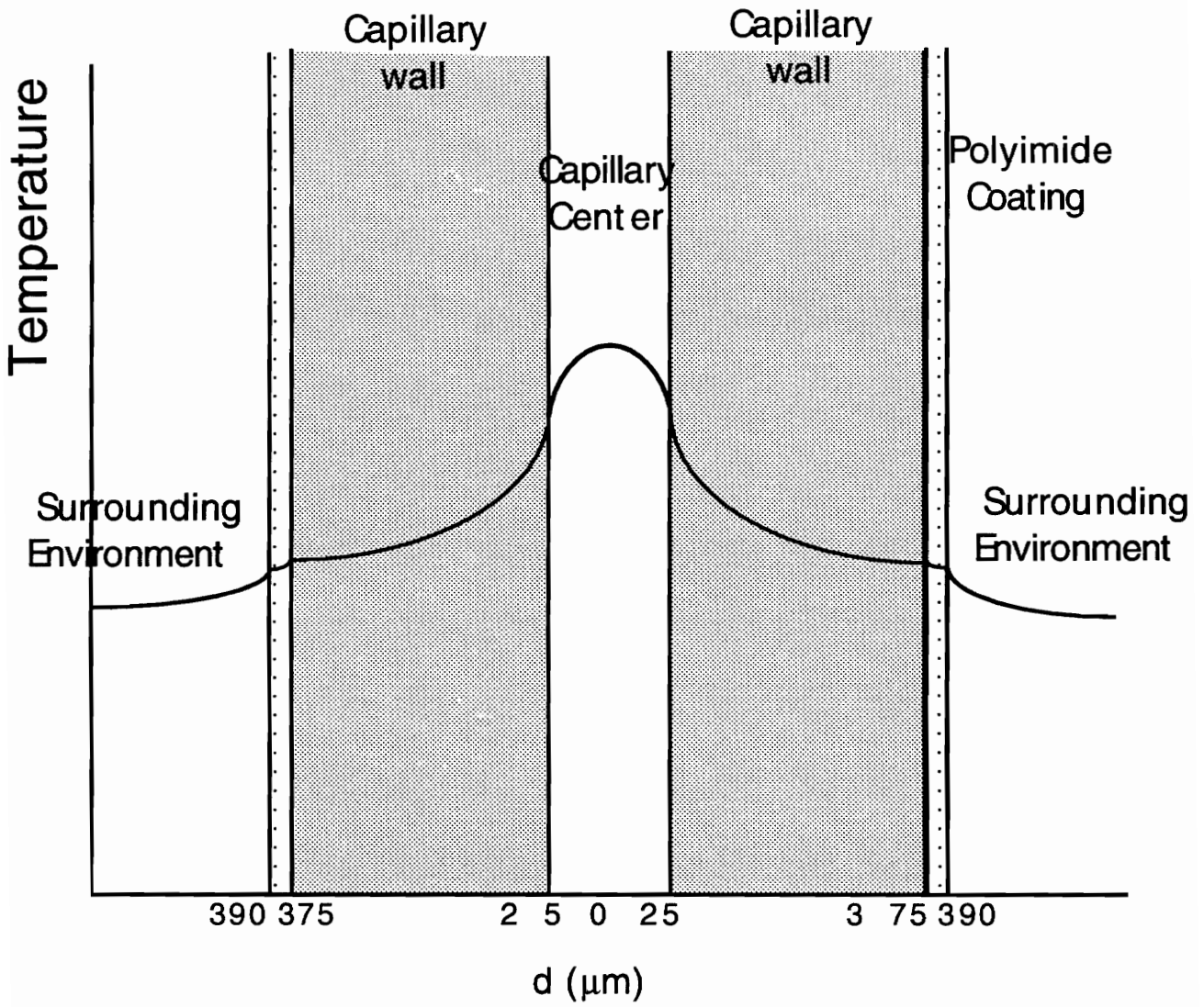


Figure 3.1: Schematic of temperature gradient from capillary center to the surrounding.

$$\Delta T_T = \frac{Qr_1^2}{2} \left[\frac{1}{\kappa_1} \ln\left(\frac{r_2}{r_1}\right) + \frac{1}{\kappa_2} \ln\left(\frac{r_3}{r_2}\right) + \frac{1}{r_3} \left(\frac{1}{h}\right) \right] \quad (3.2)$$

where Q is the power density; κ_1 is the thermal conductivity of the silica (1.5×10^{-2} W/cm/K); κ_2 of the polyimide (1.6×10^{-3} W/cm/K); r_1 is the inner capillary radius; r_2 is the outer capillary radius; r_3 is the outer radius of the polyimide; and h is the thermal transfer rate from the capillary. Equation 3.2 implies that it is advantageous to use narrow inner diameters as the thermal gradient is proportional to the square of the inner radius. Unfortunately, narrow capillaries cause severe problems with sample loading capacity and optical detection. A larger outer diameters is also recommended. Although the polyimide coating is only a few microns thick, its thermal conductivity is lower than that of fused silica, limiting efficient heat transfer.

Although mobility will increase approximately 2% per degree centigrade, this is not a problem if temperature can be controlled. In addition to minimizing the effect of joule heating, temperature can be also used as a parameter to optimize a separation. Poor temperature control results in irreproducible migration times and peak areas. Area irreproducibility is more severe relative to migration time irreproducibility as the latter reflects the average conditions over a relatively long time, while the area is determined by the actual conditions during short periods such as passage through the detector window or during injection.

Commercial CE systems differ in their form of capillary temperature control. Most thermostating is achieved through liquid or forced air convection. Some instruments are also capable of subambient cooling as well as heating.

3.1.2. INJECTION PLUG LENGTH

The contribution of the injected plug length to system dispersion can be expressed as (43):

$$\sigma^2 = \frac{l_{inj}^2}{12} \quad (3.3)$$

where l_{inj} is the injection plug length. Very small sample volumes are necessary due to the small capillary diameters. Ideally the limit of injection plug length should be less than 1-2 % of the total column length. For a 70 cm column, a 1 % length corresponds to a 7 mm plug length (14 nl for a 50 μm id column) (44). Unfortunately, while instruments are capable of such injections, detection limits demand larger injections. A compromise has to be reached.

3.1.3. ELECTRODISPERSION

When the conductivity of a solute zone is considerably different from that of the background buffer, three effects can take place: 1) skewed peak shapes; 2) solute zone focusing or defocusing; and 3) a temporary state of isotachopheresis may occur. These zone deformation effects are due to electromigration dispersion. (8).

For reasons of electroneutrality, solute ions tend to displace the buffer ions in the solute zone. Differences in mobility within the zone result in localized changes in conductivity and consequently resistance. Since the current has to be constant throughout the capillary, it follows from Ohm's law that local differences in field strength would result. Figure 3.2 illustrates how different solute conductivity results in differing peak distortions. When the solute has a higher mobility than the background electrolyte ($\mu_A > \mu_E$), the solute zone has higher conductivity, lower resistance and consequently is in a lower field. The ions that diffuse forward out of the zone, are met by more resistance and a higher field and are therefore slowed down and overtaken by the solute zone. Those ions that diffuse backwards are similarly slowed down, but in their case they never reach the zone and tail behind. The result is tailing peaks. The opposite (fronting peaks) results with solutes of much lower conductivity. When both mobilities are equal a symmetrical peak results. Electrophoretic dispersion effects can be reduced by either matching the mobilities or reducing the concentration of the solute in the first case (tailing peaks), or that of the buffer in the second case (fronting). In the interest of optimizing resolution, the latter change is some times not beneficial. Electrodispersion problems are most apparent with indirect detection methods, due to the difficulty of finding a suitably matching background electrolyte.

3.1.4. SOLUTE WALL EFFECTS

CZE as a technique has gained a reputation for its ability to separate both large and small molecules with very high efficiencies. Macromolecules such as proteins for example, with their low diffusion coefficients are,

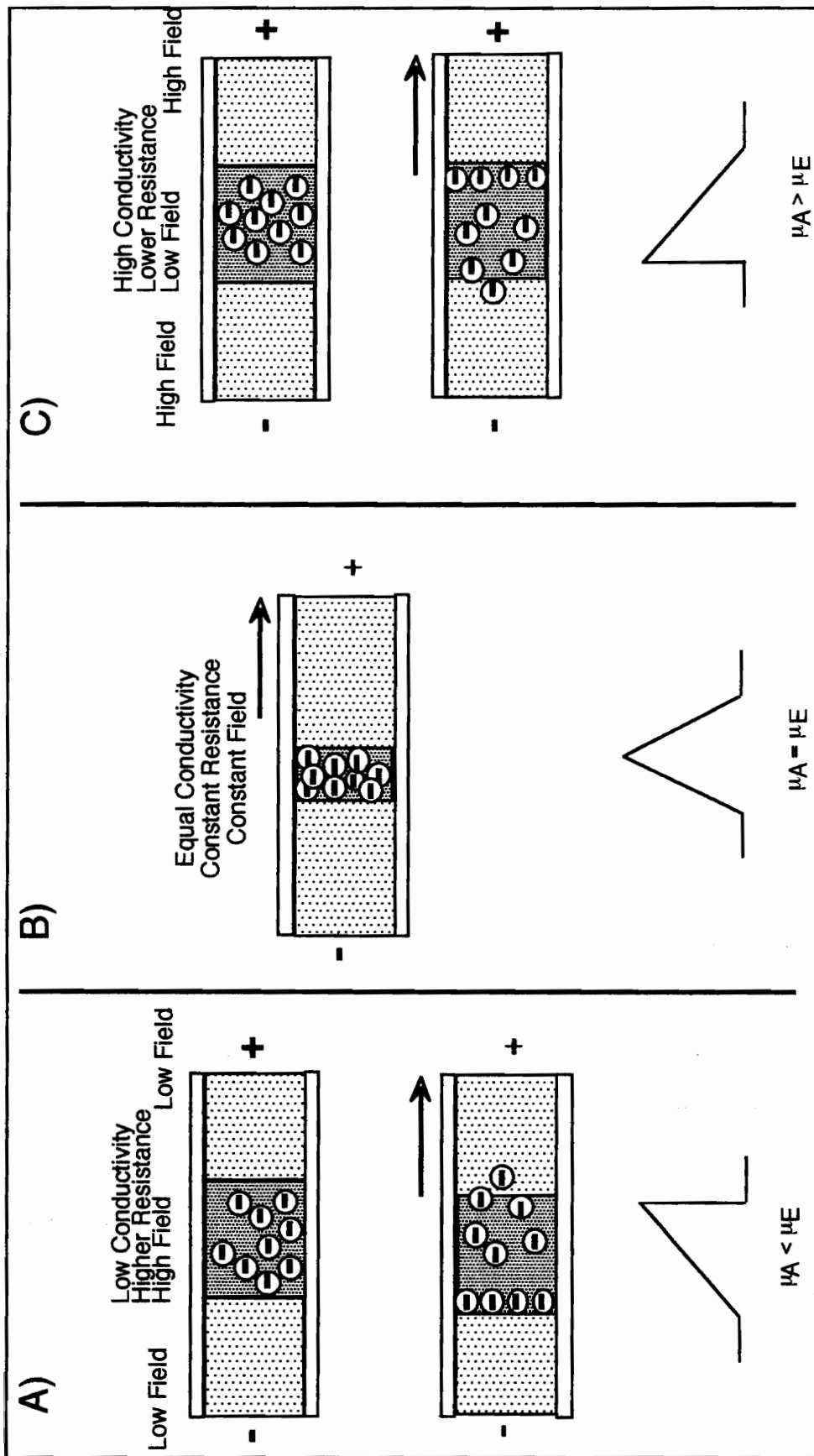


Figure 3.2: Electrophoretic Dispersion

theoretically, expected to exhibit efficiencies of one million theoretical plates⁽³⁷⁾. However, it has been found that interactions with the capillary surface causes greatly reduced efficiencies and often result in peak tailing and even total retention in the capillary. Proteins tend to exhibit variability in charge, hydrophobicity, size and conformation. Their separation without such surface interaction, would necessitate the use of extreme pHs ⁽⁴⁵⁾ or surface modification ⁽⁴⁶⁾ . While the former practice has been effective in reducing some surface ionic interactions, unfortunately it often results in protein denaturation. On the other hand silica surface modification, while diminishing solute adsorption, results in a reduction of the electroosmotic flow. Modification can be either permanent or dynamic (reversible).

Permanently capillary surface modifications commonly involve silylation followed by deactivation with a suitable functional group. Polyacrylamide ⁽⁴⁷⁾, polyethylene glycol ⁽⁴⁸⁾, proteins ⁽⁴⁹⁾, Methylcellulose ⁽⁵⁰⁾ and Polyethyleneimine ⁽⁵¹⁾ are some of the common deactivating agents. The choice of modification is dependent on the coating's pH stability, hydrophobicity and the effect on μ_{EO} . Deactivation with cationic groups reverses the μ_{EO} direction and with amphoteric groups ⁽⁵²⁾ yields tunable control of μ_{EO} depending on the pH of the buffering solution.

Dynamically coated capillaries involve additives in the buffer that will temporarily alter the charge and hydrophobicity of the surface. This technique is easier to implement and easier to optimize and it allows for easy surface regeneration. Examples include quaternary amines, surfactants, polyvinyl alcohol, alkyl cellulose, and organic solvents such as methanol. Such

additives, however, affect the analytes as well as the capillary surface and they may require some equilibration time.

Much research now involves investigation of polymeric tubing material as a replacement for fused silica. Examples to date include modified polypropylene hollow fibers. Materials that would be inexpensive, prevent protein adsorption, be flexible, UV transparent, and obtainable with homogeneous inner diameters are now under investigation (53).

3.1.5. COMPARATIVE EVALUATION OF THE DIFFERENT DISPERSIVE EFFECTS

As is obvious from above, separation efficiency is affected by a combination of the above dispersive forces. Liu and co workers (54) have evaluated the various dispersive forces in CZE as well as in CGE for 10-100 μm capillaries. Using a Fluorescence detector dispersive forces were not prominent due to their use of low sample concentrations. In addition to diffusional dispersion they found adsorption effects to be of significance especially at high field strength where the sorption-desorption kinetics become important, manifesting themselves as tailing peaks. Thermal effects were found to be of little significance in small bore capillaries (<50 μm), but are more pronounced in larger bore capillaries (>75 μm). Diffusion and thermal contributions are minimized in gel filled capillaries with diameters less than 50 μm . An equation is developed which takes into account the contributions of injection, axial diffusion, adsorption and joule heating to plate height in capillary electrophoresis;

$$H = \frac{I^2}{12L_d} + \frac{2D}{(\mu_i \pm \mu_{eo})E} + \frac{c_f(1-c_f)^2(\mu_i \pm \mu_{eo})rEn}{Z\alpha} + \frac{\delta_i^2 \kappa^2 \mu_i^2}{K^2 D} \cdot \left[K_1 \frac{E^5 r^6}{(\mu_i \pm \mu_{eo})} + K_2 \frac{E^6 r^8}{LD} \right] \quad (3.5)$$

where,

I	Initial width of the sample plug (cm)
L _d	Effective capillary length (cm)
c _f	Fractional concentration of a free solute
r	Inner radius of the capillary (cm)
Z	Number of molecules striking a unit surface area/sec
n	Number of molecules/unit volume inside the tube (cm ⁻³)
α	Fraction of molecules which adhere on collision
δ _i	Temperature coefficient of the mobility of component i (K ⁻¹)
κ	Specific conductance of the background electrolyte (S.Cm ⁻¹)
K	Thermal conductance of the background electrolyte (W.cm ⁻¹ .K ⁻¹)
K ₁	6.5x10 ⁻⁴
K ₂	4.34x10 ⁻⁵
E	Electric Field Strength

Equation (3.5) is analogous to the Van Deemter equation in chromatography. From the equation injection is not influenced by the applied potential whereas dispersion due to diffusion effects decreases while adsorption and joule heating contributions increase with increasing field strength.

3.2. CHOICE OF OPERATIONAL PARAMETERS

Operational parameters such as field strength and capillary dimensions should also be chosen carefully to minimize further contributions to band broadening.

3.2.1 VOLTAGE EFFECTS

Fast analysis is an advantage in CE. Both the electrophoretic mobility and electroosmotic flow are directly proportional to the electric field. Intuitively, higher field strength will bring about faster migration times (equations 2.3 and 2.7). Jorgenson ^(34,35) by assuming that axial diffusion was the exclusive dispersion factor in CE (equation 2.12), obtained a linear relationship between efficiency and the applied voltage. The higher the applied voltage the higher the efficiency (equation 2.14), and the better the resolution (equation 2.17). This relationship however, fails at high voltages and in addition to the deterioration in efficiency, Ohms law and the linearity of v_{eo} with E , equation (2.7) no longer applies. These deviations from linearity are caused by increased heat generation at the higher potential differences.

However when v_{eo} is plotted versus current, the relationship still holds. According to theory ⁽⁵⁵⁾ voltage can be exchanged by i / κ and equation (2.7) becomes,

$$v_{eo} = \frac{\epsilon \zeta i}{4 \pi \kappa \eta} \tag{3.6}$$

Thus ε and ζ vary only slightly with temperature and their variation is such that their product is independent of temperature. The specific conductance κ and η , the viscosity, exhibit large dependencies on temperature, however, their product, too, cancels out (Walden Rule) ⁽⁵⁶⁾. As such, the electroosmotic velocity v_{eo} depends only on the current density i , with the linearity unaffected by the temperature. Operation in the constant current mode is, therefore, preferable to the constant voltage mode in CE.

3.2.2. CAPILLARY DIMENSIONS

The heart of every capillary electrophoresis system is the capillary column. The material used for the column should be UV transparent, have high thermal conductivity to allow efficient heat dissipation, be ionic enough to allow electroosmotic flow, prevent compound adsorption to the surface and be malleable but not fragile. Several capillary materials have been investigated. Initial attempts used Pyrex borosilicate glass and Teflon, but currently the most frequently used material is fused silica.

Fused silica capillaries, available from a variety of manufacturers, are usually, 10-100 μm in internal diameter, 190-375 μm in outer diameter, 10-100 cm in length and have an approximate 12 μm external coating of polyimide for improved flexibility. For on-column detection 1-2 mm of the polyimide has to be removed to expose the transparent fused silica and allow detection (fig 3.3). This is usually achieved through burning, the use of concentrated acid or mechanical etching. The latter two methods are more frequently used with chemically derivatized or gel filled capillaries. Other less popular forms of fused

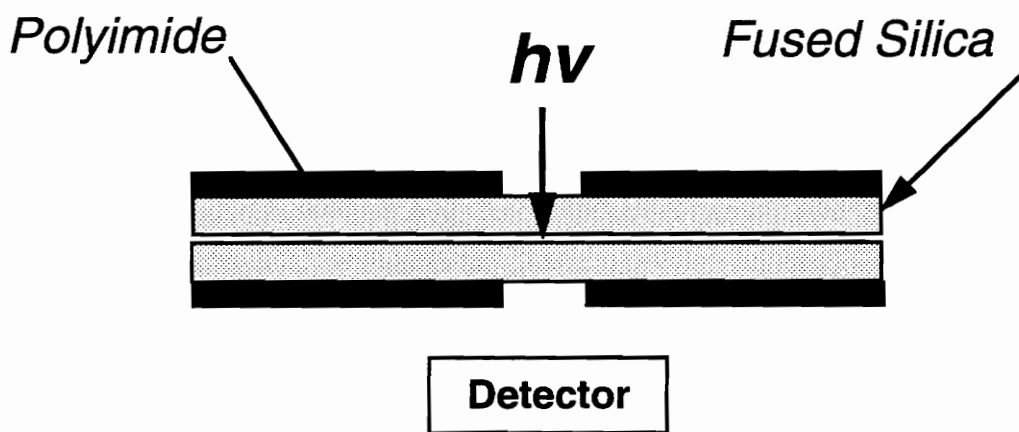


Figure 3.3 : On-Column Detection; Polyimide can be removed by burning, acid etching or mechanical scraping.

silica capillary columns available use UV transparent flexible polymeric coatings instead of polyimide or are rectangular in shape instead of circular.

The choice of capillary material and dimensions is very important as it has an effect on several factors such as applied voltage, migration time, resolution, efficiency, detection sensitivity, heat dissipation and sample adsorption.

As is obvious from equation (2.14), while an increase in the length beyond the detector increases resistance and allows for use of higher voltages, a decrease in efficiency results. Additional capillary length contributions are shown when the voltage is substituted by EL_v and equation (2.17) becomes

$$R = 0.177 \cdot (\mu_1 - \mu_2) \cdot \sqrt{\frac{EL_d}{D_m \cdot (\bar{\mu} + \mu_{eo})}} \quad (3.7)$$

showing resolution to be directly proportional to the $\sqrt{L_d}$. A detailed investigation of the effect of capillary length on efficiency and resolution is provided by Jorgenson (36). In this work capillary length longer than 100 cm contributed more to migration times than to efficiency, while capillaries shorter than 100 cm showed dramatic decreases in efficiency. The latter effect was attributed to the increase in joule heating as a result of the decrease in resistance.

Decreased inner diameter results in better heat dissipation due to the larger surface area to volume ratio, currents are reduced due to the higher resistance ($I \propto r^2$) (57), making it easier to control the temperature, and use higher voltages. Adsorption effects, too, are decreased. However, there is loss

in a sensitivity due to the shorter UV path length, lower possible mass loading, less ease in detector alignment and limitations in injection mode possibilities.

3.3. THE ELECTROLYTE SYSTEM

Selectivity in CE, as in most separation techniques, is the most critical factor for optimization. In chromatography (especially HPLC) variations in type and composition of both the mobile phase as well as the stationary phase together contribute to selectivity. In CE, however, method optimization in terms of selectivity is limited to optimization in the mobile phase; the electrolyte system.

The electrolyte system, or buffer, in capillary electrophoresis, assuming both the role of the mobile phase and the stationary phase in chromatography plays a central role, influencing solute mobility, peak shape, efficiency; selectivity and ultimately resolution. The buffer maintains the required pH, which determines the silica surface charge and is the most important selectivity factor for the electrophoretic separation of ampholytes. Its ionic strength and concentration not only determine the system's degree of Joule heating, but also has a marked effect on the double layer thickness, the viscosity and consequently the electrophoretic mobility and electroosmotic flow. In addition the buffer's composition can improve efficiency and selectivity in more ways than one, facilitating the separation.

3.3.1 THE BUFFER IONIC STRENGTH

Electroosmotic mobilities, or equivalent linear velocities and migration times, have been related to buffer concentration (58) and ionic strength (59). While ionic strength was proven to be a more meaningful quantity than concentration (58), studies confirm that, at a fixed pH, mobility decreases with increasing concentration, but confusion exists about the mathematical model that should be used to describe this behavior.

Cohen et al (57) described the interrelationships of buffer concentration, current, viscosity, radius and zeta potential:

$$c = \frac{I\eta}{\pi r^2 \epsilon E \zeta} \quad (3.8)$$

and proved it experimentally. They found that when working at higher voltages, an increase in the ionic strength results in temperature and viscosity increases which in turn influences the mobility, increasing the migration times dramatically. The studies indicate that, at a fixed pH, mobility decreases with the increase in ionic strength. The exact relationship, whether this decrease is linear or proportional to the square root, is a point of controversy.

Moreover, the negative charges on the capillary surface are better balanced by counterions with an increase in ionic strength, thus leading to a general decrease of the surface charge and, consequently, of the zeta potential. An increase in ionic strength also, in some cases, results in an improvement in peak shape and efficiency due to suppression of the electrophoretic dispersion.

3.3.2. THE pH

The buffer's pH in CZE, is the most important separation parameter for changing the selectivity of the system. Separations in electrophoresis are based on the differences in electrophoretic mobilities of the analytes. These, in turn, depend on the size and net charge of the analyte. While the size is dependent on the molecular weight and the hydrodynamic radius (the later being dependent on the solution polarity and ionic strength), the net charge is dependent on the buffer's pH and the extent of ionization of the analyte pKa.

The net charge on a solute at any pH can be calculated using the Henderson-Hasselbalch equation for acids:

$$pH = pK_a + \log \frac{[A^-]}{[HA]} \quad (3.9)$$

and for bases:

$$pH = pK_a - \log \frac{[A^-]}{[HA]} \quad (3.10)$$

When the pH of the buffer is close to the pKa value, the analytes occur in partially ionized states. As the net charge changes with pH, the electrophoretic mobility of the analytes changes too. By appropriately selecting the pH of the buffer, mobility differences can be induced between ions with similar absolute

mobilities. Absolute mobilities of analytes, μ^0 , are determined when the analyte is totally ionized, while the net or apparent mobilities, μ^n , are dependent on the extent of ionization α at a particular pH, times the absolute mobility.

$$\mu^n = \mu^0 \cdot \alpha \tag{3.11}$$

Absolute mobilities can be obtained from Offord's empirical equation (59)

$$\mu_{rel} = \frac{Z}{\sqrt[3]{M^2}} \tag{3.12}$$

(where Z is the total net charge and M is the molar mass) or can be determined experimentally by referring them to an internal standard of known mobility.

For monovalent ions, calculations of the extent of ionization is straight forward, while for small zwitterions such as amino acids, the contribution of the acidic, basic and side chains need to be combined to calculate the net charge. For the larger and more complex zwitterions, such as proteins, the situation requires a more complex approach. However, when their pI values are accessible (60) working above, at or below this value will change the solute charge and cause the solute to migrate either faster, the same or slower than electroosmotic flow. If the pH is below the pI value the analytes are cationic; if equal to the pI they are neutral; and when pH is above the pI they are anionic. Basic proteins are usually a problem in CE. At physiological pHs these proteins are cationic and tend to adsorb to the silica surface. A high pH is required,

which in turn is limited by the silica solubility and the pH stability of the other sample constituents.

While optimal separation conditions can be predicted using various models (61,62), the calculations are effective only as a first approximation. For separation, one is ultimately interested in the net mobility differences. A plot of mobility verses pH for the various analytes would suffice to indicate the optimum pH.

In addition to affecting the solute charge, changing the pH will cause a concomitant change in the electroosmotic flow (fig 3.4). The surface silanols of the silica behave like a weak acid and dissociate with increasing pH. As a consequence, the overall charge of the surface increases, which leads to growth of the zeta potential. At pHs higher than 7-8 the silanols are totally dissociated, and there is no effect on the zeta potential.

Adjustment of pH solves many separation problems. Some separations, however, require additional additives to effect selectivity.

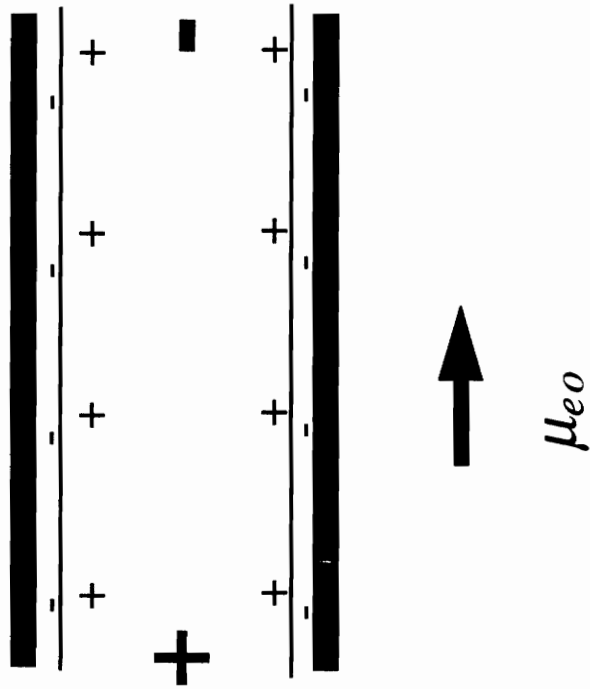
3.3.3. BUFFER ADDITIVES

Buffer additives are used to address several problems (63): to modify mobility and electroosmotic flow; to solubilize samples; to reduce or eliminate solute-capillary interaction; and finally to change the mechanism of separation.

a) Complex Formation

One of the major disadvantages of capillary electrophoresis is it's inherent lack of selectivity for hydrophobic compounds. To overcome this

pH of 3.0 - 4.0



pH of 6.5-7.5

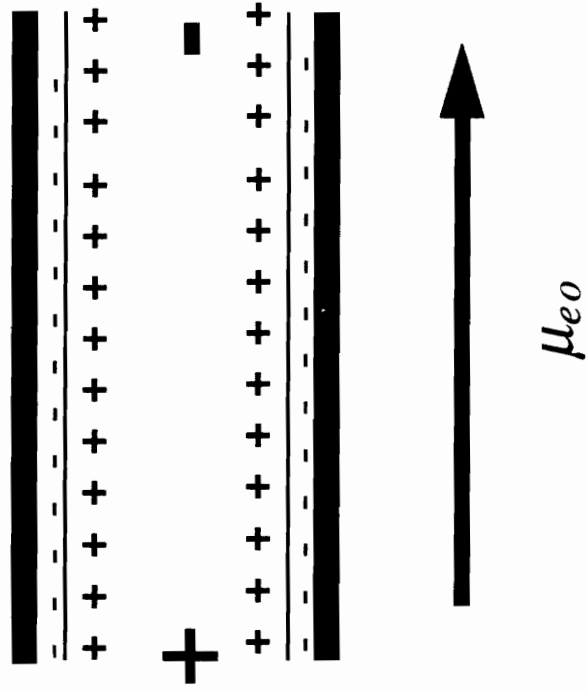


Figure 3.4: Effect of pH on the surface charge and electroosmotic flow

drawback additives are incorporated into the buffer system to interact with the analytes. In addition to micellar employment, as in MEKC, complexing agent can be added to introduce a charge to a neutral compound or to eliminate the adverse effects of charge. Separation takes place based on different electrophoretic mobilities of the associated or complexed species based on the different complex formation constants of each analyte.

ION PAIRING AGENTS

Addition of ion pairing agents facilitates the separation of a number of neutral compounds and reduces the effects of capillary wall adsorption for some of the others. Some of the common ion pairing agents include the tetraalkylammonium salts, such as tetrabutylammonium (TBA) sulfate and tetrahexylammonium (THA) perchlorate. Through solvophobic interactions PAHs were separated using THA dissolved in 50 % acetonitrile (64).

METAL ADDITIVES

The first chiral separation in CZE was reported by Gassman et al using Cu(II)-L-histidine for the resolution of a mixture of amino acid enantiomers (65). Other metals used to coordinate to nitrogen, oxygen and sulfur containing compounds have included Zn(II), Mg(II), Ca(II), Mn(II) as well as Fe(II), (63).

CYCLODEXTRINS

A lot of attention has been given to the use of inclusion complexes, such as cyclodextrins (CD), as additives. CDs are nonionic cyclic oligosaccharides consisting of six (α cyclodextrin), seven (β cyclodextrin), and

eight (γ cyclodextrin) glucose units (fig 3.5 and table 3.1) They are hollow truncated cones in shape, with a hydrophobic interior and a hydrophilic rim of secondary hydroxyl groups at the opening with the larger diameter. Selectivity results from inclusion of a hydrophobic portion of the solute in the cavity and also from hydrogen bonding to the hydroxyl moieties. CDs can effectively solubilize solutes, provided the size and the shape of the compounds conform to the interior dimensions of the cone. The larger the binding constant for a solute, the longer time it spends within the cavity, altering its electrophoretic mobility relative to that of its free uncomplexed form. The use of cyclodextrins are well known to analytical chemistry, with most of the applications in the field of chiral recognition. Only a few applications are, however, reported for aromatic hydrocarbons (66), peptides (67), PCBs (68) and corticosteroids (69).

SURFACTANTS, (Micellar Electrokinetic Chromatography, MEKC)

The addition of surfactants to capillary electrophoresis by Terabe in 1984 (21), marked a new era and a profound contribution to the technique allowing the separation of neutral as well as hydrophobic compounds. As such, inclusion of the surfactants bridged the gap between electrophoresis and chromatography, in the form of Micellar ElectroKinetic Capillary Chromatography (MEKC or MECC).

Micelles are molecular aggregates of amphiphilic character, with monomers having hydrophobic tails and (usually charged) hydrophilic heads. At low concentrations in aqueous media the surfactant monomers are in a molecular disperse stage, where they may be associated as dimers, trimers or

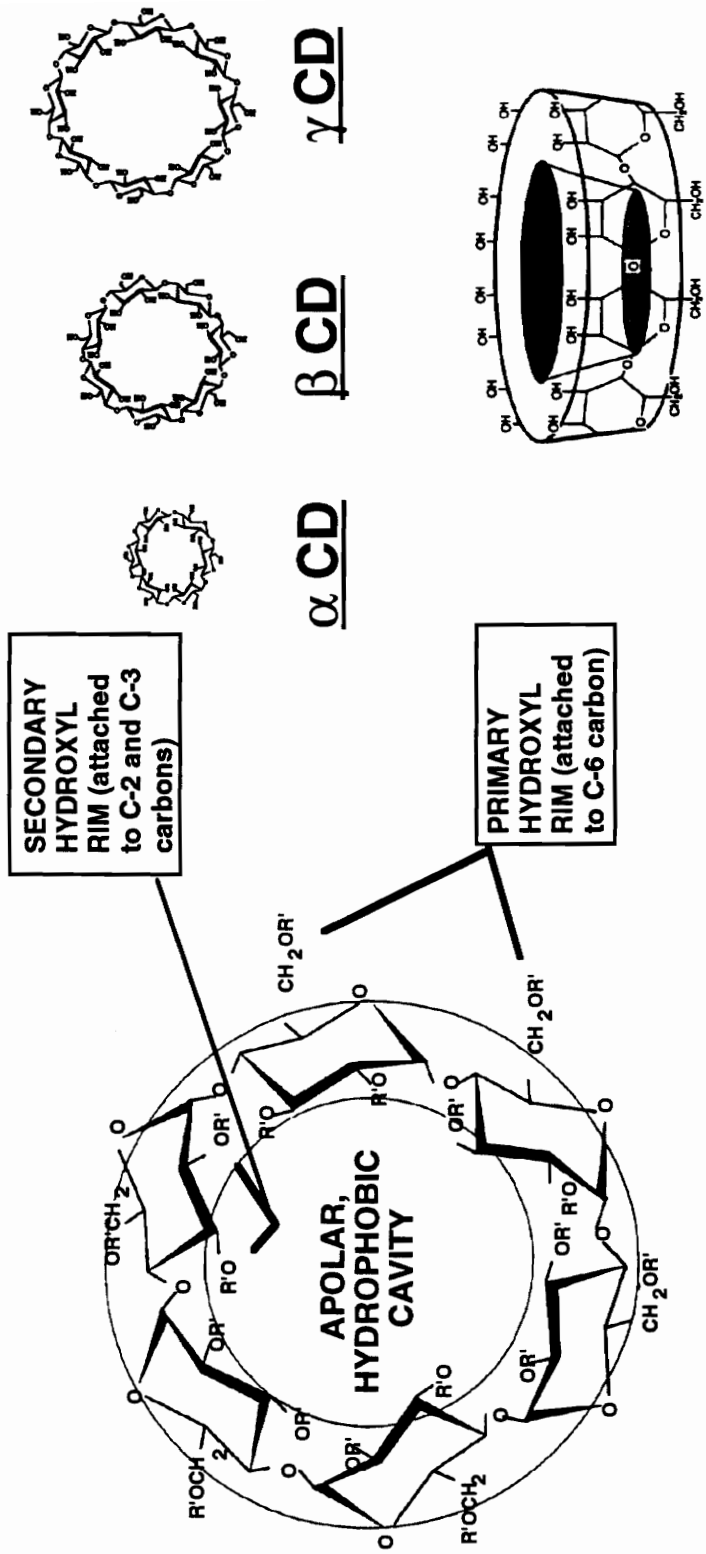


Figure 3.5: Molecular structures of Cyclodextrins (CD)

Table 3.1: Physical data of Cyclodextrins
(Chromatographia 34 (1992) 505)

	α CYCLODEXTRIN	β CYCLODEXTRIN	γ CYCLODEXTRIN
NUMBER OF GLUCOSE UNITS	6	7	8
MOLECULAR WEIGHT	972	1135	1297
INNER DIAMETER Å	4.7-6	8	10
OUTER DIAMETER OF CAVITY Å	14.6	15.4	17.5
VOLUME OF CAVITY Å ³	176	346	510
SOLUBILITY IN WATER 25°C (g/ml)	14.5	1.85	23.2

oligomers depending on the type of surfactant (70). When their concentration exceeds a certain critical micellar concentration (cmc) the molecules aggregate to form spherical micelles. This cmc value depends on the type of surfactant and on external parameters like temperature, ionic strength, pH of the media as well as the presence of chaotropic ions and organic solvents. The latter additives decrease the polarity of the surrounding media and destabilize the micellar structure. The average number of molecules per micelle is termed the aggregation number and differs according to the monomer molecular structure (Table 3.2). The micellar system is labile and is in constant equilibrium with the monomer in the surrounding media. Micelles can be anionic, cationic, nonionic or zwitterionic (Table 3.2). In aqueous solutions, micelles are oriented so that their hydrophobic moiety is in the interior while their hydrophilic counterpart is on the exterior. As the surfactant concentration increases the micellar number in solution increases and the shape, size and conformation may change significantly.

In MEKC, micelles, when charged, have their own electrophoretic mobilities μ_{ep} in solution. Sodium dodecyl sulfate (SDS), a commonly employed anionic surfactant will move with a mobility $\mu_{mc} = \mu_0 - \mu_{ep,mc}$. When the electroosmotic flow is high enough the SDS micelles will move in the same direction as the buffer, but at a slower velocity. (fig 3.6a).

Analytes will distribute themselves between the aqueous phase and the hydrophobic portion of the micellar phase, with a partition coefficient dependent on the molecules hydrophobicity. Very polar compounds will not enter the micellar phase and will elute with the electroosmotic flow, at t_0 . This is the shortest time possible for nonionic compounds to elute. Highly hydrophobic

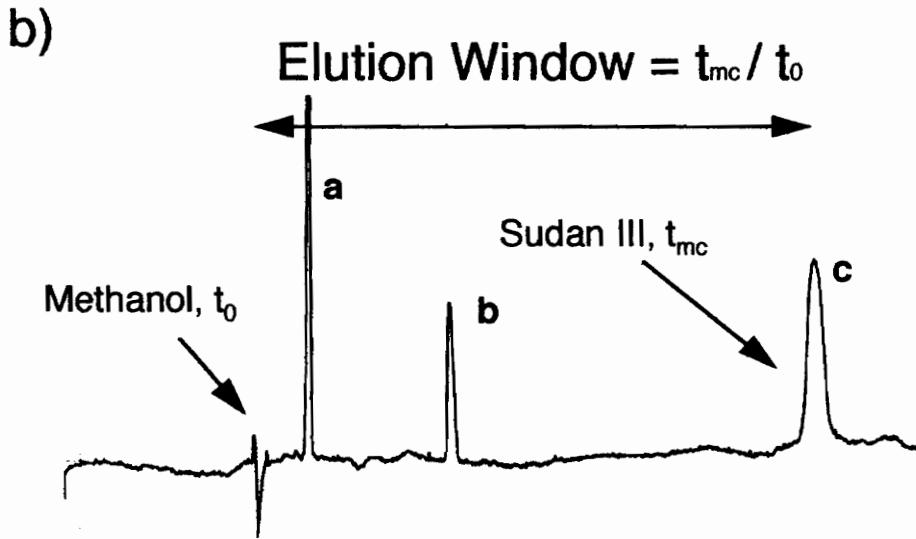
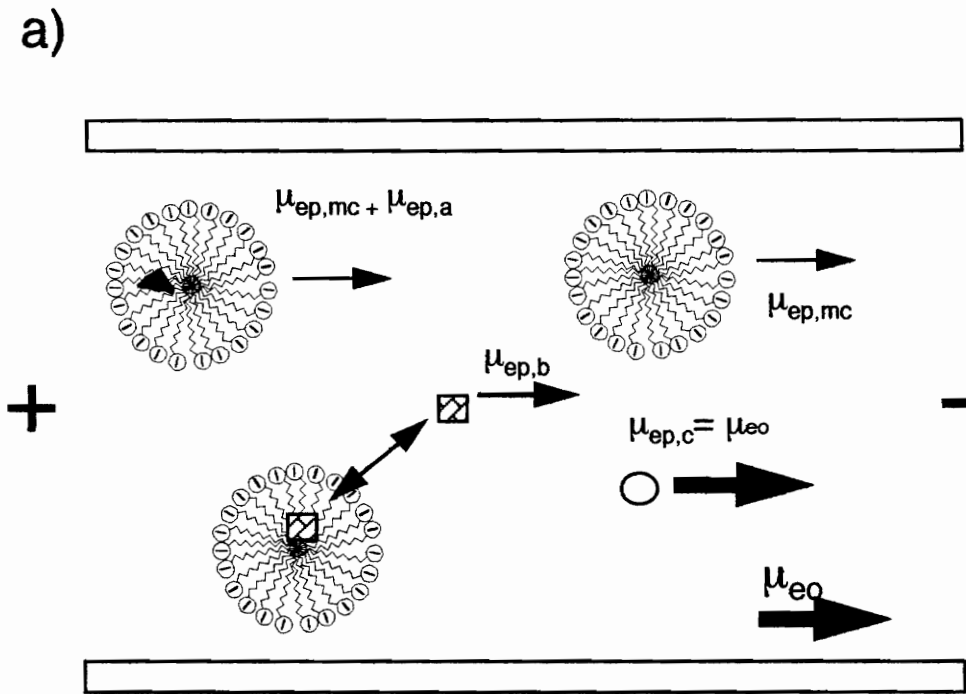


Figure 3.6: a) Separation in MEKC,
b) Resultant Chromatogram.

Table 3.2: Critical Micellar Concentration (CMC) and average Aggregation No. (A.N.) of surfactants in water at 25 °C. (71)

SURFACTANT	CMC	A.N.
ANIONIC		
Lithium dodecyl sulfate	8.77×10^{-3}	
Sodium dodecyl sulfate	8.10×10^{-3}	62
Sodium tetradecyl sulfate	2.20×10^{-3}	138
Sodium dodecanate	2.4×10^{-2}	56
Sodium cholate	1.40×10^{-2}	3
Sodium deoxycholate	5.00×10^{-3}	4-10
Sodium taurodeoxycholate	3.00×10^{-3}	8
CATIONIC		
Cetyltrimethyammonium chloride	1.3×10^{-3}	
Cetyltrimethyammonium bromide	9.2×10^{-4}	23
Dodecylammonium chloride	1.5×10^{-2}	55
ZWITTERIONIC		
Sulfobetain SB12	3.3×10^{-3}	55
Propane sulfonate (CHAPS)	$4.2-6.3 \times 10^{-3}$	9-10
NONIONIC		
Octylglycoside	2.5×10^{-2}	27
Digitonine	$6.7-7.3 \times 10^{-4}$	60
n-dodecylglucoside	1.9×10^{-4}	
Brij 35	9.0×10^{-5}	40
Tween 80	1.0×10^{-5}	

molecules residing only in the hydrophobic interior of the micelles, will elute with the micellar flow μ_{mc} at time t_{mc} . All other compounds of varying polarity must elute within this window, between the two elution times (fig 3.6 b), with a retention time t_r (72);

$$t_r = \frac{1 + k'}{1 + \frac{t_0}{t_{mc}} k'} \bullet t_0 \quad (3.13)$$

by inversion, defining the capacity factor;

$$k' = \frac{t_r - t_0}{t_0 \left(1 - \frac{t_r}{t_{mc}} \right)} \quad (3.14)$$

Equations (3.13) and (3.14) above look different from the conventional chromatographic equations. The difference is due to the moving (pseudo-stationary) phase. If the micelles were to be made stationary, a situation where $\mu_{eo} = -\mu_{ep,mc}$, then t_{mc} would become infinite and the equations would simplify to the familiar chromatographic equations.

Calculation of capacity factors requires knowledge of both t_0 and t_{mc} . As in CE, t_0 is determined by measuring the migration of a neutral, but in this case, using very polar compounds to avoid partitioning into the micelle. On the other hand t_{mc} is measured by adding a highly hydrophobic dye to the sample. Being completely included into the micelle, the migration behavior is considered to be representative of the micelle itself. Examples of compounds used include

Sudan III (most common) (72), Sudan IV (73,74), Yellow OB and Orange OT (75,76). When organic solvents are part of the mobile phase, no suitable tracer can be used, instead, an iterative procedure has been proposed using a series of homologous compounds to check the validity of t_{mc} (78).

Although MEKC was originally conceived for the analysis of neutral molecules, it is of equal benefit and enhances the selectivity of ionic and ionizable compounds. Real samples usually contain a mixture of both neutral and ionic compounds and the presence of micelles not only helps separate ionic molecules of close electrophoretic mobilities but may also change their conventional CE elution order .

The addition of cationic surfactants, such as decyltrimethylammonium sulfates and its homologues, reverses the electroosmotic flow (fig. 3.7). The cationic moiety of the monomer at low concentrations adsorbs to the surface of the fused silica (fig. 3.7a) until it totally counteracts the SiO^- , reducing the electroosmotic flow to zero. Further increases in the concentration results in the formation of hemimicelles (79) reversing the electroosmotic flow direction (fig 3.7b). Beyond the cmc of the cationic surfactants micelles begin to appear.

Efficiency

Terabe et al have theoretically evaluated the contributions to band broadening in MEKC (80). They concluded that axial diffusion was more important than resistance to mass transfer and micelle microheterogeneity. Sepaniak et al (81) and Davis (82) have observed and discussed nonequilibrium effects relating band broadening to linear velocities or applied voltage.

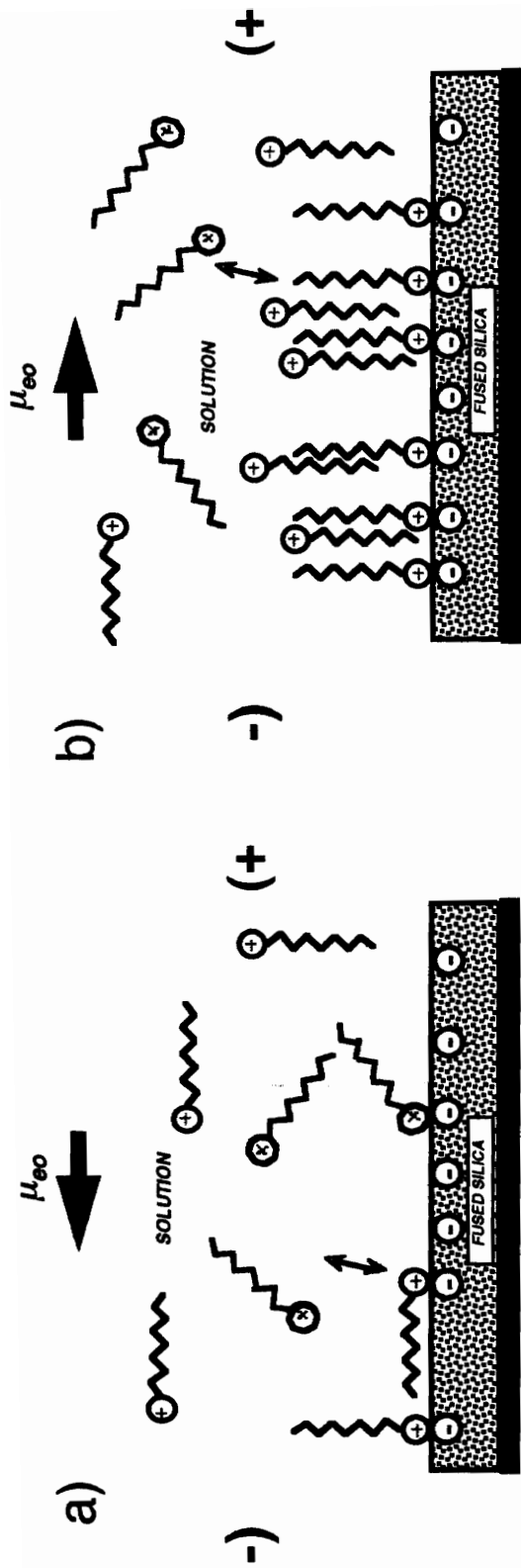


Figure 3.7: Effect of addition of cationic surfactants. a) decrease in electroosmotic flow, b) reversal of electroosmotic flow and formation of hemimicelles. (79)

From the Golay equation,

$$H = \frac{B}{v} + Cv \quad (3.15)$$

as long as the axial diffusion predominates, highest efficiency is obtained at high velocities. In MEKC, the contributions from resistance to mass transfer are small relative to the stationary phase's contribution in liquid chromatography, hence the superior efficiencies of the former technique. The micelle is a small labile entity, with a radius close to the length of the hydrophobic chain (83). The micelle itself has a life time of 100-1000 msec. The risk of irreversible trapping or slow mass transfer is strongly reduced. Table 3.3 shows the relative contributions of the various parameters.

Resolution

The resolution of two analytes is derived through inserting equation (3.14) into the classical master resolution equation (84), to show that;

$$R = \frac{\sqrt{N}}{4} \cdot \frac{\alpha - 1}{\alpha} \cdot \frac{k_2'}{1 + k_2'} \cdot \frac{1 - \frac{t_{eo}}{t_{mc}}}{1 + \left(\frac{t_{eo}}{t_{mc}}\right) \cdot k_1'} \quad (3.16)$$

Assuming that conditions are chosen so as to obtain optimal efficiency, and selectivity is predetermined by the surfactant choice, the last two components of equation (3.16) are the most important parameters for resolution optimization. Resolution can be increased by decreasing the term t_0 / t_{mc} . This

TABLE 3.3: Typical values for several plate height contributions ⁽⁸⁰⁾

VARIANCE	h (mm)
AXIAL DIFFUSION h_{diff}	5.4
MICELLAR MASS TRANSFER h_{MC}	0.2
INTERMICELLAR DIFFUSION h_{aq}	$5 \cdot 10^{-6}$
JOULE HEATING $h_{\Delta T}$	< 1.0
MICELLAR POLYDISPERSITY h_{disp}	$3.0 \cdot 10^{-5}$
INJECTION PLUG h_{inj}	0.17

can be accomplished by suppressing the electroosmotic flow) or optimizing the capacity factor, k' (manipulations in the surfactant concentration, $k' = \beta K_{eq}$).

MECC, however, suffers from a limited elution range. Analytes must elute in the time between t_0 (the elution time of an unretained solute) and t_{mc} (the elution time of the micelle). In addition, selectivity for hydrophobic compounds is restricted by the limited variety of useful micelles for MECC applications and the tendency for hydrophobic compounds to partition largely into the micelle, hence eluting close to t_{mc} . Attempts to overcome these limitations involve addition of organic modifiers to the buffer system (78,85-87), changing the micellar electrophoretic characteristics (chain length and hydrophobicity) and decreasing of the electroosmotic flow (u_{eo}). The u_{eo} can be decreased through an increase of the buffer ionic strength (87), adjustment of the buffer pH (88-89), deactivation of the capillary surface (90) and manipulations in the surfactant concentration (72).

b) Organic Modifiers

Organic modifiers when added to the mobile phase alter the physicochemical characteristics of the system. Both the viscosity and the polarity of the mobile phase are affected, in turn affecting the electroosmotic mobility as well as the electrophoretic mobilities. Additionally, organic solvents are widely used to solubilize poorly soluble analytes. Fujiwara and Honda (91) have investigated the influence of the addition of methanol and acetonitrile on electroosmosis and found that methanol decreased it while acetonitrile increased it. They also reported that both methanol and acetonitrile raised electrophoretic mobilities, due to intramolecular hydrogen bonding, improving

resolution. Others ⁽⁹²⁾ obtaining the same results attributed the mobility changes mainly to viscosity, assuming that viscosity has more influence on mobility than the dielectric constant or the zeta potential.

Other higher alcohols have been investigated ⁽⁹³⁾. The μ_{eo} showed a decrease with the chain length: methanol < ethanol < n-propanol < butanol. Diols or polyols are more efficient in changing the viscosity of the mobile phase: ethylene glycol < glycerol < PEG 400.

Other organic modifiers frequently used to decrease the zeta potential and hence the electroosmotic flow, include methylcellulose and hydroxypropylmethyl cellulose. These compounds not only decrease the μ_{eo} but also limit the adverse effects of adsorption to the silica silanols, and behave as entangled polymers with an additional sieving effect.

Sepaniak et al ⁽⁹⁴⁾, Fujiwara ⁽⁹¹⁾ and Terabe ⁽⁸⁸⁾ studied the effects of addition of organic modifier with micellar phases. In addition to interacting with the capillary wall and changing the electroosmotic flow, organic solvents alter the elution window, the partition coefficients, enhance selectivity (in some cases), increase the capability to handle hydrophobic solutes, increase the cmc values of micelles and allow for gradient elution.

CHAPTER IV

INSTRUMENTATION

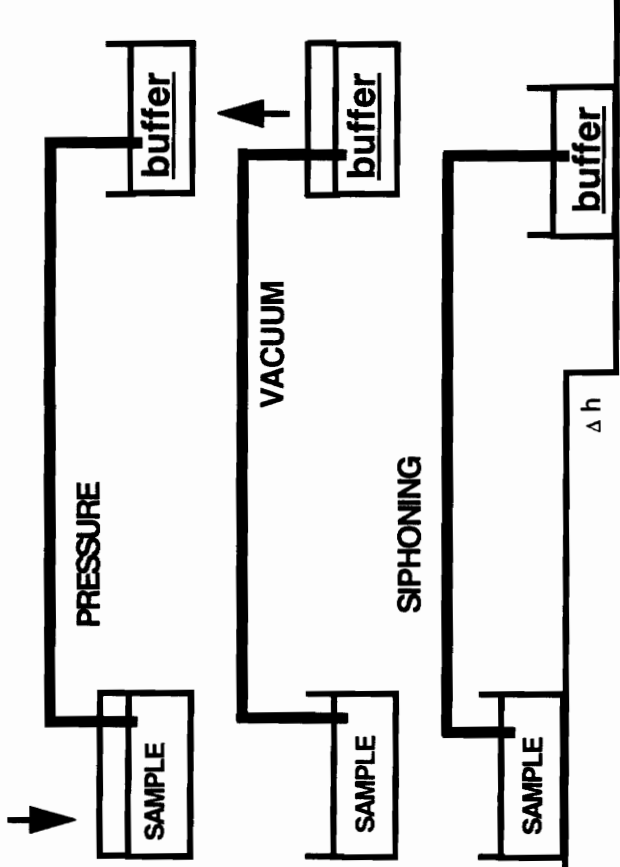
4.1. SAMPLE INTRODUCTION

The small dimensions of capillary columns results in system overloading by large sample volumes. The significant zone broadening introduced acts to counteract the system's inherent high efficiency. An injection method capable of delivering small volumes of sample (< 100nL) into the column efficiently and reproducibly, is therefore important. Direct on-column methods employing electrokinetic migration and hydrodynamic flow are, consequently, the best methods. Electrokinetic and hydrodynamic injection methods are, to date, the two most popular ways to introduce sample into the CE capillary (fig 4.1). Other more specialized techniques, such as electric sample splitter, rotary injector, and a microinjection system, have been described ⁽⁹⁵⁾.

4.1.1. HYDRODYNAMIC INJECTION

For hydrodynamic injection (fig 4.1 A) a pressure drop has to be applied along the capillary. The volume introduced is then a linear function of the applied pressure difference and it's duration. The injection is accomplished by temporarily placing one end of the capillary into the sample solution. Either pressure (or vacuum) is applied to the appropriate buffer vial for a fixed period of time.

A) HYDRODYNAMIC



B) ELECTROKINETIC

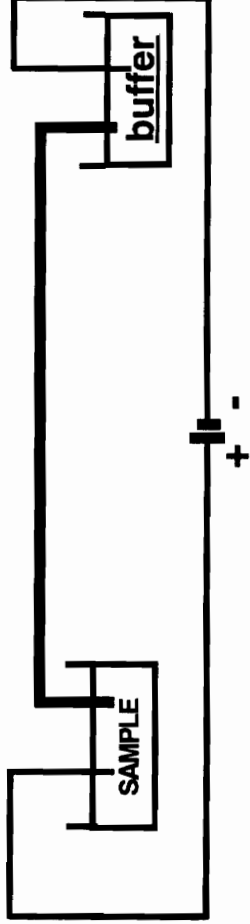


Figure 4.1: Modes of Sample Introduction in Capillary Electrophoresis

The quantity of sample introduced is governed by the following equations;

a) Pressure and vacuum,:

$$Q = \Delta P_{inj} \cdot t_{inj} \cdot c_{inj} \cdot \frac{1}{\eta} \cdot \frac{\pi d_c^4}{128 L_v} \quad (4.1)$$

ΔP_{inj} is the applied pressure or vacuum, η is viscosity, t_{inj} is the duration of injection, d_c is column diameter and c_{inj} is the concentration of sample injected.

b) Siphoning;

$$Q = \Delta h_{inj} \cdot t_{inj} \cdot c_{inj} \cdot \frac{g\rho}{\eta} \cdot \frac{\pi \cdot d_c^4}{128 L_v} \quad (4.2)$$

Δh_{inj} is the height difference between the two buffer levels on lifting the sample vial, g is the gravity constant and ρ is the solution density.

The above two equations show that the sample plug injected depends on the column diameter, column length, mobile phase viscosity (therefore column temperature) and can be varied by changing the duration of pressure, vacuum or elevation and by the extent of pressure, vacuum or elevation. If all the above

can be kept constant, quantitation is then dependent on the vacuum or pressure pump, and lever precision for height elevation (siphoning).

4.1.2. ELECTROKINETIC INJECTION

Electrokinetic injection (fig 4.1 B) is an alternative mode of sample introduction in CE. Temporary application of voltage to the sample vial causes electrophoretic and electroosmotic movement of the contents. The injected sample quantity is then given by ⁽⁹⁶⁾;

$$Q_{inj} = \frac{V_{inj} \cdot t_{inj}}{V \cdot t_r} \cdot c_{inj} \cdot \frac{\pi \cdot d_c^2 \cdot L_d}{4} \quad (4.3)$$

Here, V_{inj} is the voltage applied during injection, while V is the analysis run voltage.

By varying the voltage and / or the introduction time, the quantity introduced into the capillary can be controlled. With this mode of injection the quantity depends on the specific electrophoretic mobility of the sample components and the electroosmotic mobility of the system. In this respect electrokinetic injection discriminates among ions based primarily on their electrophoretic mobility. Species with high mobilities are drawn in at a faster rate into the capillary than those with lower mobilities. Oppositely charged ions would only migrate into the capillary if their electrophoretic mobility is smaller than the electroosmotic flow; and neutral molecules would be introduced only when there is electroosmotic flow. In addition electrophoretic mobility and

electroosmotic flow change with different matrixes of the samples, adding yet another possibility for sample bias.

Hydrodynamic injection seems, therefore, to be the preferred mode over electrokinetic injection in terms of non-bias sampling. However, there are certain cases where the latter injection mode would be necessary; when gel columns are used (hydrodynamic injection would simply extrude the gel), or when deliberate discrimination is required to eliminate an undesirable matrix or perhaps to concentrate an analyte in a dilute sample.

To further improve efficiencies and enhance detection sensitivity, sample plugs may be further concentrated during or just after sample injection. Such focusing attempts, or "stacking" are based on field strength differences between the sample plug and the running buffer. The sample is dissolved in water or diluted buffer, with a resultant lower conductivity. The lower ionic strength in the sample plug, results in higher electroosmotic flow and sample mobility. At the running buffer boundary the sample is once again slowed down resulting in a more focused band. If the sample cannot be diluted, stacking can be induced by injecting a water plug prior to the sample. A third form of stacking involves partially filling the capillary with sample, reversing the electroosmotic flow to stack the sample at the head of the column, then resuming the original flow direction and commencing the electrophoresis ⁽⁹⁷⁾.

4.2. POWER SUPPLY

Analytes in CE only migrate when a field strength (E) is applied across the capillary. The necessary voltage can be obtained from a DC power supply

capable of applying up to 30 kV and current levels of 100 to 200 μA . Stable regulation of voltage ($\pm 0.1\%$) is required to maintain migration time reproducibility.

Normal conditions in CE entail injection in the anode side and detection close to the cathode. However, should the surface of the silica be cationic instead of anionic, or should the electroosmotic flow be so weakened that the electrophoretic mobility of analytes, traveling in the opposite direction, is stronger, or if gels are used, it may be necessary to reverse the polarity of the electrodes. The power supply, in this case, should have the capability to switch polarity. Polarity switching should be software controllable even during the analysis.

Both constant voltage (isoelectrostatic) as well as constant current (isorheic) modes should be available from the power supply. When capillary temperature is not adequately controlled, in the isoelectrostatic mode, the buffer viscosity changes and consequently the migration time. While constant voltage analyses are most common, it would be more beneficial in this case to use the constant current mode. In this mode, any viscosity changes would be compensated for by proportional changes in the applied voltage, maintaining constant migration time.

Another feature of the power supply, should be the ability to run voltage, or current gradients during an analysis. Low voltages at the beginning of an analysis would prevent the sudden temperature rises that may result in the premature thermal expulsion of the sample plug just injected into the capillary. Gradients would also be used to cut analysis time by ramping up to higher

voltages speeding up the late eluters. Ramping down gradients, at the end of a run may also be beneficial during sample collection (98).

4.3. DETECTION

The volume restrictions that apply to injection are equally valid for detection. In CE, this is a major challenge and detectors must be miniaturized according to the column dimensions. If detachable detection cells serving as part of a stand alone detector were used, as they are in HPLC, a cell volume of nanoliters or even subnanoliter levels would be required. According to Yu and Dovichi (99) the maximum allowable detector dead volume V_d is given by;

$$V_d = \frac{\Theta^2 V_c}{\sqrt{N}} \quad (4.5)$$

where Θ^2 is the fraction of allowable peak broadening, and V_c is the column volume in ml. For a 1-m long, 75 μm id capillary providing 250,000 theoretical plates, the detector volume that introduces a 10 % peak broadening ($\Theta = 0.22$) has to be about 1 nl. The construction of such cells is not yet practical. In view of this restriction a small section of the column itself is commonly used in CE as the detection volume (i.e. on-column detection). The detection window is made as described in section 3.2.2. above, the length of which according to Wang et al (100) who in agreement with Otsuka and Terabe (101) suggested it should be less than 1 mm for efficiencies of 300,000. Such a detection configuration, nevertheless, poses two major problems. First, the capillary dimensions, less

than 100 μm , define a very short path length. Second, unlike the plane-parallel arrangement in conventional detection cells, cylindrical capillaries are poor optical surfaces, that result in refractive index effects. Another possible contributor to detector band broadening is the detector time constant or rise time. Insufficient detector time constant settings needlessly sacrifice signal/noise ratio, whereas higher values can result in band broadening. The time constant should be no greater than 10% of the temporal peak variance (102).

Two main types of detectors can be distinguished, selective and non-selective detectors. While the first measures a specific property of the analyte (UV/VIS absorbance, fluorescence, electrochemical (ED) and mass spectrometry (MS) detection, the second measures differences in physical properties of the analytes relative to the bulk solution (refractive index (RI) and conductivity detection).

Another way detectors can be categorized is whether they are mass or concentration sensitive detectors. In CE; UV/VIS, fluorescence and conductivity detectors are concentration sensitive detectors, while the electrochemical and mass spectrochemical detectors are considered mass sensitive detectors. The former's response is proportional to the concentration of the solute in the buffer as it transmits the detection window and shows a continuous baseline rise when the flow is stopped during the passage of solute through the detection window. The solute area for concentration sensitive detectors are flow dependent in HPLC, where the peak velocities and peak width on-column are a function of the solute's retention characteristics until they leave the column where they are all swept past the detector at the pre-determined column flow. In CE, however, the migration velocity of each solute through the capillary is a

function of its electrophoretic mobility in conjunction with the electroosmotic flow. Therefore peak areas are solute dependent rather than electroosmotic flow dependent, the slower they move, the larger the area counts (103).

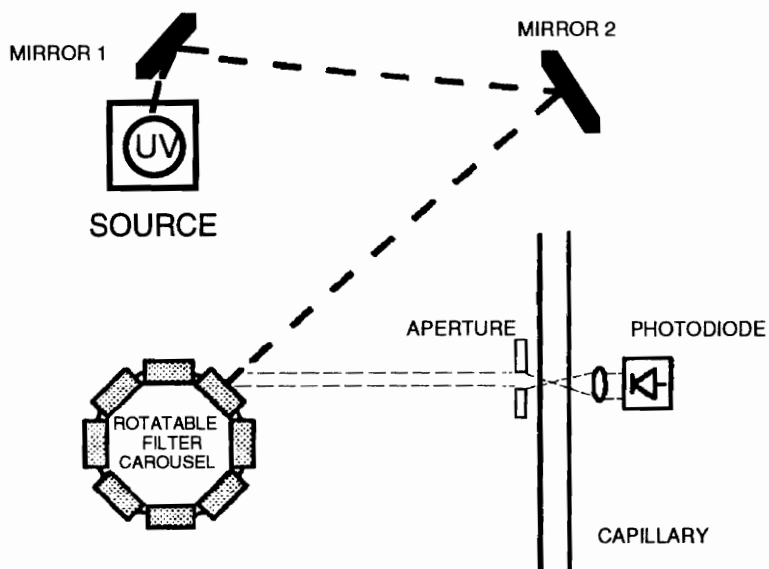
Mass sensitive detectors on the other hand are not affected by the buffer, but respond only to the mass of the analyte present. The area is flow independent. Additionally, when the buffer flow is stopped an immediate decrease in signal results.

A number of detection methods are available for CE, many of which are similar to those employed in HPLC. Only a few, however, are practical enough to be available commercially. Table 4.1 contains a list of many of the detection methods investigated, along with their detection limits, advantages and disadvantages (104).

4.3.1. UV/VIS ABSORPTION DETECTION

UV/VIS absorption is by far the most popular technique used in CE today. Detection is performed on-column towards the end of the column. The benefits of fused silica are here, once again apparent. High quality fused silica has a UV cut-off at 170 nm as opposed to glass capillaries with a cut-off around 300 nm. Several designs for light transport through the capillary window, are available (fig 4.2). Some have fixed wavelength detection that use mercury, zinc or cadmium lamps with wavelength selection by filters, while others offer variable wavelengths through the use of deuterium or tungsten lamps with monochromator or filter wavelength selection. Multiwavelength UV detectors employ either a photodiode array or employ a scanning monochromator. The spectrophotometric types are most valuable because spectral information as

a) Single beam spectrophotometer



b) Double beam Spectrophotometer

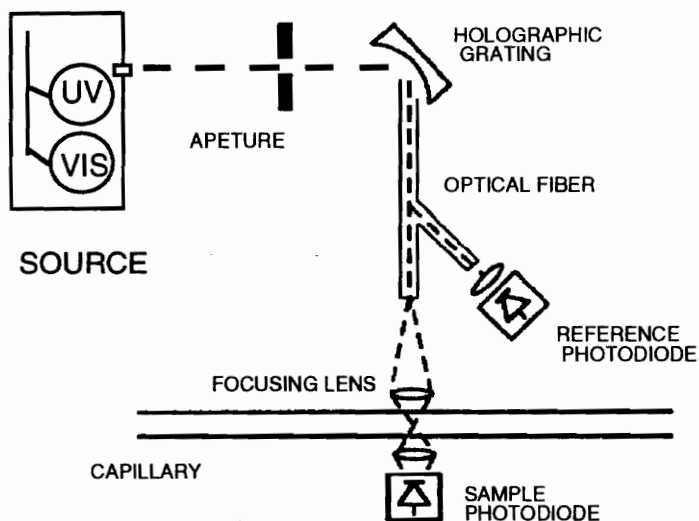


Figure 4.2 : Schematic diagram of two different UV detection devices for CE. a) Optical layout of a spectrophotometer with a single-beam system. b) Optical layout of a spectrophotometer with a double beam system. (108)

Table 4.1: Available methods of detection in Capillary Electrophoresis (104)

<u>Method</u>	<u>Mass detection limit</u> (moles)	<u>Concentration detection limit</u> (moles) (10nl inj.)	<u>Advantages/ disadvantages</u>
<u>UV-Vis absorption</u>	10 ⁻¹³ -10 ⁻¹⁶	10 ⁻⁵ -10 ⁻⁸	<ul style="list-style-type: none"> • Universal • Diode Array offers spectra.
<u>Fluorescence</u>	10 ⁻¹⁵ -10 ⁻¹⁷	10 ⁻⁷ -10 ⁻⁹	<ul style="list-style-type: none"> • Sensitive, Selective. • Usually requires sample derivatization.
<u>Laser-induced fluorescence</u>	10 ⁻¹⁸ -10 ⁻²⁰	10 ⁻¹⁴ -10 ⁻¹⁶	<ul style="list-style-type: none"> • Extremely sensitive • Usually requires sample derivatization. • Expensive.
<u>Amperometry</u>	10 ⁻¹⁸ -10 ⁻¹⁹	10 ⁻¹⁰ -10 ⁻¹¹	<ul style="list-style-type: none"> • Sensitive. • Selective but useful only for electroactive analytes • Requires spectral electronics and capillary modification.
<u>Conductivity</u>	10 ⁻¹⁵ -10 ⁻¹⁶	10 ⁻⁷ -10 ⁻⁸	<ul style="list-style-type: none"> • Universal • Requires spectral electronics and capillary modification.
<u>Mass Spectrometry</u>	10 ⁻¹⁶ -10 ⁻¹⁷	10 ⁻⁸ -10 ⁻⁹	<ul style="list-style-type: none"> • Sensitive and offers structural information. • Interface between CE and MS complicated.
<u>Indirect UV fluorescence, amperometry</u>	10-100 times less than direct method	—	<ul style="list-style-type: none"> • Universal. • Lower sensitivity than direct methods.

well as electrophoretic information can be displayed. However, these detectors are frequently considered less sensitive when scanning the whole UV range, as signal averaging must be carried out more rapidly than when narrow wavelength detection is used. In this respect, single wavelength detectors are at an advantage.

One of the major problems in UV detection is focusing the light onto the capillary center. Unfocused light that strikes the rim of the capillary is dispersed increasing the background noise and reducing the amount of light reaching the capillary. Narrowing the source slit width to further narrow the ray of light, will only serve to reduce the light intensity through the capillary. By using various ball lens designs and materials, sensitivity has been greatly improved.

Nevertheless, with the current technology, limits of detection are still in the 10^{-4} - 10^{-7} M range. Several attempts have been made to extend the path length and increase sensitivity. This is usually at the expense of efficiency and resolution (105). Examples include commercially available rectangular borosilicate capillaries, for sideways illumination (fig 4.3 a). A 3 mm Z-shaped longitudinal on-column cell has resulted in a six-fold increase in sensitivity with a tolerable loss in efficiency (fig 4.3 b). Hewlett Packard has introduced a bubble cell. The bubble shaped blown glass at the detection window is three times the width of the column's internal diameter and results in an approximate three fold increase in sensitivity (fig 4.3 c). Another detector has employed an on-column multireflection absorption cell with an internally silvered surface (fig 4.3 d). Finally, detection by shining laser light or conventional light down the axis of the column (as opposed to perpendicular), takes advantage of the entire length of each solute band for absorption measurements (106,107).

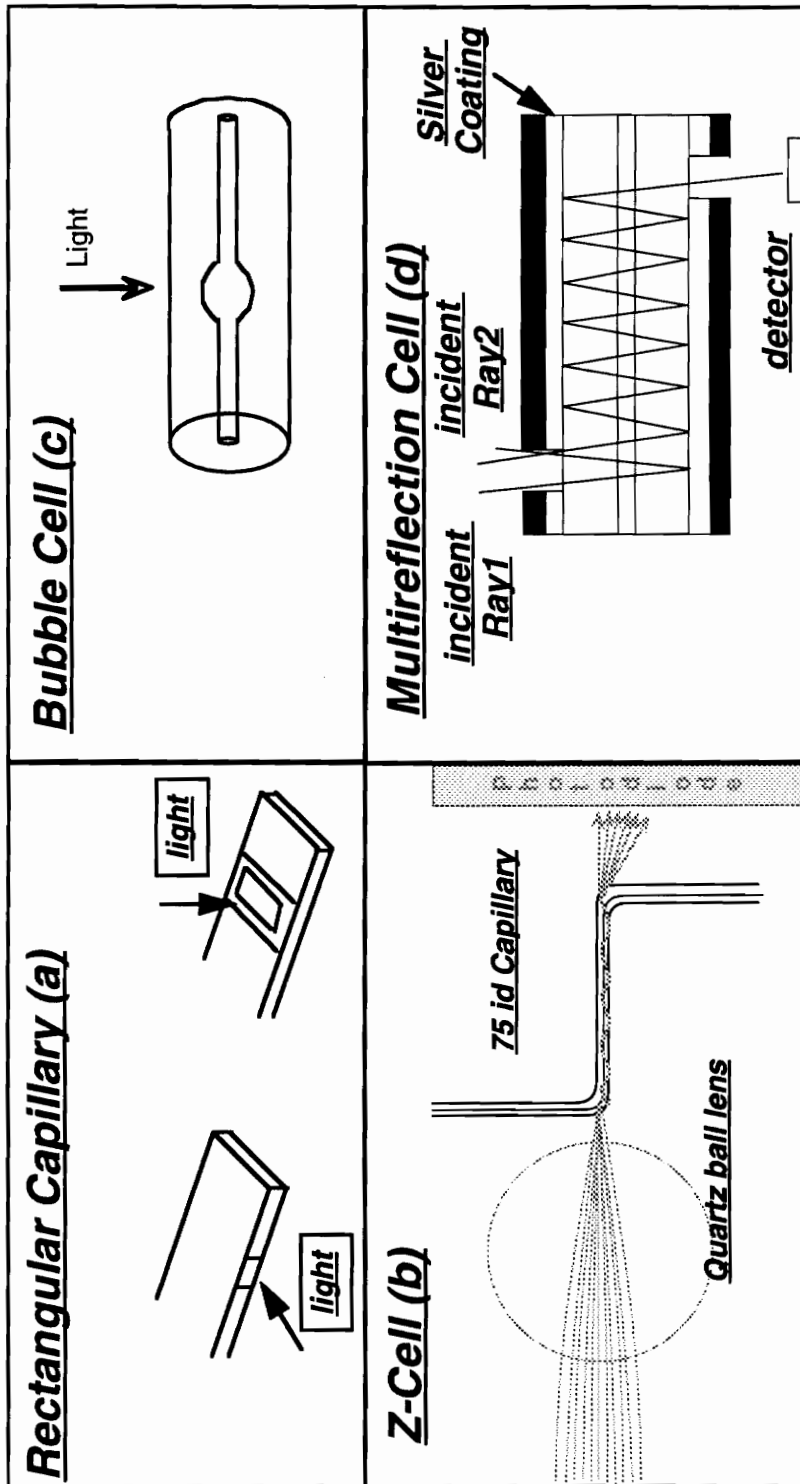


Figure 4.3: Methods to enhance sensitivity in CE, Anal Chem,65 (1993) 489A

4.3.2. FLUORESCENCE DETECTION

Fluorescence detection is both more sensitive and selective than UV absorption, especially when laser sources are used. Excitation radiation from an arc lamp or a laser is focused onto a section of the capillary where the polymer coating has been removed. The resulting fluorescence is collected usually at an angle of 90° relative to the excitation beam through a system of lenses or through an optical fiber⁽¹⁰⁸⁾. The increased sensitivity of fluorescent detection is due to the non-fluorescing buffer background which allows for high amplification of low analyte signals relative to UV absorption detection where the measurement is a small difference between two high signal intensities.

In its selectivity, fluorescence detection is less versatile than UV detection. Many solutes do not exhibit native fluorescence, and when possible must be derivatized with some type of fluorophore to benefit from the technique's inherent sensitivity.

When employed lasers are superior excitation sources relative to the conventional arc lamp sources. They result in better focusing on the capillary reducing stray light and increasing the throughput of excitation energy reaching the small volume capillaries with diameters less than $50\ \mu\text{m}$. However, unlike the arc lamp, laser radiation is not readily available in a broad range of wavelengths necessary to detect many compounds. Tunable lasers are too expensive and too complicated for CE use. In general, continuous lasers are more stable in intensity, easier to focus and are less likely to cause optical damage. Helium-Cadmium lasers, emitting with wavelength of 325 and 422 nm and with powers of 5-10 mW are the most frequently employed. Argon ion lasers can be adapted to different wavelengths in the green, blue and the U.V.

range of the spectrum (most often to 350-360, 476, 488 and 514 nm), and are available with powers ranging from a few to 10 W. The use of diode lasers in the near IR (109) as well as with frequency doubling are also rapidly gaining popularity. Frequency doubling allows detection in the UV region where good fluorophores are more abundant .

4.3.3. ELECTROCHEMICAL DETECTION

Electrochemical detection is one of the most sensitive and equally selective detection modes available to CE. It is a detection mode well suited for microseparations with improvements in detection limits as the capillary volume decreases. There are two basic modes of electrochemical detection; potentiometry and amperometry.

a) Potentiometric Detection

Potentiometric detection in capillary electrophoresis can be divided into one electrode and two electrode systems. One electrode systems involve measurement of potential at one working electrode relative to a reference electrode in an open circuit, or by passing a small current through the working electrode. Although introduced as early as 1974 by Virtanen (15) for 200 μm capillaries, it has found little application in today's modern CE. Two electrode potentiometric detection, also known as conductivity detection, and first introduced to CE in 1979 (8) involves the measurement of the potential between two indicator electrodes when a small constant current is passed through. Analytes are detected because of a difference in conductance relative to that of a background electrolyte. The larger the difference the greater the

sensitivity. To minimize electromigration dispersion, however, the buffer concentration has to be high, thus decreasing the sensitivity.

Two on-column designs are popular. One design by Foret et al (110) involves three platinum wires cast into a polyester resin block protruding from the wall of the capillary at the cathodic end in contact with the solution electrolyte. Another more recent design (fig. 4.4), by Huang and Zare (111) involves the implantation of two platinum wires opposite each other, into the fused silica capillaries. A computer controlled CO₂ laser is used to make the necessary 40 μm holes into 50 or 75 μm capillaries. The platinum wires are placed exactly opposite each other in order to minimize the interference from the background of the high electric field used for the separation. This detector end of the capillary is also the cathode. A specially designed conductivity meter is necessary to isolate it from the system potential. The detector is most applicable to small inorganic compounds and carboxylic acids. The detector suffers from baseline drift and high detection limits. Recent developments involving suppressed conductivity (112,113), has resulted in increased sensitivity.

b) Amperometric Detection

Amperometric detection measures the current created by the constant potential electrolysis of species in a flowing stream. It is one of the most sensitive and selective detection techniques afforded to CE. In amperometry, current is measured at a working electrode as analytes are oxidized or reduced. The working electrode, is held at a constant potential, relative to a reference electrode, and the current is recorded verses time. The choice of working

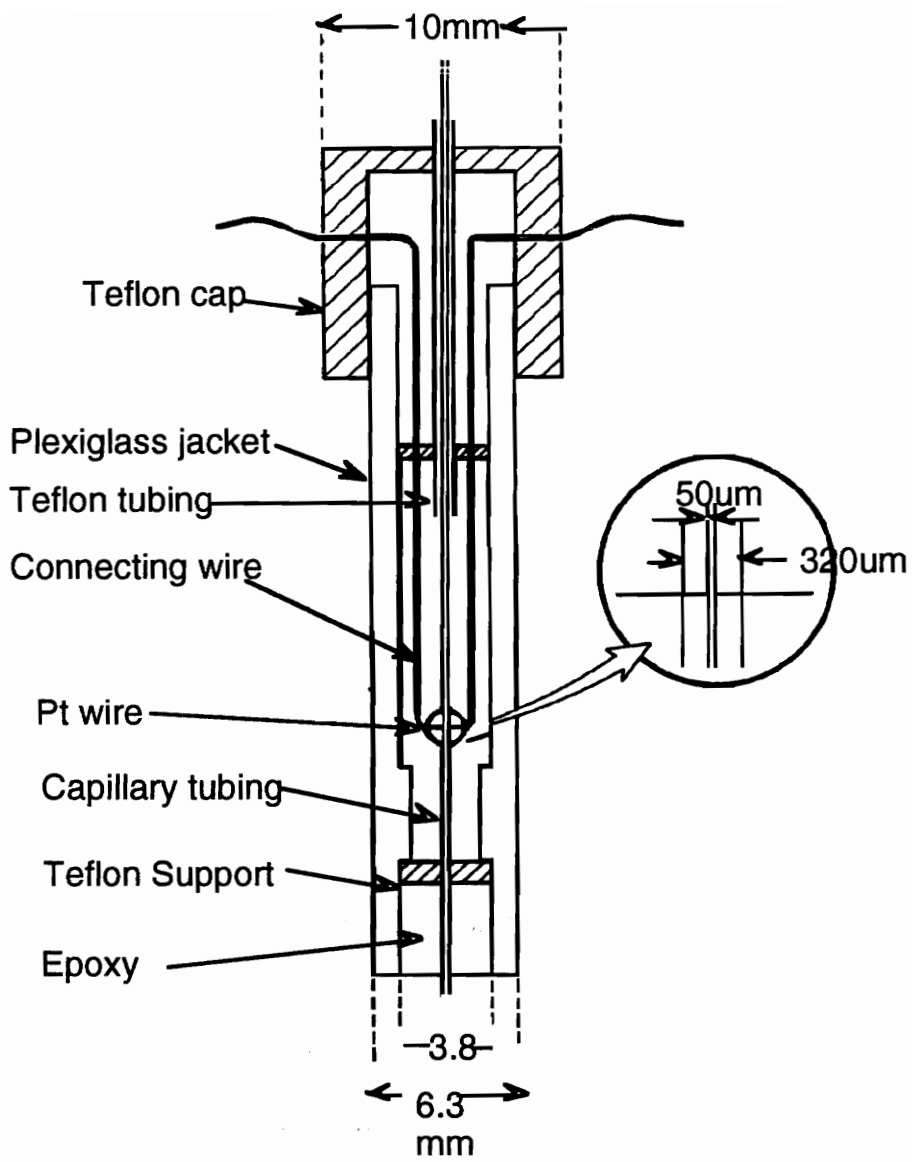


Figure 4.4: Schematic for conductivity cell for detection in capillary electrophoresis (111)

electrode material can have a significant effect on the selectivity. Commonly employed electrode materials include platinum and carbon. Different working electrodes have different potential windows but they are typically between 0 and 1 V.

Good selectivity can also be achieved by the control of the working electrode potential, because it can be set to just oxidize (or reduce) any analyte. The electrochemical properties of a molecule can be determined by the nature of the electroactive functional groups. Electroactive molecules can be either oxidized, reduced or both. Their suitability for amperometry depends on their voltammetric behavior. Cyclic voltammetry evaluation of the solute would determine its reaction kinetics, stability and reversibility. The potential from the scan that gives the maximum current relative to the background should be the one chosen for the CE amperometric analysis. Some solutes are easier to oxidize or reduce than others, requiring lower potentials, and their detection limits are consequently higher. Additionally the signal in amperometric detection is proportional to the efficiency of the oxidation reaction.

In a potentiometric cell a term iR_s known as the ohmic potential drop, is characteristic of the bulk solution resistance and residual current. This adverse voltage drop has to be included in the measured potential of the cell (114). The current from the CE system's high potential is usually several orders of magnitude higher than the actual faradiac current measured at the working electrode. The iR_s term is substantially increased resulting in a high background. Several approaches have been taken to minimize this high background.

A Post column amperometric detection interface (fig 4.5), developed by Wallingford and Ewing (115) involved a crack in the capillary at the cathode end. This crack is covered with a porous glass (115) or Nafion (116) coatings. The joint, although difficult to construct, allows passage only of the small electrolyte ions and serves as the ground end of the MECC system, dropping the potential. This separates the electrochemical current and minimizes background interference with the electrochemical detection carried out post fracture. The electroosmotic flow pumps the solute through the remaining short section of a 25 or 50 μm id capillary. The working electrode, generally, a 10 μm carbon fiber is threaded and epoxyed to a glass pipette tip centered on a microscope slide which is attached to a three way micro-manipulator. Requiring meticulous preparation and manipulation, the electrode is carefully introduced into the outlet end of capillary with the aid of the micromanipulator and a microscope.

This system has allowed sensitive detection of neurocompounds down to 50-20 fmols in the presence of SDS with efficiencies ranging from 10,000 - 200,000 theoretical plates. When 5 and 2 μm id columns were used (117) for the analysis of single cell cytoplasm, 36 pl samples were injected with 960,000 theoretical plates and 3 attomoles of catechol were detected.

Another successful approach to electrochemical detection developed by Haung et al (118) known as End-column amperometric detection, eliminated the need for the fractured joint design, while keeping a low background current with the use of 5 μm capillaries and a 10 μm cylindrical carbon fiber microelectrode. Since the electrode is larger in diameter it was aligned with the bore of the capillary and positioned up against but not into the capillary (fig 4.6a). Creating

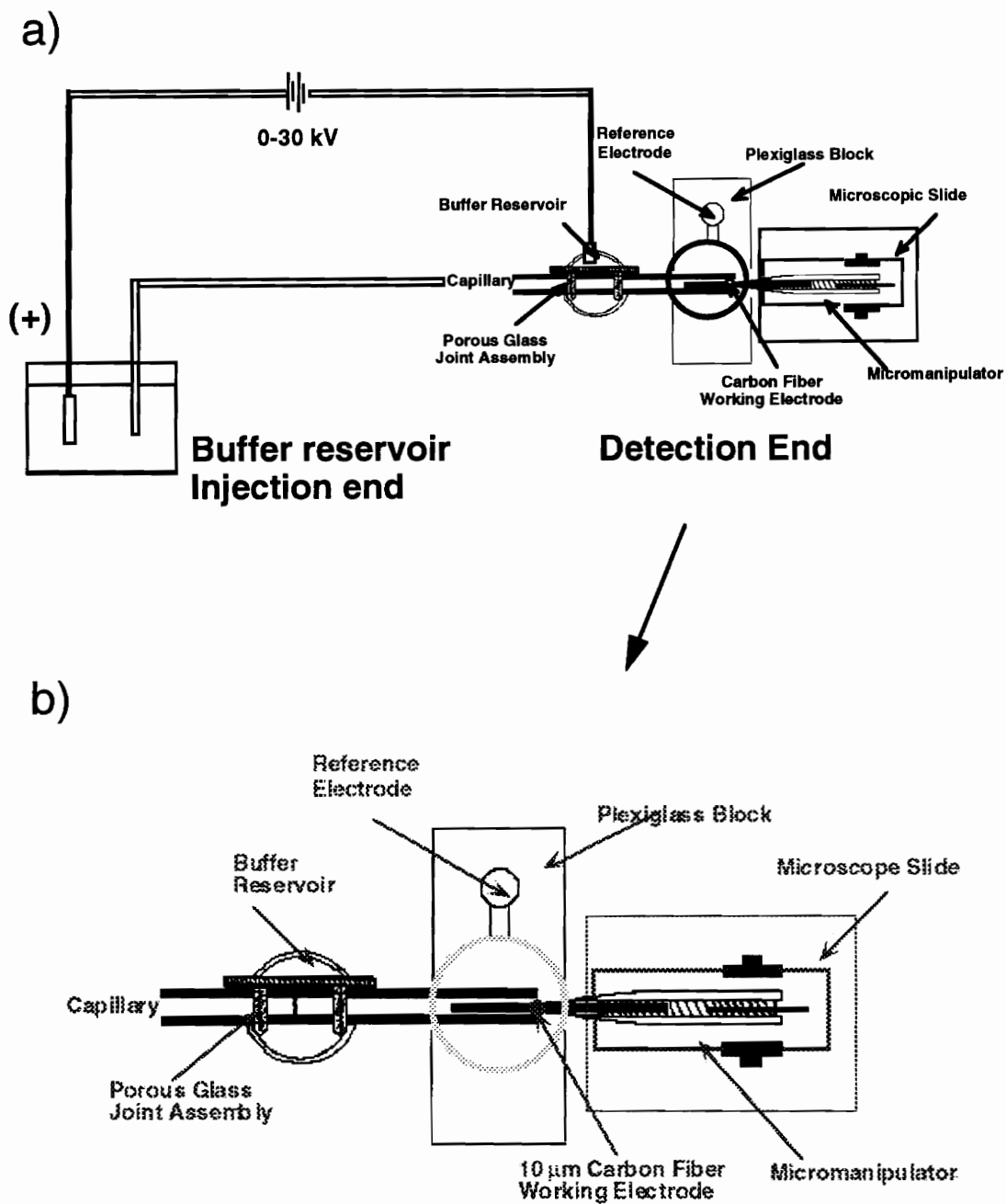
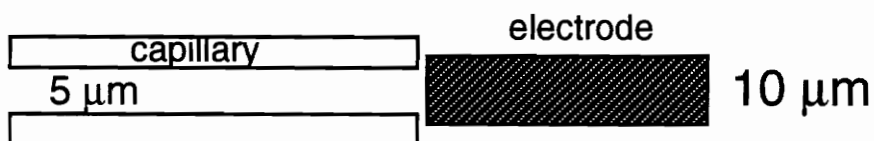
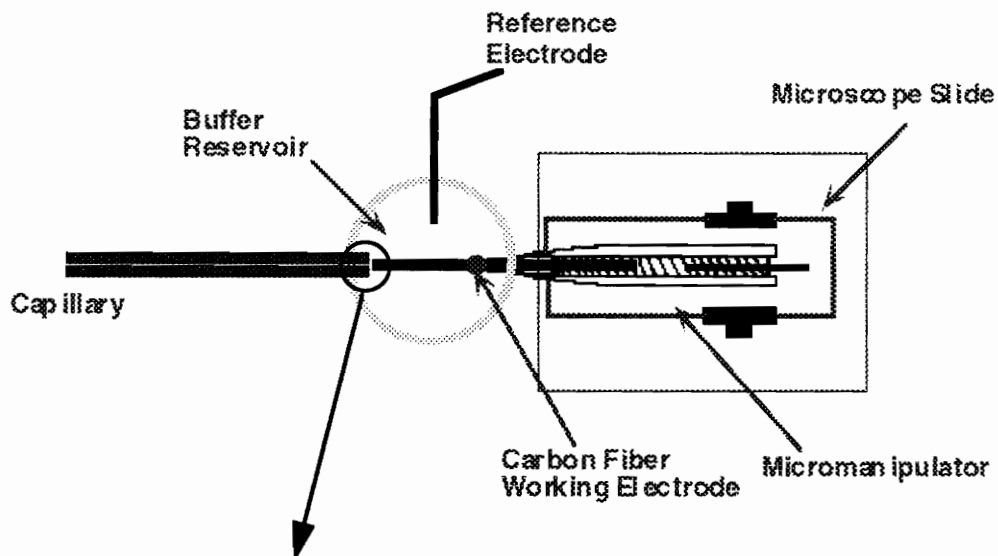


Figure 4.5: Capillary Electrophoresis
 Post-column electrochemical detection (115)

a) End column detection



b) Optimized End column detection



Figure 4.6: Capillary Electrophoresis
End column electrochemical detection (118)

a thin layer at the output with a diameter twice that of the capillary, good oxidation efficiencies were achieved. Detection limits as low as 56 attomoles with a linear range of 5×10^{-5} - 5×10^{-7} M. These results, however are tempered by difficulties in placement of the electrode, leading to low precision.

A solution to this problem was proposed by Sloss and Ewing (119) in the form of a conical entrance to the capillary (achieved by etching) (fig. 4.6 b). Although the detection limits were similar to those achieved, the results were more reproducible.

Electrode diameters larger than the diameter of the column have recently been investigated (119), and efficiencies for different electrode positions at the end of the capillary were found to be highly dependent on electrode placement. Lu and Cassidy (120) reported a potential gradient that formed at the end of fused silica capillaries (important only for 25 μm and larger) exposing the working electrode to significant potential fields, and rapidly changing the electrodes physical appearance. This lead them to the investigation of the various electrode positions relative to the capillary concluding that the best efficiencies are obtained when the electrode is inserted into the capillary. With the capillary inserted, the influence of analyte diffusion and convection currents are minimized.

Although electrochemical detection is a highly sensitive method it's selectivity limits the range of observable analytes. Much research intended to expand this range involves the use and development of different electrode materials and detection schemes (122-124)

4.3.4. MASS SPECTROMETRIC DETECTION

Mass spectrometric detection for CE is recently gaining much attention and developing very rapidly. Since it was first reported by Olivares et al (125) the earlier problem of interfacing has now been eliminated only to be succeeded by the lack of sensitivity. There are two popular ionization techniques currently under investigation, Electrospray (ES) and Fast Atom Bombardment (FAB).

Smith and co-workers (125-127) developed an interface based on the electrospray ionization technique developed by Mack et al (128) and Whitehouse et al (129). Figure 4.7 is a schematic of this interface. A metal needle attached to the capillary or a thin film of metal is deposited on the column end and provides the electrical contact with the buffer solution. Electrospray ionization is performed at atmospheric pressure and at a voltage slightly higher than ground. The technique requires make-up flow to elevate the total flow to 1-10 μ l. This can be achieved either by passing heated N₂ across the electrospray through a coaxial sheath flow that provides a slight vacuum, or through a liquid 'T' junction where make-up buffer is introduced using a syringe pump.

Analyte sensitivity and the quality of the mass spectrum obtained depend on the ESI voltage, the buffer composition, the nebulizer efficiency and the ion focusing parameters. One of the biggest problems facing sensitivity of this technique is cluster formation, a phenomenon that occurs when using aqueous buffers.

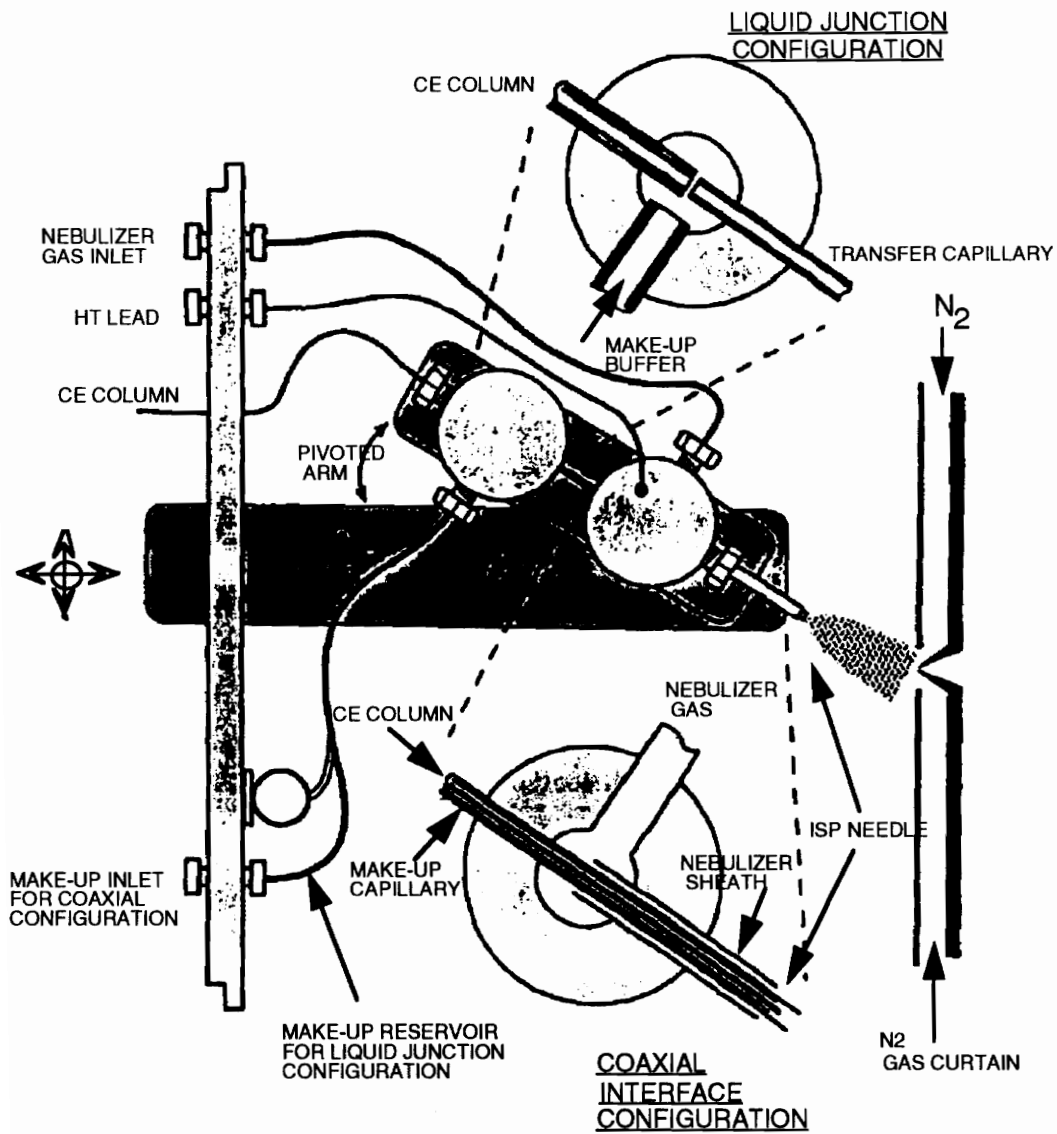


Figure 4.7 : Schematic of liquid junction and coaxial interface between CE and MS
 J. Chrom. 591,325 1991.

To date this technique has been applied to quaternary ammonium salts, dipeptides, amines, proteins, carbohydrates, pesticides, small organic and inorganic molecules (125-127). Future developments will probably lie in volatile organic based buffers.

4.3.5. INDIRECT DETECTION

Indirect detection is gaining more acceptance as a universal detection mode, in CE. The signal is derived from a reduction in the background electrolyte instead of the analyte itself. The background buffer is added in such concentrations, low enough so as not to over saturate the detector but high enough to affect a proper separation. In addition, the buffer's mobility has to be close to that of the analytes for minimum electrodispersion effects and higher efficiencies. Common buffers include chromate, benzoic acid, phthalates, salicylate, benzoate and p-hydroxybenzoate. The analyte, when added, displaces the background buffer resulting in a decrease in the available signal and consequently a negative peak in the electropherogram. Indirect UV absorbance, indirect fluorescence as well as indirect amperometry, have been reported (130).

CHAPTER V

EXPERIMENTAL

5.1. MEKC OF PUNGENT COMPOUNDS USING SIMULTANEOUS ON-LINE ULTRAVIOLET AND MODIFIED ELECTROCHEMICAL DETECTION

5.1.1. Apparatus and Instrumentation.

The instrumentation used for this work is pictured in Figure 5.1. The experiments were performed using a home built CZE system. A high-voltage power supply, Spellman CZE 1000 R (Spellman, Plainview, NY), provided the variable voltage of 0-30kV. The power supply is equipped with a home built (Virginia Tech) variable timer for electrokinetic injections.

The fused silica capillaries (Scientific Glass Engineering, Austin TX) of 100 μm and 25 μm id were 65 cm in length with the transparent window for the on-column detection at 45 cm. The window was made by burning off approximately 2 mm of the polyimide coating, following the procedure of Schomburg et al (131), using a gas chromatograph glow plug. The capillary surface was regenerated constantly by first flushing it with 0.1 M NaOH for two minutes, then with 0.01M NaOH for two more minutes followed by five minutes of de-ionized doubly distilled water and finally for five minutes with the running buffer. Flushing with pressure was found to be more efficient for the smaller diameter columns over the conventional suction under vacuum. This was achieved using a GC capillary solvent reservoir (Alltech, Deerfield IL), which was filled with the flushing solution and connected to an air cylinder, under

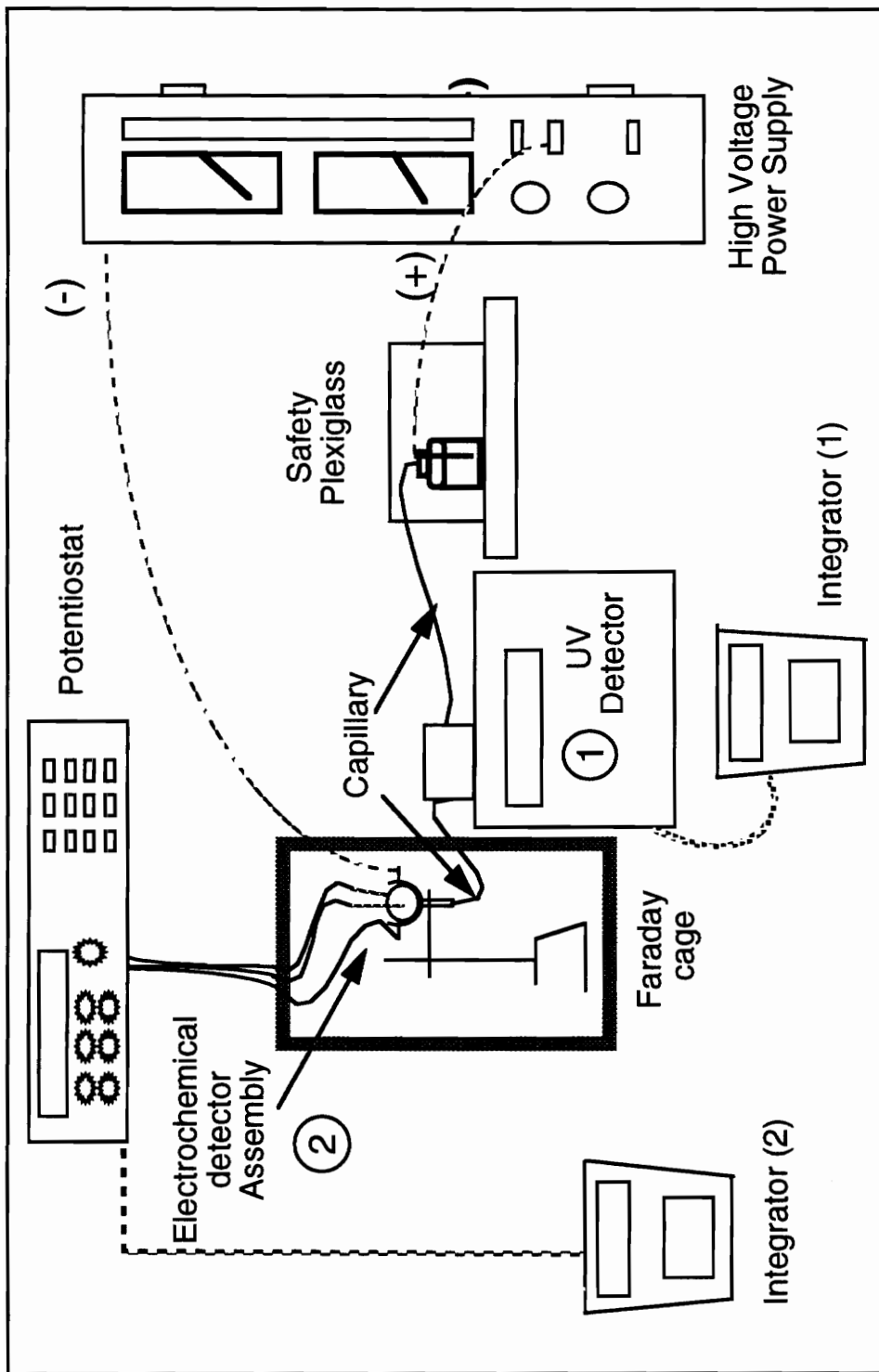


Figure 5.1: Experimental set up for simultaneous on-line UltraViolet and Electrochemical detection

pressure of approximately 60 psi. The fused silica capillary was immersed into the solution in the reservoir. During analysis, one end of the fused silica capillary was immersed into one buffer reservoir, at the high voltage end of the system (anode). This 'live' end is usually housed in the Plexiglass box equipped with a safety interlock, to prevent operator shock (~100 μ m Amps). Samples were introduced electro-kinetically at this end of the capillary.

For UV detection, a Linear model 206 stand alone PDA detector (Spectra Physics, Fremont CA) equipped with a micro quartz lens cell was used. The detector was laid sideways for capillary insertion convenience and the capillary was threaded through the flow cell and secured with Upchurch PEEK nuts and 320 μ m tees (Upchurch Scientific, Oak Harbor, WA)

The ground end of the column, 15 cm from the UV detector was entered into a three electrode configuration wine cup cell design through a pre-punctured GC septa (Hewlett Packard, Palo Alto, CA), Figure 5.2. This cell also acted as the buffer reservoir for the MECC ground end. A working carbon fiber microelectrode (BAS, West Lafayette, IN) was inserted into the electrochemical cell and butted to the capillary outlet. The micro hed between runs with Gamma micropolish #3 (0.05 microns) Alumina A (Buehler, Lake Bluff IL) to remove adsorbed impurities. The polishing is carried out in a figure 8 circular motion to keep the electrode glass surface as flat as possible. Both 33 and 10 μ m diameter carbon electrodes were tested. Refined adjustments were made using a micromanipulator with the aid of a (x50) pocket microscope (Edmund Scientific Co., Barrington NJ.) clamped to a stand. The distance of the capillary from the working electrode was adjusted by first butting the two together, then applying pressure to the other end of the capillary. The thrust of emerging liquid

**REFERENCE
ELECTRODE**

**WORKING
MICROELECTRODE**

**MICRO-
MANIPULATOR**

**MECC
GROUND**

**AUXILIARY
ELECTRODE**

CAPILLARY

Figure 5.2: Modified Amperometric Electrochemical Detection Cell - 88

pushed the capillary end away from the electrode a reproducible distance. This distance proved sufficient to prevent suppression of electroosmotic flow (caused by back pressure due to blockage), but close enough for peak detection and symmetry.

Two platinum wires implanted in the glass reservoir and protruding about 1cm outside, acted as the auxiliary electrode and the MECC ground connections. A sodium saturated Ag/AgCl electrode was used as the reference electrode. When KCl was used as the electrode cell electrolyte it precipitated the SDS in the MECC buffer (132). The KCl was replaced, by a saturated solution of NaCl. Due to the need for measurements of very low currents, the entire electrochemical detector assembly was housed in a Faraday cage.

The potential of the working electrode was controlled with an EG & G PAR model 273 Potentiostat (Princeton Applied Research, Princeton ,NJ.). Hewlett Packard 3390 and 3394 integrators were used for the recording of the dual outputs. UV spectra of the capsaicins and the piperines were obtained using a Perkin Elmer 235 array detector system (Perkin Elmer Cooperation, Norwalk CT).

5.1.2. Chemicals.

Fresh 0.01 M borate buffer pH 9.2 (Aldrich Milwaukee, WI), 5 mM phosphate pH 7.2 and 20 mM MES buffer (2-morpholine ethene sulfonic acid) pH 6.2 (Sigma Chemical Company, St. Louis, MO) were prepared fresh with nanopure deionized and filtered water (Millipore, Bedford, MA). HPLC grade methanol and acetonitrile (Fisher Scientific, Pittsburg, PA) were used. 50 mM Sodium dodecyl sulphate SDS (Sigma Chemical Company, St. Louis, MO) was

used as the surfactant. Prior to use, all phases were filtered daily through 0.2 μm nylon filters (Supelco, Bellefonte, PA).

Stock solutions of 0.01 M Capsaicin (C), dihydrocapsaicin (DC) , piperine (P), homovanillic acid (HVA) and hydroquinone (H) (Sigma Chemical Company, St. Louis, MO) were prepared in 50:50 methanol : buffer solutions. Care has to be taken when using capsaicin as it is a powerful irritant with acrid vapors. Stock solutions of 0.01 M dopamine (D) and 3,4 dihydroxybenzylamine (DBA) (Sigma Chemical Company, St. Louis, MO) were prepared in 0.1 M perchloric acid and diluted with the MES buffer.

5.2. CAPILLARY ZONE ELECTROPHORETIC SEPARATION OF ISOMERIC BENZOIC CARBOXYLIC ACIDS; THE EFFECT OF ADDITIVES.

5.2.1 Apparatus

Two commercially available instruments were used to perform this work. The first was a Spectraphoresis 1000 system and software (Thermoseparations, Fremont, CA). Low Inertial Scanning (LIS) UV/VIS capabilities, three dimensional plots, offering electropherogram as well as UV spectral information, are possible with this system. LIS allows rapid movement of the holographic grating to focus on a single photodiode, as opposed to the PhotoDiode Array (PDA) instruments, where a fixed grating diffracts light to an array of photodiodes. UV spectra of all analytes were collected from 200-350 nm for identification. The anodic buffer is stored in a large reservoir (250ml or 500ml) that is constantly sparged (for bubble removal) in between runs, and is used to flush the anodic reservoir with fresh buffer in between runs. The cathodic buffer remains unflushed.

A second instrument, also used to continue this work, was a Beckman P/ACE 2100 and it's Gold software (Beckman, Fullerton, CA). It's UV detector employs a deuterium lamp with wavelength selection by filters. Only one wavelength can be monitored at any one time. The capillary housed in a cartridge is liquid peltier cooled. No external reservoir is available and the buffers are not replenished or sparged.

Fused silica capillary columns (Polymicro Technologies Inc., Phoenix, AZ), were 50 μm in internal diameter and were 44 / 38 cm long when using the Spectraphoresis system but 55 / 57 cm long when using the Beckman system.

The differences in length were due to instrumental limitations of the cartridge design. The capillaries in both instruments are housed in a cartridge and (peltier) cooled with forced air in the Spectraphoresis system but with fluoroorganic fluids in the Beckman system.

5.2.2. Materials

Cetyltrimethyl ammonium bromide (CTAB), tetrabutylammonium bromide (TBAB), dodecyltrimethylammonium bromide (DTAB), α , β and γ cyclodextrin, sodium tetraborate and benzoic acid (BA), 1,4-benzenedicarboxylic acid (terephthalic acid (TA)), 1,3-benzenedicarboxylic acid (isophthalic Acid (IA)), 1,2-benzenedicarboxylic acid (phthalic acid (OA)), 1,2,3-benzenetricarboxylic acid (hemimellitic acid (HMLA)), 1,2,4-benzenetricarboxylic acid (trimellitic acid (TMLA)) and 1,3,5-benzene tricarboxylic acid (trimesic acid (TRA)), were all obtained from Sigma (Sigma Chemical Co., St. Louis, MO). Methanol and acetonitrile were obtained from Fisher (Fisher Scientific, Pittsburgh, PA). The 1N NaOH solution is from Aldrich (Aldrich, Milwaukee, WI). De-ionized doubly distilled water was obtained from Millipore (Millipore, Bedford, MA). All solutions were prepared fresh and always filtered through 0.45 μm filters, (Supelco, Bellfonte PA).

5.2.3 Procedure

A standard 80 ppm mixture of all the acids was prepared by dissolving 800 ppm of each acid in basic water (pH 13) diluting and filtering using a 0.45 μm filter. Fresh borate buffer is prepared as it's boric acid

equivalent (207), where 0.05 M borate is prepared by weighing (0.05 / 4) M sodium tetraborate hexahydrate (also known as Borax).

Triplicate, 1 sec, 30 mbar hydrodynamic injections were made when using the Spectraphoresis instrument (2 sec, 0.5 psi when using the Beckman). Based on the UV spectra, two different wavelengths 210nm and 235nm were constantly monitored to confirm the identities of the peaks (214 nm filter with the Beckman). All electropherograms were obtained at 25°C, unless otherwise stated.

The capillary, after burning off 2mm of the polyimide and installing it into the respective instrument's cartridge, was prewashed with 0.05 M NaOH for 1min; de-ionized, distilled water for 2 mins; and finally with the running buffer for 4mins, before every analysis.

A number of electrolyte systems of varying pH, buffer concentration as well as additive content were investigated and compared for their selectivity, efficiency and resolution of the mono-, di- and tri-carboxylic acids. Some industrial samples from a confidential source were run to test the ruggedness of the electrolyte systems and the methods.

5.3. EVALUATION OF AN OLIGOMERIZED SODIUM UNDECYLENATE AS A SURFACTANT FOR THE SEPARATION OF VITAMINS.

5.3.1. Apparatus

The HP ³DCE (Hewlett Packard, Littlefalls, DE) system used for this work, is equipped with a photodiode array detector (2nm spectral resolution) that has been especially developed for capillary electrophoresis. The optical part of the detector has been optimized for both standard capillaries and HP's extended light path capillaries with inner diameter of 50 and 75 μm . The HP ³DCE Chem station, which controls the system, enables full spectral information to be retrieved as well as single wavelength and multiwavelength detection. Peak purity algorithms and spectral library searches can greatly facilitate method development in CE. The peak purity function can be especially useful for differentiating peak shapes distorted by mobility differences between analytes and running buffer from those that represent actual impurities.

The extended light path capillaries (the Bubble Cell, figure 4.3) contain a three times expanded diameter section (bubble) at the point of detection offering a three fold increase in sensitivity over the 'straight' capillaries. In the region of the bubble the electrical resistance is reduced and thus the field is decreased. Moreover, the flow decreases because of the expanded volume. On entering the bubble region, the sample front speed is reduced and the zone stacks as it shrinks. The sample zone expands radially (across the capillary) and contracts longitudinally (along the capillary), with a constant total volume. The zone concentration is unchanged but the optical pathlength is increased three fold.

The capillary used in this work (Hewlett Packard, Little Falls, DE) was 50 μm in internal diameter, 64 cm long with the transparent straight (or bubble cell) window at 56 cm. A temperature of 25°C was maintained with a peltier forced air convection system.

5.3.2. Material

Of each of the water soluble vitamins Riboflavin (B2), Ascorbic acid (C), Niacinamide (B3), Thiamin (B1), Pyridoxine, Pyridoxal and Pyridoxamine (B6) and Cyanocobalamin (B12), 200-400 ppm were prepared in water, while saturated solutions of the fat soluble Retinol (A) (70% all trans), and (\pm)- α -Tocopherol (E) (95%), were prepared in 20% methanol: buffer solutions (Aldrich, Milwaukee, WI). Vitamins are not the easiest compounds to work with as indicated by Table 5.1. Much of the sample preparation had to be carried out under low light conditions and had to be stored in amber vials which were consistently flushed with He after usage.

All solutions were prepared fresh and always filtered through 0.45 μm filters (Supelco Bellefonte, PA). Fresh 0.1M sodium tetraborate decahydrate (99%) buffer (Borax) was prepared as it's boric acid equivalent, and mixed with 0.05 M disodium hydrogen phosphate buffer to provide the appropriate pH (Sigma Chemical Co., St. Louis, MO). Assuming a molecular weight of 2000 (10 monomer units), 0.01 g/ml of the synthesized oligomer sodium 10-undecylenate (UDO) was weighed into solution to give 0.005 M. A comparison of the vitamin separation was made using three different surfactants, the oligomer, sodium 10-undecylenate (SUA 98%) and sodium dodecylsulphate (SDS 98%) (Sigma).

Table 5.1: Vitamin Stability Conditions

VITAMINS	pH=7	pH<7	pH>7	O ₂ / Afr	Light	Heat
RETINOL (A)	S	U	S	U	U	U
TOCHOPHEROL (E)	S	S	S	U	U	U
ASCORBIC ACID (C)	U	S	U	U	U	U
COBALAMINE (B12)	S	S	S	U	U	S
THIAMIN (B1)	U	S	U	U	S	U
RIBOFLAVIN (B2)	S	S	U	S	U	U
PYRIDOXINE (B6)	S	S	S	S	U	U
PYRIDOXAL (PL)	S	U	S	U	U	U
PYRIDOXAMINE (PN)	S	U	S	S	U	U
NIACINAMIDE (B3)	S	S	S	S	S	S

S=Stable, U= unstable.

concentration plot still exhibited an inflection point (0.1 M) similar to the cmc inflection induced by formation of micelles. This, however, has been attributed to the onset of intramolecular micellar aggregation ().

The intrinsic viscosities of aqueous solutions of the monomeric and polymerized material have shown that the polymerized micelle has a hydrated size equal to the size of the monomeric micelle (177).

Fluorescence studies with the micropolarity probe pyrene show that the fluorophore penetrates the intermolecular polymeric micelle less than the monomeric one. This is expected of the more compact structure of the polymeric micelle due to the presence of polymerization-induced covalent bonds among the terminal methylene groups of the undecylenate chains (177).

The present study involves characterization of this sodium 10-undecylenate oligomer synthesised by free radical initiation instead of γ radiation. Carbon-13 and proton NMR studies are used to confirm the structure molecular weight and aggregation number. Molecular interactions with a number of vitamins are used to shed some light on the oligomer's behavior as a MECC surfactant.

6.3.2. Oligomeric synthesis and NMR characterization

The synthesis of the polymer in this work has followed the procedure of Dujurai and Blum (133) as detailed in the experimental section. The polymerization is induced by catalytic initiation using potassium persulfate instead of γ radiation. The achieved yield was 7% (2.67g) which is low but generally expected from free radical polymerization of α -olefins, which additionally result in low molecular weight oligomers due to autoinhibition by allylic hydrogens (178).

Methanol, ethanol and acetonitrile were used as organic modifiers (Fisher Scientific, Pittsburgh, PA). De-ionized doubly distilled water was obtained from Millipore (Bedford, MA). All solutions were prepared fresh and always filtered through 0.45 μm filters, (Supelco, Bellfonte PA).

5.3.3. The Oligomer synthesis

The undecylenate oligomer (UDO) was oligomerized according to Dujairaj and Blum (133). Into a three necked 200 ml round bottomed flask, fitted with a nitrogen inlet (at the top of a distillation column), a thermometer and magnetic stirrer, were added 40 g of sodium undecylenate, 80 ml of deoxygenated water (2.5 M carboxylate salt) and 1.2 g (4 mmols) of potassium persulfate. The reaction mixture was heated to 65-70 $^{\circ}\text{C}$ for about 50 hours while the contents of the flask were stirred under a continuous flow of nitrogen. Care has to be made to ensure efficient mixing. The reaction mixture was then poured into a beaker of previously cooled 0 $^{\circ}\text{C}$ ethanol (Fisher Scientific, Pittsburgh, PA), 400 mls, to precipitate the oligomer. The oligomer (a white product) was filtered washed several times with 20 ml aliquots of cold ethanol, and dried under vacuum at 65 $^{\circ}\text{C}$ to give a whitish crispy powder. The product yield for the batch used was calculated to be approximately 7 % (2.65g). The reaction is depicted in figure 5.3.

Carbon-13 and Proton NMR were measured for two preparations of the oligomer dissolved in D_2O (Aldrich, Milwaukee, WI), on Varian Unity 400 (Varian, Palo Alto, CA), at a frequency of 100.57 MHz and 399.95 MHz respectively. The ^{13}C NMR chemical shifts were measured relative to TSP 3-

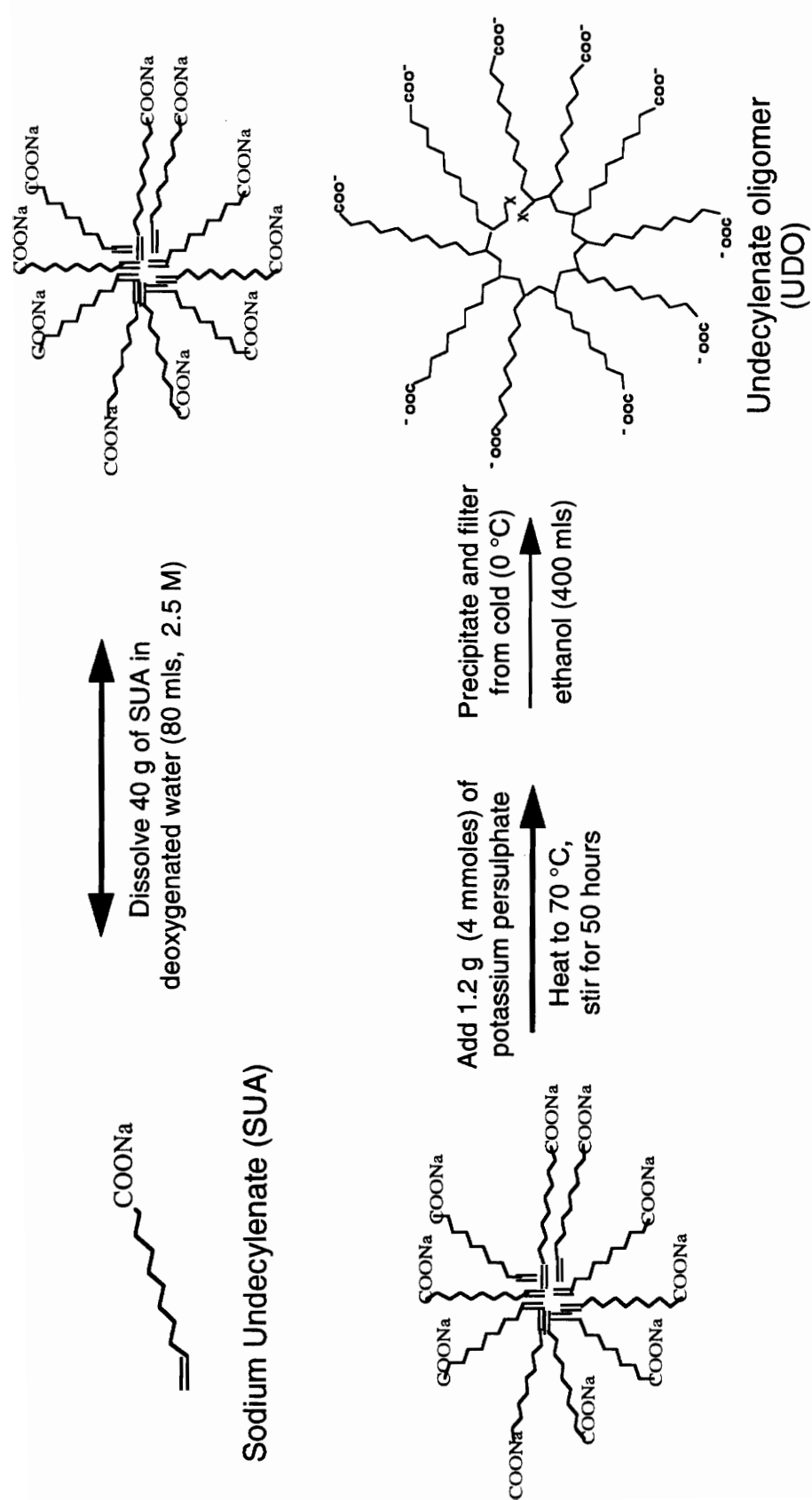


Figure 5.3: Synthetic Scheme for Oligomeric Sodium Undecylenate (UDO).⁽³⁾

(trimethylsilyl)propionic acid, sodium salt (Aldrich, Milwaukee, WI). For the ^{13}C NMR 80 mg were used while 5 mg were used for the ^1H NMR.

5.4. THE SEPARATION OF PHOSPHOLIPIDS AND THEIR USE AS SURFACTANTS IN MICELLAR ELECTRO-KINETIC CHROMATOGRAPHY.

5.4.1. Apparatus

The experiments were performed using a home assembled CZE system (fig. 1.2). A high-voltage power supply, Spellman CZE 1000 R (Spellman, Plainview, NY), provided the variable voltage of 0-30 kV. For UV detection, a Linear model 206 stand alone PDA detector (Thermo Separations Products, Fremont, CA) equipped with a micro quartz lens cell, was used. The detector was laid sideways for capillary insertion convenience and the capillary was threaded through the flow cell and secured with Upchurch PEEK nuts and 320 μm tees (Upchurch Scientific, Oak Harbor, WA). Detection was set at 210 nm.

The fused silica capillaries (Scientific Glass Engineering, Austin TX) of 75 μm id were 65 cm in length with the transparent window for the on-column detection at 45 cm. The capillary surface was regenerated constantly by first flushing it with 0.1 M NaOH for two minutes, then with 0.01M NaOH for two minutes followed by five minutes of de-ionized doubly distilled water and finally for five minutes with the running buffer.

During analysis, one end of the fused silica capillary was immersed into one buffer reservoir, at the high voltage anode end of the system. This 'live' end is usually housed in a Plexiglass box equipped with a safety interlock, to prevent operator shock ($\sim 100 \mu\text{m}$ Amps). Samples were introduced hydrodynamically through siphoning. The other end of the capillary was

immersed in the other buffer reservoir, the cathode. Care has to be taken to maintain the reservoir levels at equal height during the analyses. Variations in temperature were achieved by simple heating of the buffer solutions to 30°C immediately before use.

5.4.2. Chemicals

For use as surfactants, D- α -Phosphatidylcholine (PC) (dipalmitoyl, synthetic, 99%), L- α -Lysophosphatidylcholine (LPC) (lauroyl, 99% synthetic), DL- α -Lysophosphatidyl-L-serine (LPS) (primarily stearic, bovine brain, 99%), and DL- α -Lysophosphatidyl-DL-glycerol (LPG) (palmitic and stearic, 99%), (Sigma Chemical Company, St. Louis, MO), were all stored at 0°C. Aqueous solution of the above surfactants with concentrations of 2.5 and 1.25 mM (LPC), 0.6 mM (LPS), and 1.6 mM (LPG) were stored in amber vials, purged with He and prepared fresh daily. Various concentrations of sodium dodecyl sulfate SDS (98%) were prepared as indicated in the text.

Analytes investigated for separation by the above surfactant solutions included a homologous series of alkyl parabens, methyl, ethyl, propyl, butyl and heptyl, (Sigma Chemical Company, St. Louis, MO). The red dye, Sudan III (Sigma) was used for t_{mC} verifications, while methanol (Fisher Scientific, Pittsburg, PA) was used for t_0 measurements.

Both sodium phosphate as well as sodium tetraborate hexahydrate buffers (Sigma Chemical Company, St. Louis, MO) were prepared fresh daily with pH adjustments increased using NaOH, or decreased using phosphoric or boric acids respectively. De-ionized doubly distilled water (Millipore, Bedford, MA) was used at all times and all solutions were filtered before use, through 0.45 mm nylon filters (Supelco, Bellefonte, PA).

For the separation of the phospholipids themselves the following: a) phospholipids; Sphingomyelin (SM) (mainly palmitic, chicken egg yolk, 99%), L- α -phosphatidylethanolamine (PE) (sheep brain, commercial grade), L- α -phosphatidylcholine (PC) (dioctanoyl, synthetic, 99%), L- α -phosphatidylcholine (PC) (didecanoyl, synthetic 99%), L- α -phosphatidylcholine (PC) (dilauroyl, synthetic, 99%), L- α -phosphatidylcholine (PC) (dimyristoyl, synthetic, 99%) L- α -phosphatidyl-L-serine (PS) (dipalmitoyl, synthetic, 99%) and; b) lysophospholipids; DL- α -Lysophosphatidyl-L-serine (LPS) (primarily stearic, bovine brain, 99%), and DL- α -Lysophosphatidyl-DL-glycerol (LPG) (palmitic and stearic, 99%), L- α -Lysophosphatidylcholine (palmitic and stearic, egg yolk), L- α -Lysophosphatidylcholine (lauroyl), L- α -Lysophosphatidylcholine (myristoyl) (Sigma Chemical Company, St. Louis, MO) were investigated.

Additives to the buffer included the surfactants sodium dodecylsulfate SDS (Sigma) and sodium tetradecylsulfate (STDS) (Aldrich, Milwaukee, WI), the base choline chloride (Sigma Chemical Company, St. Louis, MO) as well as the organic modifier, methanol (Fisher Scientific, Pittsburg, PA).

5.5. THE ANALYTICAL SEPARATION OF *TRICHODERMA REESEI* CELLULASES BY CAPILLARY ZONE ELECTROPHORESIS; MANIPULATION OF THE OPERATING CONDITIONS.

5.5.1 Apparatus

Two instruments were used in this work an H.P.^{3D}CCE (Hewlett Packard, Avondale CA), and an abi model 270A-HT (Applied Biosystems of Perkin Elmer, Norwalk CT). While both systems attempt to improve sensitivity through extended light path capillary design with the bubble cell for the HP system and the Z-cell of the abi system (fig. 4.3), their capillary formats are different. The HP^{3D}CCE capillary can come in the two common internal diameters (50 μm , 75 μm) with the bubble cell three time the id. The capillary is housed in a cartridge and peltier heated with forced air. The abi uses only the 75 μm id with it's Z-cell (not lower capillary ids due to the fear of clogging and not larger ids for fear of efficiency loses). The cartridge hangs loose with forced air convection heating.

The detection for the HP system is a UV photodiode array with multiple tasking software support. The abi detects with a multiple UV detection using interchangeable deuterium and tungsten lamps.

When using the HP system the capillary was 50 μm in internal diameter, bubble cell 150 μm id and 56/60 cm long. The capillary installed in the abi system was 75 μm in internal diameter with a 3mm Z-Cell and 60/80 cm long.

Injection with the HP was for 3 sec under a pressure of 50 mbar, while when using the abi it was for 1 sec.

Several coated columns were used: 1) the J&W μ Sil 50 μ m 75/100 cm long (J&W, Folsom, CA), 2) the CElect-P175 and 3) the CElect-H75 both 75 μ m in id and 65/100 long (Supelco, Bellefonte PA).

5.5.2 Materials

Standard samples of the cellulase enzymes used were a culture filtrate of the fungi, *Trichoderma Reesei* obtained and purified at Iogen (Iogen Corporation, Ottawa, Canada). The cellulase complex contains three types of components: 1) 1,4- β -D-glucanohydrolases (endoglucanases, EG); 2) 1,4- β -D-glucan cellobiohydrolases and 1,4- β -D-glucan glucohydrolases (exoglucanases, CBH); and 3) β -D-glucoside glucohydrolases (β -glucosidases). Methods of their preparation and purification are confidential. However, such information is not crucial at this stage. The standards (CBH II 20g/l, EG I 39g/l, EG II 20 g/l and CBH I 33g/l) were diluted a hundred fold (CBH II was diluted only 50 times). Phosphate buffer and alkyl sulfonate (Aldrich, Milwaukee WI) were prepared as usual with de-ionized doubly distilled water (Millipore, Bedford, MA). Changes in pH were made with NaOH (Aldrich, Milwaukee WI) and phosphoric acid (Fisher Scientific, Pittsburgh, PA). All solutions were prepared fresh and always filtered through 0.45 μ m filters (Supelco, Bellefonte PA).

The capillary, after burning off 2 mm of the polyimide and installing it into the respective instrument's cartridge, was regenerated with 0.05 M NaOH for 1 min; de-ionized, distilled water for 2 mins; and finally with the running buffer for 4 mins, before every analysis. This regenerating procedure is not recommended for any of the coated capillaries.

CHAPTER VI

RESULTS AND DISCUSSIONS

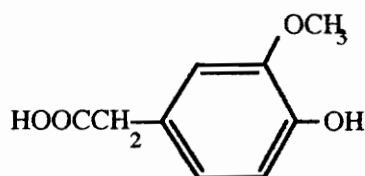
6.1 MEKC OF PUNGENT COMPOUNDS USING SIMULTANEOUS ON-LINE ULTRAVIOLET AND MODIFIED ELECTROCHEMICAL DETECTION.

Spicy foods are a rapidly expanding part of the food industry.

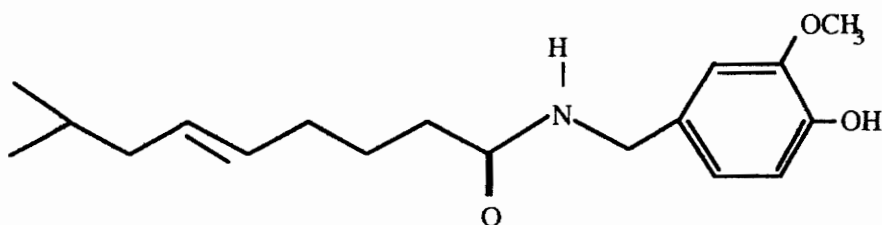
Consequently, the determination of the pungent principles of such products is of increasing interest. Common pungent principles include capsaicin (8-methyl-N-vanillyl-6-nonenamide) and its analogues, the capsacinoids. Found in the capsicum fruit, hot red and green peppers (134), capsaicin (C) and dihydrocapsaicin (DC) constitute more than 90 % of the burning taste of these foodstuffs (135). The compounds occur in some herbs and spices, such as oregano, cilantro and cinnamon. The capsacinoids (Figure 6.1), associated with other oleoresins, they are a powerful irritant with acrid vapors. Another, frequently co-existing pungent principle, piperine (2-trans-4-trans-N-piproylpiperidine) (Figure 6.1), is a common ingredient of Black Pepper (136). On exposure to light piperine is photoisomerised to its non pungent isomers, Chavicine (cis-cis), isochavicine (trans-cis) and isopiperine (cis-trans).

These two classes of compounds, the capsacinoids and piperines, produce a burning taste and induce a long lasting desensitization of the primary taste neurons and mucus membranes through excitation of the pain receptors on the tongue and in the mouth. To reduce such irritations the brain causes the

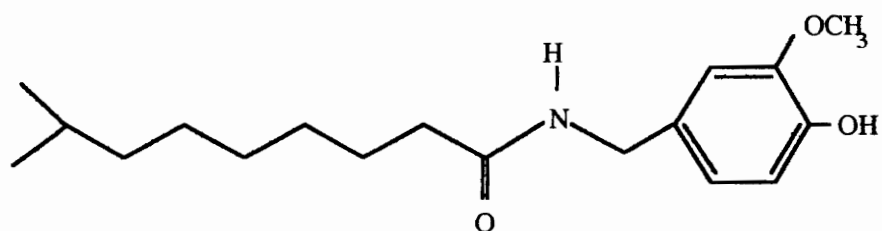
**HOMOVANILLIC ACID
(HVA)**



CAPSAICN (C)



DIHYDROCAPSAICN (DC)



**PIPERINE (P)
trans-trans**

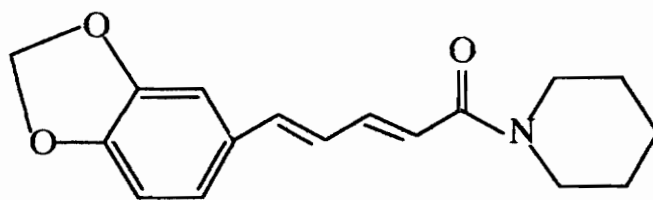


Figure 6.1 : Molecular structures of the pungent compounds

mouth to salivate, the nose to run and the gastrointestinal track to work hard, while the body sweats to cool itself. One explanation of the chili addiction is that when the body encounters pain, the brain secretes endorphins, an excess of which causes a feeling of pleasure (135).

In addition to their importance in the food industry, interest in capsaicins has been directed to their chronic and acute toxicity, their effects on the nervous system, and their nutritional benefits (137). Exerting its major pharmacological effects on C-fiber afferent sensory neurons, capsaicin's action results in a series of responses which range from stimulation of the sensory fibers to irreversible destruction of the nerves. This biological activity has been attributed to metabolic changes of the 4-hydroxy-3-methoxy benzyl(vanillyl) group (138,139). Further more, capsaicin is of importance to plant biochemists as the suspected dimer, formed through oxidation, cross links plant cellular and subcellular components (140).

Various methods of detection and quantitation of these pungent compounds have been attempted in the past. These have included High Performance Thin Layer Chromatography (141), Gas Chromatography (135,142,143) and HPLC (136,144). These methods either suffer from sample decomposition, laborious sample preparation, long analysis times and or poor resolution, especially when the capsaicins coexist with the piperines. In an attempt to achieve total and simultaneous separation of both classes of compounds with short analysis times and to handle ultra small samples typical of pharmacological investigations, the use of Micellar Electrokinetic Capillary Chromatography (MECC) is explored in this work.

MECC, as explained in chapter three, suffers from a limited elution range. Analytes must elute in the time between t_0 (the elution time of an unretained solute) and t_{mc} (the elution time of the micelle). In addition, selectivity for hydrophobic compounds is restricted by the limited variety of useful micelles for MECC applications and the tendency for hydrophobic compounds to partition largely into the micelle, hence eluting close to t_{mc} posing resolution problems. Attempts to overcome these limitations involve addition of organic modifiers to the buffer system (78,145-147) and decreases in the electroosmotic flow (μ_{eo}). The μ_{eo} can be decreased through an increase of the buffer ionic strength (147), adjustment of the buffer pH (88,148) and deactivation of the capillary surface(149).

Another notable limitation for MECC lies in detection sensitivity. The path length across CE capillaries is very narrow (typically 50 μm), limiting sensitivity of the on-column spectroscopic techniques. On the other hand, hydrophobic compounds have poor solubilities in the largely aqueous phases of MECC, hindering detection of low concentrations. As a result, detection limits are in the range of 1 ppm. Much attention is devoted to the development of more selective and sensitive techniques, such as Laser Fluorescence (150,151) and Electrochemical detection (115-118, 152-153).

The capsaicins and the piperins are both electrochemically active and are easily oxidized. However, there is still much controversy concerning the product structure. The formation of a diketone or a dimer both have been suggested but not conclusively confirmed. The previous electrochemical set-ups referred to earlier are impractical and laborious. An extension of end-column electrochemical detection employing a modified set-up of the

electrochemical cell was found necessary. The unprecedented use of commercially available microelectrodes and larger 25 μm id columns are reported here for the first time. In addition, efficient separation and detection of both the piperine and the capsaicins were achieved using dual simultaneous detection, (UV and ED).

6.1.1. The Chromatography

The separation of the two hydrophobic compounds capsaicin and dihydrocapsaicin required manipulations of several parameters. It was found that 50 mM SDS surfactant and the use of low buffer ionic strength (5 mM phosphate) afforded the best separations in the shortest analysis times. Both 100 μm and 25 μm id fused silica capillary columns were compared (Figure 6.2). Analyte sensitivity was much higher for the 100 μm id column, but high currents and the resultant joule heating effects prevented use of the higher voltages needed for shorter analysis times (eq. 2.9) and better efficiency (eq. 2.14). The limitation of the smaller 25 μm id column lay in the shorter on-column UV cell path length resulting in the need for larger sample injections.

Samples were injected electrokinetically (hydrodynamic injections are not possible with 25 μm id columns) with variations in voltages and times of injection. Injection duration were found to affect peak efficiencies, resolution, shape and (especially evident in 25 μm id columns) elution times (fig 6.3). Intuitively, the longer the duration and the higher the voltage of injection, the deeper the analyte will have traveled into the column before starting the actual separation. This increases greatly the band broadening due to injection (σ_{inj}^2) and the resultant resolution. Injection at 5 kV for 2 seconds afforded the best results (fig. 6.3).

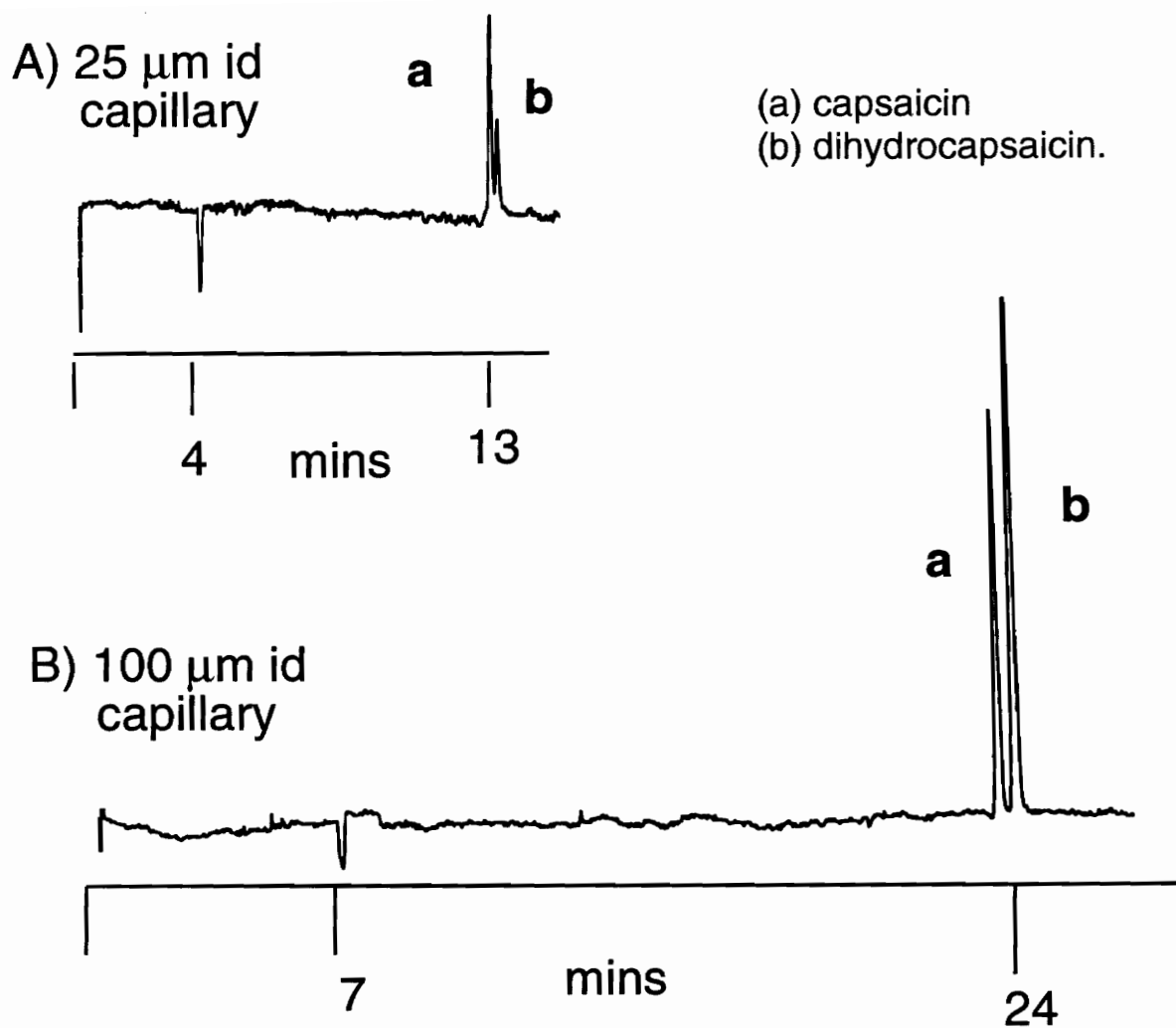


Figure 6.2 : Separation of (a) capsaicin and (b) dihydrocapsaicin.

Conditions: 5 mM Phosphate, 50 mM SDS.

Capillary: L_d 50 cm / L_v 70 cm.

A) Electrokinetic Injection. (5kV / 2 sec)

25 μm id column, 30 KV (4 μA)

B) Electrokinetic Injection (5kV / 6 sec)

100 μm id column, 12 KV (57 μA)

Electrokinetic injection 5kV

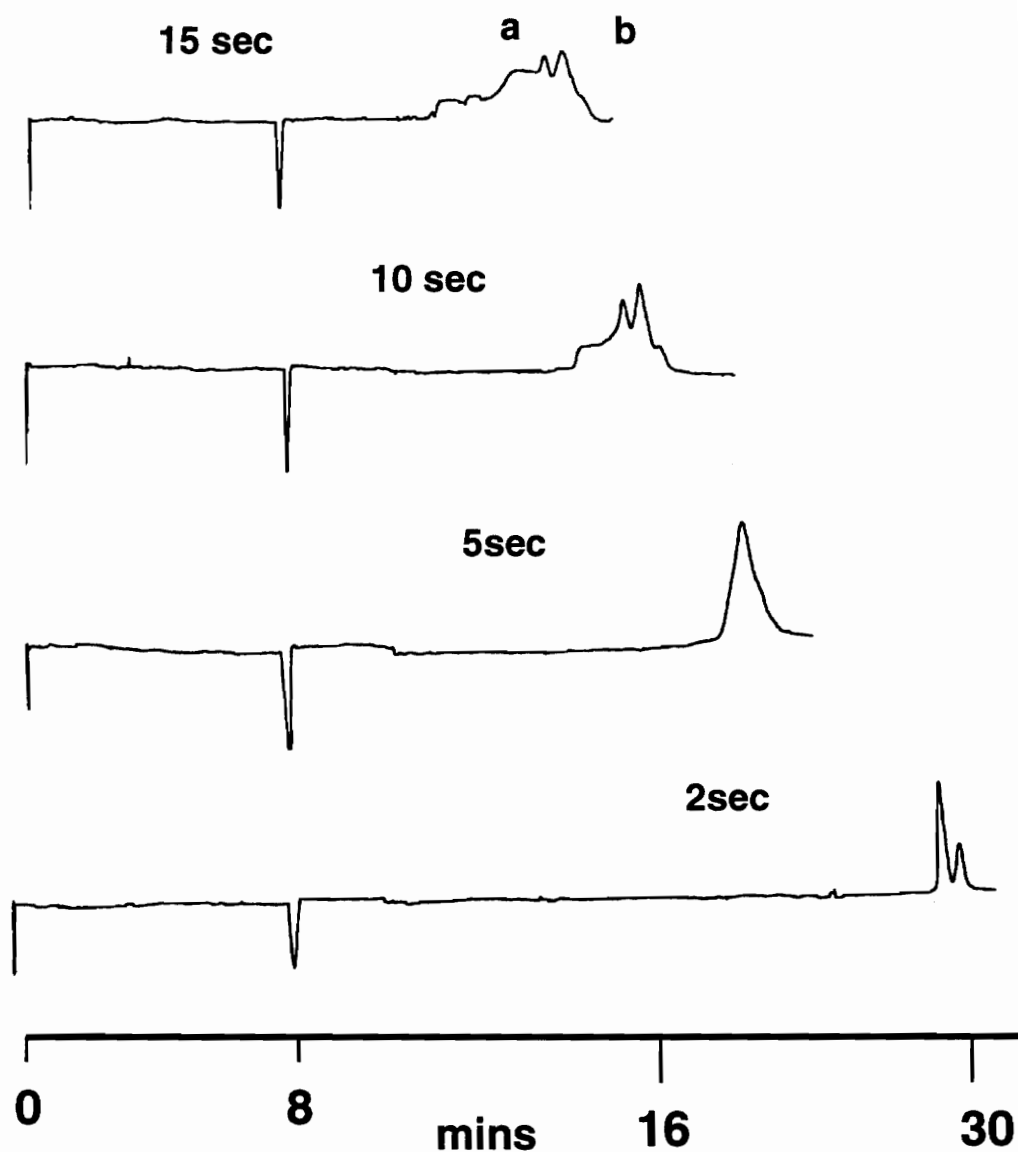


Figure 6.3: Effect of injection time using the 25 μ m id capillary column with conditions as in Figure 6.2 A) and a separation potential of 12kV. (a) capsaicin and (b) dihydrocapsaicin.

As expected from equations 2.9 and 2.14, increasing the applied potential enabled faster separations but (due to joule heating effects) at a cost in efficiency and resolution (fig 6.4). Choice of an optimum potential is a compromise between resolution and analysis time (154).

To enhance resolution, addition of organic modifiers was investigated. As mentioned earlier organic modifiers have been known to affect the electroosmotic flow through changes in the zeta potential, viscosity and / or dielectric constant (31). If the electroosmotic flow is decreased, analytes with only slight differences in electrophoretic mobility will be better resolved (18). In addition, organic modifiers influence the analyte peak shape and increase their partitioning into the mobile phase, a situation beneficial for highly hydrophobic compounds. The concentration of organic modifiers, however, is restricted by its effect on the surfactant cmc. Concentrations higher than 10 % methanol in a mobile phase of SDS begin to show deterioration of peak shape; a situation comparable to using low concentrations of surfactant (146). Addition of acetonitrile to the mobile phase resulted in very poor peak shapes and no resolution. Methanol surprisingly showed little effect on the electro-osmotic flow but seemed to affect the elution range or electrophoretic mobilities (fig 6.5). The best separation of the capsaicins was obtained with 2 % methanol (fig. 6.6).

When a mixture of piperine and capsaicins was analyzed, the piperine coeluted with the capsaicins (fig 6.7). Attempts to separate the three components simultaneously proved impractical, diverting direction to the need for selective detection.

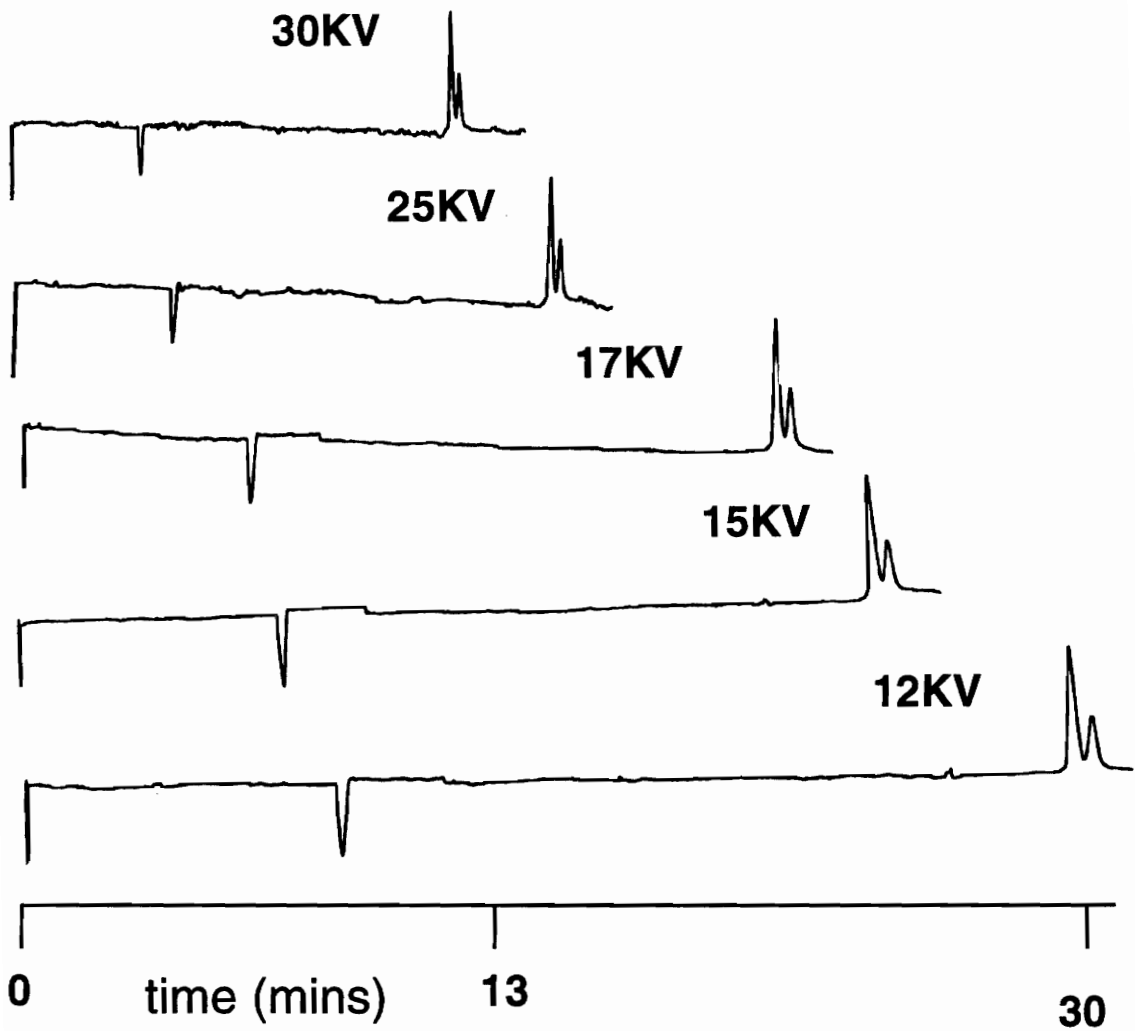


Figure6.4: Effect of separation potential on resolution and elution time. (Conditions as in Figure 6.2 A).

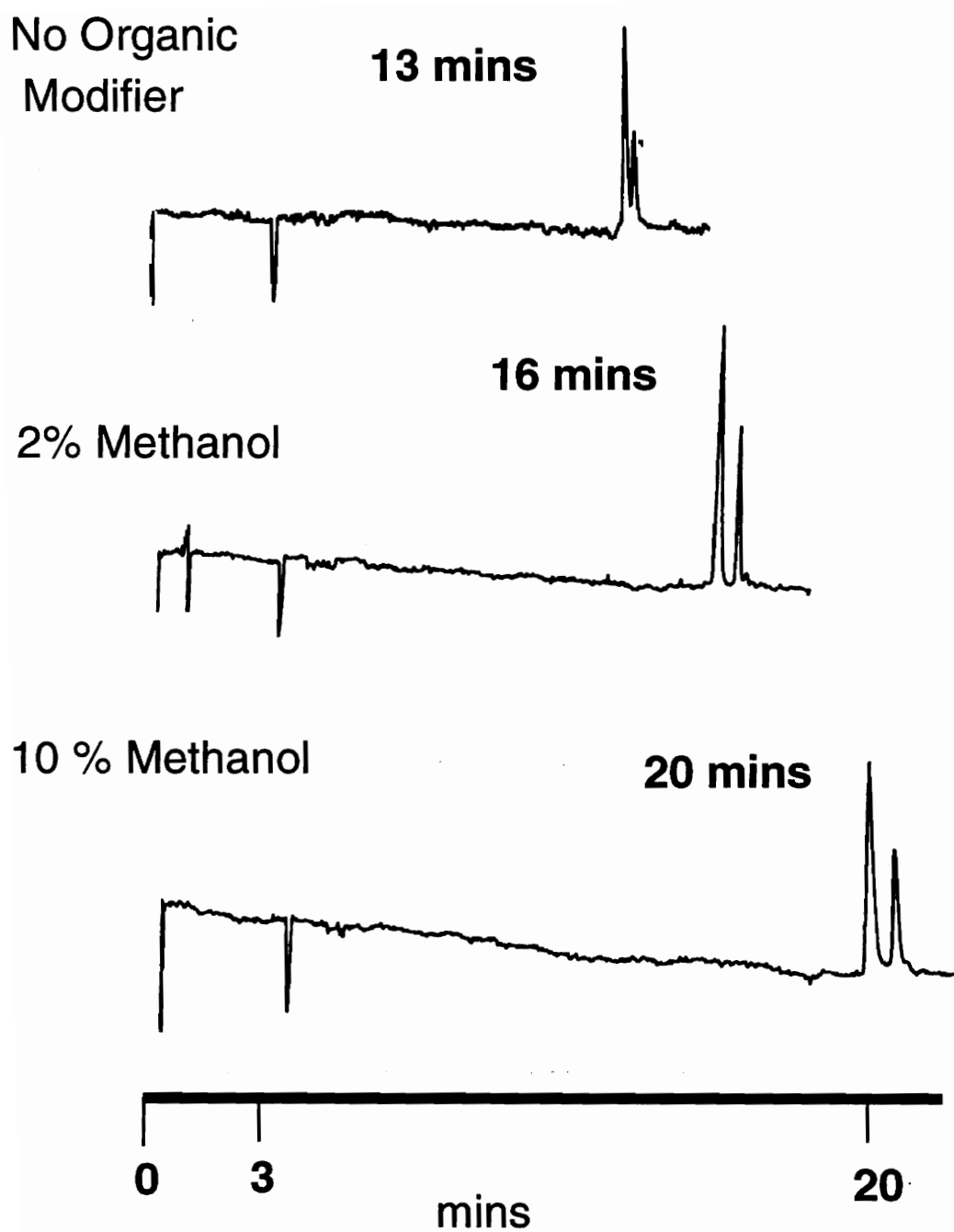


Figure 6.5: Effect of organic modifier. Conditions as in Figure 6.2 A).

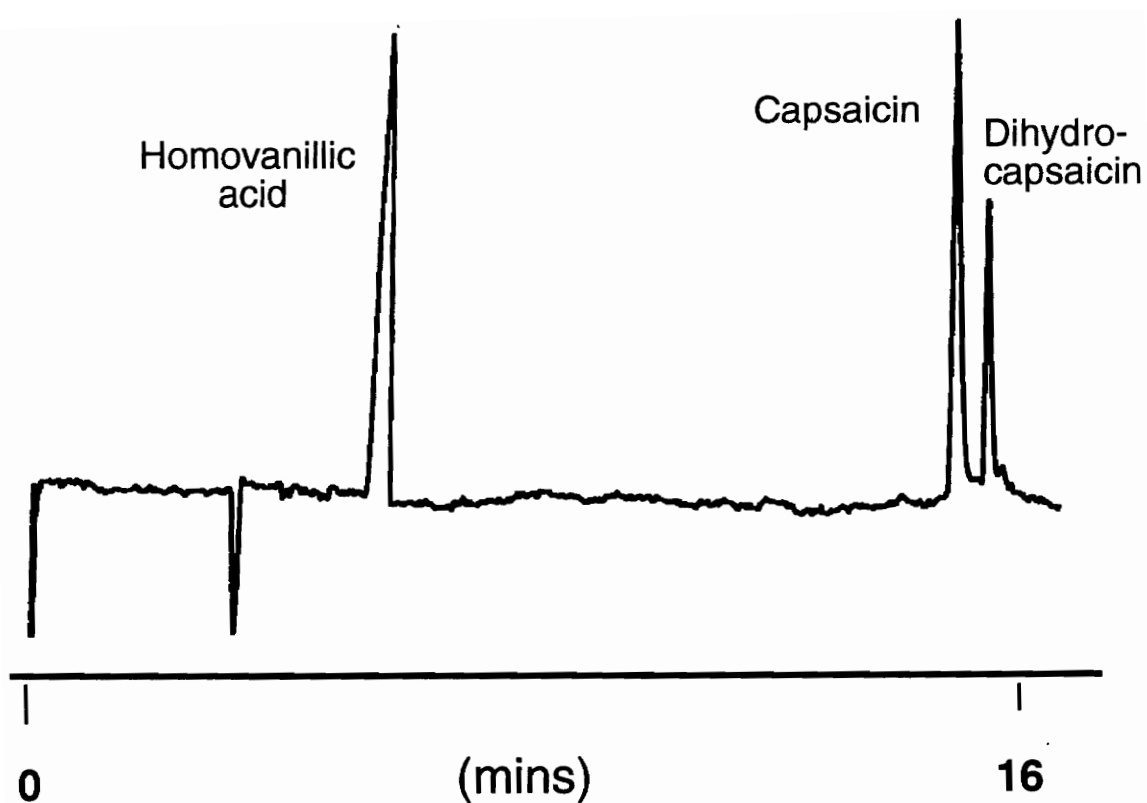


Figure 6.6 : Optimal MECC Separation Conditions.

Mobile Phase - 5 mM Phosphate, 50mM SDS, pH- 7.2
Capillary- L= 65 / 45 cm, 25 μ m id
Potential applied- 30 KV
Electrokinetic injection- 5 kV / 2sec
Absorbance Wavelength- 230 nm
Modifier- 2% methanol

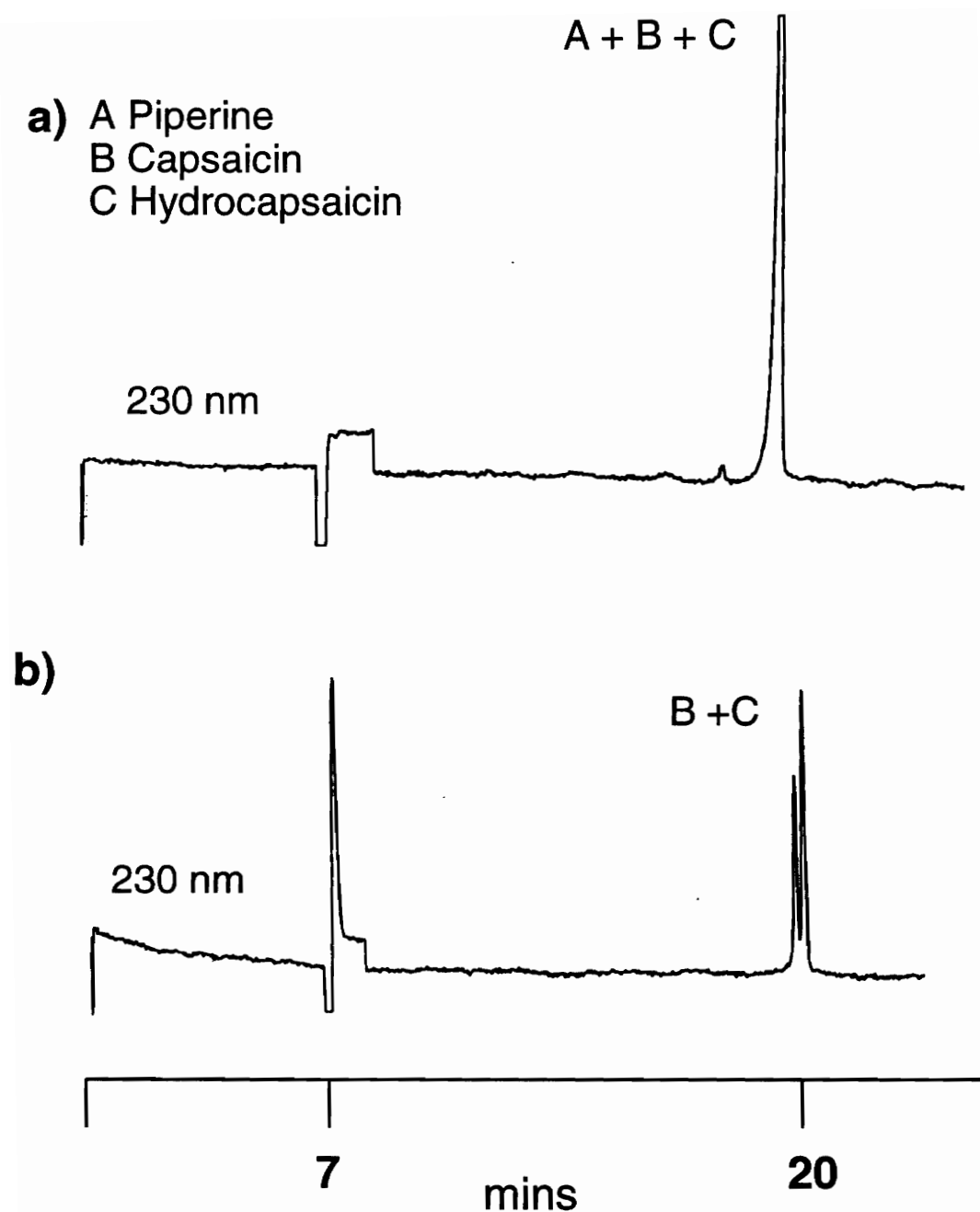


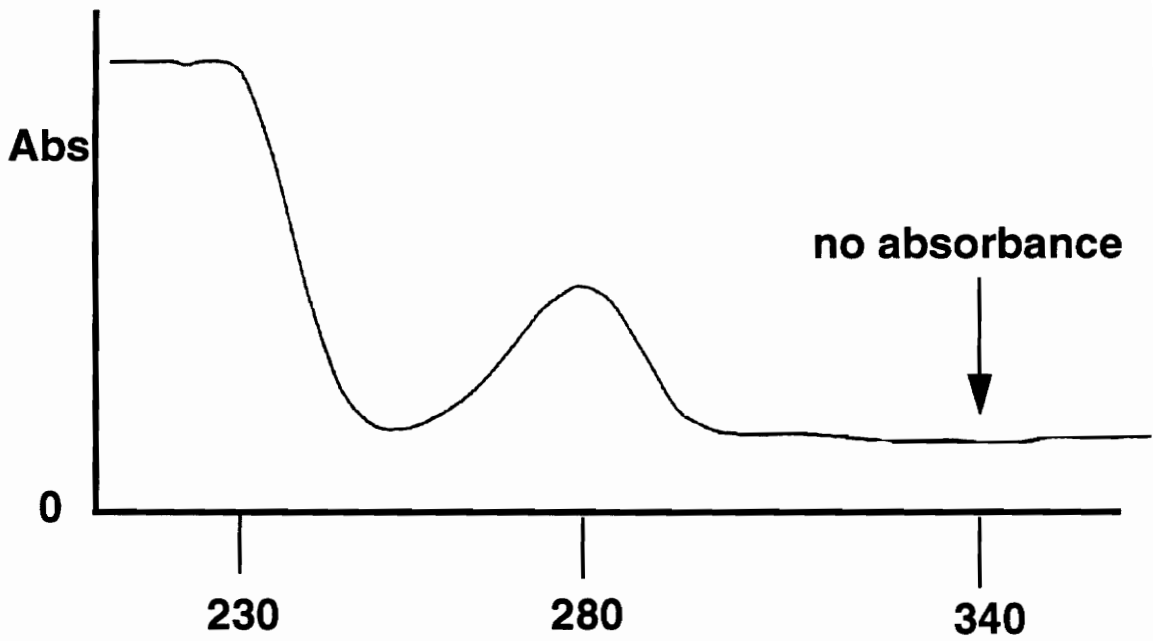
Figure 6.7: UV detection of
 a) coeluting mixture of piperine, capsaicin,
 dihydrocapsaicin at 230 nm.
 b) capsaicin and dihydrocapsaicin at 230 nm,
 no piperine. Conditions as in Figure 6.2 B).

6.1.2. The Detection

The UV absorbance spectra (fig 6.8) show that at 340 nm selective on-column UV detection of only the piperines is possible even in the presence of the capsaicins. Cyclic voltammetry experiments indicates the potential for selective amperometric electrochemical detection of the capsaicins and compounds of similar structures at 0.9 V versus Ag / AgCl (fig. 6.9). Placing the end-column electrochemical detector cell in-line after the on-column UV detector allowed selective, simultaneous UV detection of piperine at 340 nm and electrochemical detection of homovanillic acid, capsaicin and dihydrocapsaicin at 0.9 V (fig 6.10). In this dual detection mode, electrophoretic separation of the piperines from the capsaicins is unimportant because the detection allows efficient separation in the detector zone.

The ohmic potential drop, iR_s , mentioned in section 3.3.3 b, inherent in the solution and increased by the CE system's large voltages has to be minimized. Usage of a three electrode electrochemical detector helps to isolate the CZE current from the detector current allowing the use of 25 μm id columns with end-column electrochemical detection. In addition to the working and reference electrodes an auxiliary electrode (platinum) is included in the system to eliminate the residual current. The potential of the working electrode is monitored relative to the reference electrode positioned close to it. A high input impedance in their circuit prevents current passage, keeping the reference electrode potential constant and equal to its open circuit value. With the excess current passing only through the auxiliary electrode circuit, the iR_s term is substantially reduced. Smaller as well as larger diameter columns should also

Capsaicins



Piperines

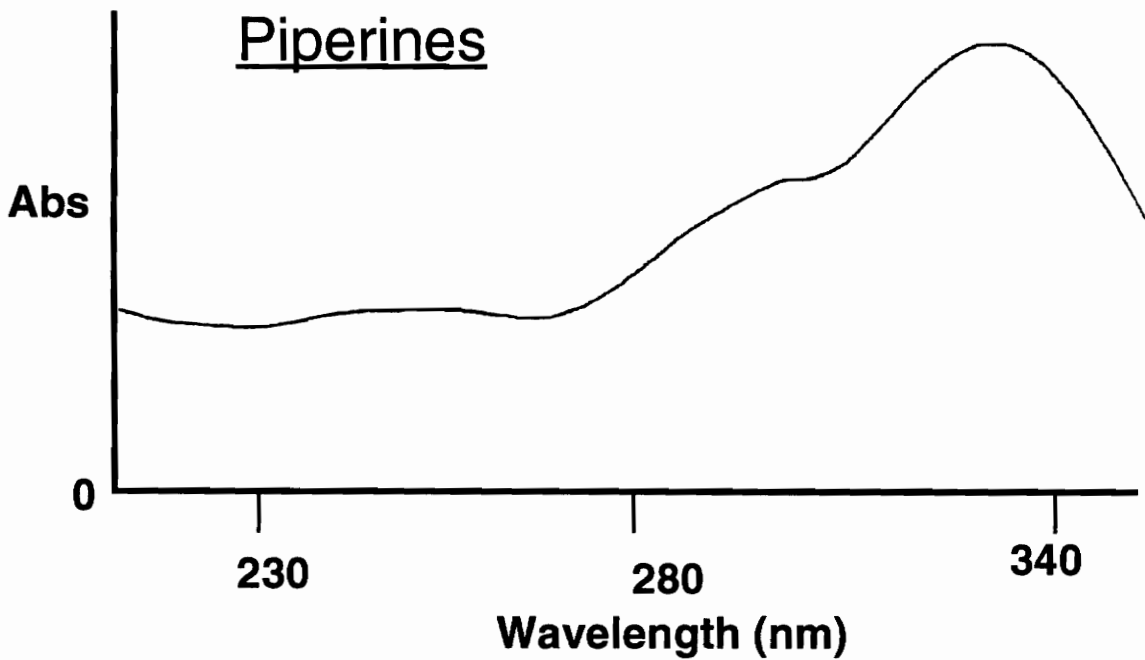


Figure 6.8 : UV spectra of a) capsaicins, b) piperine.
At 340 nm, only piperine would absorb.

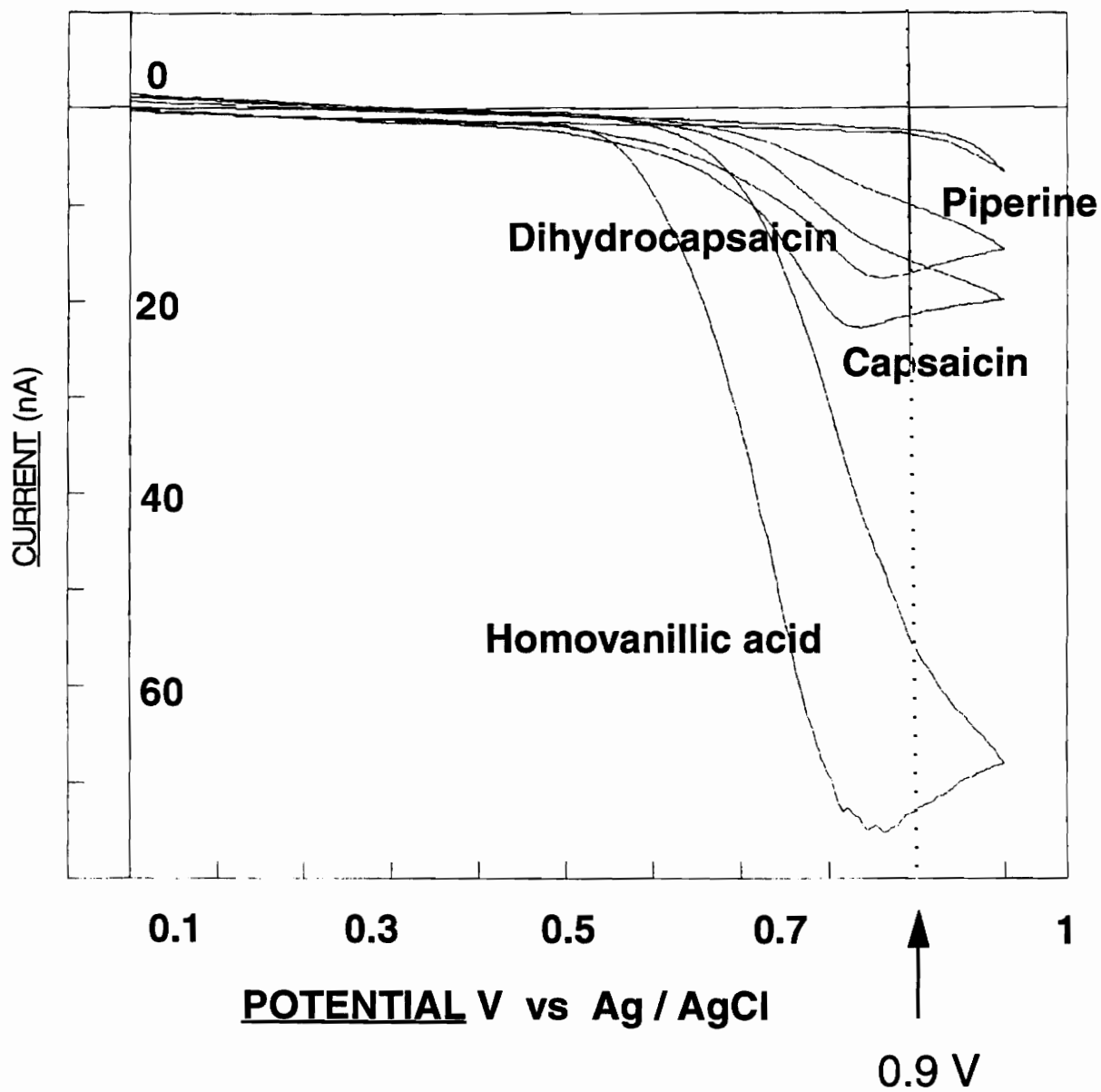


Figure 6.9 : Cyclic voltammetry of the pungent compounds
Scan rate of 100 mV/ sec.

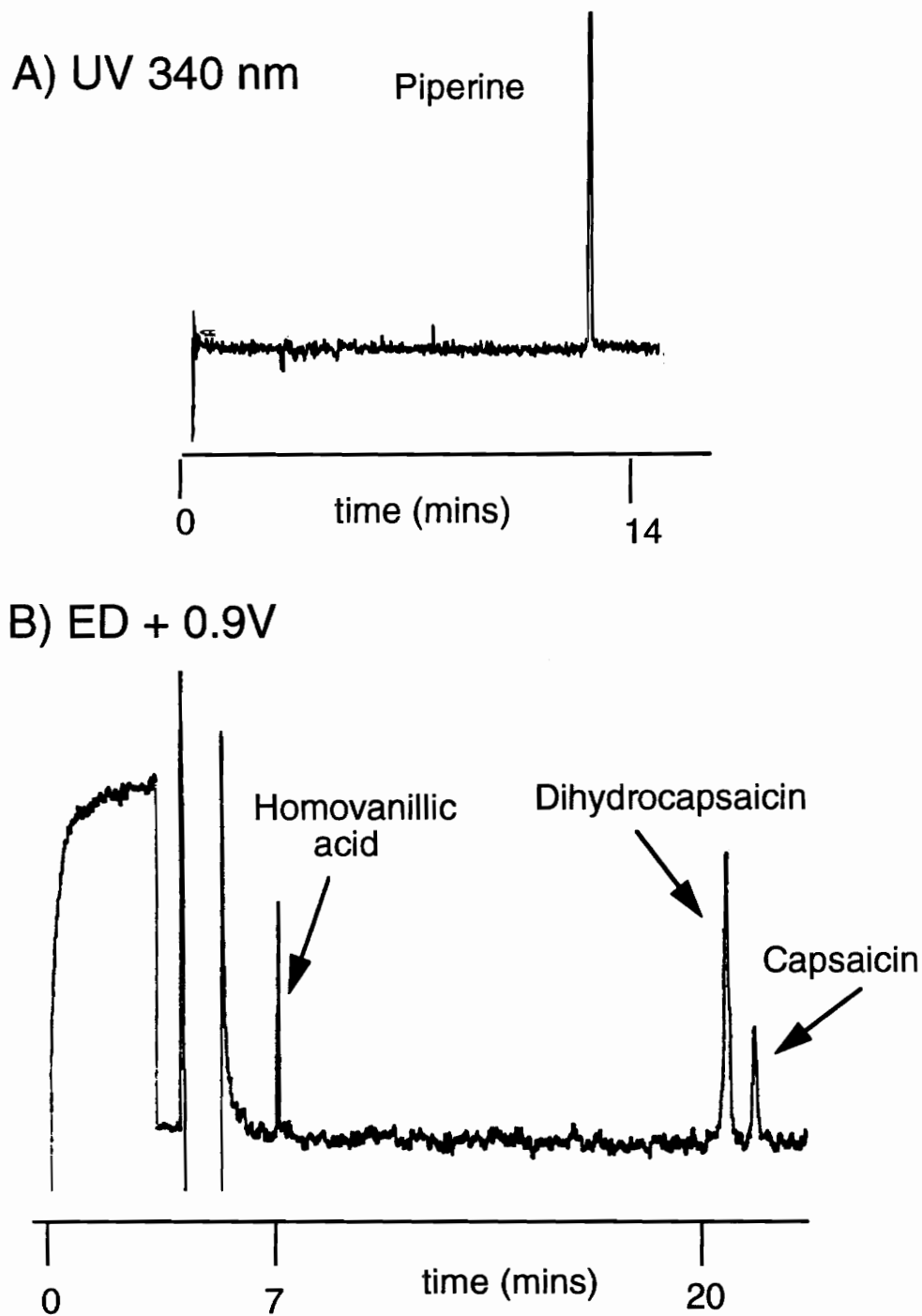


Figure 6.10: Simultaneous online detection of piperine and capsaicin.

Concentration of analytes 1m M. A) UV at 340 nm, $L_d=45\text{cm}$.

B) Electrochemical detection at 0.9V versus Ag/AgCl. Carbon $33\mu\text{m}$ electrode, $L_d=65\text{cm}$. Conditions as in Figure 6.2 A) with 2 % methanol.

prove successful with this cell configuration. Both 10 and 33 μm diameter microelectrodes showed comparable sensitivities and efficiencies.

Quantitation was carried out using equation (4.3) by Rose et al. (96). Minimum detectable quantities and efficiencies are shown in Table 6.1. The detector exhibited linearity from 1×10^{-2} M to 1×10^{-5} M for hydroquinone with a regression coefficient of 1.0. (fig. 6.11); and for the capsaicin and dihydrocapsaicin with a linear range of 1×10^{-2} to 5×10^{-4} M and a linear regression of 0.995 each, (fig. 6.12).

The % Relative Standard Deviation for area and elution time are listed in table 6.2. The capsaicins did not seem to poison the electrode surface as was observed by Boercsh et al (139). In any case, the electrode was easy to assemble and disassemble and was polished every two runs.

In the separation of dopamine and 3,4-dihydroxybenzylamine, with only MES as the buffer (fig.6.14), baseline noise was notably decreased. The increase in background noise for the other analyses may be related to the presence of SDS. Further manipulation of buffer type and pH should eliminate the evident peak tailing of the amines.

Table 6.1: Resultant efficiencies and MDQ using the modified end column detection.

COMPOUND	MDQ (Femto- moles)	EFFICIENCY (N)	LINEAR REG. COEF.
Homovanillic Acid	28	162,000	0.995
Capsaicin	160	92,000	0.995
Dihydrocapsaicin	80	152,000	0.995
Hydroquinone	2.5	191,000	1.0
Dopamine	56	Tailing Peaks	-
3,4 Dihydroxy- benzylamine	56	Tailing Peaks	-

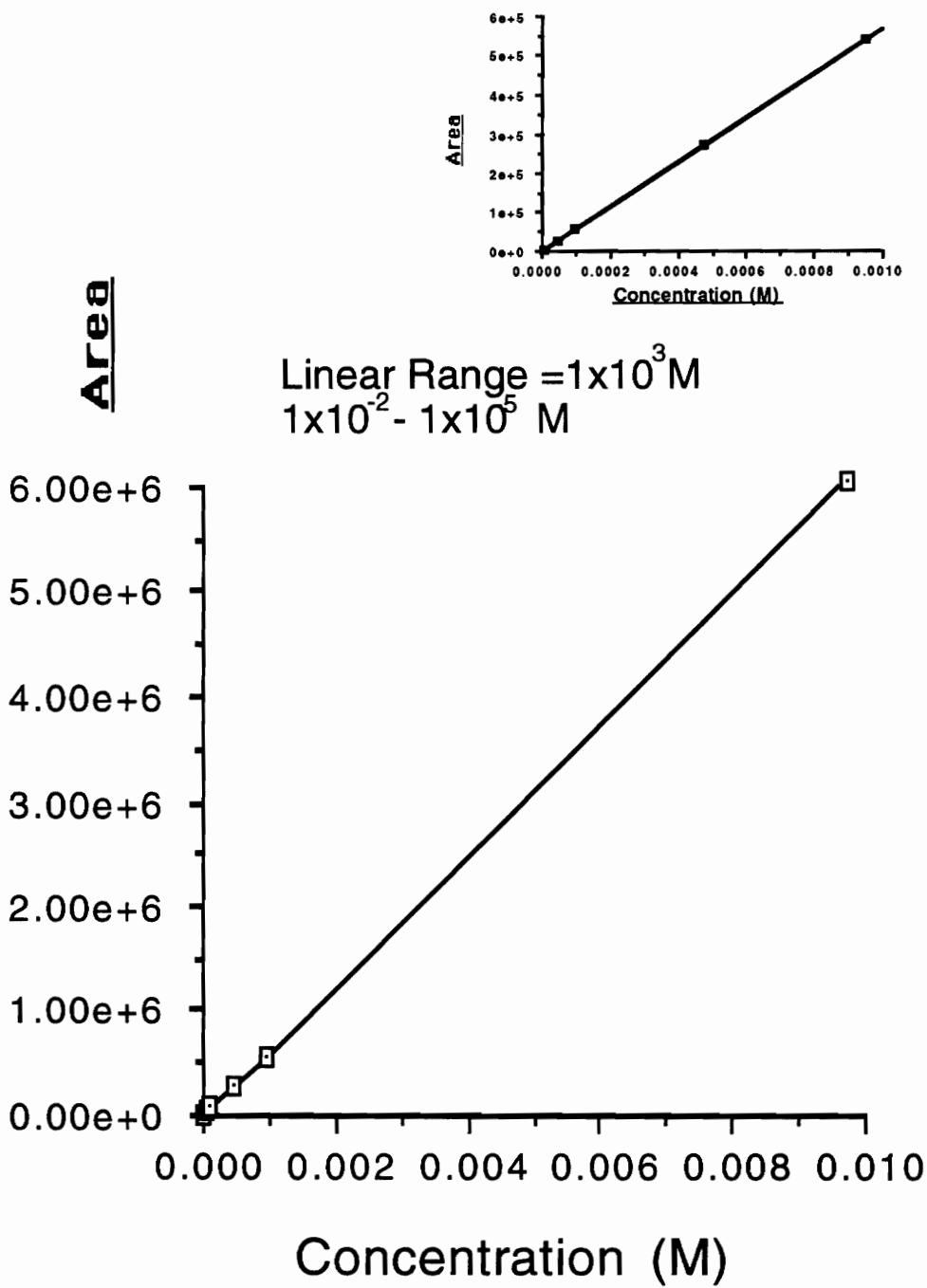


Figure 6.11: End-column electrochemical detector linear range for hydroquinone.

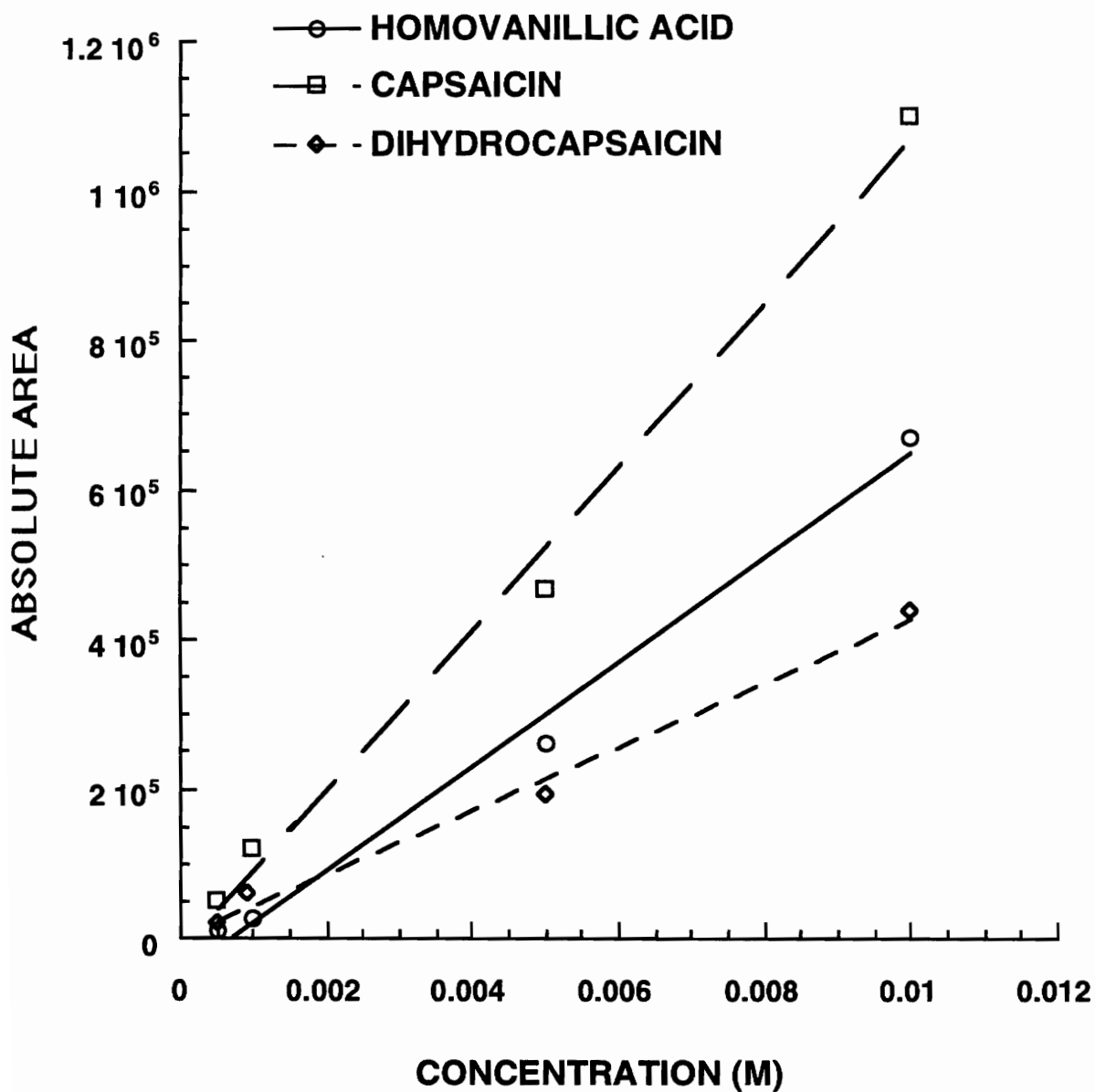


Figure 6.12: Calibration curve for Homovanillic acid, Capsaicin and dihydrocapsaicin.

Table 6.2 : % RSD values for peak areas.

CONCENTRATION	HOMOVANILLIC ACID	CAPSAICIN	DIHYDROCAPSAICIN
$5 \cdot 10^{-3}$ M	0.85%	3.38%	10.2%
$5 \cdot 10^{-4}$ M	28.9%	29%	4.4%

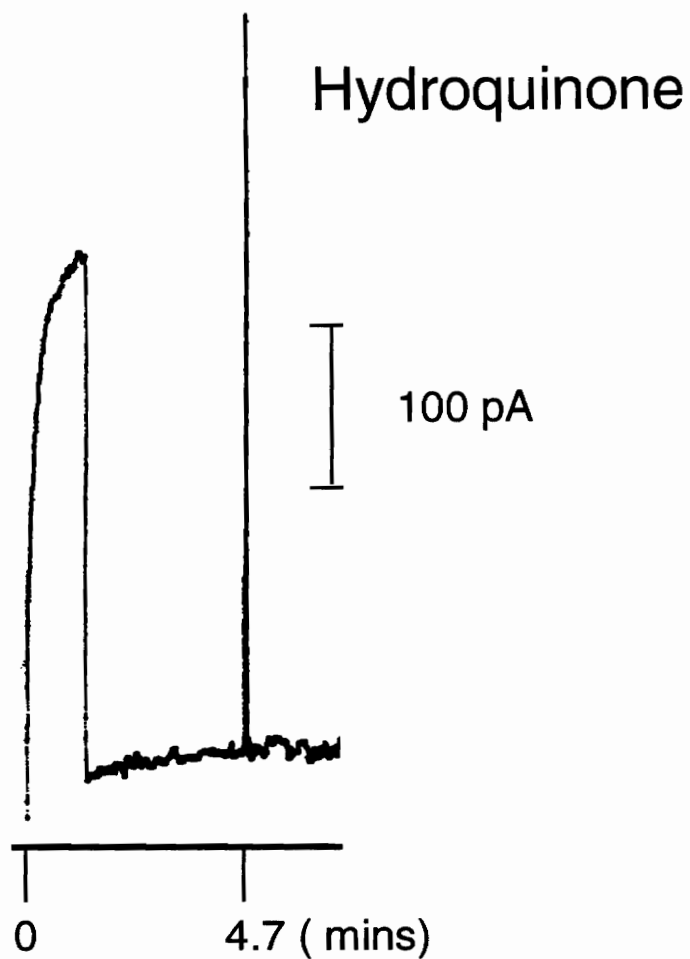


Figure 6.13: End-column electrochemical detection of hydroquinone.
Analyte concentrations 0.1 mM
Conditions as in Figure 6.11.

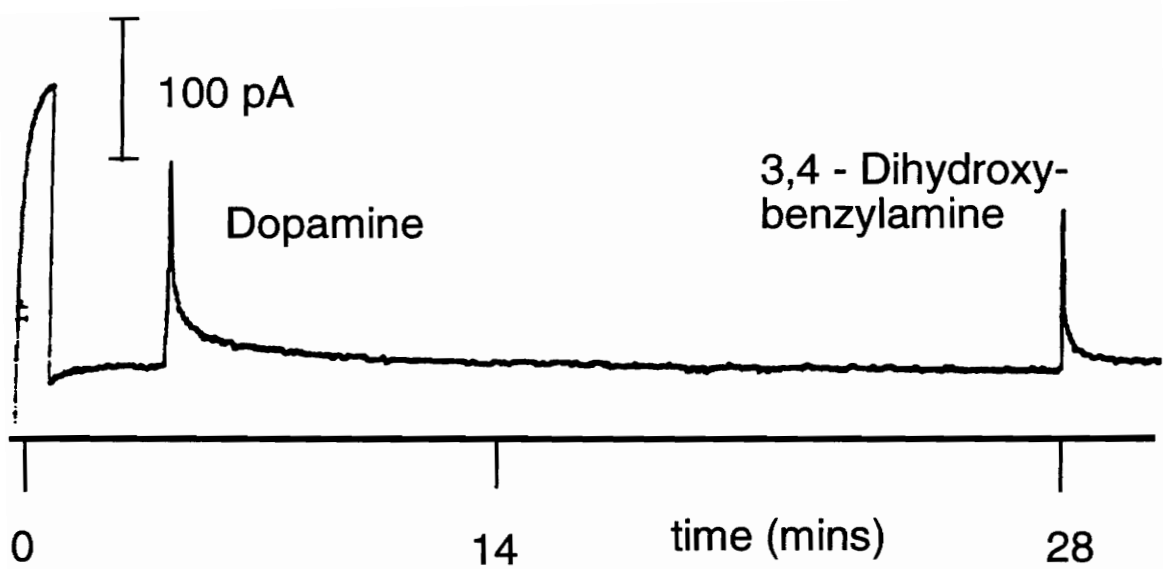


Figure 6.14: End-column electrochemical detection of Dopamine and 3,4-Dihydroxybenzylamine . Analyte concentrations 0.1 mM. Conditions as in Figure 6.2 except buffer 0.02 M MES pH 6.2.

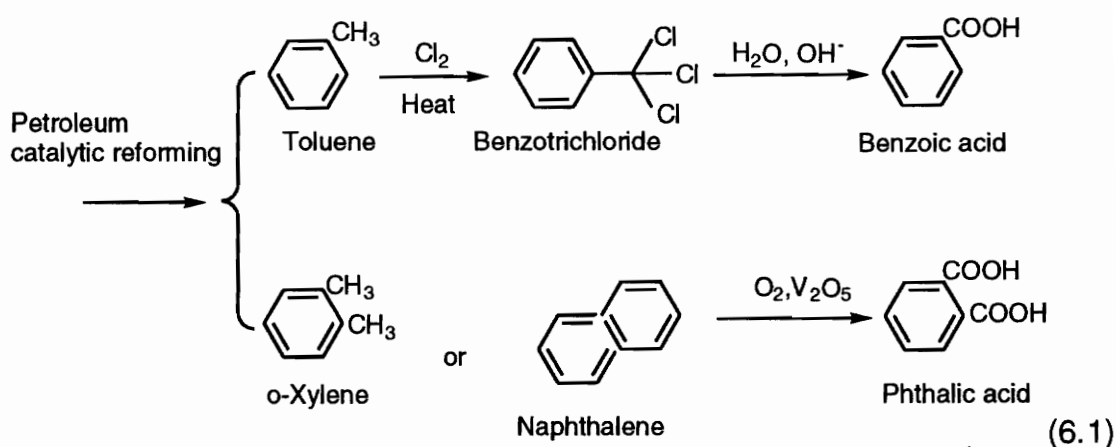
6.2. CAPILLARY ZONE ELECTROPHORETIC SEPARATION OF ISOMERIC BENZOIC CARBOXYLIC ACIDS; THE EFFECT OF ADDITIVES.

Capillary Zone Electrophoresis is expected to compliment, if not compete, with High Performance Liquid Chromatography (HPLC). However, while HPLC cannot offer the extremely high efficiencies available to CZE, HPLC's selectivity, through solvent optimization and wider stationary phase availability, is superior to CZE. Through changes in the buffer pH or by use of buffer additives, selectivity can be enhanced in CZE. As mentioned earlier in section 3.3.3, various additives such as cyclodextrins, surfactants and organic modifiers, are available for increased selectivity.

A lot of attention has been given recently to the use of inclusion complexes, such as cyclodextrins (CD), and they are being widely incorporated in CE separations. However, most of the applications are in the field of chiral recognition. Terabe ⁽¹⁵⁵⁾ was the first to use ionic cyclodextrins (M 2-O-carboxymethyl- β -cyclodextrin) for the separation of o-, m-, and p-isomers of cresol, nitroaniline, chloroaniline, nitro- and dinitrophenol. Fanali et al ⁽¹⁵⁶⁾ investigated the effect of β -CD and derivatized β -CD on the resolution of optical isomers, and used Isotachophoresis for the separation of a series of amino, nitro- and hydroxybenzoic acids ⁽¹⁵⁷⁾. Terabe et al ⁽¹⁵⁸⁾ explored the applicability of γ -CD in the presence of micelles for the separation of highly hydrophobic and closely related compounds such as polychlorinated biphenyls, tetrachlorodibenzidioxin (TCDD) isomers and polycyclic aromatic hydrocarbons (PAHs). Nishi and Matsuo ⁽¹⁵⁹⁾ with the addition of CD to SDS were able to

improve separations of lipophilic compounds, corticosteroids and aromatic hydrocarbons. Moreover Li et al used γ CD-MECC to separate vitamins E and A.

The application of cyclodextrin in this work, however, is for the separation of a series of isomeric polycarboxylic benzoic acids. Terephthalic, isophthalic, phthalic, hemimellitic, trimellitic and trimesic acids (fig. 6.15), are of considerable interest and importance to the polymer industry.



Once formed these acids are used for polymer synthesis. It is essential, therefore, for process control to resolve these compounds to a degree which allows their accurate identification and quantitation. Earlier attempts to resolve these acids have involved Gas Chromatography (after derivatization) (160), Ion Chromatography (Strong Anion Exchange, SAX) (161) and Ion Suppressed Reversed Phase Liquid Chromatography (162). Capillary Electrophoresis presents an alternative method that offers high efficiencies with short analysis time and low solvent consumption.

In an attempt to separate these mono-, di- and tri-carboxylic acids and their isomers for practical use, manipulations of the selectivity and optimization

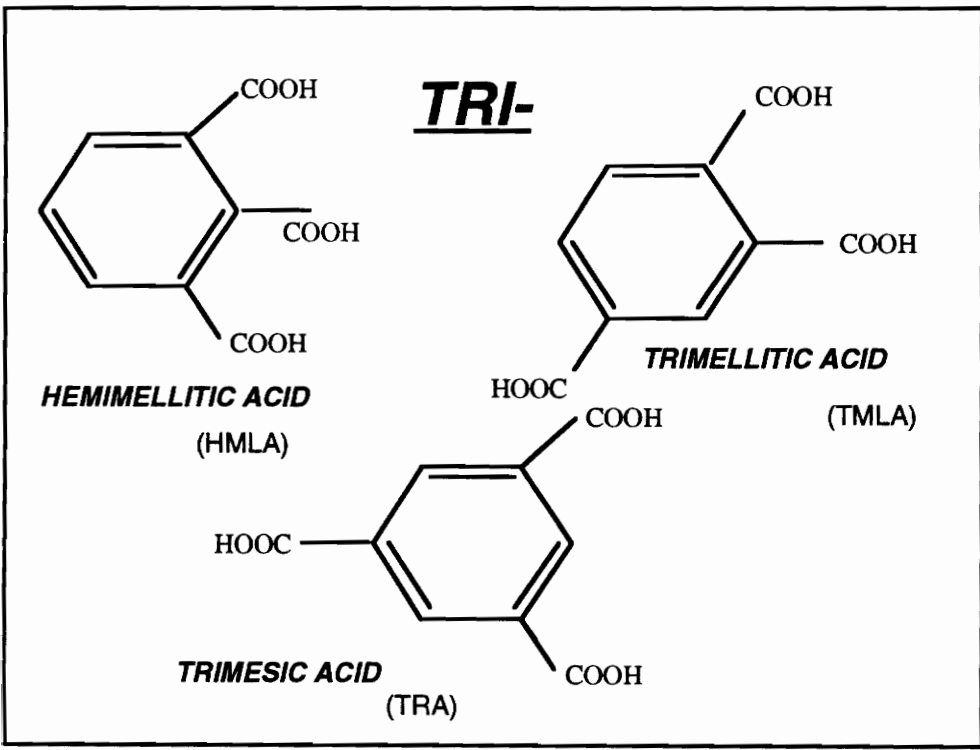
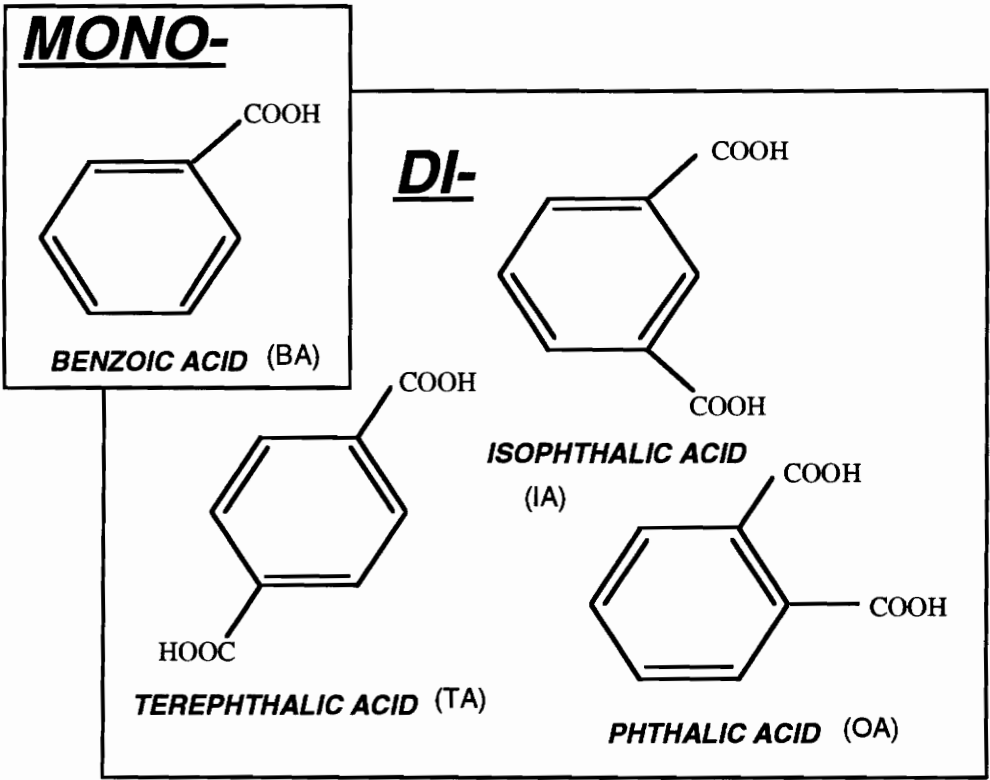


Figure 6.15: Molecular structures of the aromatic carboxylic acids

of the separation and peak shapes entailed changes in buffer pH, ionic strength, composition, cyclodextrin type and CD concentration. Finally, the effect of polarity reversal (with cationic surfactants) and applied potential were also investigated.

6.2.1. Electrolyte system a) Positive Polarity, with 0.05M borate buffer;

At pHs above their pKa (Table 6.3) the acids are negatively charged with electrophoretic mobilities opposite to the inherent electroosmotic flow of the system. With a positive potential of 440 V / cm (25 kV) and using 0.05 M borate buffer at pH 10, separation of all the acids, except Terephthalic acid (TA) and the Isophthalic acid (IA), was possible (fig. 6.16). The more negative and the smaller their hydrodynamic radius, the larger their effective electrophoretic mobilities (equation 2.3 and 2.4) and consequently the longer their elution time. The triacids elute the latest implying that their charge to hydrodynamic radius is larger relative to the diacids.

The tri-carboxylic acid's peak shapes, in this mode, seem to always show pronounced tailing. This becomes more evident on applying lower potential fields (fig. 6.17), when real sample matrix components (requiring more rigid electroosmotic flow manipulations) are investigated. This, most probably, is due to the earlier mentioned electrophoretic dispersion phenomenon (section 3.1.3). Mismatched mobilities of the highly charged ions relative to the background buffer result in tailing peaks. The carboxylic ions, at pH 10, are totally charged and have higher mobilities and conductivities relative to the borate buffer (fig. 3.2 c). The electric field in the sample zone will be lower than in the buffer zone.

Table 6.3: pKa and molecular weight values of the aromatic carboxylic acid isomers. ⁽¹⁶³⁾

ACID	pK_{a1}	pK_{a2}	pK_{a3}	MW
BENZOIC ACID (BA)	4.19	–	–	122.13
PHTHALIC (OA)	2.94	5.43	–	166.13
ISOPHTHALIC (IA)	3.70	4.60	–	166.13
TEREPHTHALIC (TA)	3.54	4.34	–	166.13
HEMIMELLITIC (HMLA)	2.80	4.2	5.87	210.13
TRIMELLITIC (TMLA)	2.52	3.84	5.20	210.13
TRIMESIC (TRA)	2.13	4.70	4.70	210.13

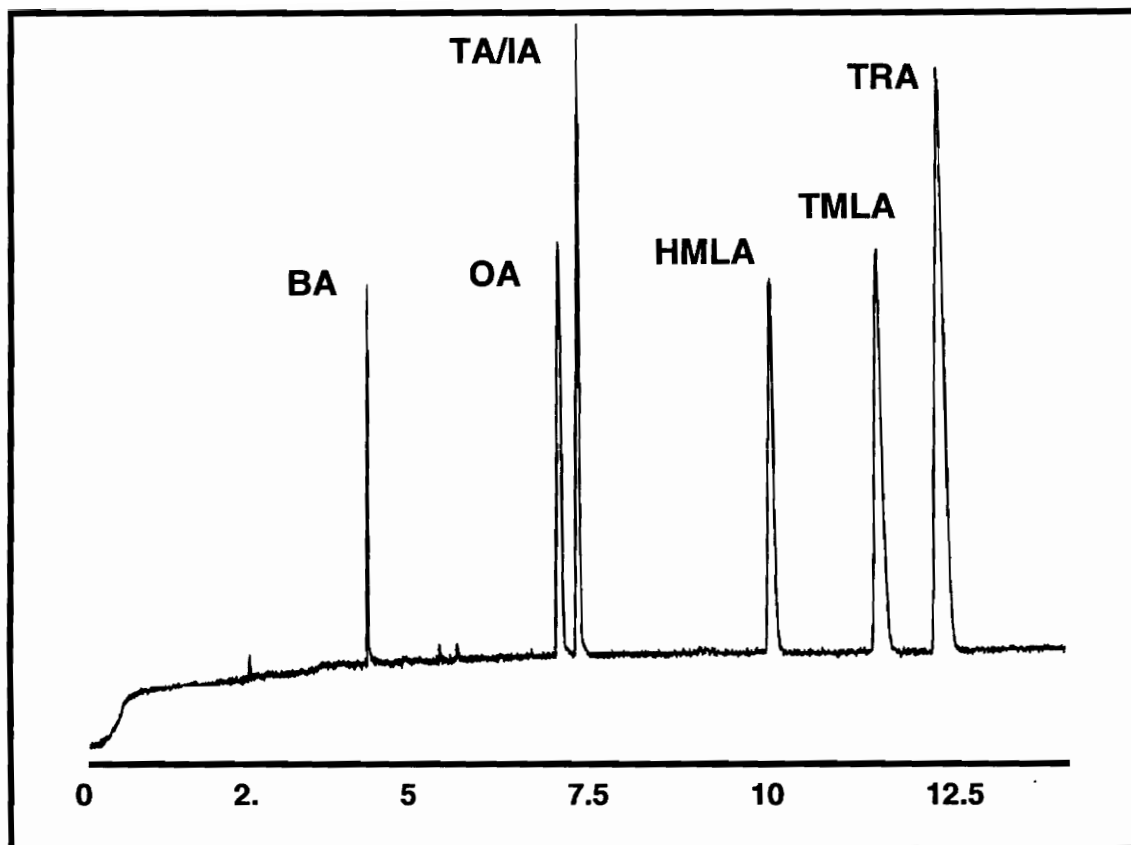


Figure 6.16: Separation of Acids under positive polarity.
Buffer : 0.05 M borate, pH 10.0, 25°C
Applied potential: + 25kV
Capillary : 50 μm id, $L_d = 55$ cm, $L_t = 57$ cm
Fig. 6.15 gives compound identification.

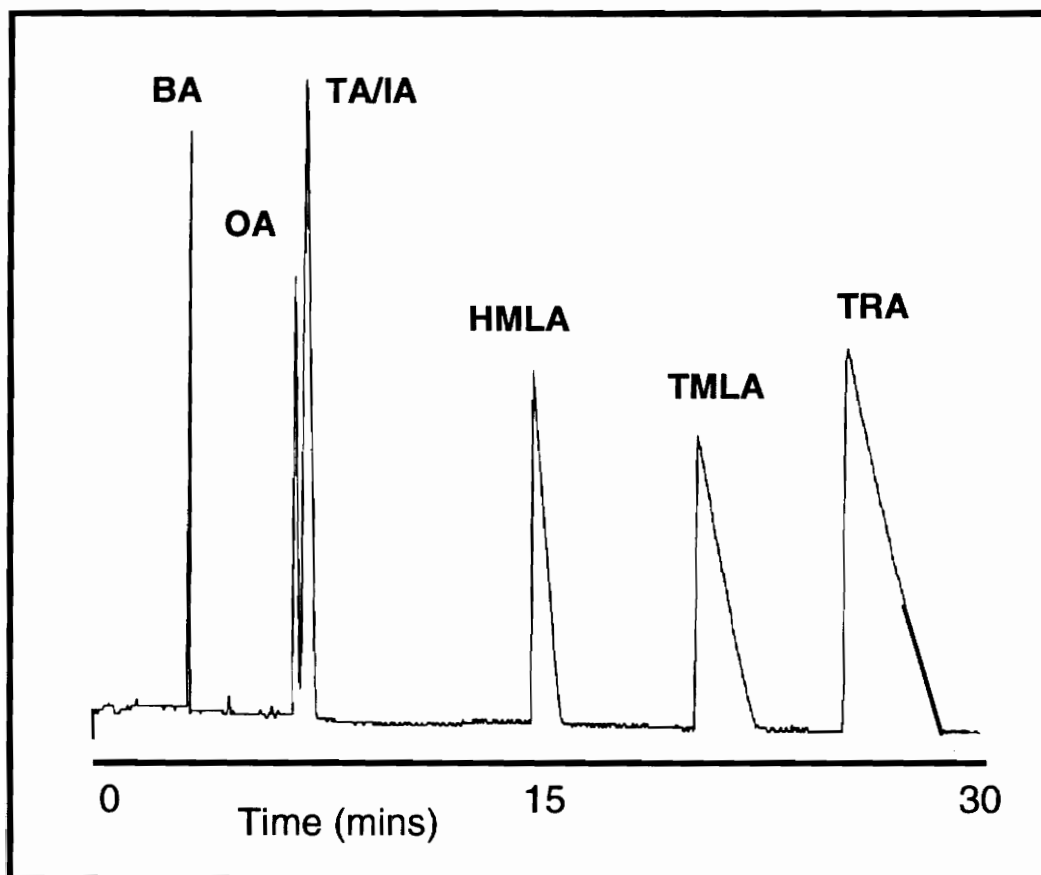


Figure 6.17: Electrophoretic Dispersion with lower applied potentials.

Buffer: 0.05 M borate, pH 10.0, 25°C

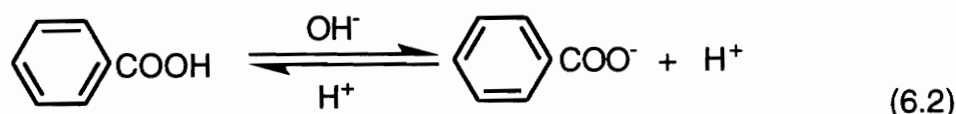
Applied potential: +12kV

Capillary: 50 μm id, $L_d = 35$ cm, $L_t = 43$ cm

(abbreviations as in figure 6.15)

Consequently, when the analyte ions migrate into the surrounding buffer by diffusion or convection, the frontal diffusion will result in deceleration of the ions due to the higher resistance. The diffused analyte ions are overtaken again by the moving analyte zone, sharpening the front end. The trailing boundary, however, tails as the ions having diffused backwards lag behind in the lower field end. The peaks show pronounced tailing. Such tailing is still evident even at low concentrations, which further diminishes possibilities for trace sensitivities.

Manipulations of pH not only affect the silica surface but also the extent of dissociation of the carboxylic acids (section 3.3.2).



Recent work ⁽¹⁶³⁾ shows the importance of subtle pH changes on resolution. With manipulations in acidic pHs close to the pK_as of the acids and under suppressed electroosmotic flow conditions, "minimum resolution within the overlapping pH ranges : 1.45-2.37, 2.60-2.71, 3.72-3.93, 4.02-4.07 and 4.21-4.33." could separate all the acids according to derived theory. Figure 6.18 a shows how slight changes in pH (0.04 pH units) can affect resolution. This of-course is an impractical approach.

In this work basic pHs were used in the presence of electroosmotic flow (fig 6.18 b). The isomers are all totally ionized at these pHs. The increase of pH thus seems to merely increase the ionic strength or viscosity of the system affecting the electroosmotic flow but not the actual charge of the analytes. The use of pHs lower than 10 resulted in loss of resolution (too low an ionic

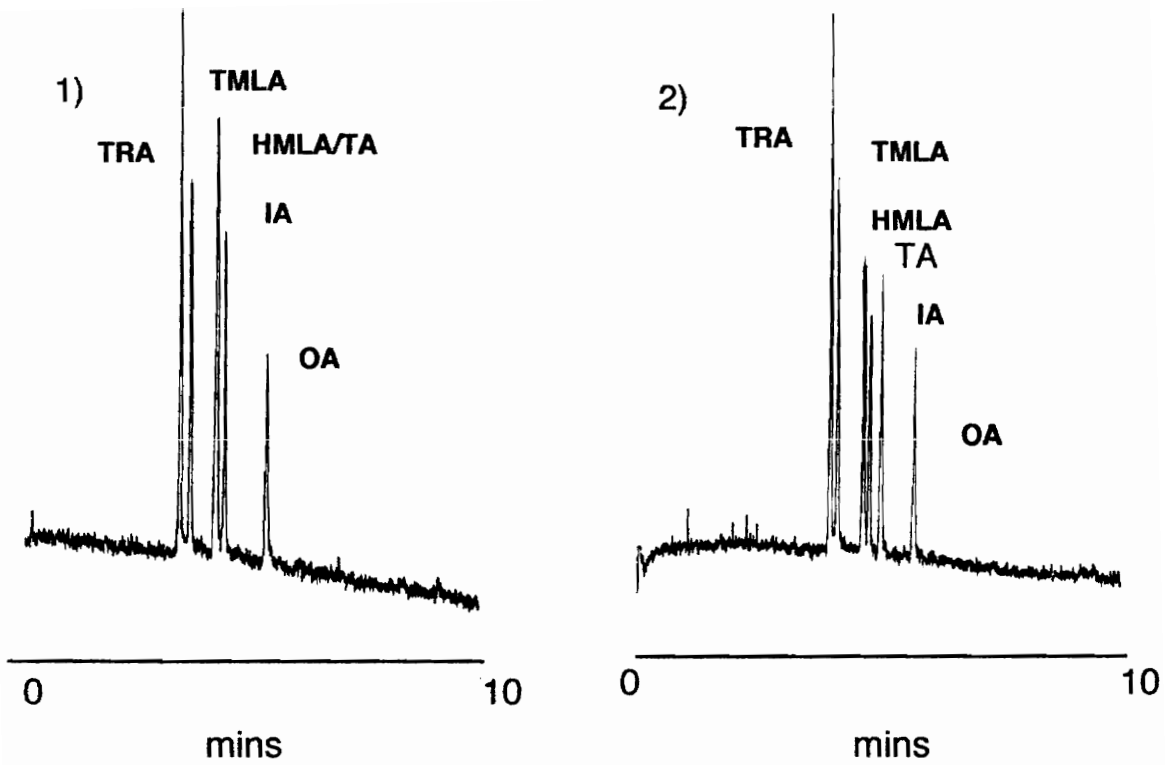


Figure 6.18a: Effect of pH changes at pKa of acids

b1) pH4.37, b2) pH4.33 ⁽¹⁶³⁾

$\lambda=214$ nm, 5 kV, 25°C

Capillary: Methylcellulose coated, id=75 μ m,

L=26.9/20.2 cm

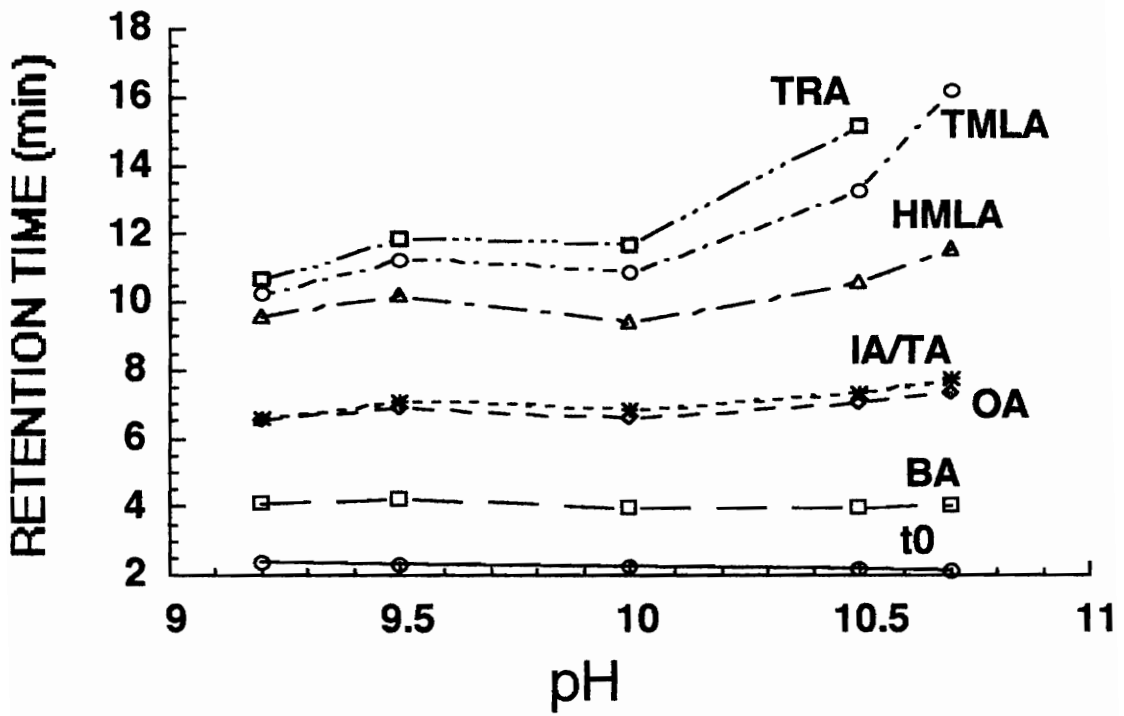


Figure 6.18 b : Effect of pH
Conditions as in figure 6.16

strength), while pHs higher than 10 seem to affect the tri-carboxylic acids retarding their elution and at pH 10.7 showing deteriorated peak shapes (fig. 6.19). Although each group of isomers is expected in this case to coelute, the ortho-isomers seem to elute earlier. This indicates some possible intramolecular coordination (perhaps with sodium ions). With an increased size their electrophoretic mobilities are decreased and they elute earlier.

Reproducibility of retention times, for this mode, ranges between 0.9 - 1.4 % RSD (n=5) and reproducibility in area ranges between 3.5 - 4.3 % RSD (n=5) fig. 6.20.

6.2.2. Electrolyte System b) Positive polarity, with 0.05 M borate buffer and cyclodextrin.

The conventional electrophoretic operating conditions failed to separate the TA/IA isomers due to the similarity in their electrophoretic properties. The electrolyte had to be modified in order to effect a different form of selectivity. In an attempt to develop a rugged method to resolve the IA / TA co-eluting pair, cyclodextrin was investigated as an additional separation mechanism to supplement the weak differences in electrophoretic mobilities. Various concentrations of both α and β as well as γ cyclodextrin were added to the buffer and compared for their retention of the acids.

All isomers were separated as shown in figure 6.21. Identification of the various peaks was facilitated with the presence of the Low Inertial Scanning capabilities of the spectrophoresis system. Figure 6.22 shows the UV spectrum of each of the acids as well as the three dimensional plot of absorbance versus elution time versus wavelength. The spectra of HMLA and TRA are similar, so are those of OA and IA.

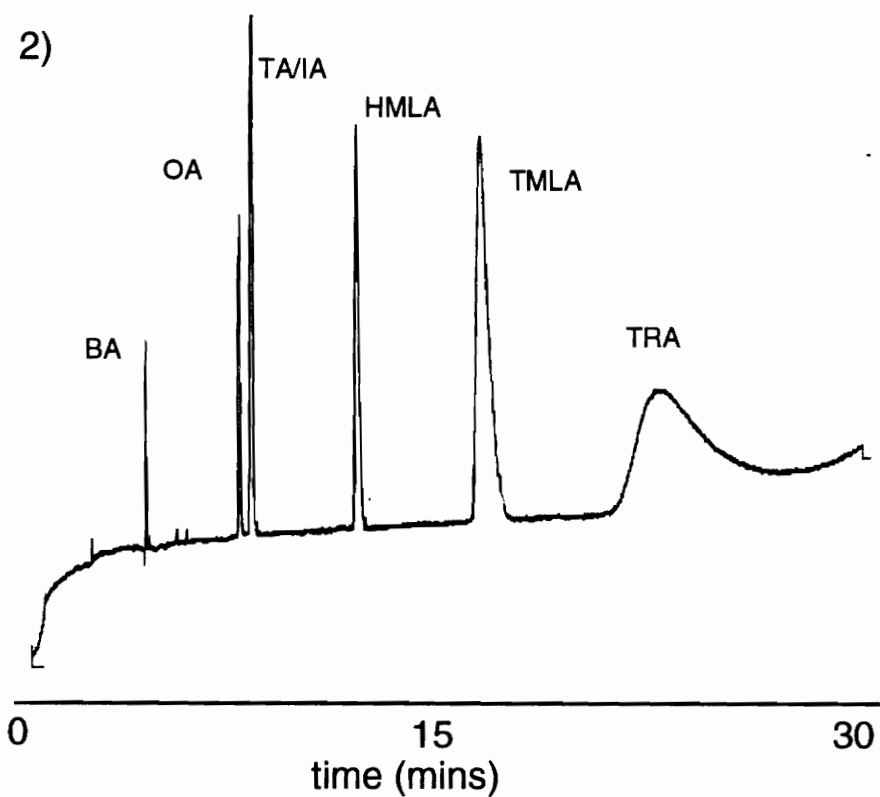
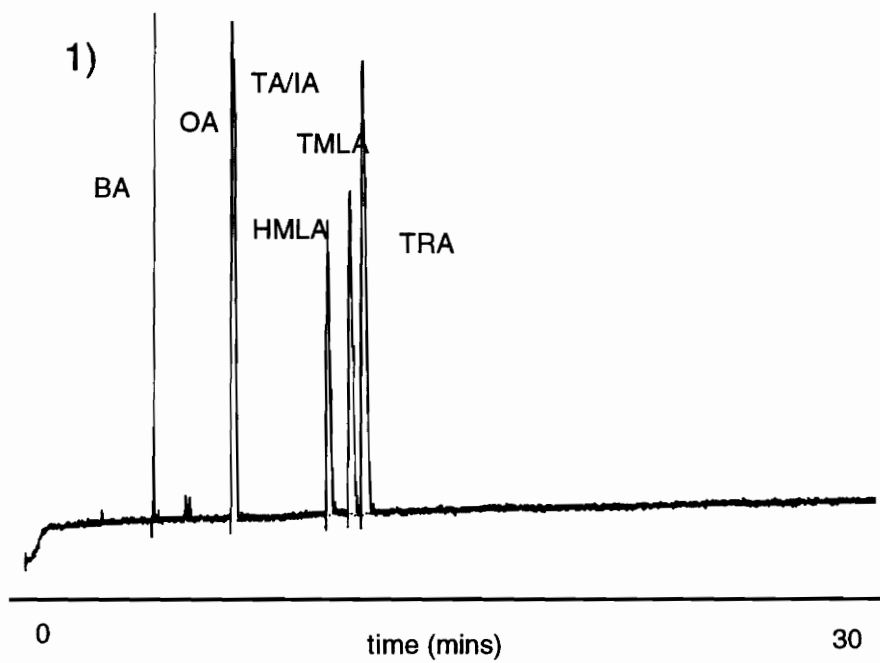
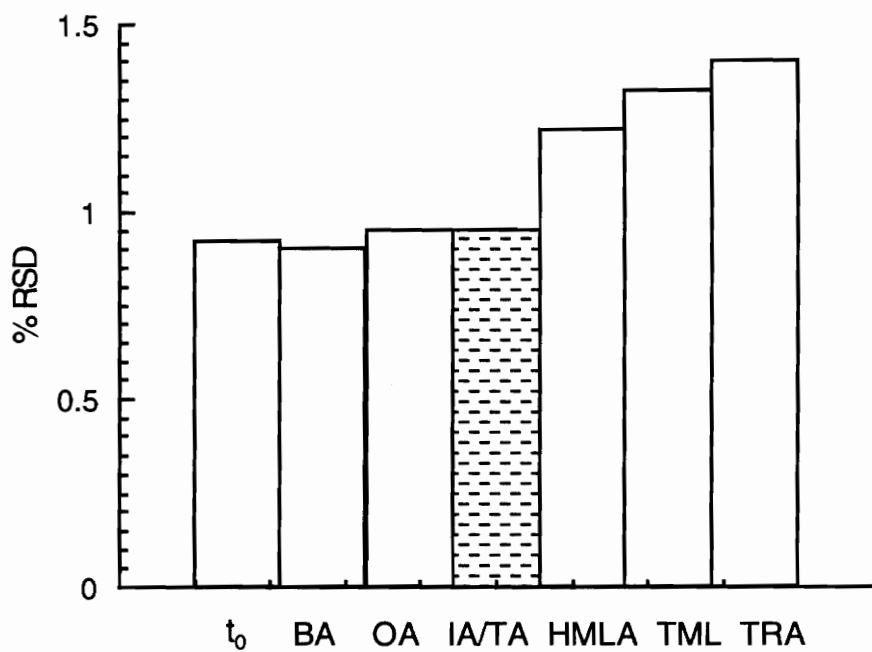


Figure 6.19 : Effect of pH
 1) pH 9.2, 2) pH 10.7; Conditions as in fig. 6.16

a)



b)

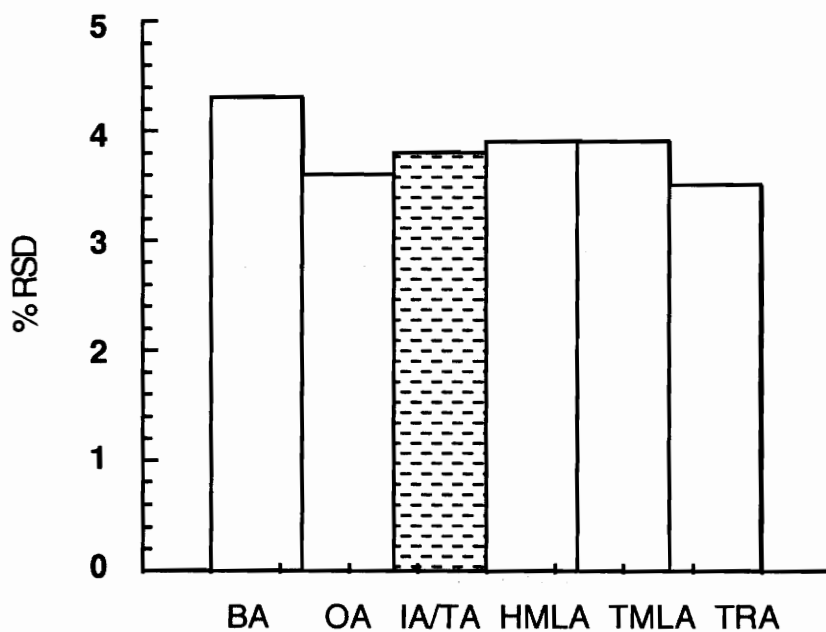


Figure 6.20: % Relative Standard Deviation

a) % RSD of time, $n=5$.

b) % RSD in area, $n=5$

Conditions as in figure 6.16

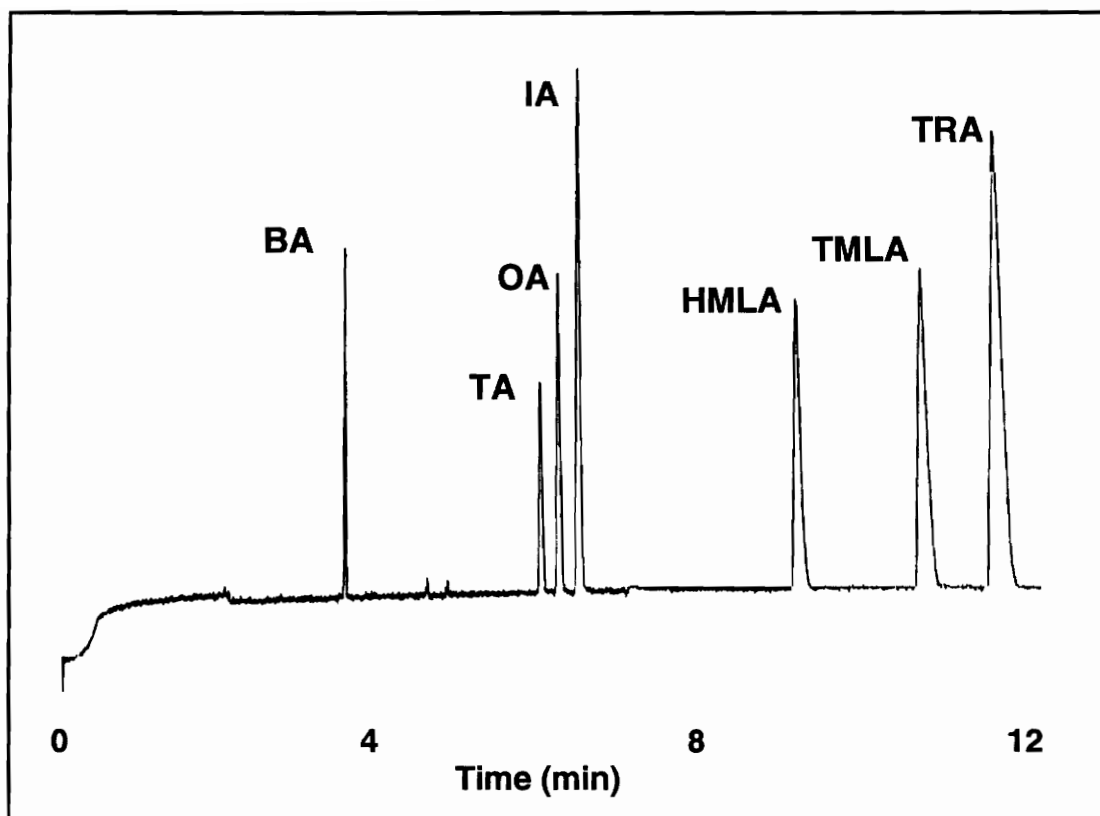


Figure 6.21 : Addition of β Cyclodextrin for the separation of the aromatic carboxylic acids.

Buffer: 0.05 M borate, 4 mM β Cyclodextrin
pH 10.0, 25°C

Applied potential: +25 kV

Capillary: 50 μ m id, L_d = 55 cm, L_t = 57 cm

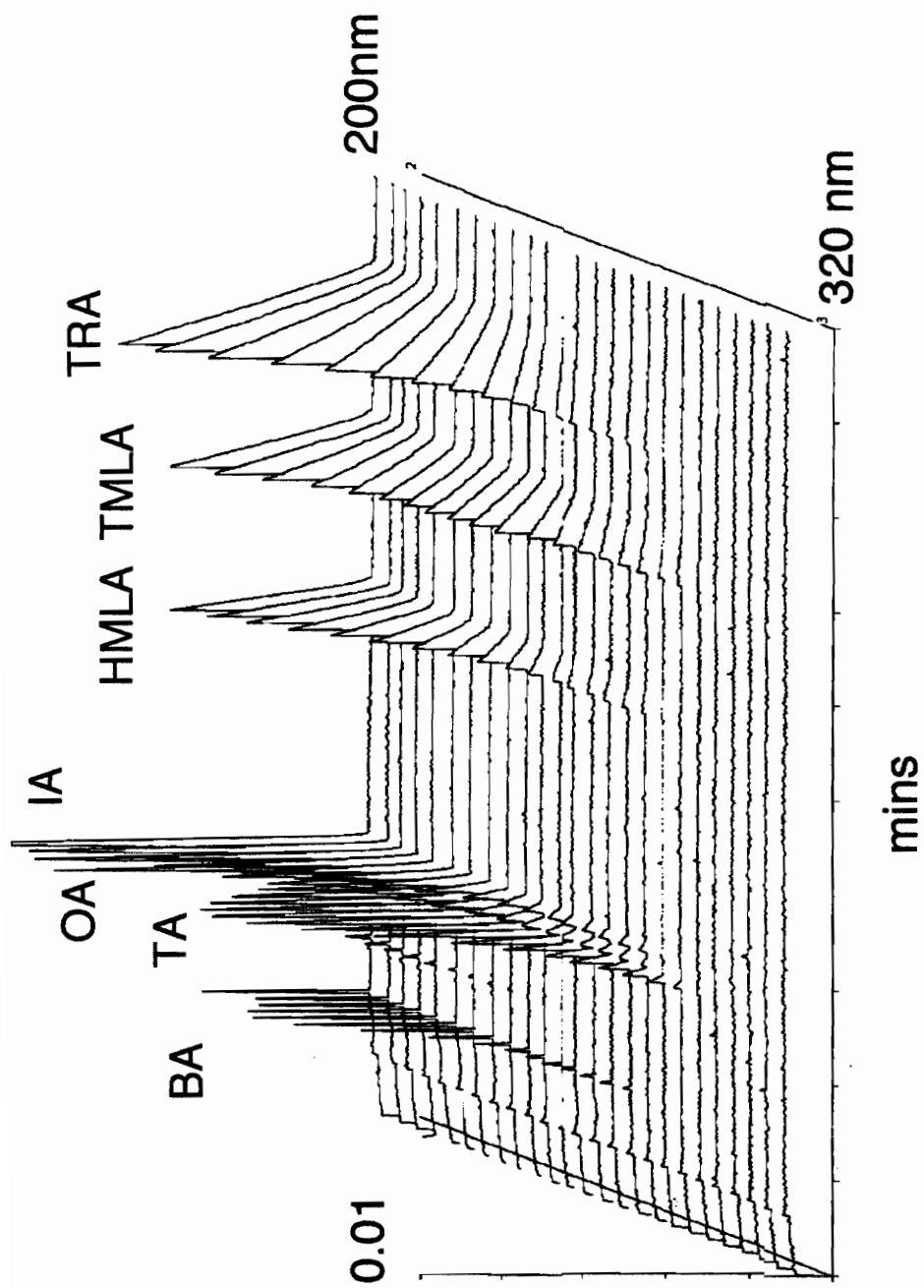


Figure 6.22a: 3-D Plot for the separation of the acids.
 Buffer: 0.05M Borate, pH 10, 4 mM β Cyclodextrin
 Capillary: $L_t = 57\text{cm}$, $L_d = 50\text{cm}$, $i_d = 50\mu\text{m}$.
 Applied Potential = +25kV

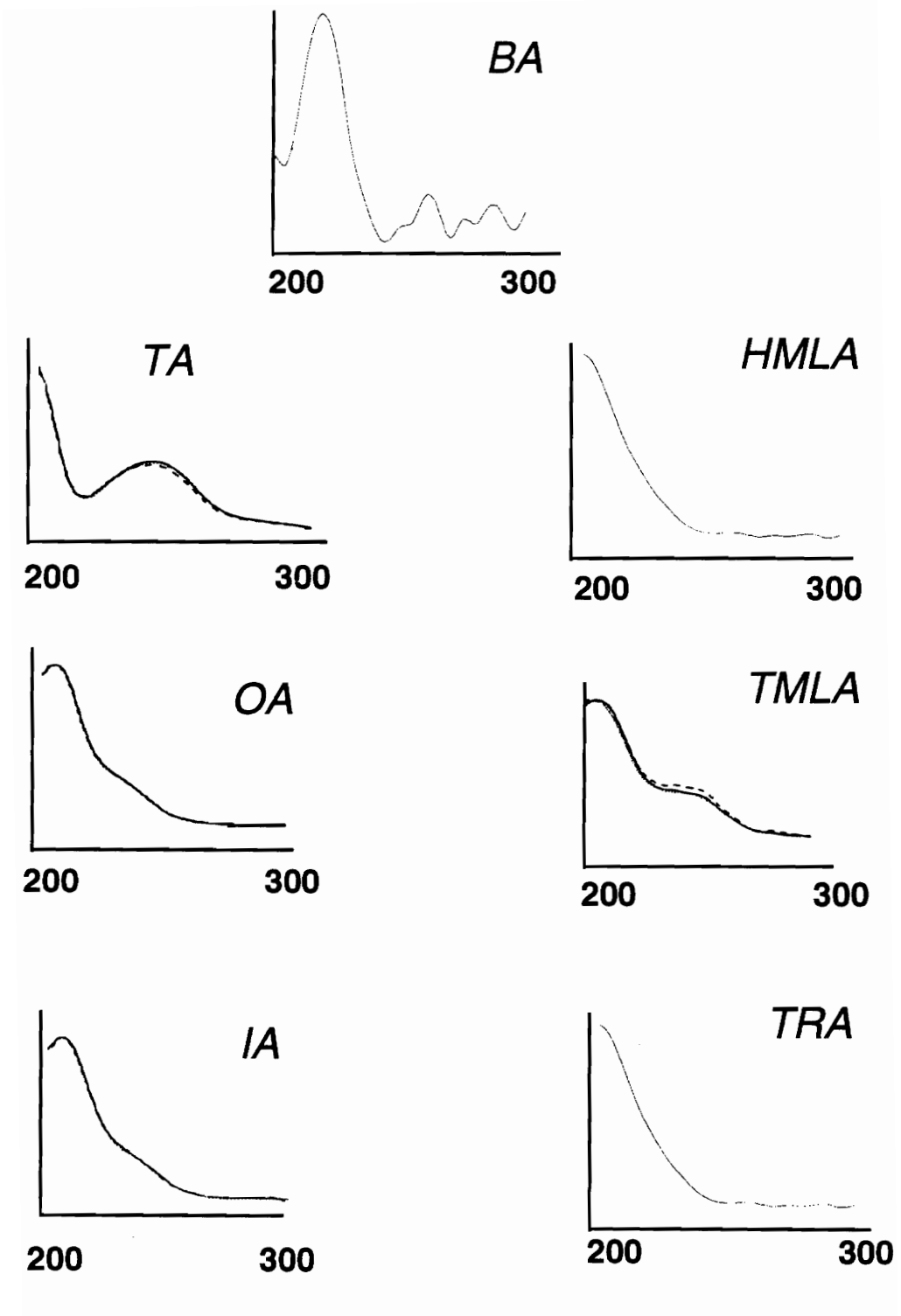


Figure 6.22 b: UV spectra of the acids

When a positive potential is applied, the slowest and least negative of the ions (least negative electrophoretic mobility), in the absence of cyclodextrin, elutes first. Cyclodextrin, having no charge, when added to the buffer system, migrates with the electrosmotic flow. When the anionic solute is complexed within the cyclodextrin hydrophobic interior, its charge to mass ratio is reduced, its charge density is lower and consequently its electrophoretic mobility decreases. The better the molecular fit into the cavity, the stronger the binding constant, the earlier the anion will appear (fig. 6.23). The selectivity of the separation systems changes owing to the different complex stabilities.

Figures 6.24 a and b, both, show that TA (the para- configuration of the di- acid) seems to be the most retained by the β cyclodextrins, decreasing in retention time, implying a possibly better fit relative to the other isomers. The TA retention is also there but to a less significant extent with the γ cyclodextrin (fig. 6.25). At a concentration of 15 mM the TA co-elutes with the OA only to re-separate at higher concentrations (results not shown). Figure 6.26 shows the successful separation of all the isomers with the three types of cyclodextrins. The elution order is reversed for the TA- OA pair for the γ and α cyclodextrins relative to the β cyclodextrin (fig. 6.27) at the applied concentrations. Rough measurements of the Van der Waal distances indicate that TA ($10.2 \times 6.5 \times 5 \text{ \AA}$) would fit the furthest into the $\sim 8 \text{ \AA}$ cavity (table 3.2) of the β cyclodextrin. All the other acids would not fit as well. The α cyclodextrin seems too small for the acids but some form of hydrogen bonding possibly takes place between the hydroxy-group on the cyclodextrin and the carboxylate end of the acids. The same rough calculations indicate that γ cyclodextrin should have retained the tri-carboxylic acids more than the β cyclodextrin due to the better fit. This,

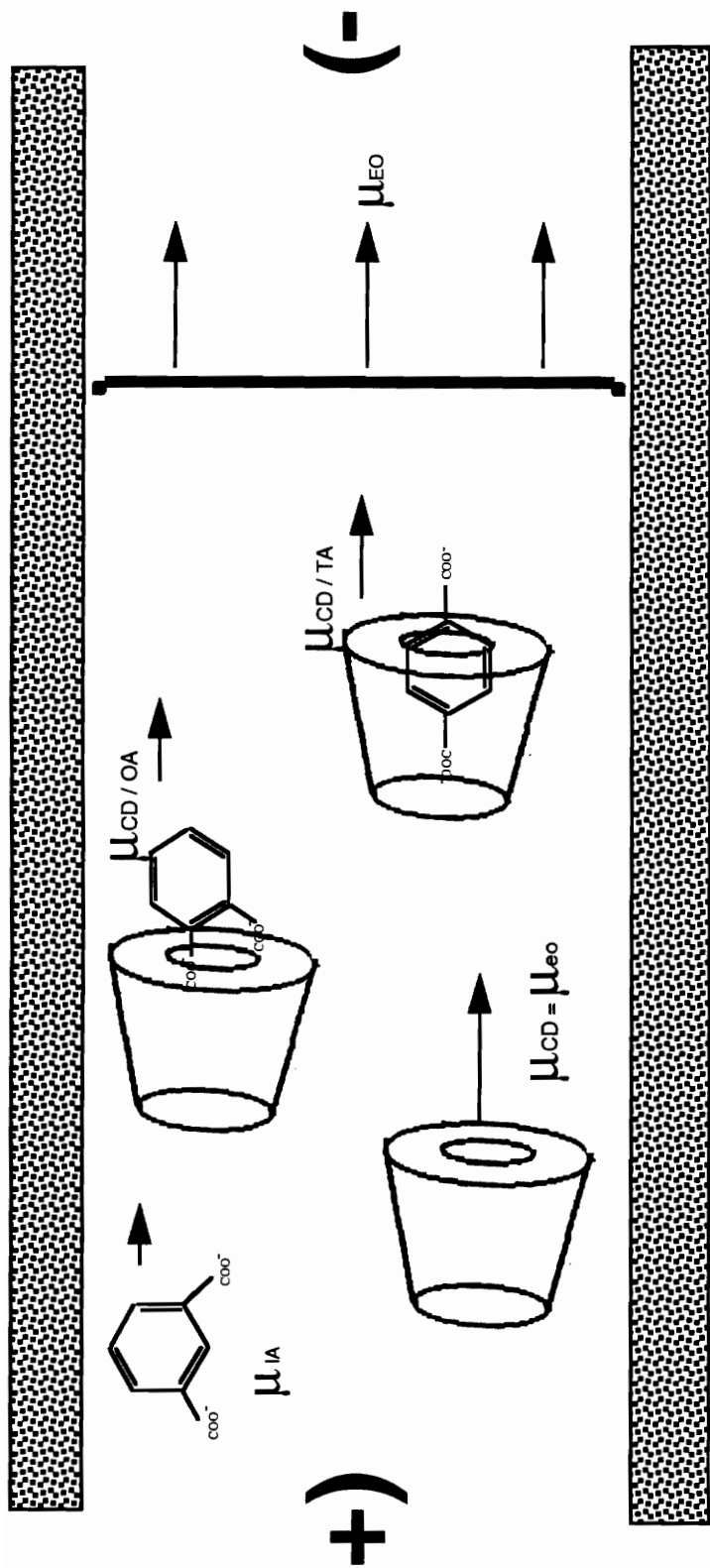


Figure 6.23: Separation mechanism for the aromatic carboxylic acids using cyclodextrins

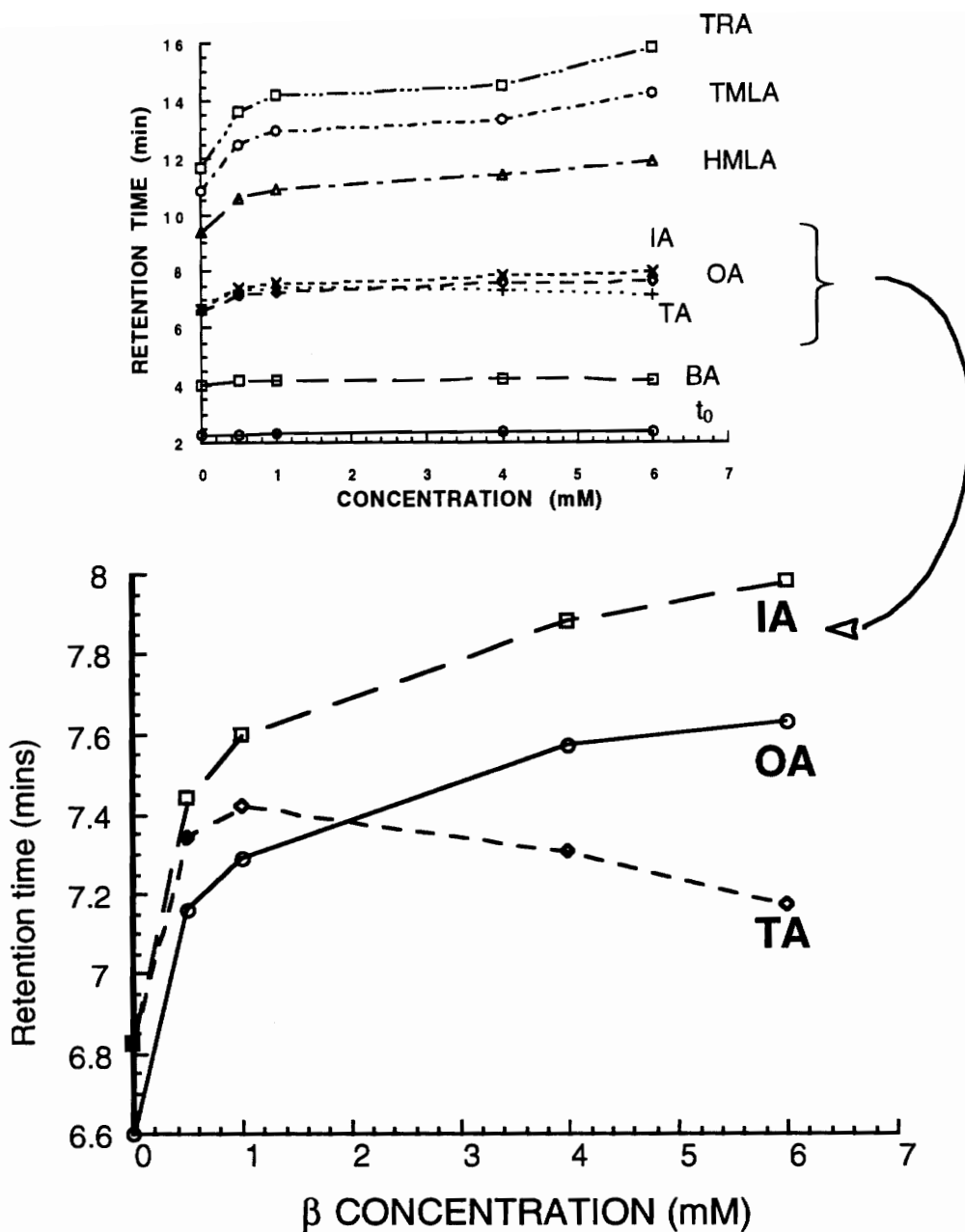


Figure 6.24: Effect of β Cyclodextrin concentration on elution order of the acids.
 0.05 M borate, β Cyclodextrin. pH 10.0, 25°C.
 Applied potential; + 25kV
 Capillary: 50 μ m id, L_d = 55 cm, L_t =57 cm

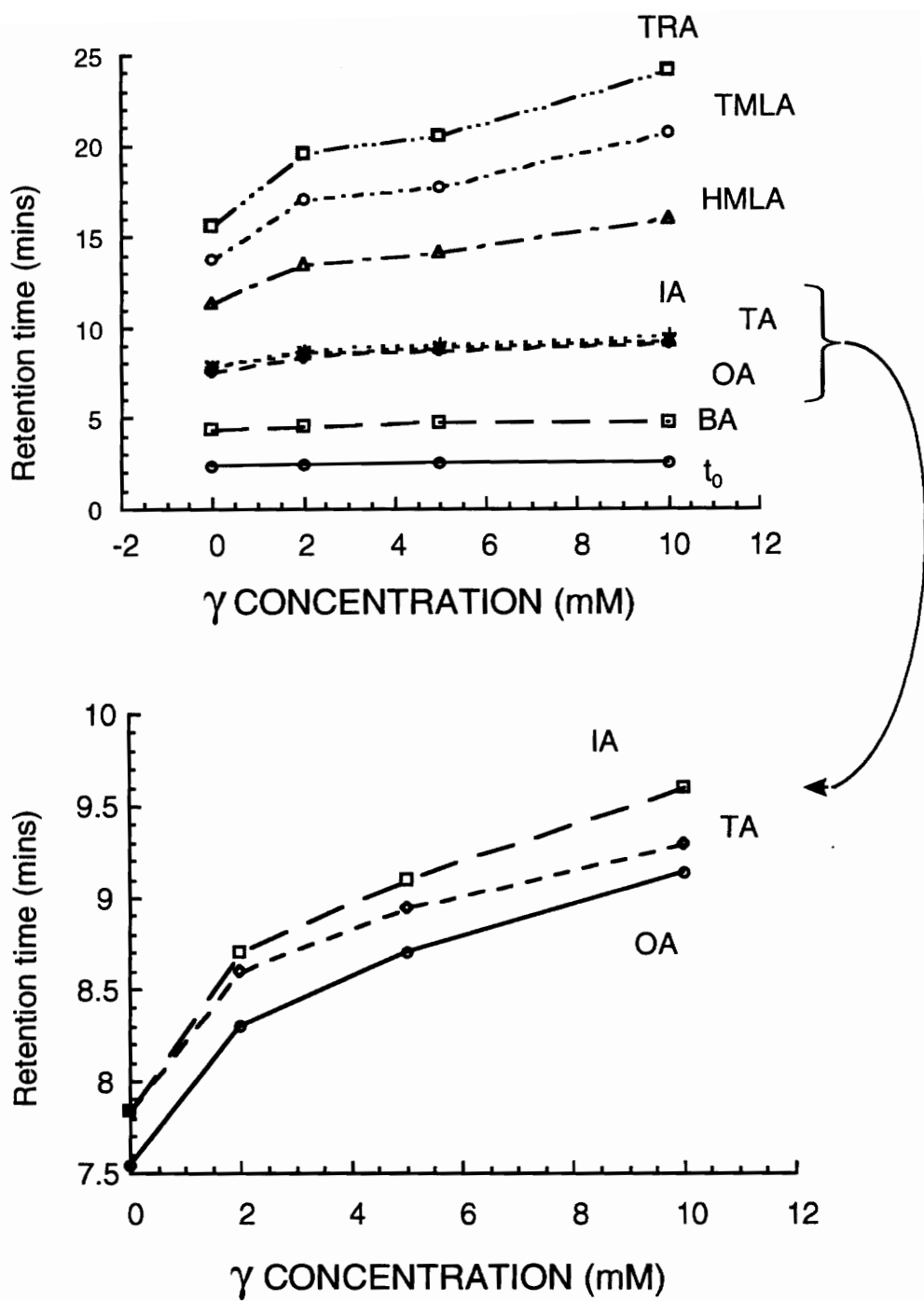


Figure 6.25: Effect of addition of γ cyclodextrin on the separation of the aromatic carboxylic acids . (conditions as in figure 6.23)

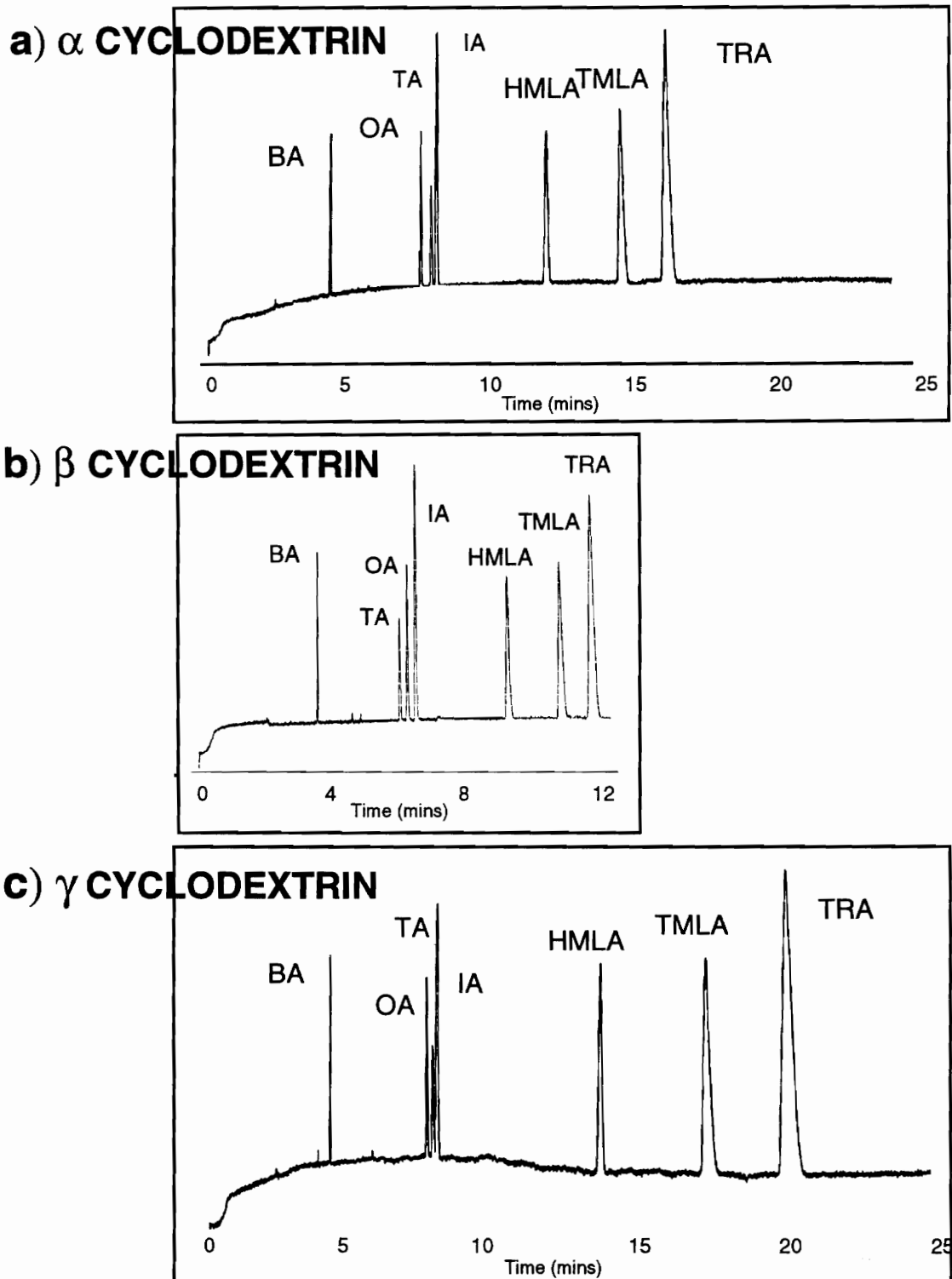


Figure 6.26: Separation of acids using cyclodextrins. Buffer: 0.05 M borate, a) 5mM α b) 4mM β c) 5 mM γ cyclodextrin. pH 10.0, +25 kV(440V/cm) (abbreviations as in figure 6.15)

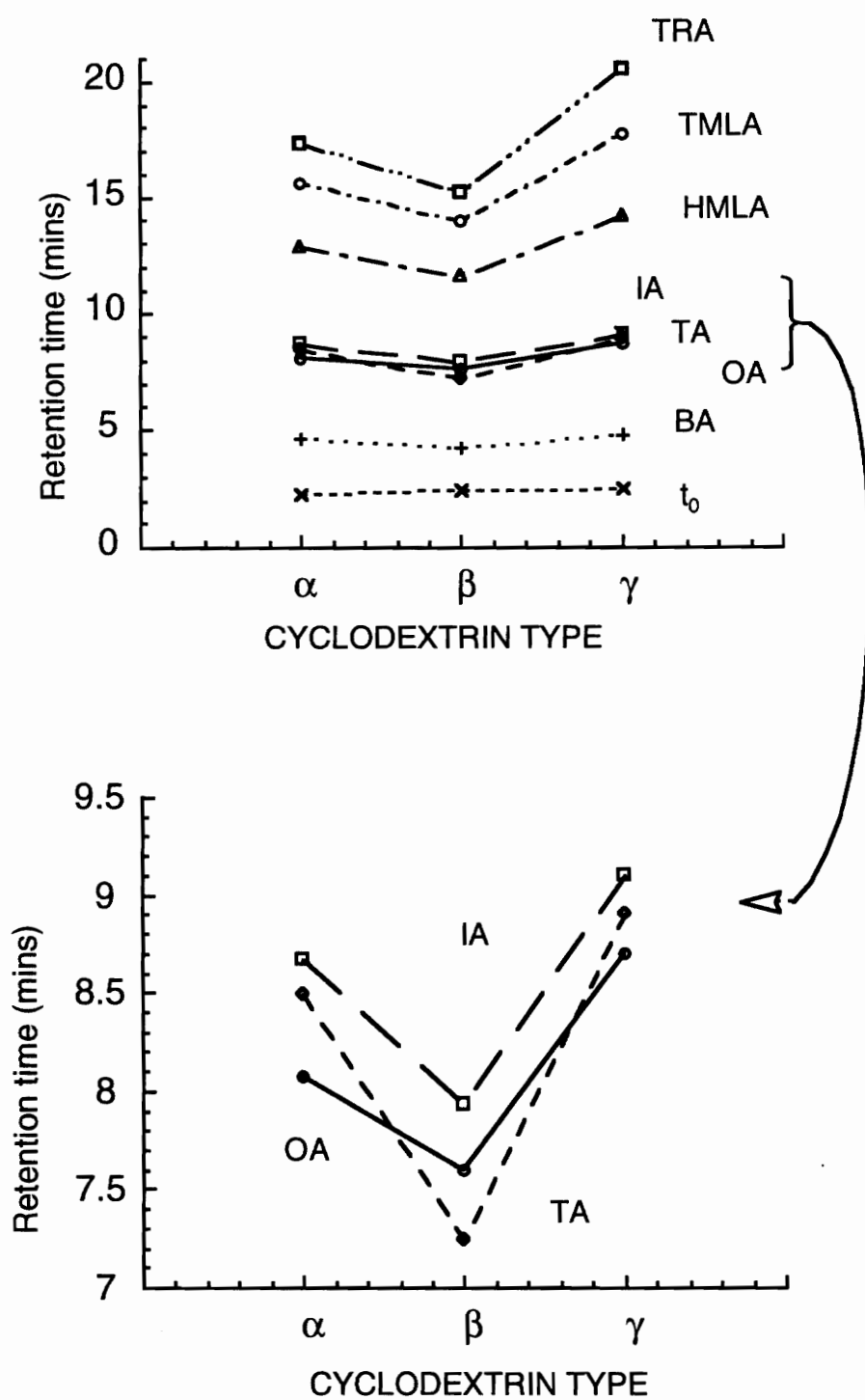


Figure 6.27: Effect of cyclodextrin type on retention of the aromatic acids. (conditions as in figure 6.24)

however, was not observed. β cyclodextrin seems to be the most successful in terms of inclusion and resolution of all the isomers.

Investigating the effect of various concentrations of both β and γ cyclodextrin on the resolution and efficiency of the acids led to some interesting results. Separation using β cyclodextrin is best using 4 mM when 25 kV is applied (fig. 6.24). Higher resolution, with larger CD concentrations, is also possible but at the expense of time and efficiency. However, optimum separation was found to vary with the potential applied, figure 6.28. At 25 kV and 2 mM β CD, both OA and TA co-eluted. Decreasing the potential results in the resolution of both isomers. This is an obvious contradiction to equation 2.17 mentioned earlier;

$$R = 0.177 \cdot (\mu_1 - \mu_2) \cdot \sqrt{\frac{V}{D_m \cdot (\bar{\mu} + \mu_{eo})}} \quad (2.17)$$

Although higher applied voltages should increase both efficiencies and resolution, as mentioned in section 3.2.1., this is limited by joule heating. The above equation only applies at low potentials. Hence, the resolution of the two isomers at lower potentials.

Testing the effect of injected amounts; 1-6 μ l injections at 0.2 psi as well as temperature 20-60 °C showed no influence on the resolution of the coeluted isomers.

Finally, % RSD values for this mode ranges from 2.9 - 4.2 %, for the retention times (n=6) and 6.8 - 7.3 % for the peak areas (n=7), fig. 6.29. A calibration curve for some of the acids showed a minimum detectable quantity of approx. 23 ppm with a hydrodynamic injection (30 mbars of 1 second

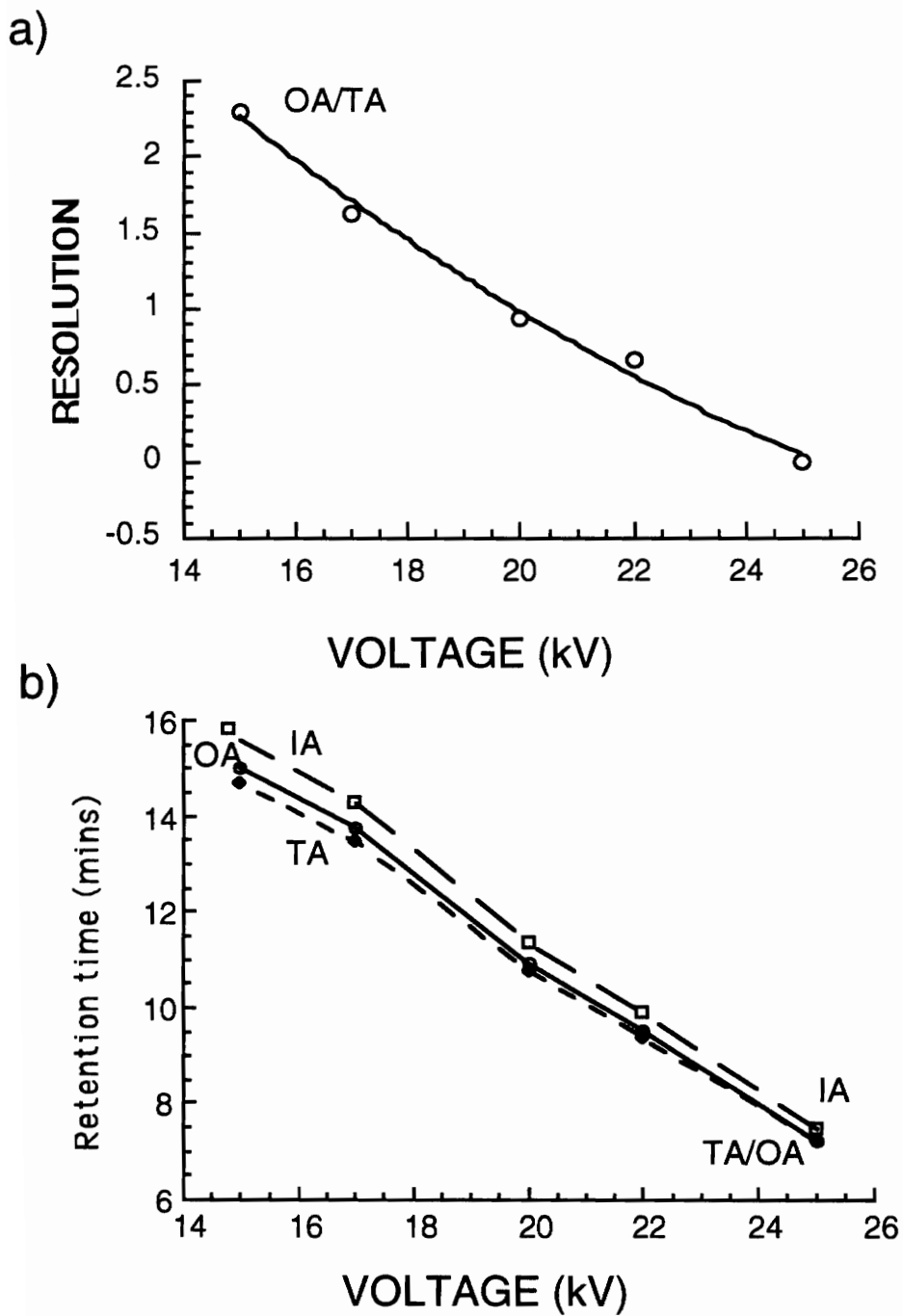
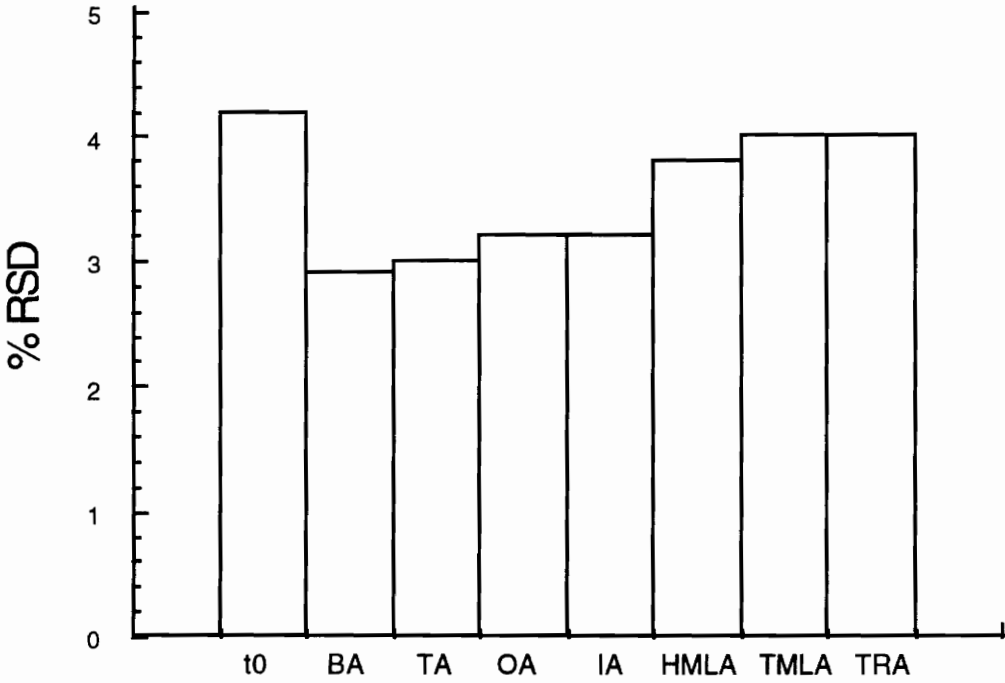


Figure 6.28: Effect of voltage on
 a) Resolution of TA from OA.
 c) Effect of Voltage on Retention time.

a) Migration time (n=6)



b) Peak area (n=7)

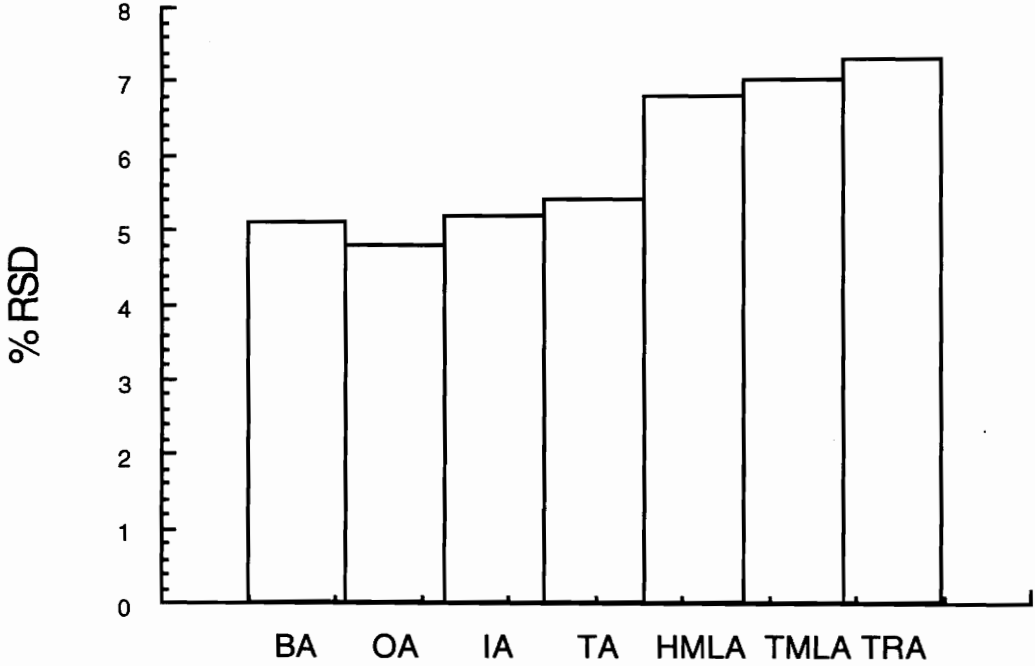


Figure 6.29: % Relative standard deviation in
a) Time n=6 and b) Area n =7
Conditions as in figure 6.24

duration). A loss in resolution due to overloading occurred for concentrations above approximately 150 ppm (fig. 6.30)

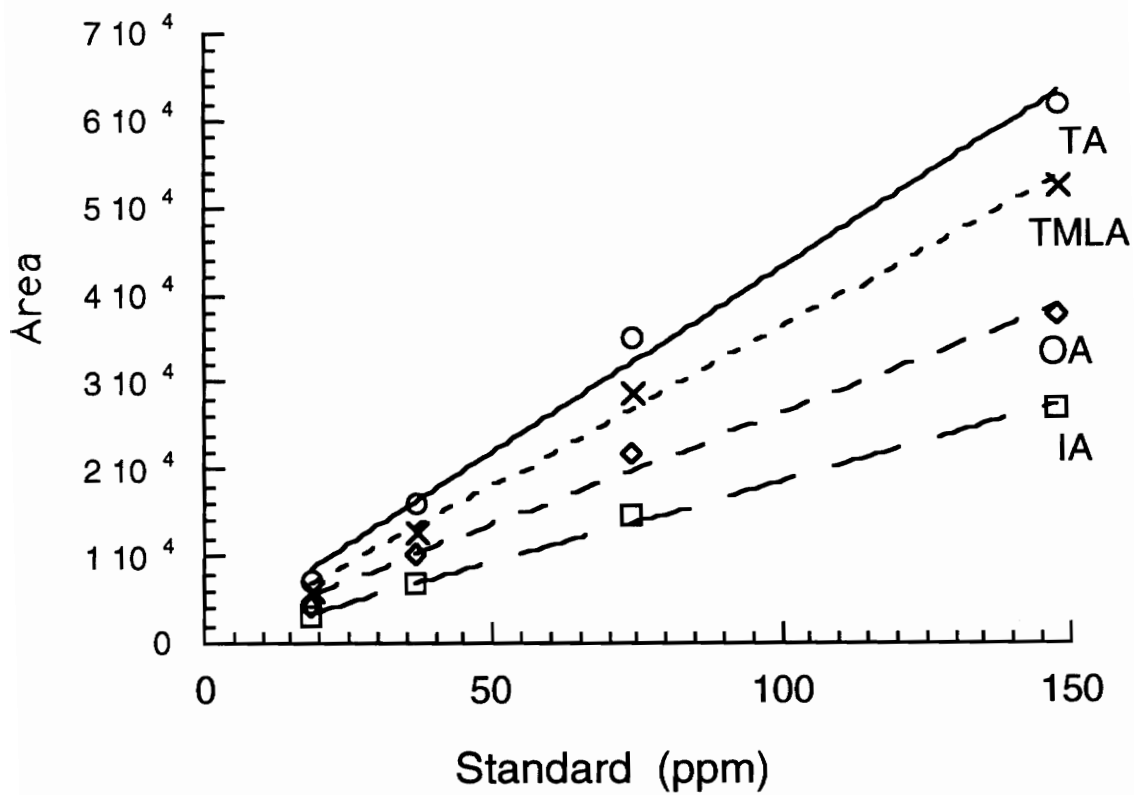


Figure 6.30: Calibration curve for acids.
 Linear regressions TA=0.996, TMLA=0.998,
 OA=0.995, IA=0.998

6.2.3. Electrolyte System c) Positive polarity, with 0.05 M borate buffer and organic modifiers

Based on the work by Fujiwara and Honda ⁽⁹¹⁾ 1-2 % methanol was added to the borate buffer, at 25 kV, in hope of some intra- and inter-hydrogen bonding interactions that may differentiate between the two isomers. No separation of IA from TA was possible. Larger additions of methanol merely resulted in an increase in retention times of the anions and decrease in the peak efficiencies and resolution. However, at +12 kV methanol addition seemed to show slightly better resolution relative to the separation at +25 kV. The other analytes however, displayed deteriorated peak shapes. Acetonitrile addition did not affect resolution.

6.2.4. Electrolyte system d); negative Polarity, 0.1 m borate buffer with cationic Surfactant

The control of electroosmotic flow is very important in capillary electrophoresis as it plays a crucial role in determining the separation and analysis time. The electroosmotic flow as mentioned earlier can be affected by manipulations in the background electrolyte. Additives such as cationic surfactants have been studied ^(79,164-168) and found to have a profound effect on electroosmotic flow. It is well documented that the addition of cationic surfactants first reduces the electroosmotic flow, next eliminates it and finally reverses it's direction. This reversal in electroosmotic flow can be advantageous in the separation of anionic compounds ^(79,169,170).

The addition of cationic surfactants was attempted here, in hope of eliminating the problem of tailing peak shapes for the tri-carboxylic acids. The

surfactant's cationic moiety adsorbs onto the silica surface reducing the electroosmotic flow (fig. 3.7a). With further additions the electroosmotic flow is totally counteracted followed by the formation of hemimicelles ⁽²⁰⁵⁾ (fig. 3.7b). The charge on the silica surface becomes positive and the direction of the electroosmotic flow is, consequently, reversed and the flow is towards the anode. Anionic solutes, consequently, elute first. Further increases in surfactant concentration (beyond the cmc) result in micellar formation. As proposed by Fuerstenau ⁽²⁰⁶⁾ and demonstrated in the work of Kaneta et al ⁽⁷⁹⁾, the electrophoretic mobilities of anions is controlled by the interaction with a) the monomer of the cationic surfactant based on ion pairing equilibria, b) the hemimicelles formed on the capillary wall and c) the micelles in the bulk solution.

This work investigates three different chain length cationic surfactants Cetyltrimethylammonium bromide (CTAB), Dodecyltrimethylammonium bromide (DTAB) and Butyltrimethyl ammonium bromide (BTAB) with variations in concentrations below their critical micellar concentration (cmc). Therefore, no micellar interactions are involved.

Reversal of the elution order was achieved as expected (fig. 6.31), with no separation of the TA and IA isomers. A delicate combination of buffer concentration, surfactant concentration and pH proved necessary to achieve optimum separation. Extensive surface equilibration between each and every run and solution replenishment were found crucial for reproducibility of the

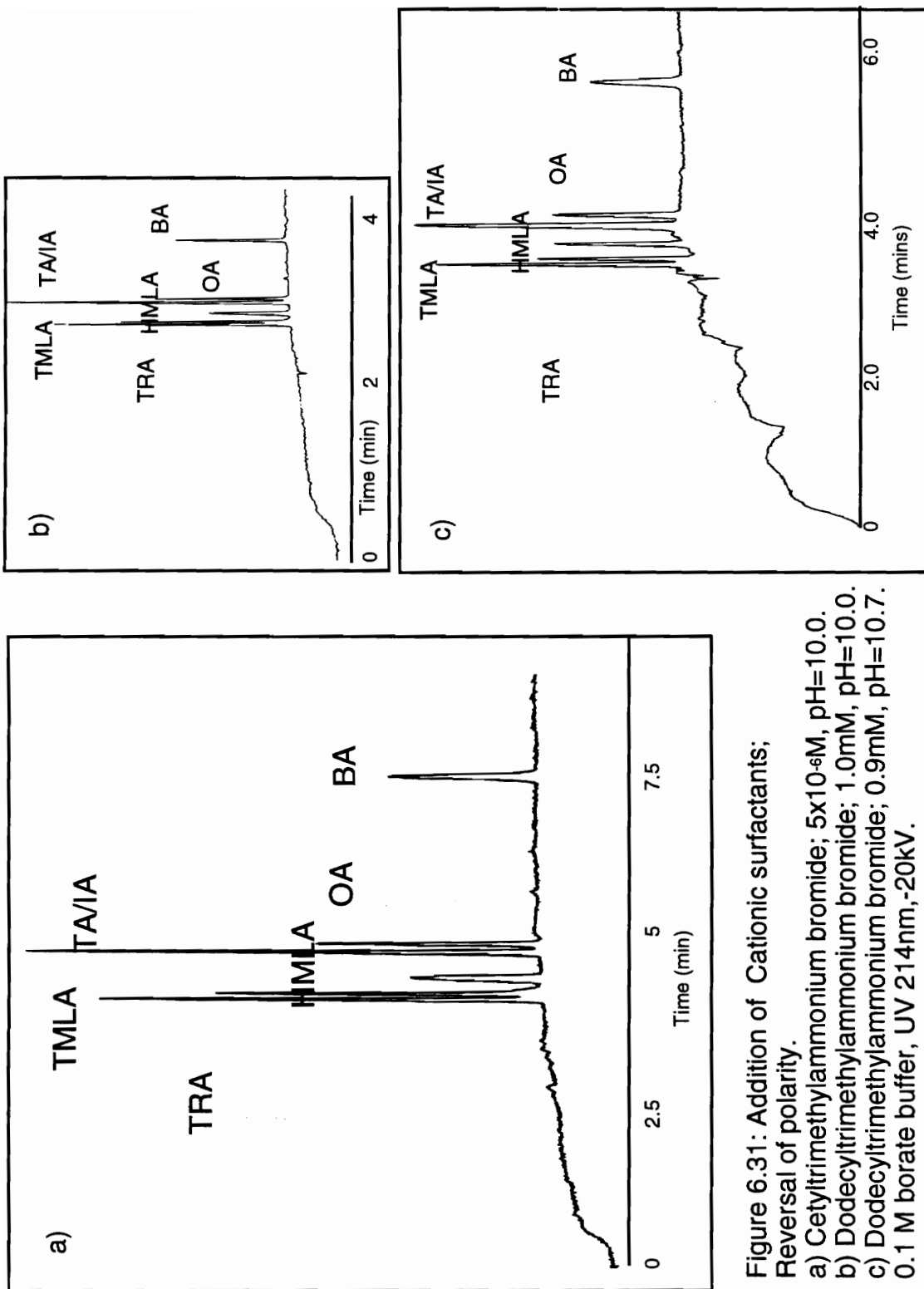


Figure 6.31: Addition of Cationic surfactants;
Reversal of polarity.

- a) Cetyltrimethylammonium bromide; $5 \times 10^{-6} \text{M}$, $\text{pH}=10.0$.
- b) Dodecyltrimethylammonium bromide; 1.0mM , $\text{pH}=10.0$.
- c) Dodecyltrimethylammonium bromide; 0.9mM , $\text{pH}=10.7$.
 0.1 M borate buffer, UV 214nm, -20kV.

method rendering it unpractical and time consuming. Additionally, signal to noise is reduced.

Attempts to add cyclodextrin resulted in further reproducibility problems and pronounced decreases in efficiency and increases in retention time. This may be attributed to the increase of system viscosity and possible competition of the surfactant hydrophobic chains for the cyclodextrin cavities (208). Use of the shorter chain 0.01 M BTAB in this configuration, to eliminate such interactions, was unsuccessful and resulted in high currents, unstable baselines and highly reduced electroosmotic flow.

The above electrolyte systems of sections 6.2.2 and 6.2.4, were tested on real samples to determine oxidation products in cake and total reactor effluent samples from the oxidation process of 2,6-dimethyl naphthalene to manufacture the 2,6-naphthalene dicarboxylic acid (2,6-NDA), (figs 6.32).

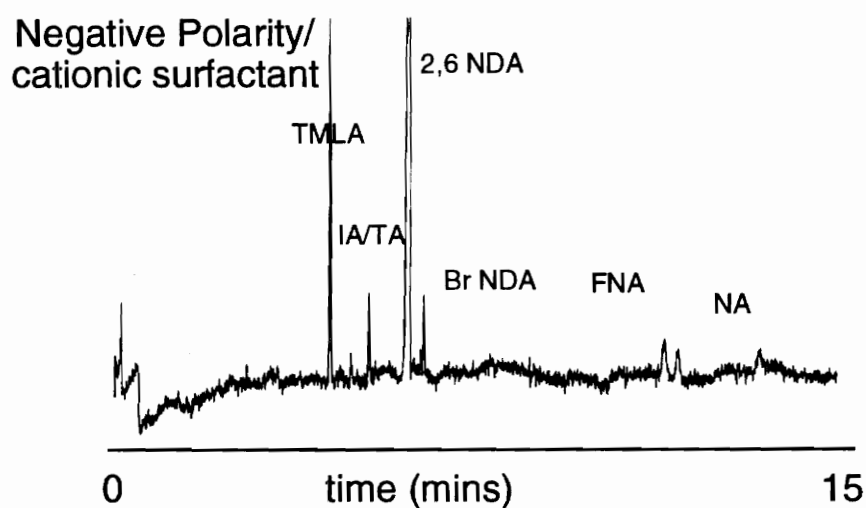
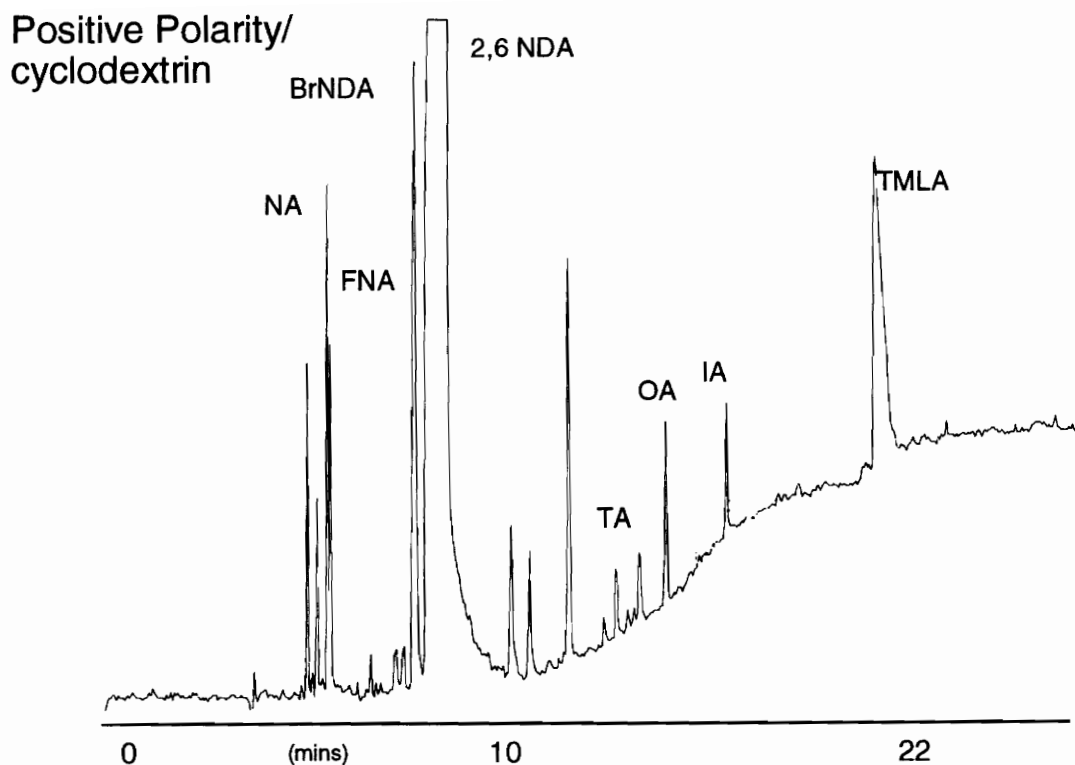


Figure 6.32: Industrial Sample

- a) Positive polarity, borate buffer, pH10.0, with β cyclodextrin,
 b) Negative polarity with cetyltrimethyl ammonium bromide, pH10.0
 Br-NDA= Bromo-2,6 Naphthalene dicarboxylic acid;
 2,6 NDA = 2,6 Naphthalenedicarboxylic acid
 FNA = 6-Formyl-2-Napthanoic acid; NA = Napthanoic acid

6.3. EVALUATION OF AN OLIGOMERIZED SODIUM UNDECYLENATE AS A SURFACTANT FOR THE SEPARATION OF VITAMINS.

The introduction of Micellar Electrokinetic Capillary Chromatography, MECC, by Terabe in 1984 ⁽²¹⁾, allowed the separation of neutral compounds, eliminating one of the then major disadvantages of the technique, (section 3.3.3). MECC, however, remains restricted by a limited elution range and difficulty in analysis of hydrophobic compound. Hydrophobic analytes not only tend to have high partition coefficients eluting very close with the micelles, but also are difficult to detect due to their limited solubility in aqueous micellar solutions. To address these problems, organic modifiers such as methanol and acetonitrile, have been experimented with to enhance partitioning of the analytes between the mobile and micellar phases. Their addition is, however, restricted to levels around 10-20% as higher concentrations tend to disrupt the micelle formation.

Attention is beginning to veer towards the replacement of micelles with polymeric components that exhibit micellar properties, but have zero cmc values which permit the addition of large amounts of organic modifiers. Ewing and Wallingford were the first to report and discuss the use of monodisperse polymer particles as pseudostationary phases ⁽¹⁷¹⁾. They separated five catechols with an anionic sulfonated polymer system (fig. 6.33). When the peaks appeared broad, they expressed their concern for the kinetics of solute-polymer interactions. Terabe ⁽¹⁷²⁾ later reported the use of cationic polymers (polydiallyldimethylammonium chloride and (diethylamino) ethyldextran) in ionic exchange MECC for the separation by ion pair formation of naphthalene-

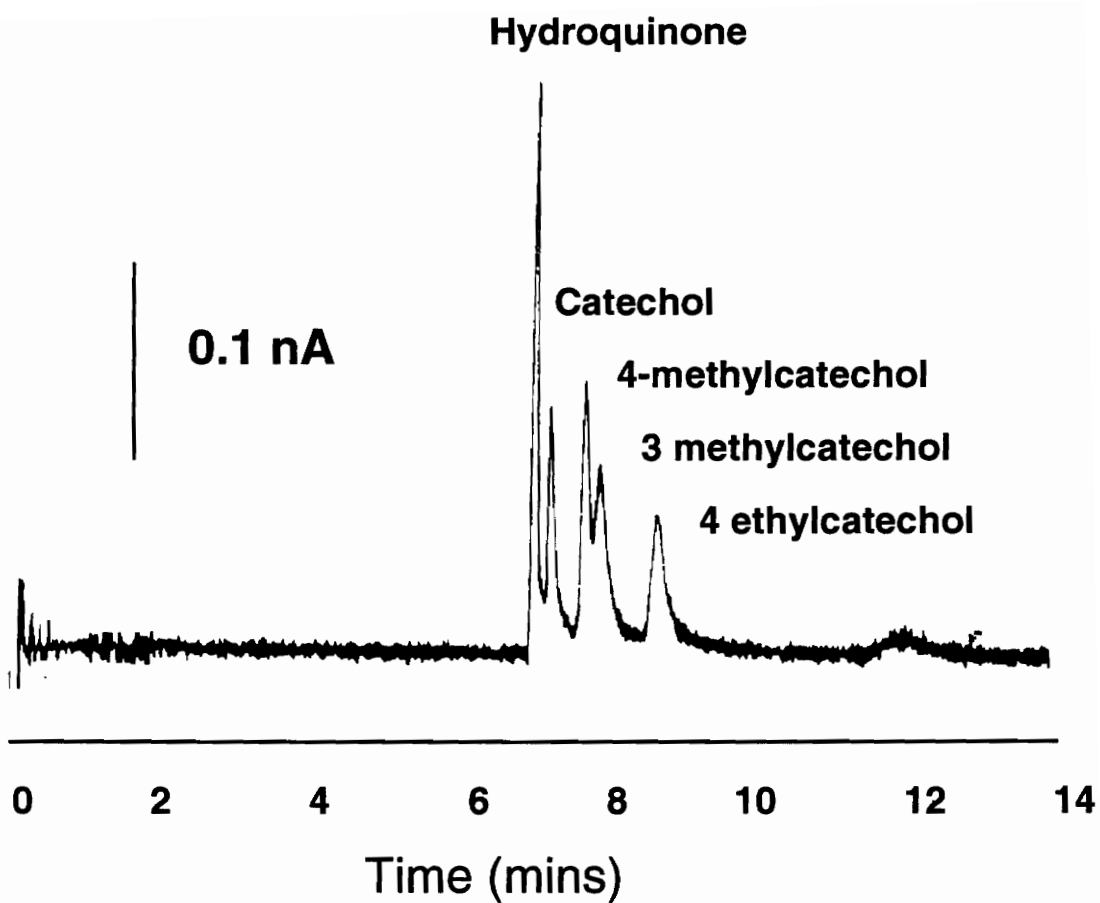


Figure 6.33: Electrokinetic separation of catechols using a monodisperse sulfonated polymer.⁽¹⁷¹⁾

sulfonates and naphthalenedisulfonates. In 1993, Palmer et al (3, 173) introduced oligomerized sodium 10-undecylenate for the most hydrophobic separation in CE of polyaromatic hydrocarbons (fig. 6.34) using up to 40% methanol or 40% acetonitrile. Phthalates and alkylbenzenes were also separated. The authors, however, noticed a non-linearity in the logarithm of the capacity factor with organic modifier content, indicating a change in the oligomer structure with solvation.

6.3.1. Micellar polymerization; Oligomerized sodium 10-undecylenate.

Larrabee et al reported in 1979 (174) that sodium 10-undecylenate can be polymerized by ^{60}Co γ irradiation, above its micellar concentration (0.04 M) to give the low molecular weight polysoap, poly (sodium 10-undecylenate). The polymerization is facilitated by the presence of the vinyl group at the end of the lipophilic chain and the organization of the polymerizable groups is induced by micellization. With vapor pressure osmometry, the polymer molecular weight was determined to be 2000 daltons and so it has a degree of polymerization equal to ten monomers. This is consistent with the separate measurements of the aggregation number of the sodium 10-undecylenate micelle, which was determined to be 12 ± 5 at 37°C (175).

Recently (176) the cmc of the monomer has been revised to 0.115 M determined with conductance measurements. The polymerization with Larrabee's earlier lower concentration has been attributed to pre-micellar aggregation rather than genuine micellization.

The polymeric micelle, having zero cmc, demonstrates micellar behavior at all concentrations. Nevertheless, the conductivity versus polymer

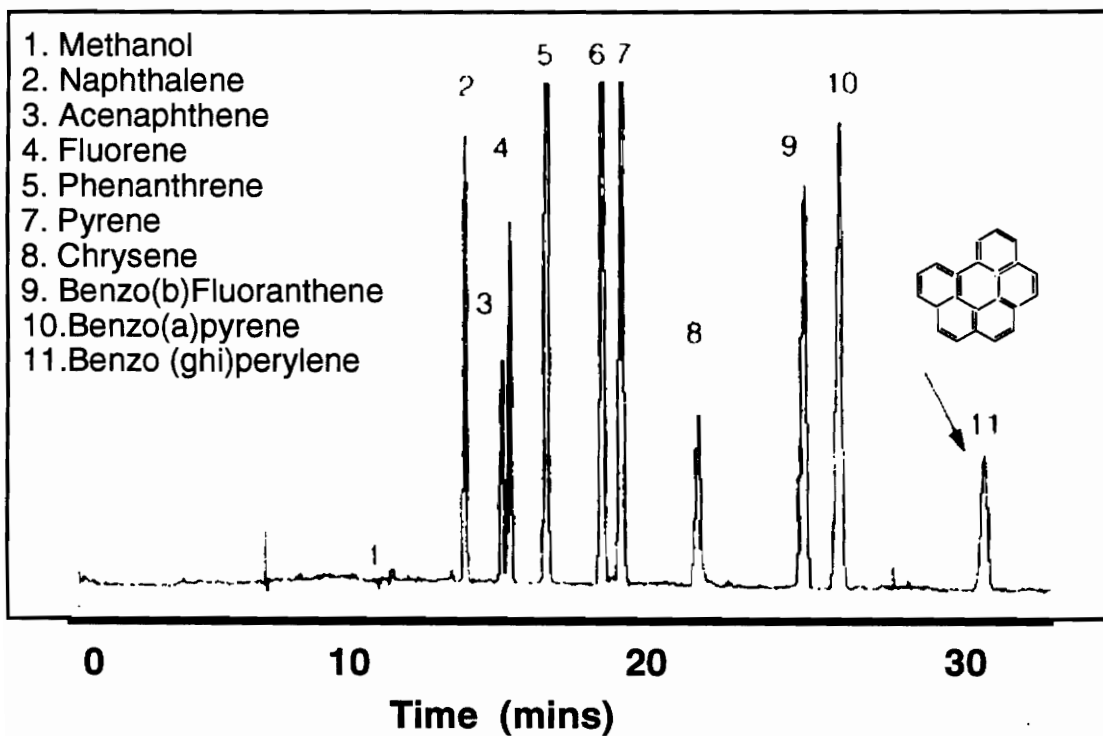
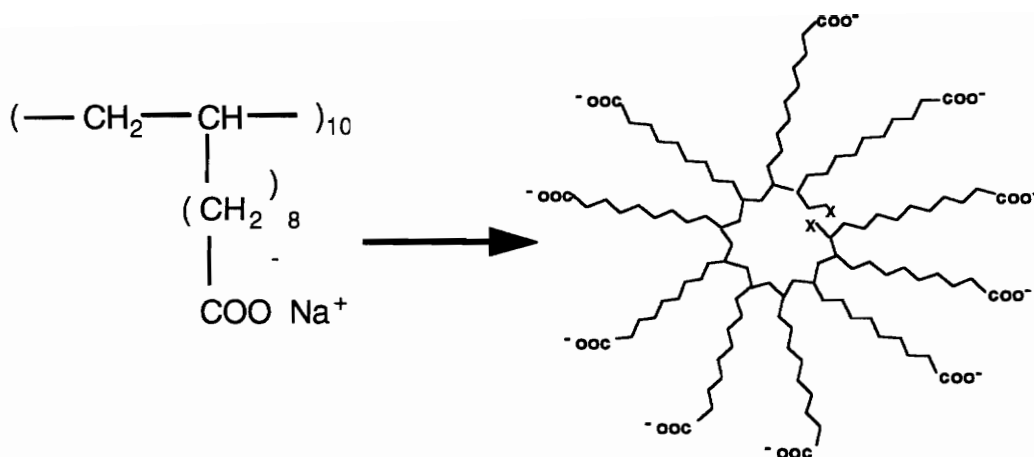


Figure 6.34: Separation of PAHs using sodium undecylenate Oligomer (35%ACN). (3)

concentration plot still exhibited an inflection point (0.1 M) similar to the cmc inflection induced by formation of micelles. This, however, has been attributed to the onset of intramolecular micellar aggregation ().

The intrinsic viscosities of aqueous solutions of the monomeric and polymerized material have shown that the polymerized micelle has a hydrated size equal to the size of the monomeric micelle (177).

Fluorescence studies with the micropolarity probe pyrene show that the fluorophore penetrates the intermolecular polymeric micelle less than the monomeric one. This is expected of the more compact structure of the polymeric micelle due to the presence of polymerization-induced covalent bonds among the terminal methylene groups of the undecylenate chains (177).

The present study involves characterization of this sodium 10-undecylenate oligomer synthesised by free radical initiation instead of γ radiation. Carbon-13 and proton NMR studies are used to confirm the structure molecular weight and aggregation number. Molecular interactions with a number of vitamins are used to shed some light on the oligomer's behavior as a MECC surfactant.

6.3.2. Oligomeric synthesis and NMR characterization

The synthesis of the polymer in this work has followed the procedure of Dujurai and Blum (133) as detailed in the experimental section. The polymerization is induced by catalytic initiation using potassium persulfate instead of γ radiation. The achieved yield was 7% (2.67g) which is low but generally expected from free radical polymerization of α -olefins, which additionally result in low molecular weight oligomers due to autoinhibition by allylic hydrogens (178).

Carbon 13 NMR (fig. 6.35) of the product yielded peaks at 185, 39, 31 and 27 ppm related to the oligomer as well as some other additional peaks 141.6, 115, 34 ppm indicative of residual monomer and ethanol. Two synthesized batches were examined and found to yield peaks at similar frequencies, however, they differed in the resonance of the peak at 30 ppm. This peak is usually broader for the polymer than it is for the monomer due to the shorter relaxation times of the chain carbons. This is in agreement with the spectra obtained by Durairaj et al (133) whose T_1 relaxation studies indicated reduced mobility at the center of the oligomerized micelle relative to the monomeric center. The difference between the two batches may be indicative of variations in the aggregation number resulting from the synthetic procedure.

Proton NMR (fig. 6.36) yielded the expected peaks at 5.75, 4.9, 4.65, 3.9, 3.5, 2.1, 1.9, 0.8-1.6 ppm. Of interest in this spectra are the two barely visible peaks at 3.9. These are probably the 3 protons close to the terminating groups (X in fig 5.3) suspected to be hydroxyls.

6.3.3. Separation of vitamins in CE

The fat and water soluble vitamins were chosen in an attempt to further characterize the oligomer and investigate its behavior relative to the other available micellar systems previously used in a capillary electrophoresis. The vitamins chosen (fig. 6.37) varied in structure, hydrophobicity and size, as well as UV absorbitivity and wavelength (fig.6.38).

Previous CE separations have involved the use of Sodium Dodecyl Sulfate (SDS) (179-182) and investigations of the additional effect of tetralkylammonium salts (183). Only two attempts thus far have been made to separate fat soluble vitamins; Ong et al in 1991(184) found that the addition of γ

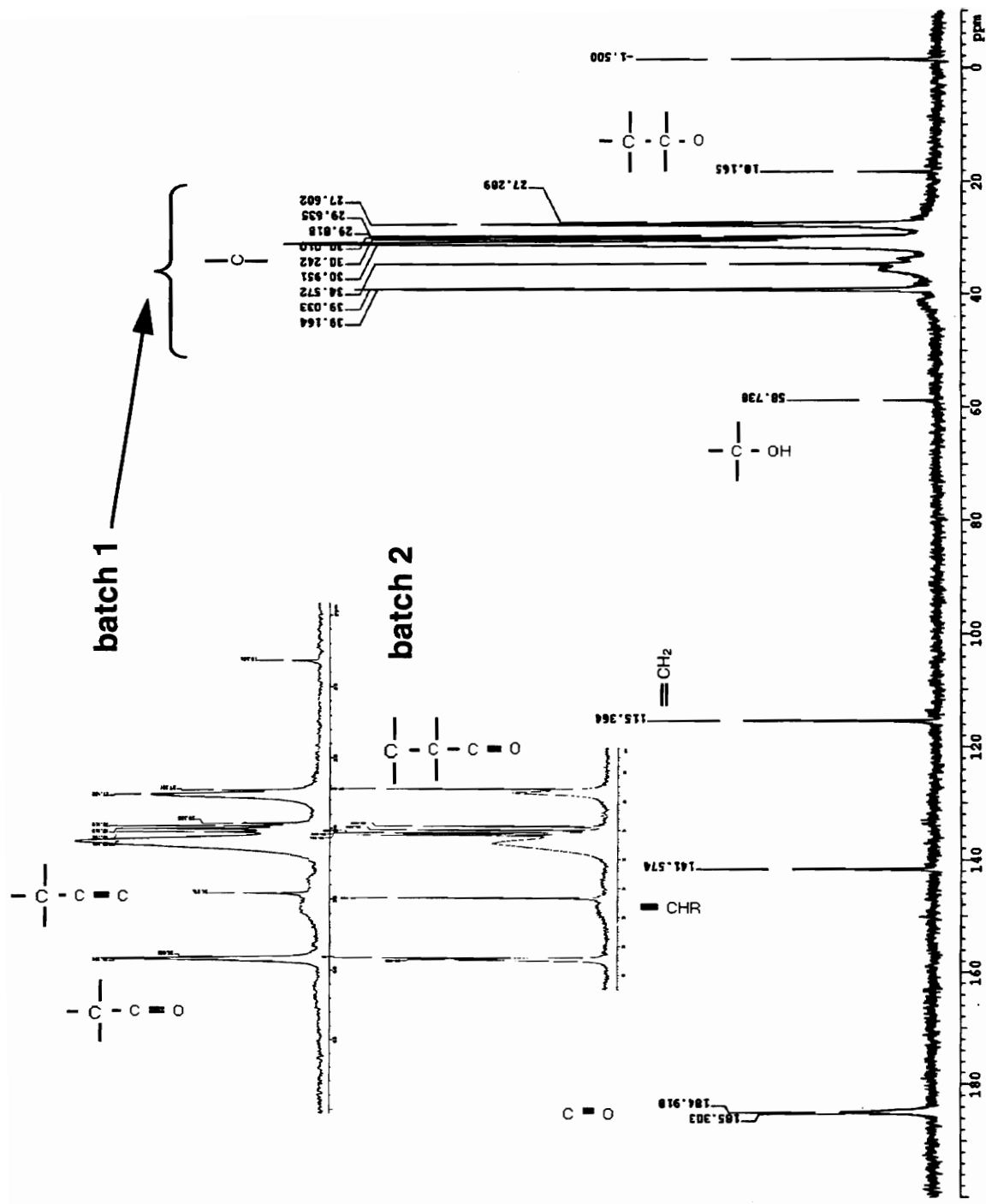


Figure 6.35: Carbon-13 NMR spectra of the Oligomerized Sodium 10-Undecylenate (UDO). Comparison of two synthesized batches.

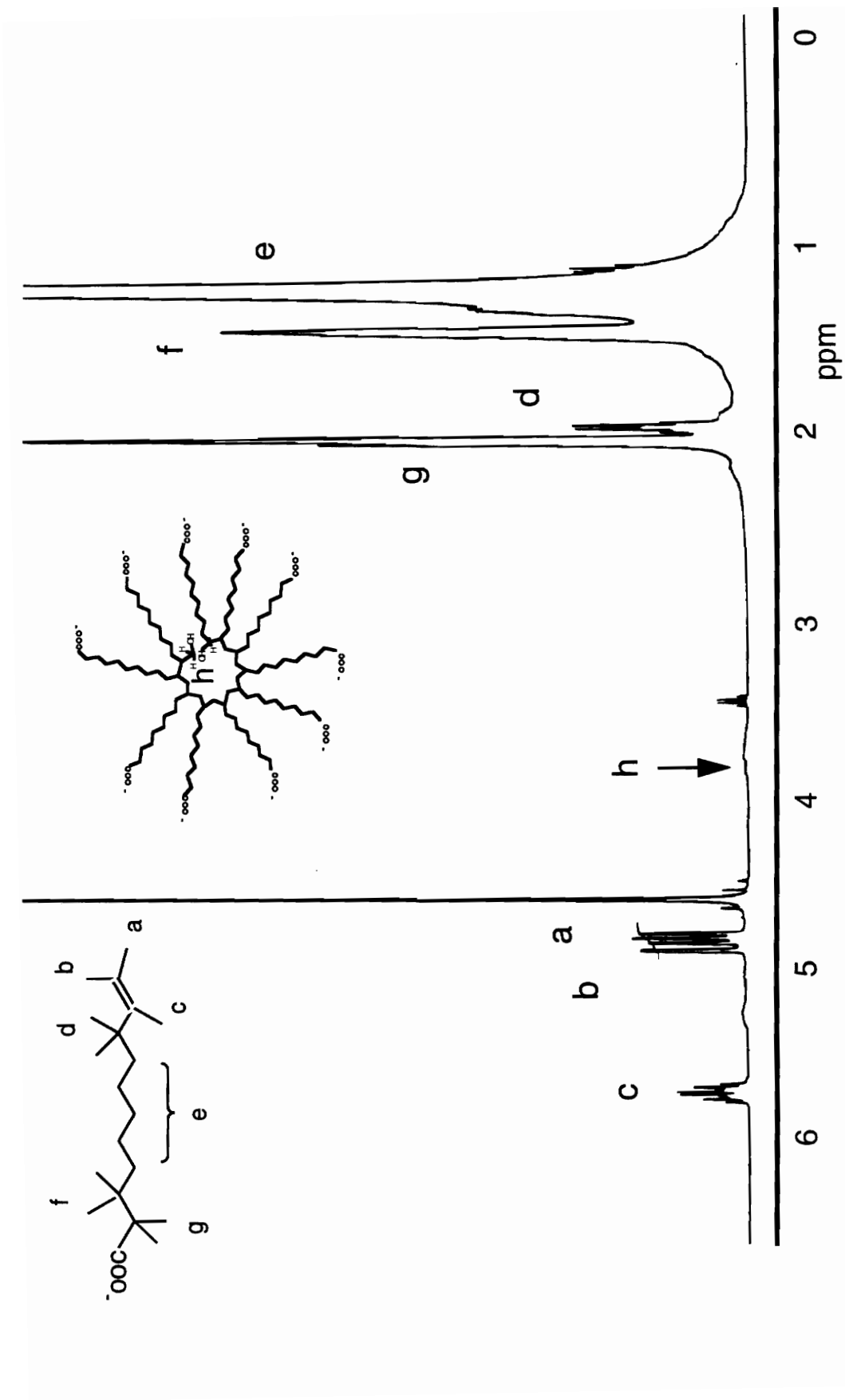


Figure 6.36: Proton NMR of sodium undecylenate oligomer

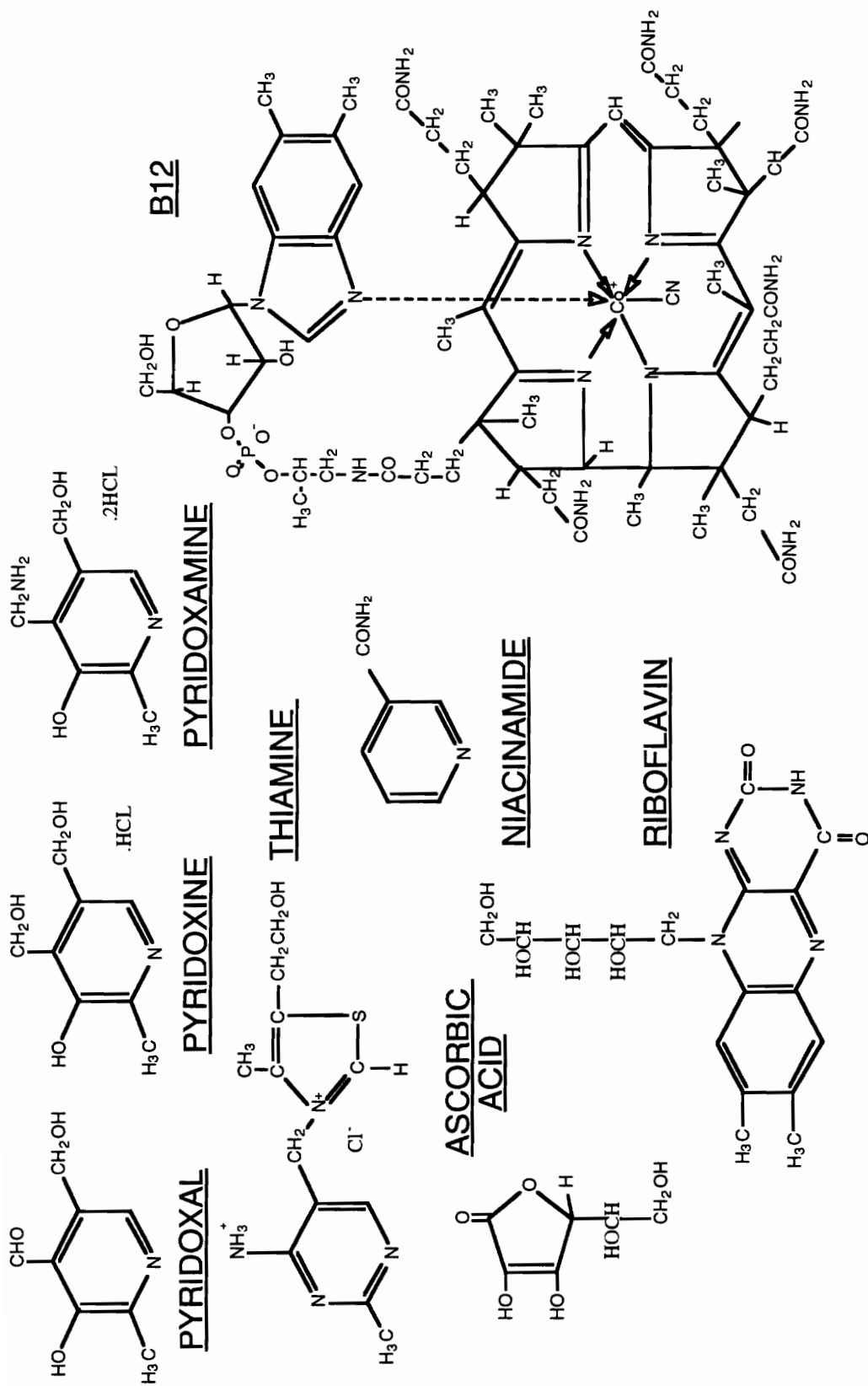


Figure 6.37: Molecular structure of water soluble vitamins

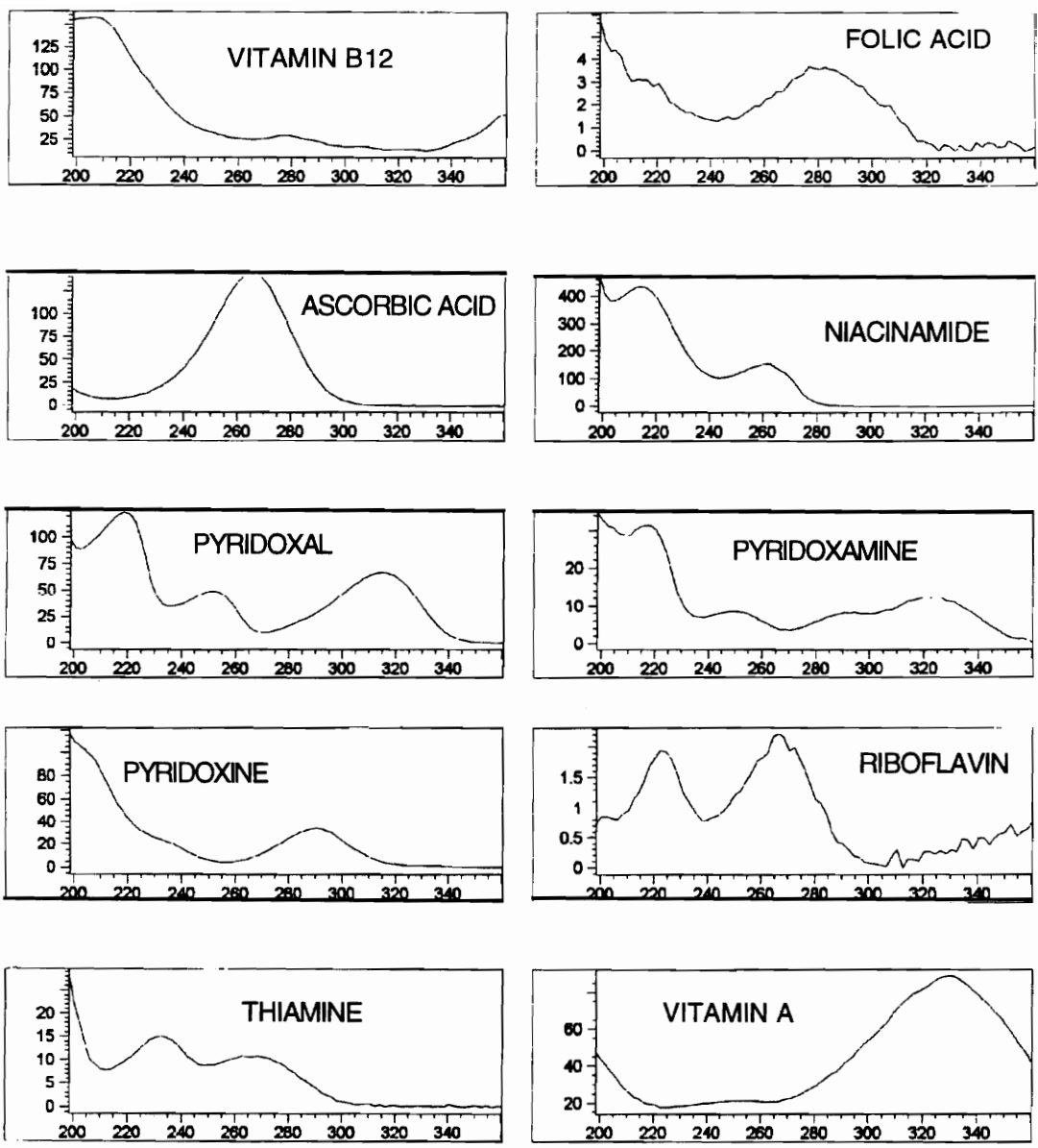


Figure 6.38: Absorbance spectra of Vitamins.

cyclodextrin or 3% isopropanol to an SDS micellar system improved the solubility of vitamins E and A and their separation. Two years later with the addition of 20 % ACN and SDS Chan et al (185) separated 5 analogs of vitamin A. This work involves the characterization of the interactions of the vitamins with the oligomer and the monomer micelle and relating the results to interactions with the commonly used SDS. This, additionally, involved variations in pH, micellar concentration, % organic modifier as well as different synthesized batches.

The effect of oligomer concentration

Figure 6.39 shows the effect of the oligomer concentration on the retention time of the water soluble vitamins, obtained by adding various amounts of the oligomer to a phosphate / borate buffer at pH 8.2. In the absence of a micellar phase all neutral vitamins (nicotinamide and B₁₂) coelute at t_0 while the cationic vitamins (thiamine and pyridoxamine) elute prior to t_0 , in a CZE type of separation. The addition of the oligomer, whose carboxylate group gives it a negative electrophoretic mobility, resulted in a different elution profile. The retention of the vitamins increased with increasing oligomer concentration. The effect was most obvious for riboflavin and thiamine. All vitamins were base line resolved at all oligomer concentrations. B₁₂ separates well from niacinamide as it interacts with the oligomer to a larger extent, probably through ionic interaction with the carboxylate groups. Thiamine, also cationic, interacts to a greater extent than does B₁₂, probably due to the latter's bulkier hindrance. Riboflavin's hydrophobicity increases its residence time within the micelle resulting in longer elution.

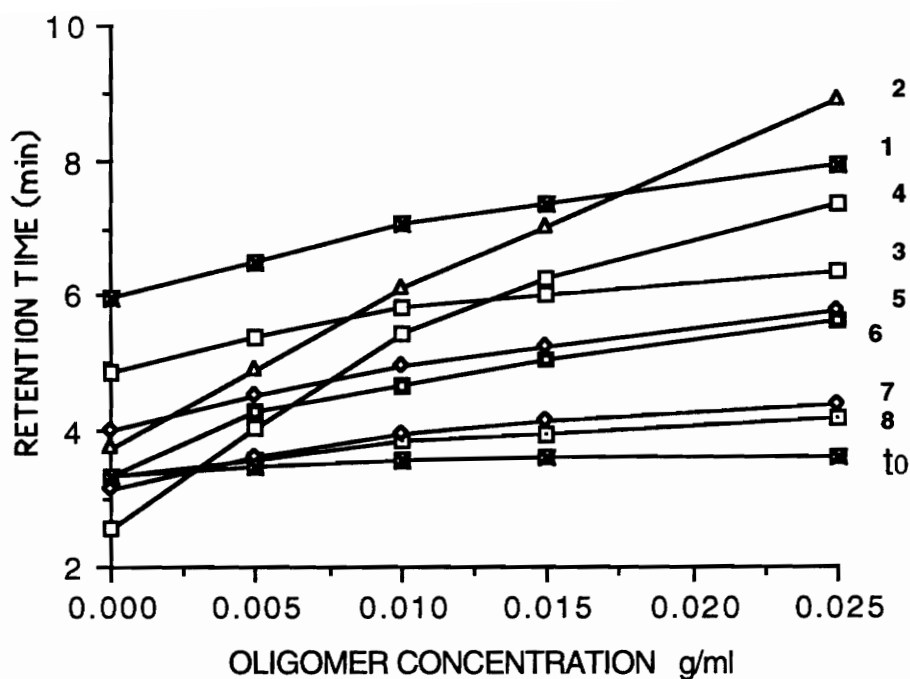


Figure 6.39: Effect of Oligomer (UDO) concentration on the elution order of water soluble vitamins.

HP ^{3D}CE; Capillary: id = 50 μ m, L=55 / 46.5 cm,

Buffer: 0.05M phosphate / 0.1M borate, pH 8.2..

1. Ascorbic acid (C), 2. Riboflavin(B₂), 3. Pyridoxine PN (B₆),
- 4.Thiamine (B₁), 5. Pyridoxal PL (B₆), 6. B₁₂,
7. Pyridoxamine PA (B₆), 8. Niacinamide(B₃')

The Effect of pH

Figure 6.40 shows the effect of pH on the retention time of the vitamins when the concentration of the oligomer is maintained at 0.01 g/ml. At pH 7.0, niacinamide, B₁₂, thiamine and pyridoxal are all overlapping with pyridoxal tailing badly (unstable at this pH). At pH 7.5 only pyridoxal and thiamine are coeluting. At pH 8.0 riboflavin and pyridoxine cross path with the former's peak shape deteriorating. The best separation may be obtain between pH 8.2 to 8.75. At pH 9.0 riboflavin and pyridoxine as well as thiamine and pyridoxal coelute. The lowest possible pH should be employed as several vitamins are unstable at alkaline conditions.

In general most of the vitamins are not affected by pH with the exception of ascorbic acid, riboflavin and thiamine, the three which happen to be unstable in basic media. Ascorbic acid, increasing in negativity with increasing pH, is possibly being repelled from the negatively charged carboxylate group of the oligomer, and consequently elutes faster. However, thiamine and riboflavin show an increase in retention despite the increase in pH. Since these two vitamins seem also to interact the most with the oligomer, the increase in pH may be further enhancing this interaction.

Changes in the electrophoretic mobilities, compound stability as well as hydrophobicity and ion pairing interactions, are responsible for this complex variation of retention with pH. The resultant plot (fig. 6.40) is different from the pH effect plots of SDS micellar systems, which shows an almost linear increase with pH for some of these vitamins (180-182).

Based on these results, the best conditions were 0.01 g/ml of the oligomer at a pH of 8.2 obtaining the separation of the water soluble vitamins

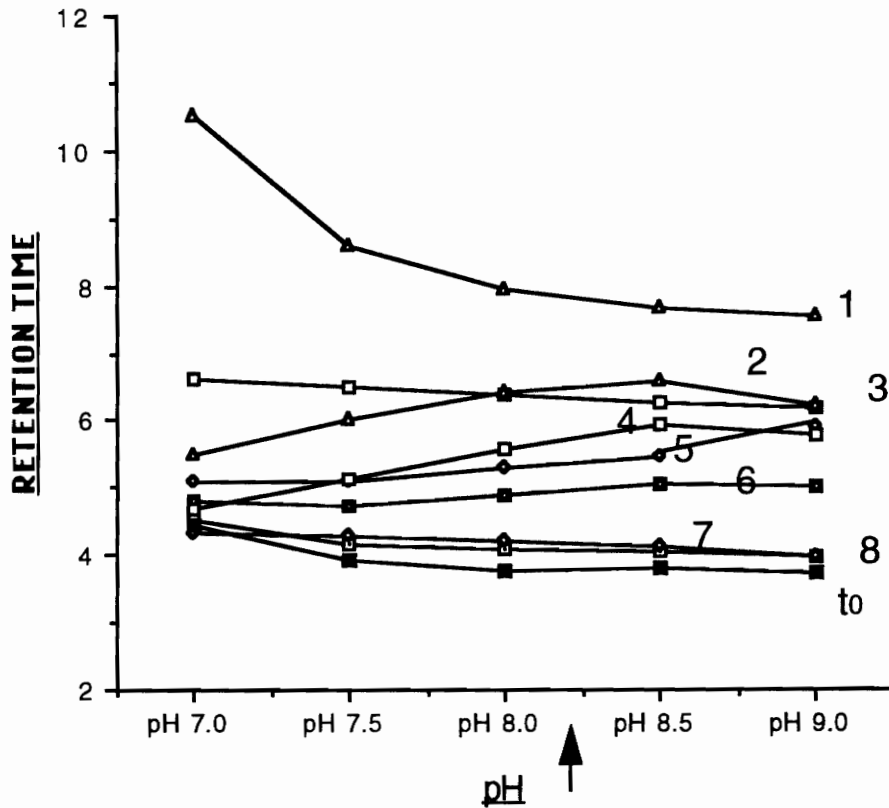


Figure 6.40: Effect of pH on the elution of the water soluble vitamins. Oligomer (UDO) concentraton 0.01 g/ ml. HP ^{3D}CE; Capillary: id= 50 μ m, L=55/46.5 cm, Buffer: 0.05M phosphate/ 0.1 M borate.

1. Ascorbic acid (C), 2. Riboflavin(B₂), 3. Pyridoxine PN (B₆),
- 4.Thiamine (B₁), 5. Pyridoxal PL (B₆), 6. B₁₂,
7. Pyridoxamine PA (B₆), 8. Niacinamide(B₃)

(fig 6.41) in less than 9 mins. Two synthesized batches were compared and showed almost equal retention times of the vitamins despite their NMR peak profile variations. The separation's % RSD s ranged between 2.7 and 10.7 % (fig 6.42) for the peak areas (n=9) with the highest values for the three vitamins unstable in alkaline pH. The % RSD for the elution time (n=9) ranged between 0.08 -0.28%, (fig 6.43).

6.4.4. Sodium dodecyl sulfate (SDS) verses sodium undecylenate (UDO).

The elution order of the water soluble vitamins with the SDS system relative to the UDO system show similarity (fig 6.44). Larger differences however, are very apparent for thiamine, riboflavin and B₁₂. SDS has an aggregation number of 62, has a cmc of approximately 8.1×10^{-3} (table 3.2) and an elution range between 2.8-4.6 (depending on the buffer conditions). UDO on the other hand is internally covalently bonded with two terminating hydroxyl groups, has zero cmc, an elution range between 2.1-4.5 and a possible aggregation number of 10. The interactions with riboflavin indicate that the interior of the SDS micelle seems more hydrophobic relative to the UDO micelle. This is further evidence to confirm the previously reported results for benzene and benzyl alcohol (173) and pyrene (177).

Thiamine reacts strongly with both the oligomer as well as the SDS micelle. This effect has been attributed to the ion pairing (183) as a result of interactions with the surface rather than the monomers in solution. With 62 monomers / SDS micelle, the micelle probably has a higher surface potential, due to the greater charge density at the surface, relative to the smaller

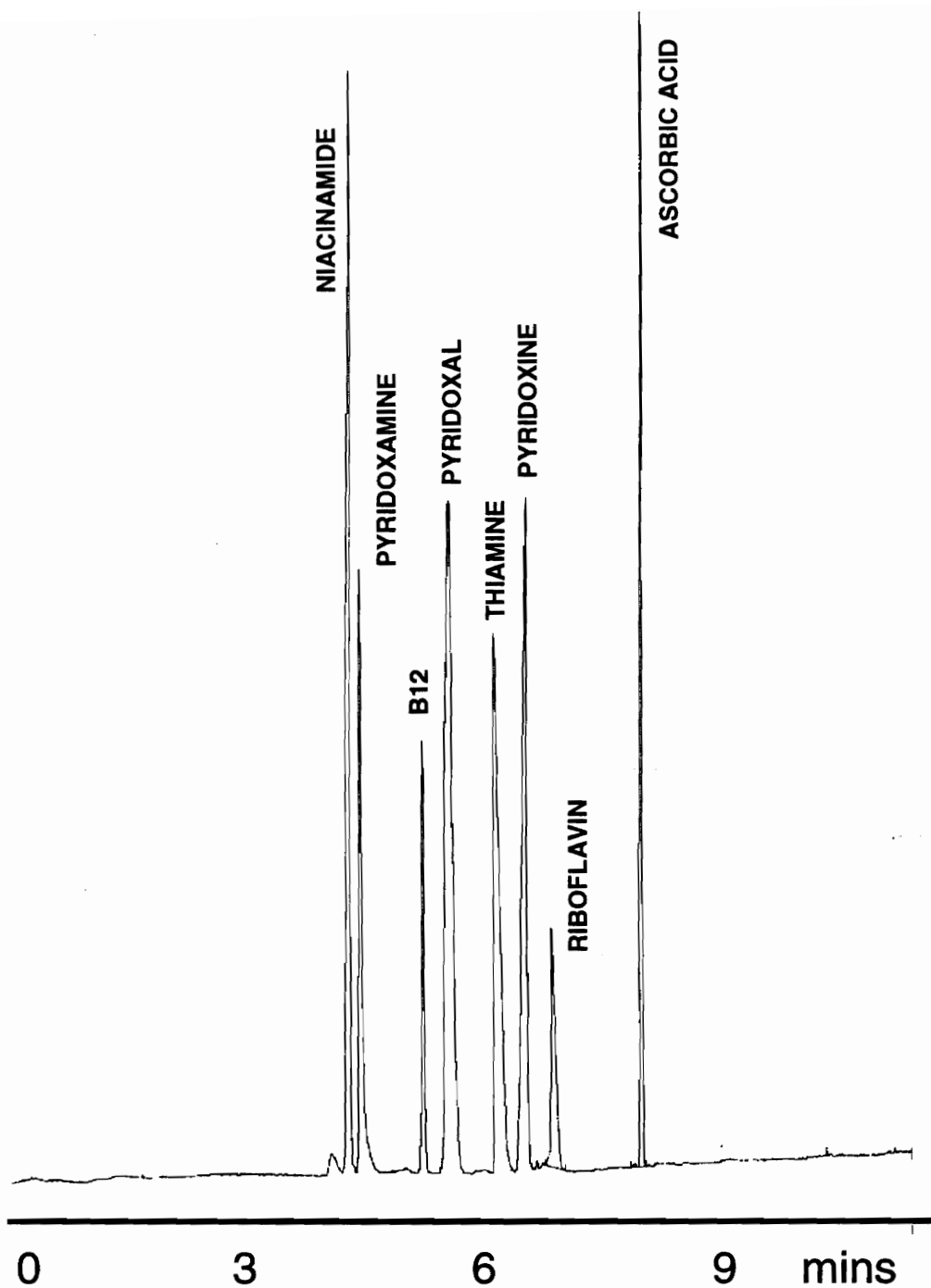


Figure 6.41: Separation of water soluble vitamins using Oligomer. HP ^{3D}CE; Capillary: id= 50 μ m, L=55/46.5 cm; Wavelength=245nm Buffer; 0.05M phosphate / 0.1 M borate, pH 8.2; UDO 0.01g / ml; Injection: 4 sec 50 mbars.

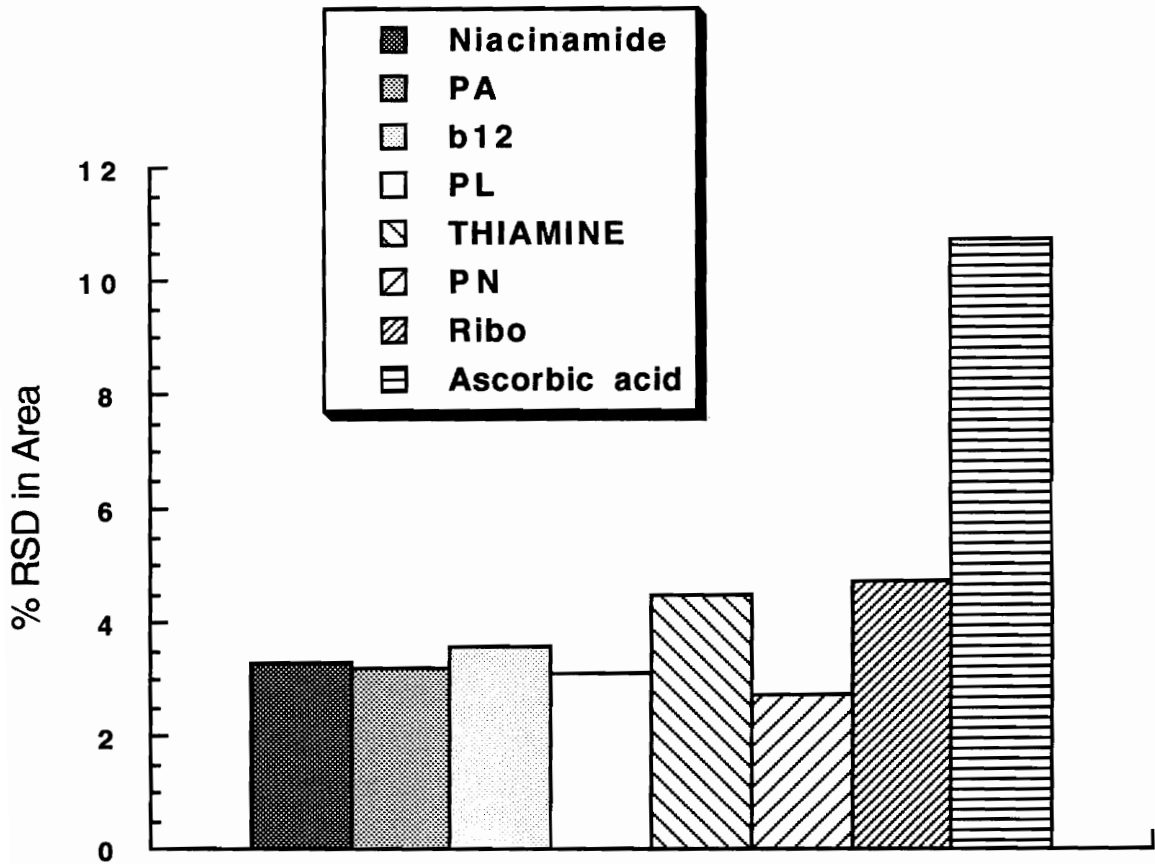


Figure 6.42: % RSD of the peak area n = 9

HP^{3D}CE; Capillary: id= 50 μ m, L=55/46.5 cm;
 Wavelength =245nm; Buffer; 0.05M phosphate/0.1 M borate,
 pH 8.2; UDO 0.01g / ml; Injection: 4 sec 50 mbars.

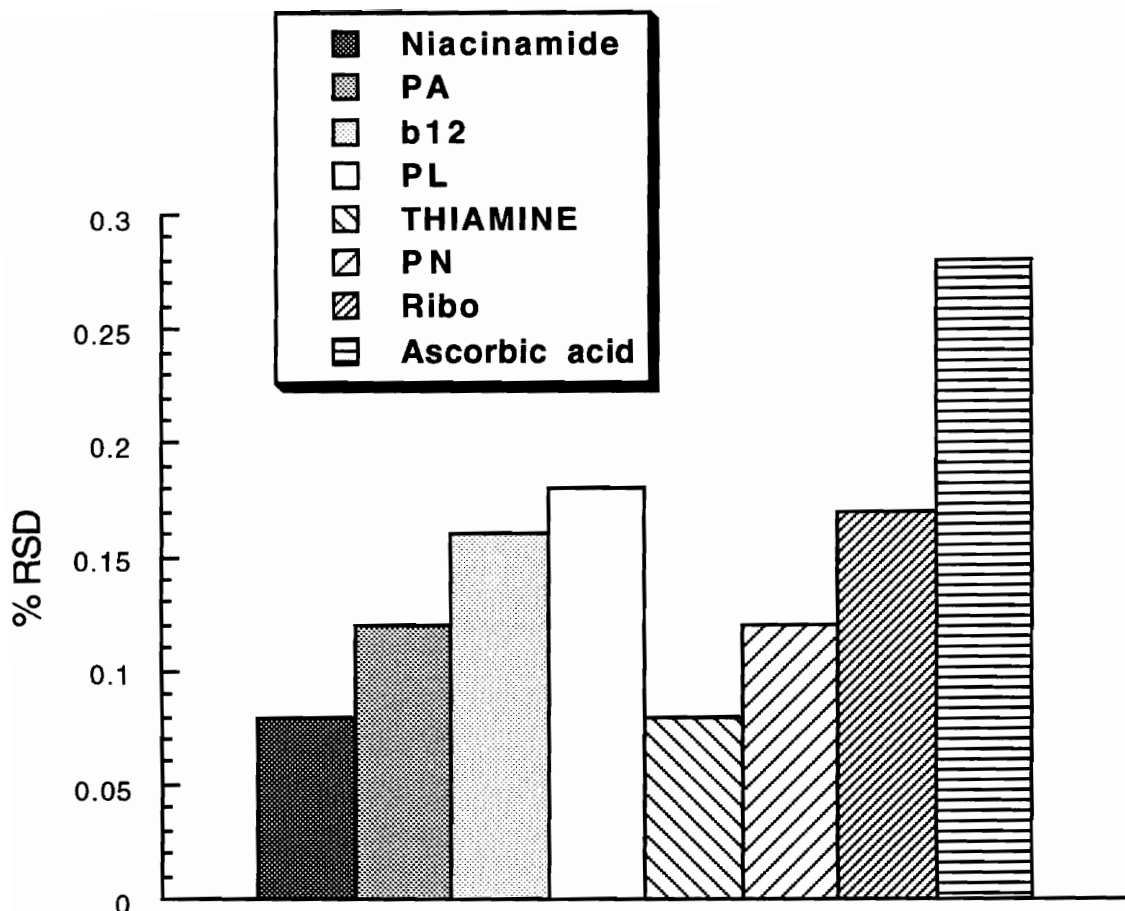


Figure 6.43 : % RSD of the elution time. n = 9

HP ^{3D}CE; Capillary: id= 50 μ m, L=55 / 46.5 cm;
 Wavelength =245nm; Buffer; 0.05M phosphate /0.1 M borate,
 pH 8.2; UDO 0.01g / ml; Injection: 4 sec 50 mbars.

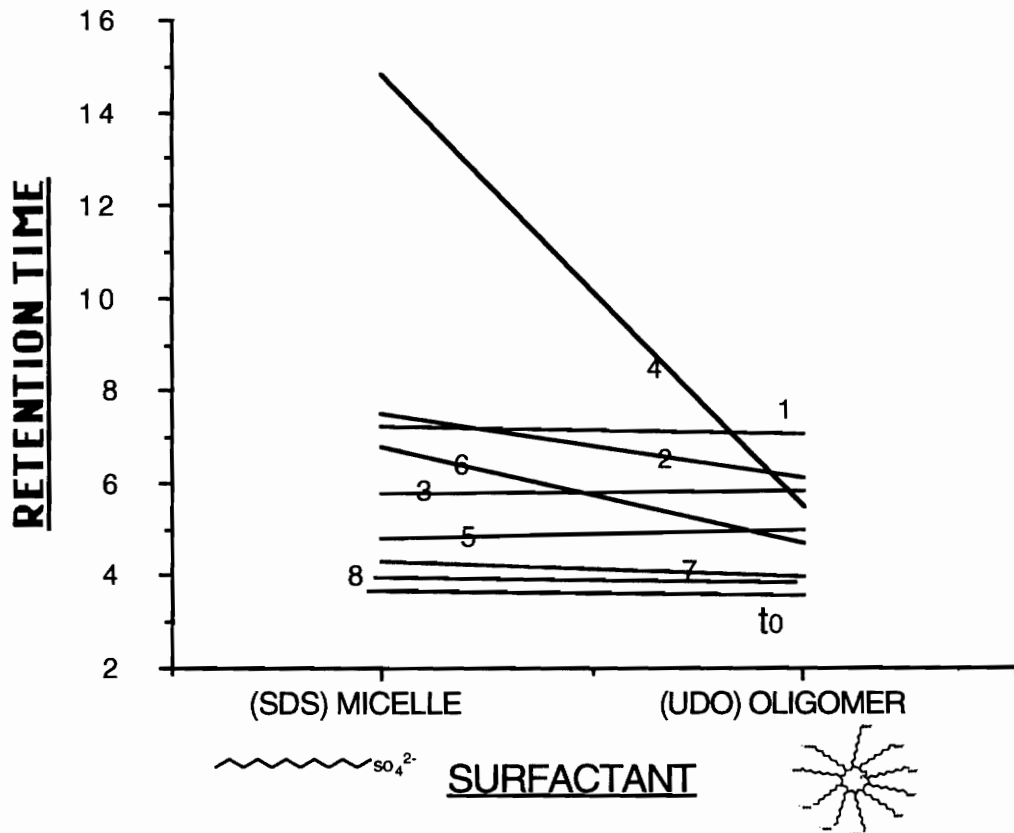


Figure 6.44: Effect of micelle type on the elution order of the water soluble vitamins SDS (0.05M) vs. UDO (0.01g/ml)

1. Ascorbic acid (C), 2. Riboflavin(B₂), 3. Pyridoxine PN (B₆),
4. Thiamine (B₁), 5. Pyridoxal PL (B₆), 6. B₁₂,
7. Pyridoxamine PA (B₆), 8. Niacinamide(B₃)

aggregates (~ 10) of the oligomer. Thus, an increased retention of the cationic thiamine.

Interestingly B₁₂ shows stronger interactions with the SDS relative to the oligomer. This can best be explained by the bulky size of the B₁₂ and thus its inability to interact with the surface of the somewhat small and more rigid oligomer. Additionally, the SDS held together by hydrophobic interactions is able to adjust the structural / conformation of its surfaces to accommodate the B₁₂ with its higher energy ionic interactions. The oligomer held together by covalent interactions, is unable to do so.

As is demonstrated through figure 6.45, the efficiency of the separations performed with the SDS and with the oligomer are very similar. This is further proof that the sorption and desorption kinetics resulting from the compactness and greater stability of the oligomer contribute very little to the resistance to mass transfer.

The monomer SUA micelle, as reported earlier, has a cmc of 0.114 M and an aggregation number of 10. Comparison of the performance of this micelle relative to the other systems was difficult as the SUA relatively high concentrations result in very higher currents, air bubble formation and the capillary walls were quick to be contaminated (173).

6.4.5. Addition of organic modifiers

In an attempt to prepare for the separation of the fat soluble vitamins, the addition of organic modifiers was investigated for their effect on the water soluble vitamins (fig 6.46). Concentrations higher than 10 % acetonitrile resulted in the loss of some of the vitamins possibly due to their insolubility. Once again both thiamine and riboflavin were the most affected as their

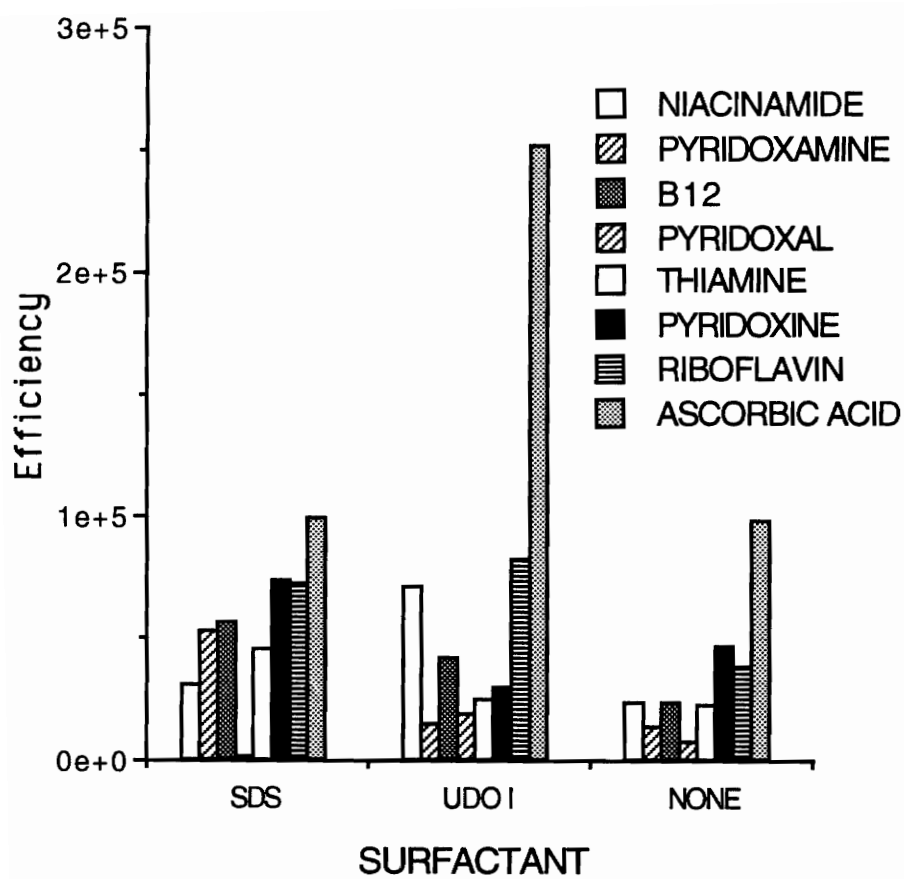


Figure 6.45: Efficiency comparison between SDS and UDO

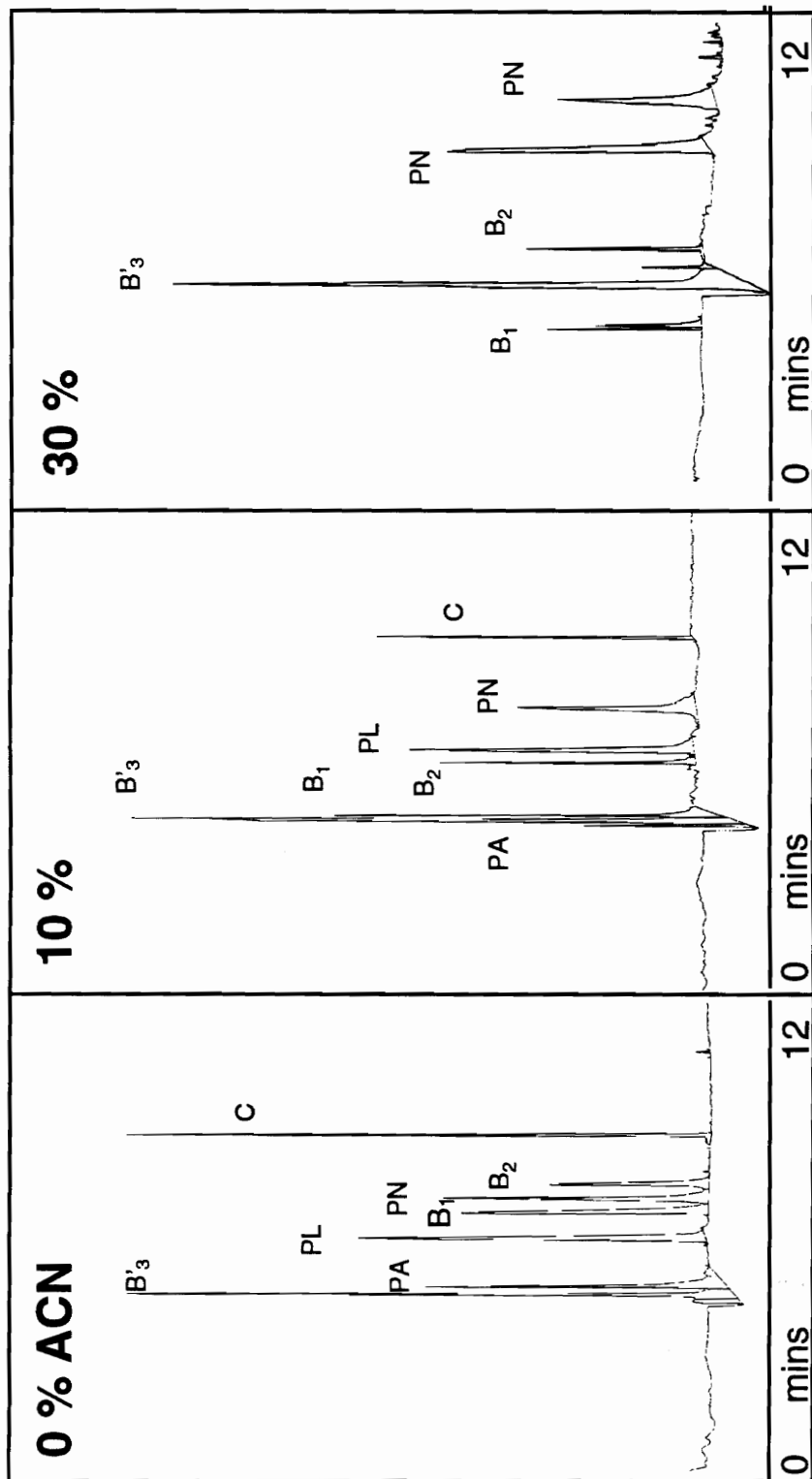


Figure 6.46: Effect of acetonitrile with oligomer on the elution of water soluble vitamins. Conditions as in 6.41

retention decreased significantly with the increases in acetonitrile. The addition of 30 % acetonitrile results in reversal of the migration direction. Since these two compounds in particular both interact strongly with the oligomer, and both show the same pattern in retention time changes, perhaps they are reflecting changes in the structure / confirmation / mobility of the oligomer. This is in support of Palmer et al's (3) suspicions of the structural or solvational changes of the oligomer under these conditions. In contrast to these results however, there is a decrease in the electroosmotic flow of the system with % acetonitrile. Worth mentioning, Palmer et al also reported that the oligomer precipitates around 55 % acetonitrile.

Niacinamide seems to be the most stable of the vitamins studied under all conditions as is validated in table 5.1, while riboflavin seems to be the most hydrophobic, partitioning more into the buffer with increased amounts of acetonitrile.. Thiamine shows split peaks with 20 % acetonitrile (fig 6.47)

The separation of the fat soluble vitamins A, E and K proved very irreproducible. These vitamins require higher percentages of organic modifier to dissolve them which precipitates the oligomer and gives no useful results.

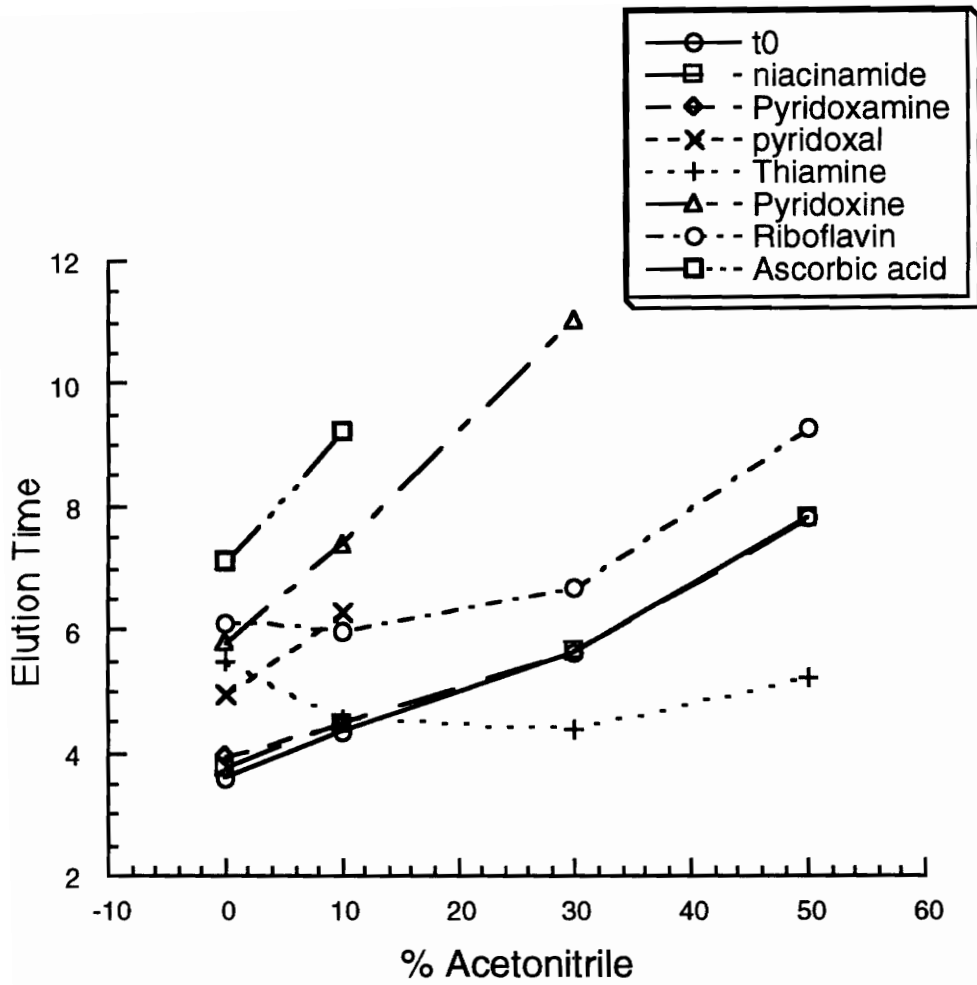


Figure 6.47: Effect of % acetonitrile on the water soluble vitamin's elution time. (Conditions as in figure 6.46)

6.4. THE SEPARATION OF PHOSPHOLIPIDS AND THEIR USE AS SURFACTANTS IN MICELLAR ELECTROKINETIC CHROMATOGRAPHY.

Selectivity, being a crucial factor in any separation technique, can be accomplished in the CE capillary only through modifications in the mobile phase (the buffer system). The conventional stationary phases of the other chromatographic techniques is only afforded in MECC through the addition of what is known as 'pseudostationary' phases, or micelles. These micelles are formed when a specific concentration of an amphiphilic molecule, with a long hydrophobic chain, is exceeded to form oriented colloidal aggregates ⁽¹⁸⁶⁾, with an abrupt change in physicochemical properties. The narrow concentration range over which these changes occur is known as the critical micellar concentration or cmc.

While a large variety of micelles are available, only a few are applicable for use in MECC. Several criteria need be met for a micellar system to be worthy of investigation. In an aqueous system a micelle has to be soluble at a concentration above its cmc; it must be hydrophobic enough to dissolve the analytes of interest; it should cause minimal joule heating; it should have a large 'tunable' elution window (t_{mc}/t_0); be selective and nondestructive towards the analyte of interest; it should allow for fast sorption-desorption kinetics for better efficiency; have a reasonable cmc value; be available in low cost and reasonable quantities; be stable for ease of use; be available in pure form and; not itself be detected. While no such universal micelle is available in CE, several anionic, cationic, nonionic and zwitterionic surfactants are available

(Table 3.2) that satisfy most of the above criteria, the most commonly reported and studied being the anionic surfactant sodium dodecyl sulfate.

Phospholipids belonging to a class of amphiphiles known as biological surfactants are of interest to the biological world. They are the major components of biological membranes, associated with many biological compounds such as proteins, carbohydrates and other lipids selectively. They are known to act as substrates to many metabolic reactions. They have very low cmcs ($<10^{-6}$ M) and form a multitude of aggregation forms in solution. This work is an investigation of the possible use of phospholipids as MECC surfactants. Their electrophoretic and chromatographic properties are studied further to help facilitate their separation as analytes.

6.4.1. Phospholipids

Phospholipids, or more accurately phosphoglycerides or glycerophospholipids are the second largest class of the complex lipids. In phosphoglycerides (fig 6.48), two of the hydroxy groups at the C-1 and C-2 positions are esterified to fatty acids while the C-3 is esterified to phosphoric acid. The phosphoric acid group, is further esterified with a group X, usually a base.

Phosphoglycerides are therefore, amphiphilic molecules having nonpolar aliphatic "tails" and polar phosphotyl-X "heads". Each of the phosphoglycerides contains differing fatty acid substituents as their tails. Saturated C₁₆ and C₁₈ fatty acids are most common, occurring at the C-1 position, while the C-2 position is usually occupied by unsaturated mostly C₁₆ to C₂₂ fatty acids.

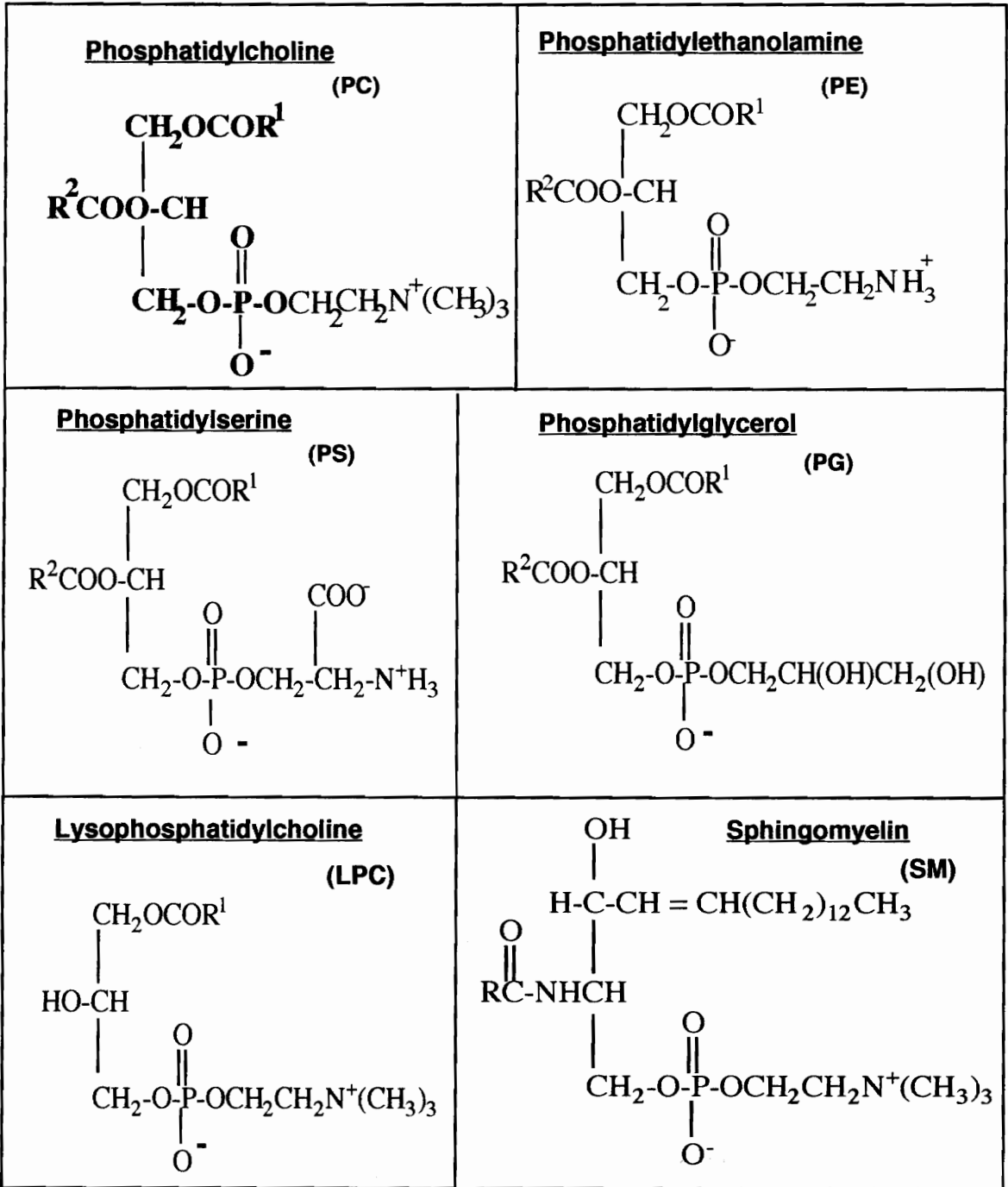


Figure 6.48: Structures of common phospholipid classes

The size, shape and electric charge of the polar heads also differ. At pH 7, all phospholipids have a negative charge on the phosphate group. Two of the most abundant phospholipids in higher plants and animals are phosphatidylcholine (PC) and phosphatidylethanolamine (PE). Their head groups contain the bases choline and ethanolamine respectively. At pH 7 both have a positive charge on their heads and therefore, the molecules are dipolar or zwitterionic with no net charge. Phosphatidylserine (PS) and phosphatidylglycerol (PG) contain serine and glycerol respectively. Both are acidic because of the additional carboxyl group of the serine and the no net charge (but quite polar) head of the glycerol. On the other hand, Lysophospholipids (LP) have only one of the two available positions of glycerol esterified to a fatty acid. Additionally as a group they contain the same polar heads as the phospholipids.

Sphingomyelins (SM) are usually included with the phospholipid class as they are related in their conformation and charge distributions. Chemically, however, they are different, and belong to the another major class of membrane lipids, Sphingolipids. Anchored to a ceramide backbone, sphingomyelins have a head group that bears a choline or an ethanolamine moiety. They are especially abundant in membranes of muscle and nerve cells.

Pure phospholipids are white waxy solids that darken on exposure to oxygen and temperature due to the peroxidation of their polyunsaturated fatty acids. The saturated phospholipids are more stable. All naturally occurring phospholipids and lysophospholipids are optically active. They are soluble in most non polar solvents containing some water and are best extracted from cells and tissues with chloroform and methanol mixtures.

In water phospholipids are insoluble forming a suspension of multilamellar vesicles that have an onion like arrangement of lipid bilayers (187). Upon sonication, these structures rearrange to form liposomes-closed self sealing, solvent filled vesicles that are bound by a single bilayer. Once formed natural phospholipid liposomes give turbid but stable solutions. Liposomes of synthetic phospholipids, however, tend to settle out quite rapidly. Lysophospholipids, on the other hand, being more polar and with only one tail, form micelles and give optically clear solutions. (fig. 6.49).

As phospholipids are very large, earlier studies (188) have indicated that they have very low conductivities in solution and low electrophoretic mobilities. The isoelectric point of phosphatidylcholine at pH 7 has been reported to be 6.7(189). On aging, phospholipid conductivities have been found to increase (188). Lysophospholipids on the other hand, with only one chain are expected to exhibit higher electrophoretic mobilities and conductivities.

6.4.2. Phospholipids as surfactants

When dissolved in water, myristoyl phosphatidylcholine and lauroyl phosphatidylcholine formed turbid solutions on sonication confirming the formation of liposomes. The filtered lauroyl phosphatidylcholine solution produced a noisy baseline and irreproducible electroosmotic flows. In order to observe 'well behaved micelles' the dihexanoyl chain of phosphatidylcholine should be used (190). The cmc for diheptanoyl phosphatidylcholine is reported as 0.001 M, so the cmc for the dihexanoyl would be expected to be around 0.01 M (190) requiring too much of the monomer. In light of the above, phospholipids should not be investigated further as possible surfactants for MECC.

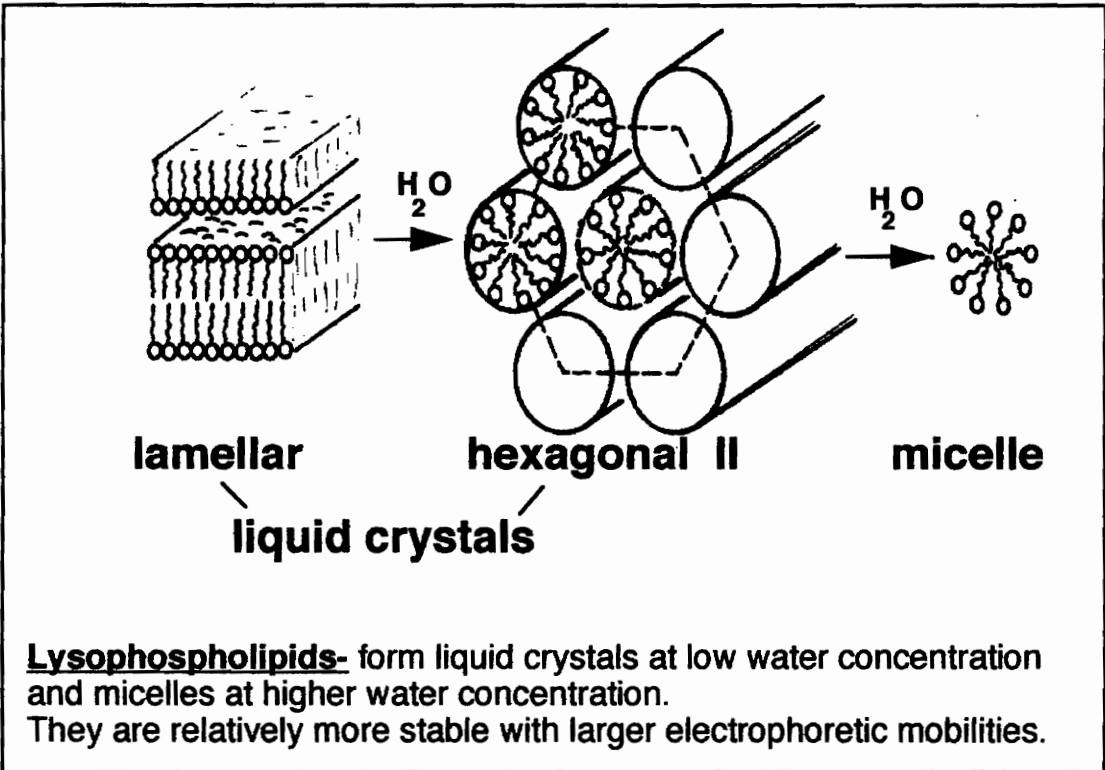
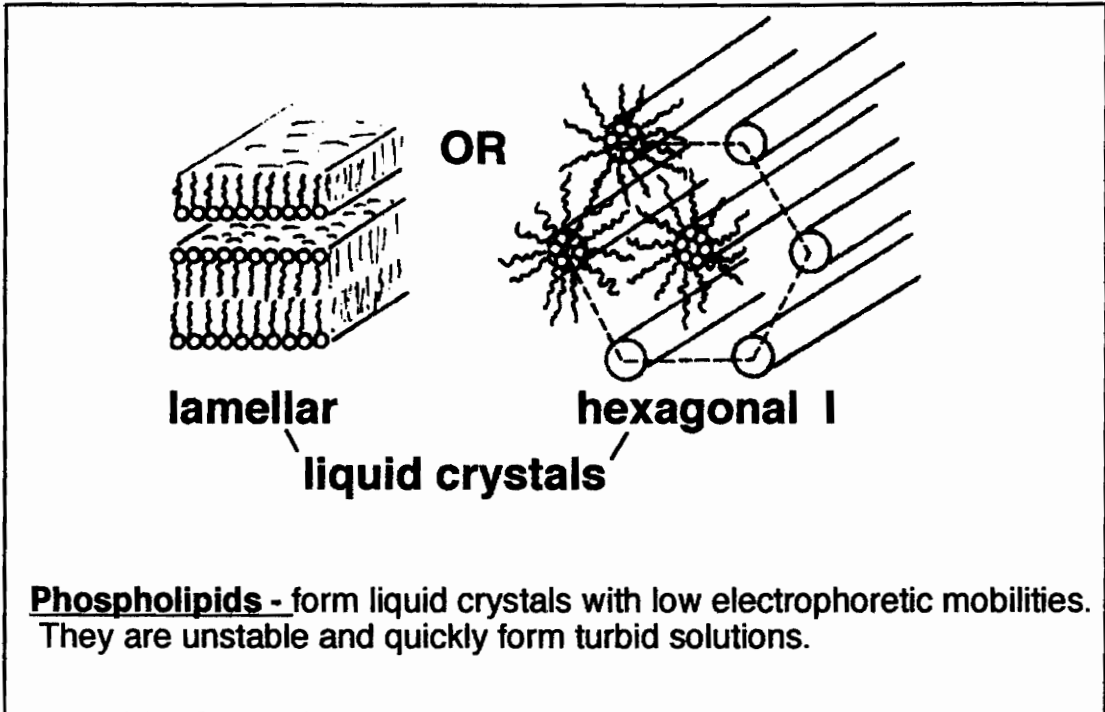


Figure 6.49: Phospholipids versus Lysophospholipids as possible surfactants

6.4.3. *Lysophospholipids as surfactants.*

For optimum solubility and cmc values the following three different classes of surfactants were investigated, lauroyl lysophosphatidylcholine, stearic lysophosphatidylserine and palmitic / stearic lysophosphatidylglycerol. Their electrophoretic mobilities were calculated at pH 9.2 using a borate buffer. All the lysophospholipids are expected to be negatively charged. The electrophoretic values (Table 6.4) showed the expected trend with the almost neutral lysophosphatidylcholine with the largest isoelectric point having the smallest effective electrophoretic mobility despite its shorter lauroyl (C12) chain. Meanwhile, lysophosphatidylglycerol exhibited a high effective electrophoretic mobility second only to sodium dodecyl sulfate. The effective electrophoretic mobilities were calculated through the independent measurement of electroosmotic flow μ_{eo} :

$$\mu_{eo} = \frac{L_V \cdot L_D}{t_0 \cdot V}$$

which was subtracted from the lysophospholipid's apparent mobility μ_i (the latter calculated as above using the dye sudan III for t_{mc});

$$\mu_{ep_i} = \mu_i - \mu_{eo}$$

It has been reported ⁽⁸⁹⁾ that the electrophoretic mobility of the micelles is virtually independent of the pH. This is confirmed by the almost nonexistent electrophoretic mobility of the lysophosphatidylcholine with increase in pH. The

Table 6.4: Electrophoretic parameters of the different micellar systems

	Lysophosphatidylcholine (LPC)		Lysophosphatidylserine (LPS)	Lysophosphatidylglycerol (LPG)	Sodium dodecylsulphate (SDS) 25 mM
μ_{ep} in 0.01M Borate Buffer (pH 9.2)	2.5 mM	1.25 mM	0.6 mM	1.6 mM	
μ_{eo} in 0.01M Borate Buffer (pH 9.2)	-0.8×10^{-9}	---	-3.86×10^{-8}	-5.07×10^{-8}	-5.21×10^{-8}
t_{mc} / t_0 in 0.01M Borate buffer	3.6×10^{-8}	5.13×10^{-8}	9.4×10^{-8}	10.4×10^{-8}	8.7×10^{-8}
	1.08	---	1.71	1.90	2.52

μ_{ep} electrophoretic mobilities of micelles. μ_{eo} electroosmotic flow of system. t_{mc} / t_0 micellar elution range

same would probably prove true for the other zwitterionic lysophospholipid lysophosphatidylethanolamine.

In an attempt to separate some paraben homologs the separation was found to depend on their hydrophobic interaction with the lysophosphatidyl choline micelle. Being partially ionized, these parabens in the absence of the surfactant have very similar electrophoretic mobilities (fig 6.50 a). The addition of the surfactant has amplified these differences with the heptyl-paraben interacting the most and accordingly arriving the fastest (fig 6.50 b).

Furthermore, Table 6.4 confirms how an increase in the surfactant concentration (lysophosphatidylcholine) results in a reduction of the electroosmotic flow. This is probably due to an increase in the buffer viscosity which is related inversely to the electroosmotic mobility (equation 2.8). This in turn results in expansion of the elution window.

On the other hand when lysophosphatidyl glycerol, with a higher more negative electrophoretic mobility (Table 6.4) is used the elution order is reversed (fig. 6.51) and heptyl arrives last. Multiple peaks of the heptyl paraben may indicate micellar polydispersity (possibly the presence of both palmitoyl and stearoyl lysophosphatidylglycerol). This is especially amplified with the heptyl paraben, as it is associated the longest with the micelle. Furthermore, this is also displayed with Sudan III. Lysophosphatidyl serine has an electrophoretic mobility that seems neither low enough (like lysophosphatidylcholine) nor high enough (like lysophosphatidylglycerol) to affect any sort of separation.

Thus by merely changing the electrophoretic mobility of a micelle total reversal in selectivity can be achieved. Additionally, zwitterionic surfactants can

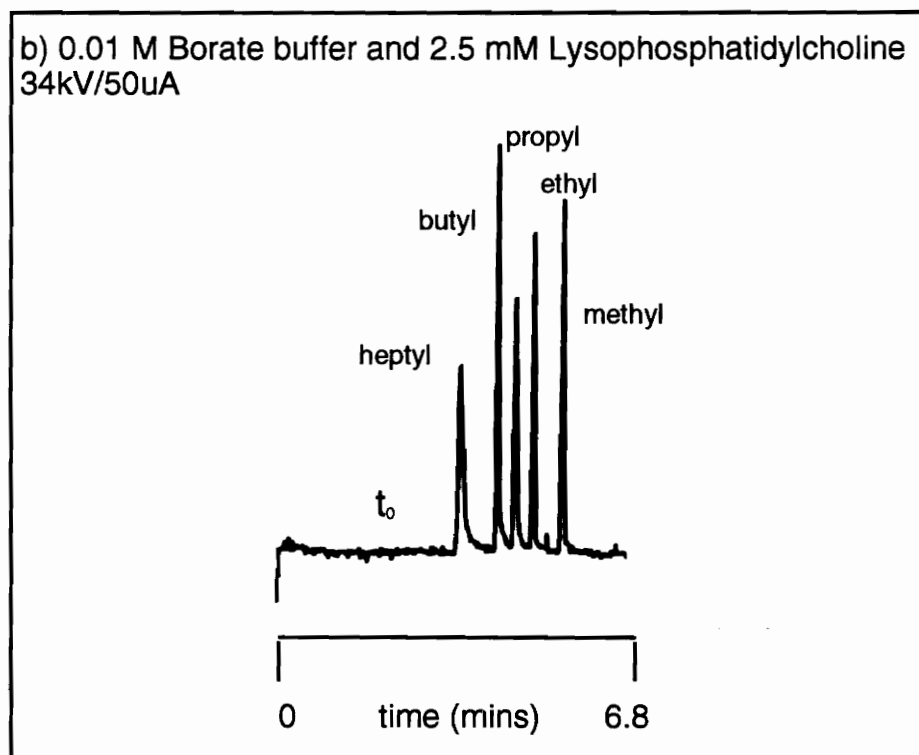
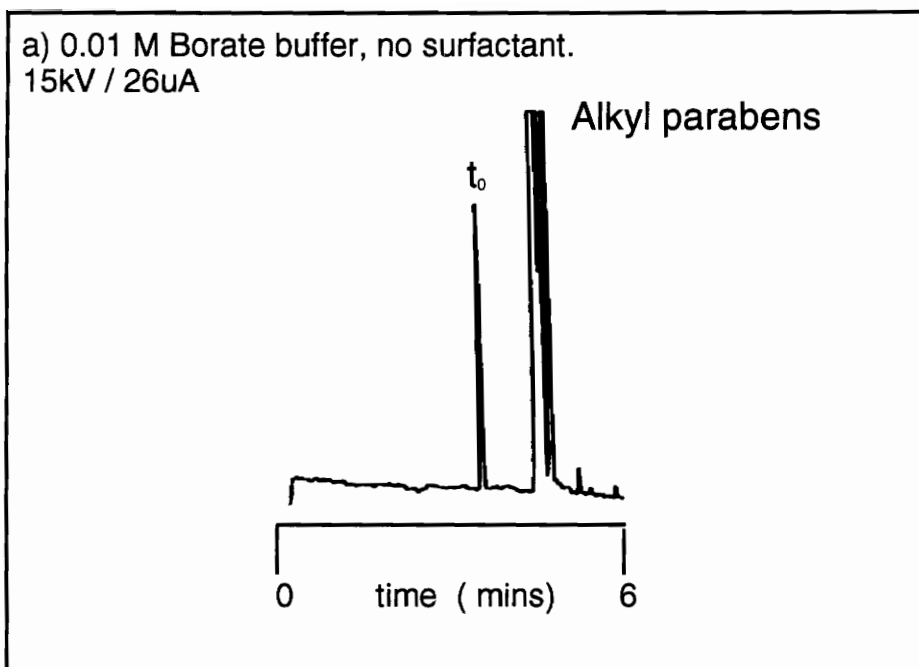


Figure 6.50: Separation of alkyl parabens a) without ,
b) with zwitterionic surfactant
pH 9.2, Capillary id=75um, L=100/50cm

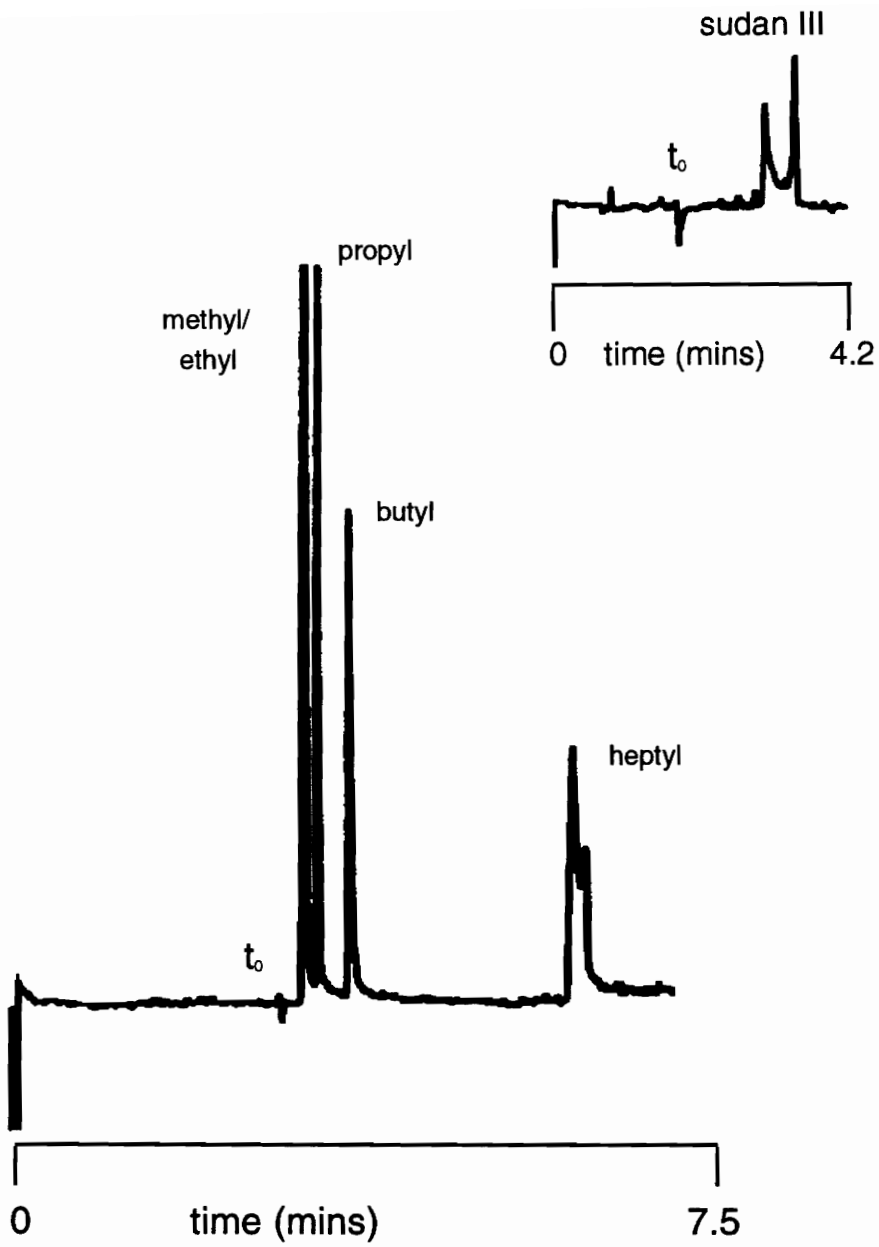


Figure 6.51: Separation of alkyl parabens with 2.2 mM of the anionic surfactant lysophosphatidylglycerol; Order reversed. 15kV/45uA. 0.01 M phosphate pH 8.8

not be used for totally unionized hydrophobic compounds, as they would all elute at t_0 (with the micelle).

The elution window

The elution window in MECC is defined as the distance between the t_0 (electroosmotic flow time) and the t_{mc} (the micelle elution time), where all neutral compounds must elute. Increasing this elution window improves resolution possibilities (eq. 3.16). This is schematically represented in figure 3.6. Manipulation of the elution windows can be achieved through changes in pH, addition of organic modifiers, coating of the capillary surface or through the use of micelles with a large electrophoretic mobility.

In an attempt to investigate the effect of pH and micellar type, calculations of the elution windows of the micelles under different conditions were investigated. Table 6.5 shows glycerol exhibiting the widest elution window after SDS. Since pH has no effect on the electrophoretic mobility of the micelles then it must solely be responsible for changes in the electroosmotic flow. This is expected and once again is illustrated in figure 3.4. Increasing the pH increases the electroosmotic flow and results in a decrease in the elution window. A decrease in pH from 9.2 to 7.2 resulted in an increase in elution range. However, the effect illustrated in figure 3.4 only applies up to pH 8 after which (the silica surface being totally ionized) there should be no effect of pH on the electroosmotic flow. Additionally, two different buffers are used and the effect of buffer type in this situation is not clear, although (contradictory to the shown results) Issaq et al ⁽²⁶⁾ have found tetraborate to result in lower electroosmotic flows relative to phosphate at the same pH and concentration.

Table 6.5: Elution Window Ranges

	Lysophosphatidylserine (LPS)	Lysophosphatidylglycerol (LPG)	Sodium dodecylsulphate (SDS)
t / t_0 in 0.01M Borfate buffer. pH 9.2	1.6	2.0	2.5
t / t_0 in 0.01M Phosphate buffer. pH 8.8	-	2.1	—
t / t_0 in 0.01M Phosphate buffer. pH 7.2	2.2	2.5	3.1
t / t_0 in 0.01M Borfate buffer + 0.025M SDS. pH 9.2	2.4	2.4	2.5
t / t_0 in 0.01M Phosphate buffer + 0.025M SDS. pH 8.8	3.2	3.2	—
t / t_0 in 0.01M Phosphate buffer + 0.025M SDS. pH 7.2	4.2	4.2	—

Gudon III

t_0 - Methanol t_{mc} -

Nevertheless elution windows did change. Both the methyl and propyl parabens are better separated however, the latter eluting peaks showed extensive tailing. The best separation with lysophosphatidyl glycerol was achieved at pH 8.8 (fig 6.51)

Mixed micellar systems

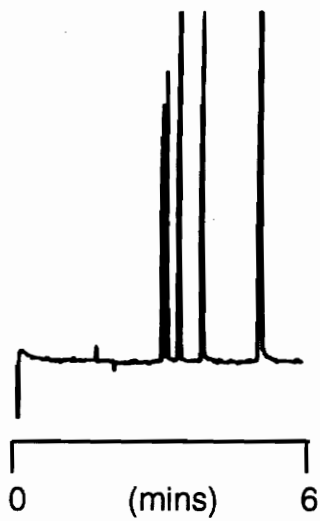
Micellar properties can be changed by using surfactant mixtures. Mixed micelles when formed have properties intermediate between the properties of each alone. The addition of lysophosphatidyl serine and lysophosphatidylcholine to a buffer solution of 0.05 M SDS shows some enhancement in the separation (fig 6.52) with no ill effects on efficiency or elution time.

6.4.4. The separation of phospholipids and lysophospholipids

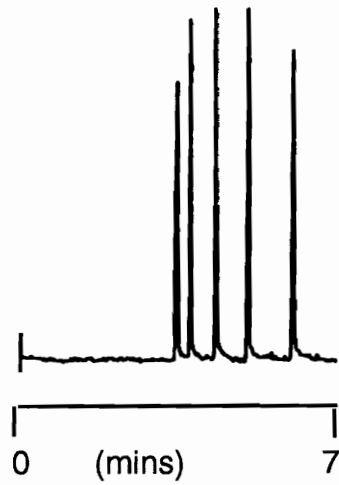
The separation of the phospholipids would be ideal if all the different classes as well as the individual chain length within each class were resolved. When electrophoresed separately, using sodium dodecyl sulfate and 5% methanol, various phospholipid classes eluted with t_{mc} (figure 6.53). Additionally, the naturally occurring phospholipids exhibited multiple peaks suggesting mixtures of chain length.

After a number of attempts with various surfactants, additives and temperatures a small separation was achieved between sphingomyelin and phosphatidylcholine (fig 6.54). Chain lengths, however were dissimilar. Sodium tetradecylsulfate (STDS) was added as a mixed micelle to enhance the hydrophobic characteristics of the SDS micelle. STDS could not be used alone due to its high Krafft point. Increasing the temperature enhanced its solubility.

a) SDS



b) SDS + LPS



c) SDS +LPC

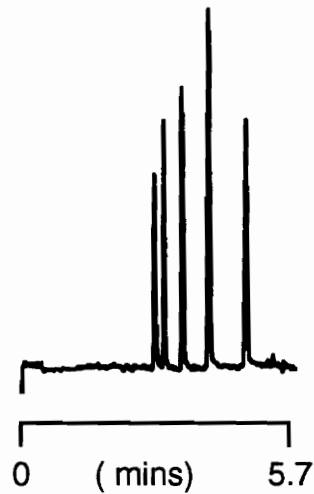


Figure 6.52: Enhancement of alkyl paraben separation with mixed micellar systems.

0.01 M borate buffer , 20 kV a) 0.025 M SDS, b) 0.025 M SDS and 0.04 mM LPS
c) 0.025 M SDS and 1.25 mM LPC

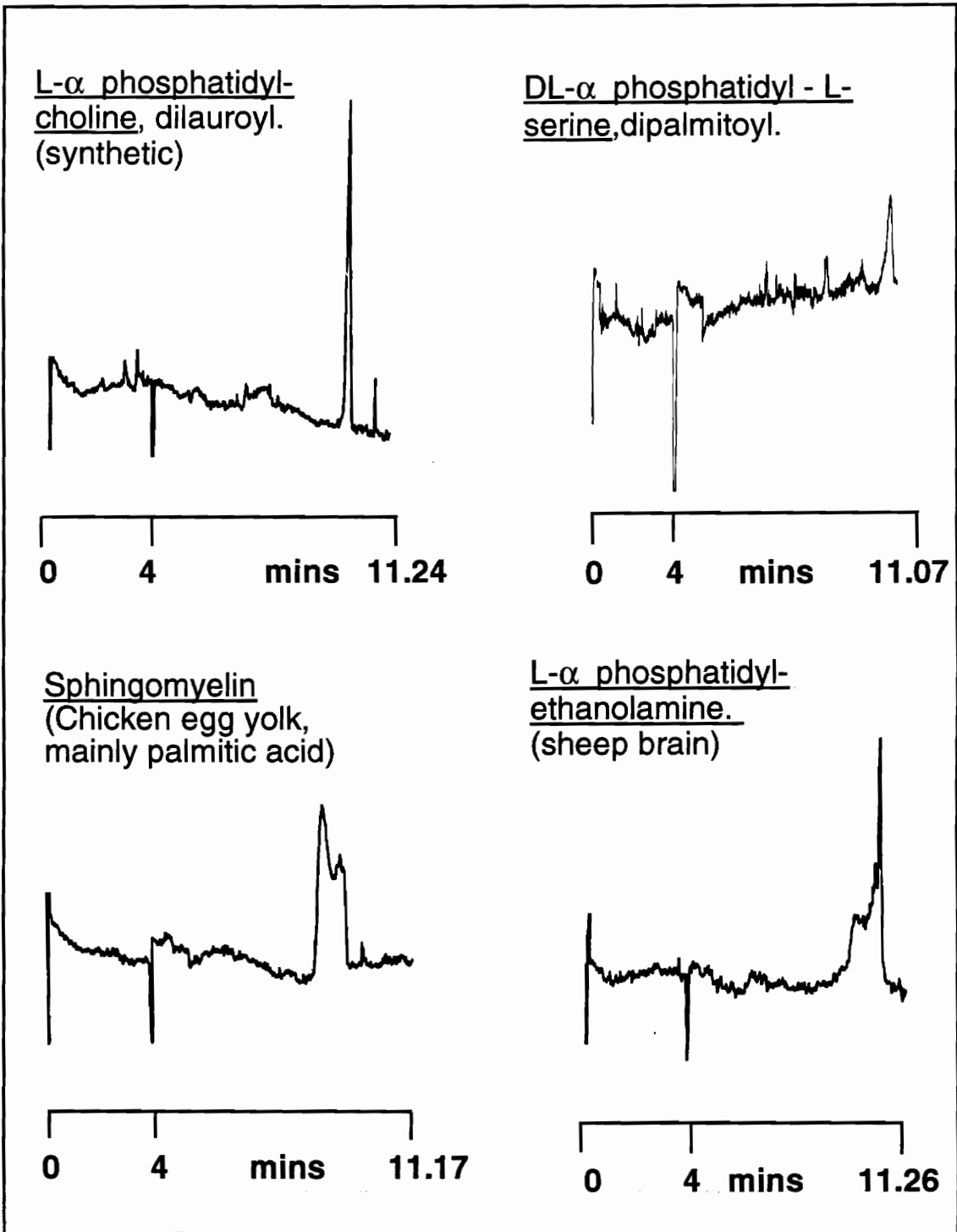


Figure 6.53: Chromatograms of commercially available phospholipids.
0.02 M borate /pH 8.2, 0.05 M SDS, 0.05 % MeOH

- 1- Methanol
- 2- Sphingomyelin
- 3- Phosphatidylcholine

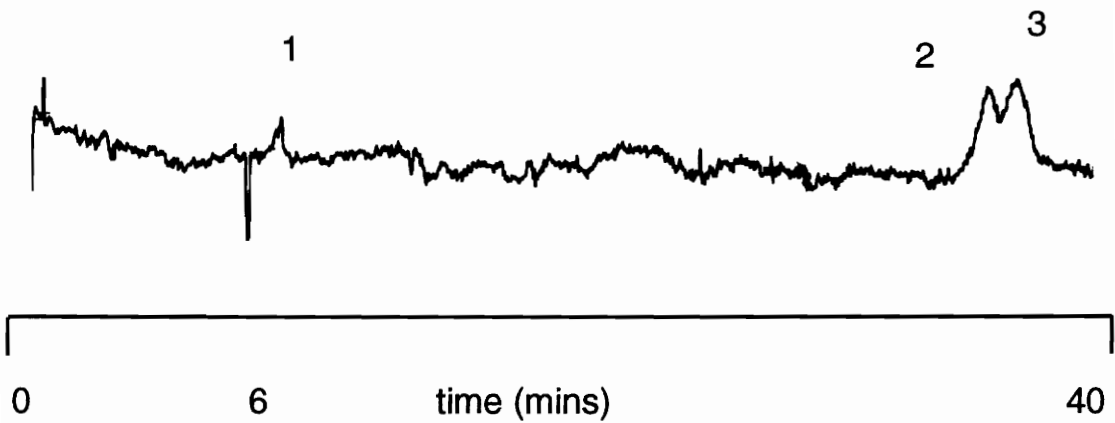


Figure 6.54: The separation of two classes of phospholipids ,
palmitic sphongomyelin and dilauroylic phosphatidylcholine
0.045 M SDS, 0.005 M STDS, 20 % Methanol, 10 mM Choline Chloride

Methanol expanded the elution range as it tends to decrease the electroosmotic flow. Choline chloride was added to further suppress the ionic properties of the micelle or lipid by ion pair associating or may even be suppressing the electroosmotic flow through interaction with the capillary surface. Separation of the phospholipids based on chain length was also achieved using a similar mixture of the buffer phase (fig 6.55).

Separation of the individual lysophospholipids exposed the extent of their purity from the supplier (fig. 6.56). Although their electrophoretic mobilities were different, they did exhibit similar retention with the SDS micelle. Their attempted resolution without micelles also resulted in their co-elution indicating a stronger affinity for each other. Slight indications of a separation was totally eliminated when the ionic strength of the buffer was increased in an attempt to suppress the electroosmotic flow to enhance the resolution. Lowering the ionic strength, addition of organic modifiers or even a slightly more polar surfactant to the buffer system may affect a better resolution.

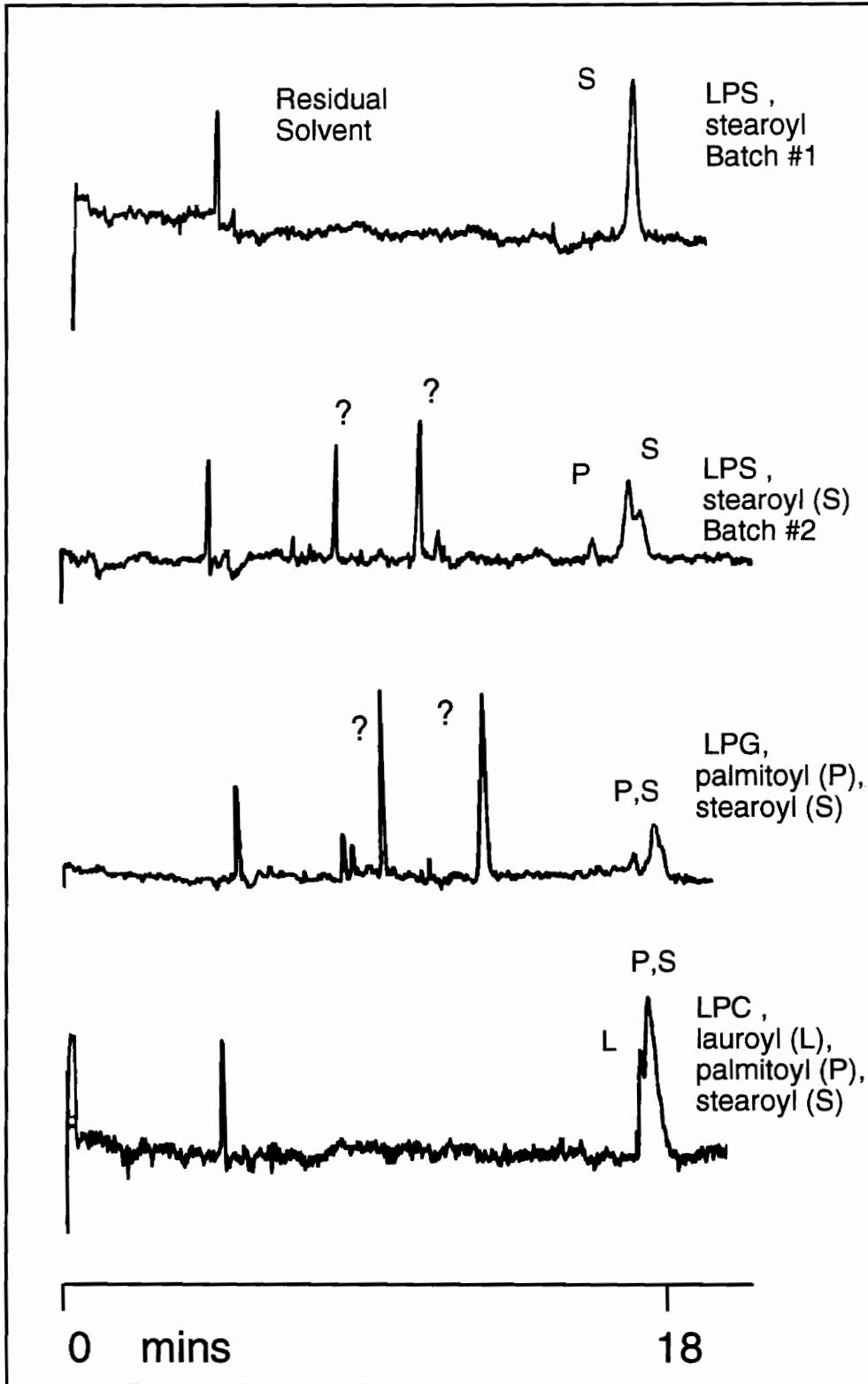


Figure 6.55: Separation of commercially available lysophospholipids
 10 mM Choline Chloride, 0.05 M SDS, 10 % MeOH
 0.01 M Borate pH 9.2. 15 kV

- a - methanol
- b - PC / dioctanoyl
- c - PC / didecanoyl
- d - PC / dilauroyl
- e - PC / dimyristoyl

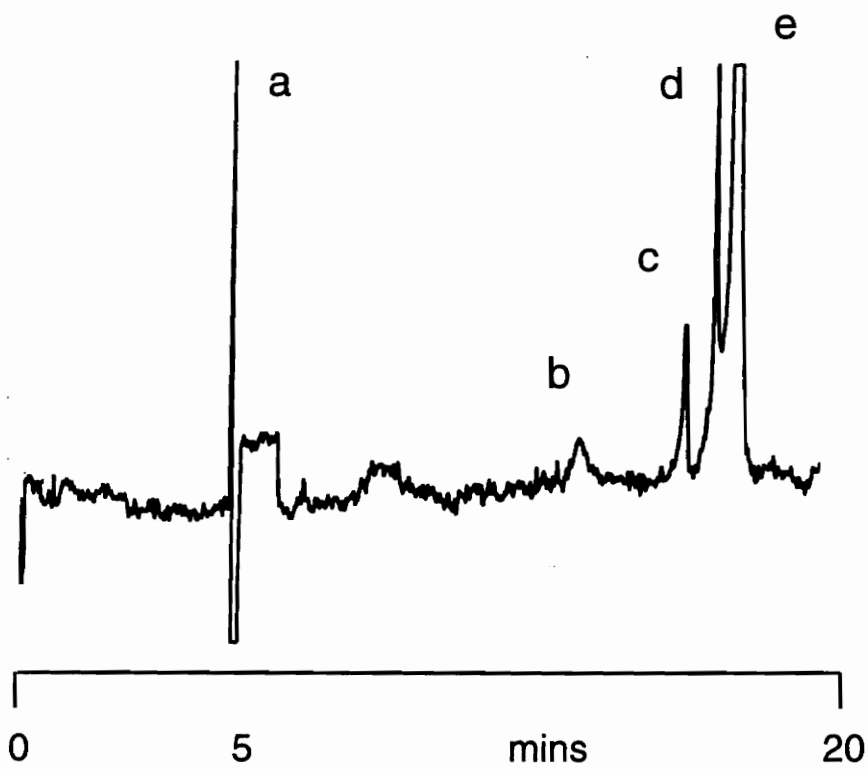


Figure 6.56: Separation of phosphatidylcholines based on different chain length.

250 V / cm, 0.02 M borate, pH 8.2

0.045 M SDS, 0.005 M STDS, 20 % Methanol, Temp. 30° C

6.5. THE ANALYTICAL SEPARATION OF *TRICHODERMA REESEI* CELLULASES BY CAPILLARY ZONE ELECTROPHORESIS; MANIPULATION OF THE OPERATING CONDITIONS.

The United States, since it depends heavily on foreign sources for its soil supply, is forced to couple its economical growth with an unpredictable foreign market. The everlasting instability in the Middle East along with the erratic and politically manipulated price fluctuations, reinforces the need for an alternative source of fuel. A solution to replace or supplement gasoline lies in the utilization of cellulose for synthesis of alternative fuels such as ethanol. Cellulose is abundant and readily available from agricultural residues, forestry products, pulp and paper industry wastes and municipal wastes. In addition to ethanol, commodity and specialty chemicals can also be produced from cellulose; these include xylose, acetone, ethyl acetate, glycine, organic acids, glycerol, ethylene glycol, furfural and animal feed (190).

Simply described, cellulose forms an intricate polymeric network and is embedded in a sheath of hemicellulose and lignin. Altogether the structure is highly complex and insoluble. Cellulose is highly crystalline with extensive intramolecular hydrogen bonding, is insoluble in water and is highly resistant to depolymerization. This makes its conversion into fermentable sugars and subsequently ethanol, very difficult. Nevertheless, using cellulose hydrolyzing enzymes (cellulases) and ethanol producing microorganisms, cellulose and hemicellulose can be converted first to fermentable sugars (glucose and xylose, respectively) and eventually ethanol, (Simultaneous Saccharification and Fermentation, SSF).

Cellulase is a multicomponent glycoprotein enzyme system with variable composition that depends on its source and requires no cofactor for its enzymatic activity. In general, fungi produced cellulases consist of three major classes of components that have molecular weights ranging from 5,600-89,000daltons; a) 1,4- β -D-glucanohydrolases (endoglucanases), b) 1,4- β -D-glucan cellobiohydrolases and 1,4- β -D-glucan glucohydrolases (exoglucanases) and c) β -D-glucoside glucohydrolases (β -glucosidases).

One common producer of Cellulase is *Trichoderma Reesei*; a fungi most intensely studied and highly recommended due to it's high productivity of the enzymes. It's cellulases consist of two endoglucanases (EG I and EG II) and two exoglucanases or cellobiohydrolases (CBH I (most abundant) and CBH II) and low levels of β glucosidases (β -G) (Table 6.6). This fungi produces cellulases that are resistant to chemical inhibitors and exhibit stability at 50°C. On the other hand, it's enzymes have low specific activities, are sensitive to product inhibition and are slowly inactivated at 50 °C.

The three components of fungal cellulases are believed to function synergistically. Endoglucanases and exoglucanases adsorb to the surface of cellulose in order to initiate hydrolysis and act at random to hydrolyze the cellulose chain internally. Endoglucanases initiate attack by randomly cleaving β -1,4-glycosidic bonds, creating shorter length cellulose chains; meanwhile exoglucanases start degrading these chains at the nonreducing termini, releasing cellobiose and glucose residues. β -glucosidases, finally, acts to liberate glucose from the cellobiose (190).

In addition to the Cellulases playing a major role in the above process, commercialization of the bioconversion technology depends largely on the

Table 6.6: Characteristics of purified *Trichoderma Reesei* Cellulases.

Enzyme	Molecular Weight	pKa
β - G *	108,000	8.5
CBH II	47,000	5.9
EG II	52,000	5.3
EG I	48,000	4.6
CBH I	52,000	4.3

*Asperigillus Niger fungi

economical feasibility of their production. The key to producing inexpensive and highly active cellulases lies in a combination of critical factors: improved enzyme quality, enhanced enzyme productivity, prolonged enzyme life time and minimal cost of media and substrate. The literature reports that several organisms, both mesophilic (20-45°C) and thermophilic (>45°C), have been employed for cellulase synthesis using as substrates soluble (lactose, cellobiose, xylose) and insoluble (cellulose, hemicellulose) carbohydrates. Media composed of nitrogen, phosphorus, magnesium and calcium sources, trace elements and vitamins have been developed to optimize enzyme productivity. For the same purpose the temperature and pH of fermentation have been manipulated in patterns in patterns depending on the microorganism used⁽¹⁹⁰⁾.

In order to evaluate the composition, levels of the individual cellulase components produced, their role in saccharification and the cellulase activity, it is necessary to screen a large number of culture filtrates, organisms and modified growth conditions as well as composition and concentration. Previous methods for the purification and separation of the various cellulase components have involved: Affinity chromatography ⁽¹⁹¹⁻¹⁹⁴⁾, Ion Exchange ^(191,195) Fast Protein HPLC ⁽¹⁹⁶⁻¹⁹⁹⁾, SDS/PAGE ⁽¹⁹⁸⁾, Isoelectric Focusing⁽²⁰⁰⁾ and Gel Filtration ^(200,196,202). Peak generally exhibit low efficiencies, poor resolution and lengthy retention times in addition to the large amounts of enzyme required and the use of costly columns.

As an alternative technique, Capillary Zone Electrophoresis (CZE) is well suited for the separation of such macromolecules. Macromolecules such as proteins, with their low diffusion coefficients are, theoretically, expected to

exhibit efficiencies of one million theoretical plates (37). However, it has been found that interactions with the capillary surface causes greatly reduced efficiencies and often result in peak tailing and even total retention in the capillary. Proteins tend to exhibit variability in charge, hydrophobicity, size and conformation. Their separation without such surface interaction, would necessitate the use of extreme pHs (45) or surface modification (46). While the former practice has been effective in reducing some surface ionic interactions, unfortunately it often results in protein denaturation. On the other hand silica surface modification, while diminishing solute adsorption, results in a reduction of the electroosmotic flow.

This work evaluates, for the first time, the separation of five different enzymes (EG I, EG II, CBH I, CBH II and β -G) produced by the fungi *Trichoderma Reesei*. Variations in buffer type, ionic strength, pH, temperature as well as reduced electroosmotic flow and their effects on the separation are investigated and presented. The separation of the enzymes achieved in less than 12 minutes, proved very reproducible.

6.5.1. The Separation

Figure 6.57 a, shows the separation of the purified standards for two of the most prominent classes of enzymes produced by the fungi *Trichoderma reesei*, the endo- (EG I, EG II) and the exo- (CBH I, CBH II) glucohydrolases. The optimal conditions, concentration and pH of the buffer was chosen after several trials. A pH (9.2) higher than the highest component pI was chosen to convert all enzymes to their anionic form and prevent solute surface adsorption. Table 6.7 shows the resultant %RSDs for the enzymes under investigation.

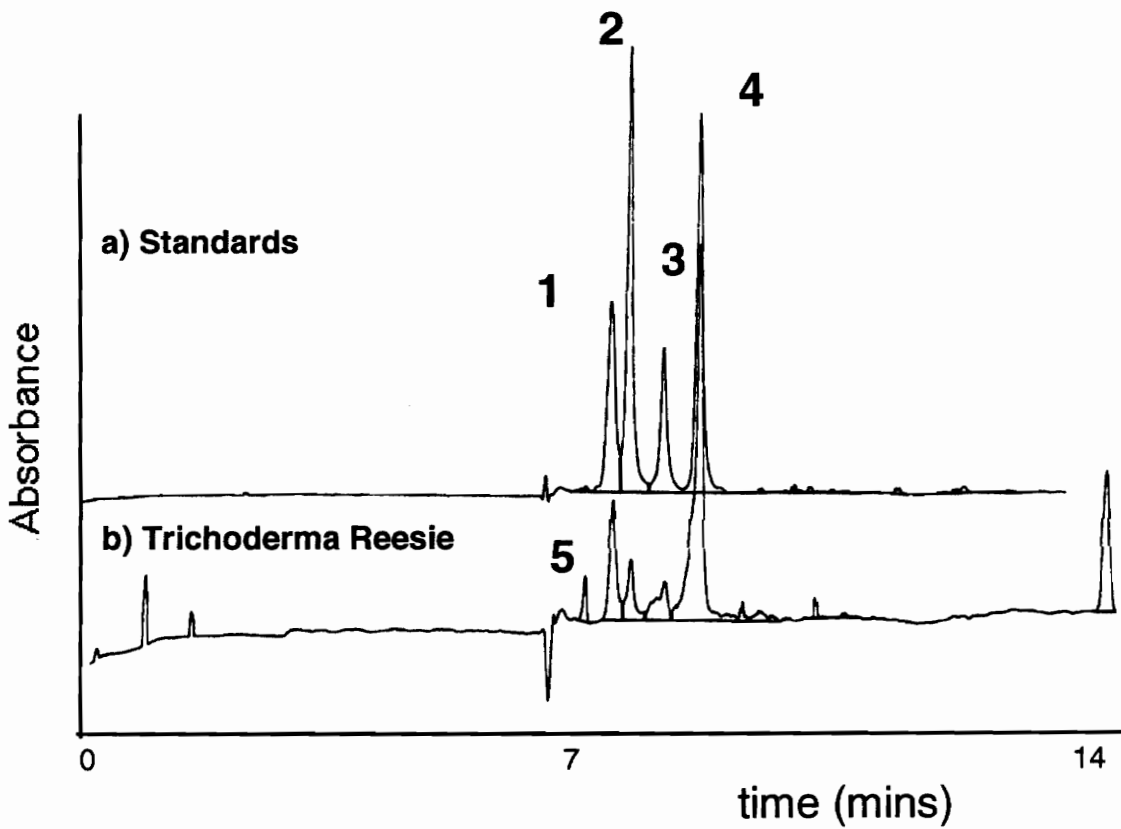


Figure 6.57: Separation of Enzymes.

Buffer 0.03 M Na_2HPO_4 , pH 9.2

Capillary : L=80/60 cm; id=50 μm ; Z-cell

Potential: 20 kV; 25°C; 210nm; 0.1 sec inj.

a) Standard sample: 1)CBH II, 2) EG I, 3) EGII, 4) CBHI, 5) β -G;

b) *Trichoderma Reesie* "X" culture filtrate.

Table 6.7: % Relative Standard Deviations (n=8)

ENZYME	RETENTION TIME	AREA
CBH II	0.48%	3.8%
EG II	0.5%	2.5%
EG I	0.59%	5.1%
CBH I	0.42%	2.4%

An actual culture filtrate is run under the same conditions. Peak five is probable that of β -G. The latest peak to elute maybe another one of the endoglucanases, with a lower pK_a .

6.5.2. Effect of pH

In an attempt to reach the above final pH choice, several pHs of the phosphate buffer were investigated (fig. 6.58). Below \approx pH 8.0 the elution sequence is EG I < CBH II < EG II < CBH I. Above \approx pH 9 the elution settles to CBH II < EG I < EG II < CBH I. The separation looks rather complicated between \approx pH 8-9. More peaks (or split peaks) appear and the sequence is in the process of transformation. Either the peak position switches or a different form or configuration of the enzymes take place. According to Eveleigh (203), multiple exoglucanase and endoglucanase forms exist due to the existence of multiple genes, post-translational and proteolytic modifications of the gene products, variable cellulase composition, presence of other proteins, glycoproteins and polysaccharides in the cellulase complex as well as variable glycosylations of the cellulase components. Additionally, variability in documented pI values may reinforce the assumption that under different pHs the enzymes changes conformational form, acquiring a different pI value. At the transient range of pHs (8-9), both forms are evident. On the other, hand this 'transient' pH range maybe just the appropriate pH for the separation of some overlapping components, possibly more endoglucanases. This can be further confirmed by acquiring some standard endoglucanases (III, IV, V and VI).

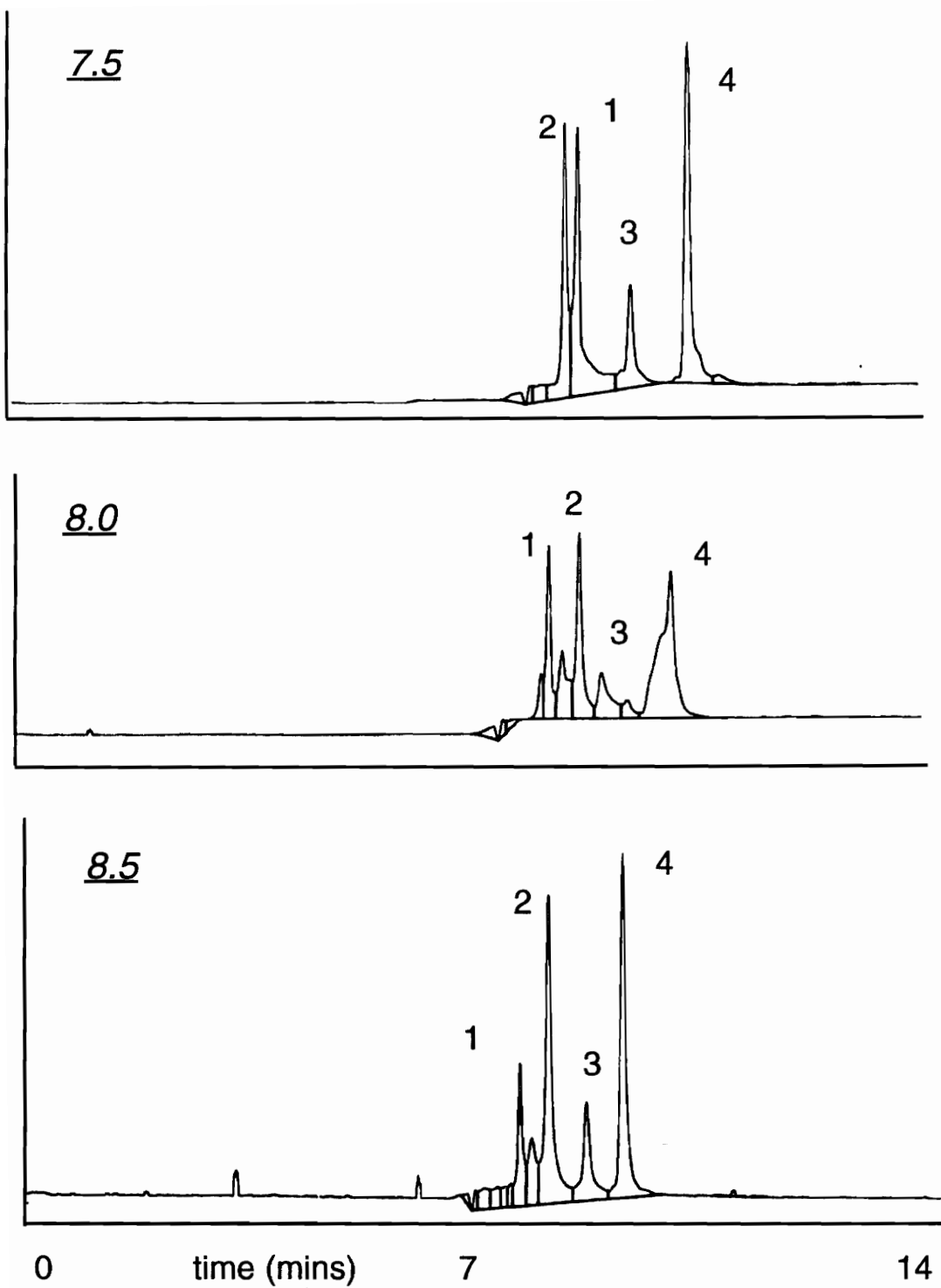


Figure 6.58b: conditions same as Figure 6.57.

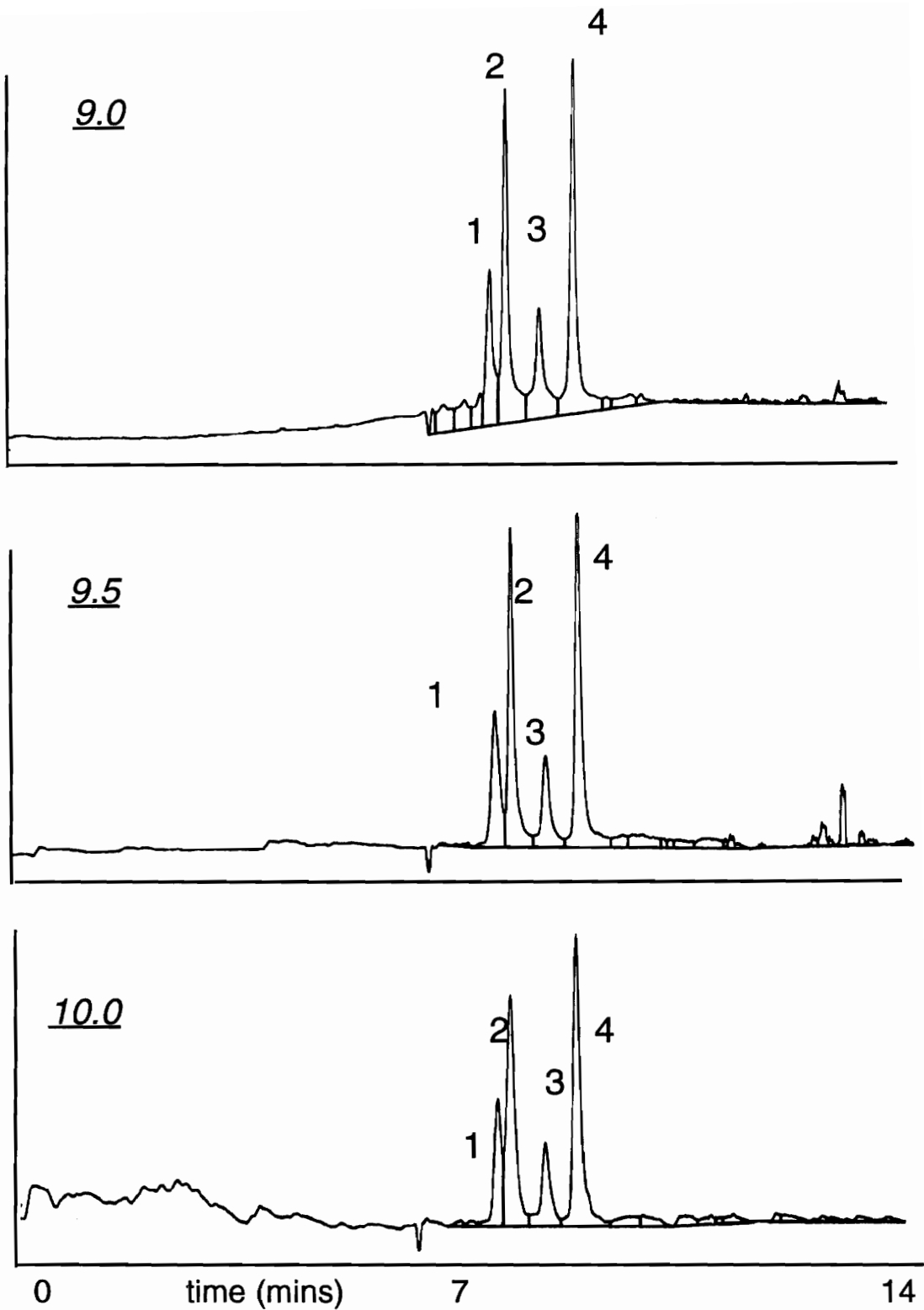


Figure 6.58 b: conditions same as Figure 6. a.

6.5.3. Effect of Buffer type and Ionic Strength

The effect of buffer ionic concentration is depicted in figure 6.59.

The greater the concentration the better the resolution, the longer the retention, the larger the viscosity and the higher the current and joule heating effect. 0.03 M concentrations of the disodium hydrogen phosphate buffer gave the best separation. Concentrations higher than 0.03 M, produced too much current and consequently, joule heating and deteriorated peak shapes.

By increasing the viscosity and decreasing the electroosmotic flow without increasing the current, alkyl sulphonates, with their low conductivities, are recently acquiring more attention as buffer additives. However, when added in conjunction with the phosphate buffer no significant improvements in resolution was recorded.

Additionally, minor temperature (20-35 °C) as well as voltage manipulations were investigated to monitor enzymatic structural changes, produced only migrational and efficiency variations.

The use of coated columns was also investigated as an alternative to the use of extreme pHs. The limited number of coatings investigated, both hydrophilic and hydrophobic, proved unsuccessful. This in no way rules out the use of coated columns but warrants further investigation of the many commercially available coatings, both permanent as well as dynamic.

Addition of Ethylene Glycol, also proved unsuccessful. Ethylene Glycol when added with the sample, is expected ⁽²⁰⁴⁾ to migrate through the column ahead of the sample, temporarily modifying the surface, minimizing silanol interactions. The only effect was an adverse one. Peak shapes as well as resolution deteriorated, possibly due to the denaturation of the enzymes.

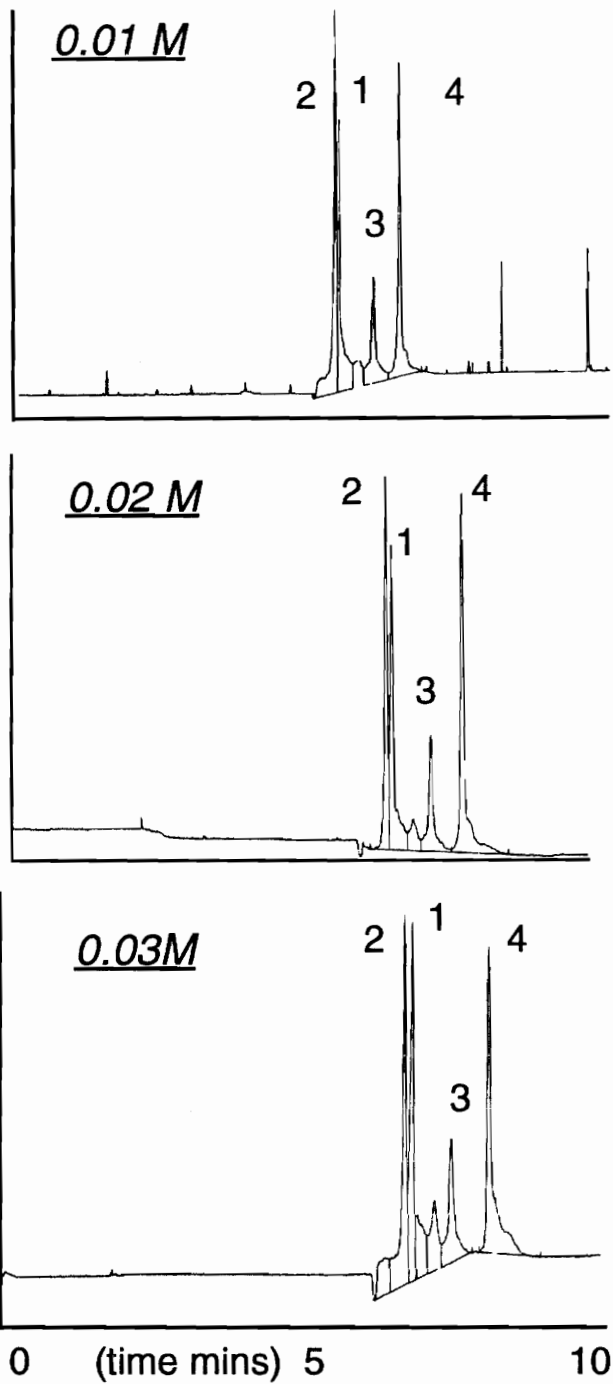


Figure 6.59: Effect of Ionic Strength. on enzyme separation. Buffer: Na_2HPO_4 , pH=7.5; Capillary: L=56/60; id=50 μm ; Bubble cell. 50mbar/3sec inj.; Potential: 20 kV

CHAPTER VII

CONCLUSIONS

Capillary electrophoresis is a rapidly advancing analytical technique. Its rapid growth and competition with some of the more established separation techniques, HPLC, GC and Electrophoresis, is a consequence of its easy adoption of much of their established theory, techniques and instrumentation. Capillary Electrophoresis thrives on its high separation efficiencies, speed of analyses, rapid methods development, low solvent consumption and low sample requirement. It is capable of separating ionic, ionizable and neutral compounds both large and small. In these respects it competes well with the other separation techniques. It lags behind, however, in concentration sensitivity, selectivity (especially for the largely hydrophobic compounds) and commercially available detectors. This work has tackled several of these problems in an attempt to accelerate the development of this technique.

In the realm of detection, MECC of pungent compounds was investigated using simultaneous on-line ultraviolet and modified amperometric electrochemical detection. Separation of the capsaicins, the pungent principles, was found possible only in the presence of SDS as a surfactant (MECC) and the addition of methanol as an organic modifier. Smaller id capillaries were found better for higher efficiency, higher voltage application and for shorter analysis times, but they showed a decreased sensitivity with UV detection. Sample injection time and voltage were found to affect resolution as well as elution time. These parameters illustrated well the need for very small

injection volumes. The addition of methanol had a minimal effect on the electroosmotic flow, but did improve the resolution.

Piperine, another of the pungent principles, coelutes with capsaicin and dihydrocapsaicin. In the presence of the several naturally occurring piperine isomers and other capsaicin analogs, attempt of a total CZE separation with mere manipulations in the buffering system, was found impractical.

Simultaneously detection using Ultraviolet detection on-line with Electrochemical detection was found to be more successful. Only Piperine was detected using UV at 340 nm while an electrochemical potential of 0.9V, selectively detected only the capsacinoids by amperometric oxidation.

The modification of amperometric end-column detection with a more practical, easy to assemble design, using commercially available microelectrodes, an auxiliary detector and larger diameter columns was successful, resulting in relatively sensitive detection of capsaisins and homovanillic acid, dopamine and 3,4-hydroxybenzylamine (2.5 to 160 femtomoles).

With the addition of better current amplification (increasing sensitivity) and reduction of column internal diameter (2-5 μm to permit in vivo injections), this end-column set up should prove useful in neuro-physiological investigations of capsaicins and their oxidation products.

In an attempt to enhance selectivity, the effect of additives such as cyclodextrins and cationic surfactants was investigated for the CZE separation of isomeric benzoic carboxylic acids. The total separation of all the mono-, di- and tri-benzoic carboxylic acid isomers using a borate buffer in the positive

potential mode was found unachievable. Additionally, when low potentials are applied, peak tailing becomes a problem for the tri-carboxylic acids. The addition of α , β , and γ cyclodextrins with manipulations in buffer pH, cyclodextrin concentration and voltage resulted in achieving total reproducible separations of all the isomers.

Although reversal of polarity, by addition of cationic surfactants below their cmc, improved the peak shape of the tri-acids (the elution order was reversed) reproducibility was poor and method development difficult. When cyclodextrin is added, a complex situation results from the competition of the cationic surfactant with the analytes for the cyclodextrin cavity. The separation not only shows very poor efficiencies but is additionally irreproducible.

A study was conducted to better understand and employ a recently introduced oligomerized surfactant. Characterization of its interactions with some vitamins (both water and fat soluble) shed some light on its behavior as a MECC surfactant. It has been shown that the oligomeric phase provides similar weak interactions with most of the water soluble vitamins as does SDS. The efficiency of the separation is good showing that the oligomer can be used for efficient separation of a variety of analytes. In contrast to SDS solutions, the oligomer does not provide ion-pairing interactions for the large B₁₂ molecule, while it does provide ion pairing interactions for the smaller thiamine molecule. This indicated that the more rigid structure of the oligomer is unable to accommodate the large analyte in the same way that the more flexible SDS micelles can.

Furthermore, two syntheses of the oligomer were made and characterized. The NMR results indicated the presence of significant quantities of the monomer. There are different residual amounts of monomer in one batch relative to the other, but the retention characteristics of the two batches are the same, confirming that the monomer has a minimal effect on the separation.

Finally, the addition of acetonitrile to the oligomeric phase, in concentrations large enough to support the solubility and detection of the fat soluble vitamins, precipitated some of the vitamins as well as the oligomer, making the use of this oligomer for the separation of these analytes impractical.

To add to the arsenal of available surfactants, a number of phospholipids (important amphiphilic components of cell membranes) were investigated. As surfactants, they were found to have very low electrophoretic mobilities, and form turbid solutions of liposomes, rendering them unsuitable for use in MECC. A sub-group, the Lysophospholipids on the other hand, being more polar with only one chain instead of two, have higher electrophoretic mobilities, are more soluble, form micelles and showed more promise in MECC as surfactants.

The electrophoretic mobilities of these micelles were different due to their different head groups as well as different tail chain lengths. The electrophoretic mobilities and elution windows were in the decreasing order of SDS>LPG>LPS>LPC. Additionally, the electrophoretic properties of lysophospholipid surfactants were found to be pH independent.

Of those examined, lysophosphatidylglycerol seems to be the most promising. It's additional chirality may prove to be useful in chiral separations. Being zwitterionic, lysophosphatidylcholine reverses the elution order of the

alkyl parabens achieved with lysophosphatidylglycerol. Additionally having no conductivity, lysophosphatidylcholine contributes little to the system current allowing higher separation voltages. Their addition as co-micelles with SDS improves resolution with no ill effects on efficiency or elution time.

The electrophoretic mobility of the various phospholipid and lysophospholipid classes are not sufficiently different to effect their own separation. With the addition of mixed micelles, SDS and STDS as well as manipulations in temperature, increasing the micelle formation/deformation kinetics, allowed reasonable resolutions. Lowering the buffer ionic strength, addition of organic modifiers or even use of a slightly more polar surfactant to the electrolyte system may affect a better resolution.

In a rapid methods development, the separation of the four common enzymes the endo- (EG I, EG II) and the exo- (CBH I, CBH II) glucohydrolases of *Trichoderma reesei*, that play a crucial role in the conversion of cellulose to ethanol, proved successful and reproducible. Underivatized fused silica capillaries were used with 0.03 M Na₂HPO₄ buffer at an optimum pH of 9.2. Additional peaks that appeared need identification. Further investigations to improve the efficiency and consequently, the resolution are necessary. Additionally, knowledge of the (confidential) methods of preparation and purification are necessary for better sample stacking and consequently, separation efficiency.

REFERENCES

1. M. Khaled, M. Anderson and H. McNair, *J. Chrom. Sci.*, 31 (1993) 259 .
2. M. Khaled and H. McNair, *HRCC*, (1994) sent for publication.
3. C. Palmer, M. Khaled and H. McNair, *HRCC*, 15 (1992) 756.
4. M. Khaled, M. A. Marochi, C. Palmer, and H. McNair, the Pittsburg Conference, Chicago IL, February 27 - March 4 (1994).
5. M. Khaled and H. McNair, *15th Int. Symp. Capillary Chromatogr.*, Riva Del Garda Italy, May 25-29 (1993).
6. O. Vesterberg, *J. Chromatogr.*, 480 (1989) 3.
7. S. Hjertén, *Chromatogr. Rev.*, 9 (1967) 122.
8. F. Mikker, F. Everearts and Th. Verheggen, *J. Chromatogr.*, 169 (1979) 11.
9. J. Jorgenson and K. Lukacs, *Anal. Chem.*, 53 (1981) 1298.
10. F. Kolrausch, *Ann. Phys. Chem.*, 62 (1897) 209.
11. J. R. Sargent and S.G. George, *Methods in Zone Electrophoresis*, 3rd ed., BDH chemicals Ltd., Poole, England (1975), Chapter 1.
12. A. Tiselius, *Trans Faraday Soc.*, 33 (1937) 524.
13. F. M. Everaerts, J. L. Beckers and Th. M. Verheggen (eds.), *Isotachophoresis-Theory and Applications*.*J. Chromatogr.*, Library Elsevier, Amsterdam- Oxford- NewYork (1976).
14. V. Pretorius, B. Hopkins, J. Schieke, *J. Chromatogr.*, 99 (1974) 23.
15. R. Virtanen, *Acta Polytechnica Scand.*, 123 (1974) 1-67.
16. J. W. Jorgenson and K. D. Lukacs, *J. Chromatogr.*, 218 (1981) 209.
17. J. W. Jorgenson and K. D. Lukacs, *Anal. Chem.*, 53 (1981) 1298.
18. J. W. Jorgenson and K. D. Lukacs, *Science*, 222 (1983) 266.
19. S. Hjertén, *J.Chromatogr.*, 270 (1983) 1.
20. S. Hjertén and M. Zhu, *J. Chromatogr.*, 346 (1985) 265.
21. S. Terabe, K. Otsuka, K. Ichikawa, A. Tsuchiya and T. Ando, *Anal. Chem.*, 56 (1984) 111.
22. J. Olivares, N. Nguyen, C. Yonker and R. Smith, *Anal. Chem.*, 56 (1987) 1230.

23. R. Wallingford, and A. Ewing, *Anal. Chem.*, 59 (1987) 1762.
24. R. Oda, T. spelsberg and J. Landers, *LC-GC* , 12 (1994) 50.
25. R. Khun and S. Hoffstetter-Khun, Capillary Electrophoresis: Principles and Practice, Springer-Verlag, Berlin (1993) 16.
26. J. Janini and H. Issaq, The buffer in Capillary Electrophoresis, Capillary Electrophoresis Technology, ed. N. Guzman, Chromatographic Science Series, Dekker, NY, 64 (1993) 130.
27. D. Grahame, *Chem. Rev.*, 41 (1947) 441.
28. S. Hjertén, *Topics Bioelectrochem Bioenerg*, 2 (1978), 89
29. B. Michov, *Electrophoresis* , 9 (1988) 201.
30. J. Vindevogel and P. Sandra, Introduction to Micellar Electrokinetic Chromatography, Hüthig, Heidelberg, (1992) 14.
31. C. Rice and R. Whitehead, *J. Phys. Chem.*, 69 (1965) 4017.
32. J. Vindevogel and P. Sandra, Introduction to Micellar Electrokinetic Chromatography, Hüthig, Heidelberg, (1992) 21.
33. J. Jorgenson, K. Lukacs, *Clin. Chem.*, 27 (1981) 1551.
34. J. Jorgenson, K. Lukacs, *Anal. Chem.*, 53 (1981) 1298.
35. J. Jorgenson, K. Lukacs, *J. Chromatogr.*, 218 (1981) 209.
36. J. Jorgenson, Capillary Zone Electrophoresis, ACS symp. Ser., 335 (1987) 182.
37. J. Knox, *Chromatographia*, 26 (1988) 329.
38. J. Giddings, "Dynamics of Chromatography Part I: Principles and Theory", Dekker Inc, NewYork, 1965.
39. R. Weinberger, Practical Capillary Electrophoresis. Academic Press, NY (1993) 28.
40. F. Foret, M. Deml and P. Bocek, *J. Chromatogr.*, 452 (1988) 601.
41. E. Gurska, R. McCormick and J. Kirkland, *Anal. Chem.*, 61, (1989) 241.
42. D. Heiger, High Performance Capillary Electrophoresis, Hewlett Packard, France, (1992) 28.
43. J. Vindevogel and P. Sandra, Introduction to Micellar Electrokinetic Chromatography, Hüthig, Heidelberg, (1992) 95.
44. D. Heiger, High Performance Capillary Electrophoresis, Hewlett Packard, France, (1992) 32.
45. H. Laur and D. McManigill, *Anal Chem.*, 58 (1986) 165.

46. S. Hjerten, *J. Chromatogr.*, 347 (1985) 189.
47. M. Novotny, K. Cobb and J. Lui, *Anal Chem.*, 62 (1990) 2478.
48. G. Bruin, H. Poppe, *J. Chromatogr.*, 471 (1989) 429.
49. J. Swedberg, *HRCC*, 14 (1991) 65.
50. S. Hjerten, *J. Chromatogr.*, 347 (1985) 191.
51. J. Towns and F. Regnier, *J. Chromatogr.*, 516 (1990) 69.
52. J. Smith and Z. El Rassi, *HRCC*, 15 (1992) 573.
53. A. Malik and M. Lee, Sixth Int. Symposium on High Performance Capillary Electrophoresis, San Diego, California, January 31 to February 3, (1994).
54. J. Liu V. Dolnik and M. Novotny, *Anal. Chem.*, 64 (1992) 1328.
55. T. Tsuda, *J. Liq. Chrom.*, 12 (1989) 2501.
56. P. Atkins, Physical Chemistry. Freeman, NY, (1990) 766.
57. A. Cohen, A. Paulus and B. Karger, *Chromatographia*, 24 (1987) 15.
58. D. Burgi, K Salomon, R. Chien, Poster presented at the 2nd International Symposium on High Performance Capillary Electrophoresis, San Francisco. January 29-31(1990).
59. B. VanOrman, G. Liversidge, G. McIntire, T. Oletrowicz, A. Ewing, *J. Microcol Sep*, 2 (1990) 176.
60. P. Reghetti, G. Tudor and K. Ek, *J. Chromatogr.*, 220 (1981), 115.
61. G. Consden, A. Gordon and A. Martin, *Biochem.* 40 (1946) 33.
62. P. Grossman, J. Colburn and H. Laur, *Anal Biochem.*, 179 (1989) 28.
63. R. Weinberger, Practical Capillary Electrophoresis. Academic Press, NY (1993) 50.
64. Y. Walbroehl and J. Jorgenson, *Anal Chem.*, 58 (1986) 479.
65. E. Gassman, J. Kuo and R. Zare, *Science*, 230 (1985) 813.
66. Y.Yik et al, *J. Chromatogr.*, 589 (1992) 333.
67. J. Liu, K. Cobb and M. Novotny, *J. Chromatogr.*, 519 (1990) 189.
68. S. Terabe et al, *J. Chromatogr.* , 516 (1990) 23.
69. H. Nishi, M. Matsuo, *J. Liq. Chrom.* 14 (1991) 973.
70. R. Khun and S. Hoffstetter-Khun, Capillary Electrophoresis: Principles and Practice, Springer-Verlag, Berlin (1993) 192.
71. U. Pfuller, Mizellen-Vesikel-Mikroemulsionen. Springer, Berlin (1986) 26
72. S. Terabe, K. Otsuka, T. Ando, *Anal Chem*, 57 (1985) 834.

73. K. Otsuka, S. Terabe, *J Chromatogr.* 515 (1990) 221
74. S. Terabe, O. Shibata, T. Isemura, *HRCC.*,14 (1991) 52.
75. K. Otsuka, S. Terabe, T. Ando, *J Chromatogr.*, 348 (1985) 39.
76. K. Otsuka, S. Terabe, T. Ando, *J Chromatogr.*, 332 (1985) 219.
77. M. Bushey, J. Jorgenson, *J Microcol Sep.*, 1 (1989) 125.
78. M. Bushey, J. W. Jorgenson, *Anal Chem*, 61 (1989) 491.
79. T. Kaneta, S. Tanaka and M. Taga, *J. Chrom.*, 653 (1993) 313.
80. S. Terabe, K. Otsuka, T. Ando, *Anal Chem*, 61 (1989) 251.
81. M. Sepaniak, R. Cole, *Anal Chem.*, 59 (1987) 472.
82. J. Davis, *Anal Chem*, 61 (1989) 2455.
83. A. Aniansson, S. Wall, M. Almgren, H. Hoffmann, I. Kielmann, W. Ulbricht
R. Zana, J. Lang and C. Tondri, *J. Phys. Chem.*, 80 (1976) 905.
84. S. Terabe, K. Otsuka, T. Ando, *Anal Chem*, 57 (1985) 834.
85. J. Gorse, A. Balchunas, D. Swaile and M. Sepaniak, *HRCC*, 11
(1988) 554.
86. J. Vindevogel and P. Sandra, *Anal Chem*, 63 (1991) 1540.
87. A. T. Balchunas and M. J. Sepaniak, *Anal. Chem.*, 59 (1987) 1466.
88. S. Terabe, H. Utsumi, K. Otsuka et al. *HRCC*, 9 (1986) 666.
89. K. Otsuka and S. Terabe, *J. Microcolumn Sep.*, 1 (1989) 67.
90. M. Sepaniak, D. Swaile, A. Powell and R. Cole, *HRCC*, 13 (1990) 679.
91. S. Fujiwara and S. Honda, *Anal. Chem.*, 59 (1987) 487.
92. A. Cohen, A. Paulus and B. Karger, *Chromatographia*, 24 (1987) 15.
93. A. Tran. et al, *J. Chromatogr.*, 542 (1991) 459.
94. A. Balchunas and M. Sepaniak, *Anal. Chem.*, 60 (1988) 617.
95. R. Wallingford and A. Ewing, Advances in Chromatography, Giddings, J.,
Ed., Marcel Dekker, New York, (1989) 14.
96. D. Rose and J. Jorgenson, *Anal. Chem.*, 60 (1980) 642.
97. R. Weinberger, Practical Capillary Electrophoresis, Academic Press,
Boston, (1993) 205.
98. D. Heiger, High Performance Capillary Electrophoresis. Hewlett Packard
GmbH, (1992) 89.
99. M. Yu and N. Dovichi, *Microchemica acta*, 3 (1988) 27.
100. T. Wang, R. Harwick, P. Champlin, *J Chromatogr.*, 462 (1989) 147.
101. K. Otsuka, S. Terabe, *J. Chromatogr.*, 480 (1989) 91.

102. R. Scott, Liquid Chromatography detectors, Elsevier (1986).
103. X. Haung, W. Coleman and R. Zare, *J. Chromatogr.*, 480 (1989) 95.
104. A. Ewing, R. Wallingford, and T. Olefirowicz, *Anal. Chem.*, 61 (1989) 292.
105. M. Albin, P. Grossman and S. Moring, *Anal. Chem.*, 65 (1993) 489.
106. J. Taylor and E. Yeung, *J. Chromatogr.*, 550 (1990) 831.
107. X. Xi and E. Yeung, *Appl. Spectroscopy*, 45 (1991) 1199.
108. R. Khun and S. Hoffstetter-Khun, Capillary Electrophoresis: Principles and Practice, Springer-Verlag, Berlin (1993) 127.
109. T. Higashimajima and N. Ishibashi, *Anal. Chem.*, 64 (1992) 71.
110. F. Foret, M. Deml, V. Kahl and P. Bocek, *Electrophoresis*, 7 (1986) 430.
111. X. Haung, T. Pang, M. Gordon and R. Zare, *Anal. Chem.*, 59 (1987) 2747.
112. P. Dasgupta, L. Bao, *Anal. Chem.*, 65 (1993) 1003.
113. N. Avdaovic, C. Pohl, R. Rocklin and J. Stillian, *Anal. Chem.*, 65 (1993) 1470.
114. A. Bard and J. Faulkner, Electrochemical Methods: Fundamentals and Applications. John Wiley, NY., (1980) 22.
115. R. Wallingford and A. Ewing, *Anal. Chem.*, 59 (1987) 1762.
116. T. O'Sea, R. Greenhagen, S. Lunte et al. *J. of Chromatogr.* 593 (1992) 305.
117. T. Olejirowicz and A. Ewing, *Anal. Chem.*, 62 (1990) 1872.
118. X. Huang and R. Zare, S. Sloss and A. Ewing, *Anal. Chem.* 63 (1991) 189.
119. S. Sloss and A. Ewing, *Anal. Chem.*, 65 (1993) 577.
120. J. Ye and R. Baldwin, *Anal. Chem.*, 65 (1993) 3525.
121. W. Lu, R. Cassidy and A. Baranski, *J. Chromatogr.*, 640 (1993) 433.
122. J. White and J. Jorgenson, *Anal. Chem.*, 58 (1986) 293.
123. D. Johnson and W. LaCourse, *Anal. Chem.*, 62 (1990) 589.
124. W. Lu and R. Cassidy, *Anal. Chem.*, 65 (1993) 1649.
125. J. Olivares, N. Nguyen, C. Yonker and R. Smith, *Anal. Chem.*, 59 (1987) 1230.
126. R. Smith and H. Udseth, *Nature*, 331 (1988) 638.
127. R. Smith, J. Wahl, D. Goolett and S. Hofstadler, *Anal. Chem.* 65 (1993) 574A.
128. L. Mack, P. Kralik, A. Rhonde and M. Dole, *J. Chem. Phys.*, 52 (1970) 4977.

129. C. Whitehouse, R. Dreyer M. Yamashita and M. Fenn, *Anal Chem.*, 57 (1985) 675.
130. E. Yeung and W Kuhr, *Anal Chem.* 63 (1991) 275A.
131. J. Lux, U. Hausig and G. Schomburg, *HRCC*, 13 (1990) 373.
132. R. Wallingford and A. Ewing, *Anal. Chem.* , 60 (1988)259.
133. B. Durairaj and F. Blum, *Langmuir*, 5 (1989) 370.
134. D. Bennett and G. Kirby. *J. Chem Soc. C* (1968) 442.
135. ESA Inc., Coulochem Applications 10-1219
136. M. Verzele, P. Mussche and S. Qureshi. *J. Chromatogr.* 172 (1979) 493.
137. T. Kawada, T. Watanabe, K. Katsura et al. *J. Chrom.*, 329 (1985) 99.
138. J. Szolcsány and A. Jansco-Gabart, *Arznein-Forsch.*, 25 (1978) 1877.
139. A. Boersch, B. Fallingham, F. Lembeck, and D. Sharman, 42 (1991) 863.
140. H. Markwalder and H. Keukom, *Photochemistry*, 15 (1976) 836.
141. D.S. Pankar and N.G. Magar. *J. Food Science* , 42 (1977) 66.
142. A. Krajewska and J. Powers, *J. Chromatogr.*, 409 (1987) 223.
143. A. Krajewska, and J. Powers, *J. Chromatogr.*, 457 (1988) 279.
144. M. Verzele, F. Van Damme, G. Schuddinck and D. Myncke, *J. Chromatogr.*, 471 (1989) 335.
145. J. Gorse, A. Balchunas, D. Dwaile and M. Sepaniak, *HRCC*, 11 (1988).554.
146. J. Vindevogel and P. Sandra, *Anal Chem*, 63 (1991) 1530.
147. A.T. Balchunas and M. J. Sepaniak, *Anal. Chem*, 59 (1987) 1466.
148. K. Otsuka, and S. Terabe, *J. Microcolumn Sep.*, 1 (1989) 67.
149. M. Sepaniak, D. Swaile, A. Powell and R. Cole, *HRCC*, 13 (1990) 679.
150. J. Liu, O. Shirota, and M. Novotny, *Anal. Chem.* 63: 413-417 (1991).
151. T. Lee, E. Yeung and M. Sharma, *J. Chromatogr.*, 565: 197-205 (1991).
- 152 R. Wallingford, P. Curry and A. Ewing, *J. Microcolumn Sep.* 1: 23-27 (1989).
153. L. Colon, R. Dadoo, R. Zare. *Anal. Chem.* 65 (1993) 476.
154. R. Cole, R. Holland and M. Sepaniak, *Talanta*, 39 (1992) 1139.
155. S. Terabe, H. Ozaki, K. Otsuka and T. Ando, *J. Chromatogr.*, 332 (1985) 211.
156. S. Fanali, *J. Chromatog.r*, 474 (1989) 441.

157. S. Fanali, *J. Chromatog.r*, 442 (1988) 371.
158. S. Terabe et al, *J. Chromatogr.*, 516 (1990)23.
159. H. Nishi and M. Matsuo, *J. Liq. Chrom.* ,14 (1991) 973.
163. W. Friedl and E. Kenndler, *Anal. Chem.*, 65 (1993) 2003.
164. J. Reijenga, G. Aben, Th Verheggen and F. Everaerts, *J..Chromatogr.*, 260 (1983) 241.
165. T. Tsuda, *HRCC*, 10 (1989) 766.
166. K. Otsuka, S. Terabe and T. Ando *J. Chromatog.*, 322 (1985) 219.
167. D. Burton, M. Sepaniak and M. Maskarinee, *J. Chromatogr. Sci.*, 25 (1987) 514.
168. T. Kanata, S. Tanaka, M. Taga and H. Yoshida, *Anal. Chem.*, 64 (1992) 798.
169. X. Haung, J. Lukey, M. Gordon and R. Zare, *Anal Chem.*, 561 (1989) 766.
170. W. Jones and P. Jandik, *J. Chromatogr.*, 546 (1991) 411.
171. R. Wallingford and A. Ewing, Advances in Chromatography, ed. J. Giddings, V29, Dekker, NY (1989) 65-67.
172. S. Terabe and T. Isemura, *Anal Chem.* 62 (1991) 650.
173. C. Palmer and H. McNair, *J. Microcol. Sep.*, 4 (1992) 509.
174. C. Larabee, E Sparague, *J. Polym. Sci.*, 17 (1979) 749
175. C. Larabee, E Sparague, *J Collo. Int. Sci.*, 114 (1986) 256.
176. E Sparague, D. Duecker and C. Larabee, *J Collo. Int. Sci.*, 92(1983) 416.
177. C. Paleos, C. Stassinopoulou and A. Mallaris, *J. Phys. Chem.*, 87 (1983) 251.
178. G. Odian, Principles of Polymerization, Wiley, NY, (1981).
179. D. Sepaniak, D. Burton, A Balchunas and M. Sepaniak, *J. Chrom. Sci*, 26 (1988) 406.
180. S. Fujiwara and S Honda, *J. Chrom.*, 447 (1988) 133.
- 181 S.Kobayashi, T. Ueda and M. Kikumoto, *J Chromatog.* 480 (1989) 179.
182. H. Nishi and S. Terabe, *J. Chromatog.*, 465 (1989) 331.
183. H. Nishi and S. Terabe, *Anal Chem.*, 61 (1989) 2434.
184. C. Ong and F. Li, *J. Chromatogr.*, 547 (1991).
185. Chan, K. Lewis, J. Phang and H. Issaq, *HRCC*, 16 (1993) 560.

186. Y. Moroi, Micelles: Theoretical and Applied Aspects, Plenum , NY, 1992.
187. P. Elworthy, B. Pharmand L. Saunders, *J. of Pharm. Pharmacol.* 8 (1956)1001.
188. Chain and Kemp, *Biochem. J.*, 28 (1934) 2052.
189. C. Tanford, The Hydrophobic Effect: Formation of Micelles and Biological membranes. Wiley Interscience,N Y, (1980).
190. R. Brown and L. Jurasek, Hydrolysis of Cellulose: Mechanisms of Enzymatic and acid catalysis. American Chemical Society, DC.(1979).
191. R. Boyer, T. Allen and P. Dykema, *Biotechnol. Bioeng.*, (29 (1987) 176.
192. C. Orgeret, E. Seillier, C. Gautier and H. Driguez, *Carbohydr. Res.*, 224 (1992) 29.
193. P. Tomme, S. McCrae and M. Claeyssems, *Methods Enzymol.* 160 (1988) 187.
194. H. Diriguez, *FEMS Symp.*, 43 91988) 399.
195. F. Bissett, *J. Chromatog.*, 178, (1979) 515.
196. A. Vorgen and W. Pilinik, *Food Sci.*, 1989 145.
197. J. Kovar and L. Kuniak, *J. Chromatogr.*, 389 (1987) 322.
198. S. Ellouz and G. Titaby, *J. Chromatogr.*, 396 (1987) 307.
199. R. Parr, *Biochem. Soc. Trans.*, 13 (1985) 452.
200. H. Tilbeurgh and M. Claeyssems, *FEBS Lett.*, 187 (1985).
201. N. Golovchenko, *J. Chromatogr.* , 591 (1991) 121.
202. R. Bhikhabhai, *Am. Lab*, 21 (1989) 78.
203. D. Eveleigh, *Phil. Trans R. Soc. Lond.*, 321 (1987) 435.
204. M. Gordon , K. Lee, A. Arias and R. Zare, *Anal. Chem.* 63 (1991) 69.
205. A. Emmer, M. Jansson and J. Roeraade, *J. Chromatogr.*, 547 (1991) 798.
206. D. Fuerstenau, *J. Phys. Chem.*, 60 (1956) 981.
207. J. Vindevogel and P. Sandra, Introduction to Micellar Electrokinetic Chromatography, Hüthig, Heidelberg, (1992) 38.
208. M. Khaldi , The 4th Annual Frederick Conference on Capillary Electrophoresis , Oct 1993.

VITAE

MAHA Y. KHALED

Maha Khaled obtained her BSc., in Chemistry, in 1983 and her MSc., in Solid State Science, in 1987, both with highest honors, from the American University in Cairo, Egypt. She obtained her Ph.D. in 1994 from the Chemistry Department of Virginia Tech., USA., working under the supervision of Professor Dr. Harold M. McNair. Her Ph.D. research was on "Selectivity and Detection in Capillary Electrophoresis".

Maha Khaled has received 5 travel awards to both national and international conferences. She has also received two other awards for her academic achievements; the Kenan award in 1992 and the American Chemical Society Analytical Division Full Graduate Fellowship Award in 1993. In addition, Virginia Tech. granted her an Excellence in Teaching award, in 1993.

Maha Khaled has had industrial experiences starting with analyzing and quality controlling soap production at Kato Aromatic (Cairo, Egypt). She worked with Gas Chromatography for pesticide and glyceride analyses, at Johnson Wax (Racine, WI); worked with High Performance Liquid Chromatography with Electrochemical Detection for the investigation of pungent compounds for Nabisco (Hanover, NJ); and used Capillary Electrophoresis for acid and enzyme separations at Amoco (Naperville, IL).

For academia, Maha Khaled has worked at the University of Kuwait as a research associate, synthesizing dithiozonate complexes for trace metal analyses with Professor A. M. Kiwan. At Virginia Tech. she worked as a graduate teaching assistant for the department of Chemistry and has assisted Professor Harold McNair in his organization and teaching of the various ACS short courses on GC, HPLC, GC/MS and CE, both at Virginia Tech. and at various conferences and industrial sites.

Maha Khaled is a member of the American Chemical Society (ACS), the Royal Society of Chemistry (RSC, England) and was President of the Chemistry Graduate Student Assembly (CGSA) at Virginia Tech..

